THE INCORPORATION OF IMPURITIES INTO SUCROSE CRYSTALS DURING THE CRYSTALLISATION PROCESS

by

GEORGES RAOUL EDOUARD LIONNET

Submitted in partial fulfilment of the requirements for the degree of Doctor of Philosophy in the Department of Chemistry and Applied Chemistry, University of Natal

Durban - 1998

ABSTRACT

The main objective of this work is to propose a mechanism for the transfer of impurities into the sucrose crystal. To this end the transfer of impurities into the sucrose crystal was investigated, under crystallisation conditions similar to those found industrially. Most of the impurities, namely, colour bodies, potassium, calcium and starch, were selected on the basis of their industrial importance, but some exotic species, namely lithium and nickel, were chosen to represent other mono- and di-valent ions respectively, and dyes, such as methylene blue, which have been used in work with single crystal sucrose crystallisation, were included to make the results more general.

A parameter to measure the rate at which impurities are transferred into the sucrose crystal was proposed. Experiments, carried out in a pilot plant evaporative crystalliser, were performed to establish the effect of selected factors on both the concentrations of impurities found in the sucrose crystal, and on the rate at which these impurities are incorporated into the crystal. All the factors selected, namely the rate of crystallisation, the temperature, the concentration and type of impurity, the diffusivity of the impurity in concentrated sucrose solutions, and the crystal dimensions, are shown to influence the rate of impurity transfer. Only the concentration in the feed and type of impurity, however, affect the final concentration of the impurity in the crystal.

Concepts involving partition coefficients and adsorption isotherms were also investigated. The experimental data did not fit the adsorption isotherm models well, but the values obtained for the partition coefficients were similar to those quoted in the literature when exchange types of reactions are operative.

Activation energies have been measured, both for the rate of crystallisation of sucrose, and for the rates of impurity transfer. The values obtained, particularly for the rate of impurity transfer, indicate that a transport mechanism is effective.

The experimental results have been used to investigate the relevance of two models, one involving a two-step approach and the other an interfacial process, for the incorporation of the impurity into the sucrose crystal. The results obtained indicate that the interfacial breakdown model describes the transfer of all the impurities studied here, except for starch.

PREFACE

The experimental work described in this thesis was carried out in the laboratories of the Sugar Milling Research Institute, Durban. I was given assistance by members of the Institute in carrying out the experimental part of this project, which is formally referred to in the Acknowledgements.

These studies represent original work by the author and have not been submitted in any form to another University.

ACKNOWLEDGEMENTS

This project was financed by the Sugar Milling Research Institute and my thanks are due to its Director and Board of Control who made it possible.

The help and cooperation of the Sugar Milling Research Institute members contributed substantially to the progress of the project. More particularly, I am indebted to and would like to thank the following staff members:

Mr R Ramsumer who carried out all the individual crystalliser runs and helped with the analytical work, particularly the affinations; all the staff of the Analytical Division of the Institute who helped with method development and did all the analytical work; Mr P Ramsuraj and Mr B Barker who carried out the crystal size distribution analyses; Mr S Markham and Mr R Ramsumer for their contribution to the experimental measurements of diffusion coefficients, and finally, to Mr M Achary and Mrs Y Naidoo who helped produce some of the drawings found in the text. I would also like to thank the staff of the Workshop who were involved with the construction and maintenance of the equipment.

The X-ray diffraction analyses of sugar crystals were carried out by Mrs L Turner of Minemet Technologies (Pty) Ltd.

I am indebted to Mrs MG Thélémaque for typing this thesis.

I was privileged to have Dr Bice Martincigh of the University of Natal and Dr Brian Purchase of the Sugar Milling Research Institute as supervisors. My thanks are due to both of them.

Finally I would like to acknowledge special thanks to my wife and family for their encouragement.

TABLE OF CONTENTS

GLOSSARY OF TERMS

The sugar industry uses a number of terms which have specific meanings. A list of those terms relevant to this work and their meanings are given here.

Brix : total dissolved solids in any sugar stream, on a percentage mass on mass basis.

Pol : apparent sucrose content of a sugar stream, on a percentage mass on mass basis.

Sucrose : true sucrose content of a sugar stream, on a percentage mass on mass basis.

Purity : the ratio of pol (or sucrose) to brix, as a percentage.

For pure sucrose streams, brix, pol and sucrose contents are exactly equivalent and purity is 100%.

Colour : of a sugar stream or product is determined by a specific analytical method. It is treated as if it was a single substance, although it is really the quantification of a mixture of many diverse compounds. Colour is quoted in "colour units", expressed on brix. A "quantity of colour" can be calculated by multiplying the colour by the brix; this is used in colour balances.

Massecuite : the mixture of sucrose crystals (30-50% by mass) and mother-liquor, found in crystallisers.

Mother-liquor : the liquid part of a massecuite.

Molasses or run-off	:	the liquid part of a massecuite, separated from the solid sugar by centrifugation.

In this work the terms mother-liquor, molasses and run-off are equivalent.

Sugar	:	the solid material obtained from the massecuite by centrifugation. Ordinary sugar consists of a crystal surrounded by a film of mother-liquor.
Crystal	:	the crystal part of sugar, that is the sucrose crystal from which the mother-liquor film has been removed. In this work crystal will always mean the crystal part of sugar from which the film has been removed by a specific laboratory affination technique.
Affination	:	a laboratory washing technique by which the mother-liquor film is removed from the surface of crystalline sugar in a reproducible manner.
Slurry	:	a dispersion of small sugar particles in alcohol. Slurry is used to instigate nucleation.
Feed	:	the sucrose containing stream fed to the crystalliser.
Liquor	:	any sucrose containing solution, generally of high brix and purity.
Wash	:	that part of the feed used to dissolve excess, small nuclei, after seeding.
Seeding	:	the introduction of slurry to instigate nucleation.
Polysaccharides:		or "gums" in the sugar industry, determined by an alcohol precipitation analytical technique.

LIST OF SYMBOLS

a	Surface area of one sucrose crystal	m^2
A	Surface area of N crystals	m^2
A_{fk}, A_{fv}, A_{fd}	Pre exponential factors	s^{-1}
B	Concentration of dissolved solids or brix	% (mass/mass)
C	Colour of material	-
D	Diffusion coefficients	m^2/s
E_a, E_v, E_d	Activation energies	kJ/mol
F	Crystal shape factor	$m^2/kg^{-2/3}$
F_i	Concentration of impurity in feed liquors	mg/kg
G	Mass growth rate of sucrose crystals	$kg/m^2/s$
k	Rate constants	s^{-1}
K	Equilibrium constants	
l_g	Linear crystal growth rate	m/s
L	Length of sucrose crystal	m
L_c	Characteristic dimension of sucrose crystal	m
m	Mass of one sucrose crystal	kg
M	Mass of material	kg
M_c	Mass of N crystals	kg
N	Number of crystals	-
P	Apparent concentration of sucrose or pol	% (mass/mass)
P_i	Partition coefficient	-

R	Gas constant	J/K/mol
R_i	Impurity transfer rate	$kg/m^2/s$
t	Time	s
T	Temperature	K
W	Width of sucrose crystal	m
X_i	Concentration of impurity in the crystal	kg/kg
Z	Empirical quantity in Equation 2.26	-

Subscript

c	crystal
cw	condensate
f	feed liquor
fn	final condition
i	initial condition or impurity
m	mother liquor
mc	massecuite
s	seed
wl	wash liquid

Greek

α	volume shape factor	-
β	surface area shape factor	-
δ	interfacial film thickness	m
η	viscosity	Pa s
ρ	density of sucrose	kg/m^3

CHAPTER 1

INTRODUCTION

The annual worldwide sugar production is about 120 million tons, all of which is produced by the crystallisation process. Commercially, two types of sugar are available, namely raw and refined, the former containing between 96 and 99% sucrose while the purity of the latter is 99,9% and higher. Quality, which commercially involves mostly the purity of the sugar, is an important parameter; it impacts on price structures, downstream processing costs and commercial applications. Sugar for infant food, for example, must meet stringent quality constraints.

Although crystallisation is a powerful purification process, impurities can and do enter the sucrose crystal. Even at very low concentrations they can affect the quality. Colour for example impacts directly on the visual appearance of the product and affects its suitability for specific applications such as baking or the soft drink industry.

The presence of impurities in the sugar is controlled through two basic steps. The first involves chemical purification during the production of raw or refined sugar. Existing processes such as carbonatation, the use of ion exchange resins or of activated carbons, are well understood, and new processes, such as the use of ozone, are being investigated. The second step involves the crystallisation process itself. This has been, and is, extensively investigated, but little or no information is available in the literature on the mechanisms of impurity transfer during the crystallisation of sucrose. A knowledge of such mechanisms would enable one to control the transfer of impurities and could reduce production costs.

The main objective of this work is to investigate those factors which impact on the transfer of impurities into the sucrose crystal and to propose general mechanisms for the incorporation of these impurities. The first step in the study was to carry out a literature review of current work concerning the crystallisation of sucrose and, where relevant, that of other products.

The results of the literature review will be described in two main sections. The first covers crystallisation itself and the factors that affect it. The second section deals with various models which have been developed to describe crystallisation and impurity transfer.

1.1 General aspects of crystallisation

The presence of impurities in the sugar crystal is well documented in the literature. In South Africa, sugar quality publications were started in 1953 when Douwes-Dekker published a report entitled "The Quality of Natal White Sugar ex Crop 1953". In 1997 Dunsmore published "The Testing of Sugars ex the 1996/97 Crop". The main impurities mentioned are colour, inorganic species such as potassium and calcium, and polysaccharides such as starch and gums.

Impurities in the sucrose crystal have been mentioned by many workers. Honig in 1953 noted that starch appeared to be strongly adsorbed on sugar crystals. Boistelle (1975) reported on the effects of the concentration of impurities, of supersaturation and of pH, on the habit of the sucrose crystal. In 1985 Mantovani *et al.* carried out extensive work on inclusions and reported on the effect of the rate of growth of the crystal. Mullin (1993) reviewed the work on inclusions and related it to the sucrose crystallisation rate. In South Africa Lionnet (1987) showed that the laboratory affination process used was a vital aspect in the study of impurity transfer: since the mother-liquor film can be 100 times more coloured than the crystal, if small amounts of liquor are left on the crystal large errors can be made when the concentrations of impurities are estimated.

Michael and Thelemaque (1984) evaluated a number of laboratory affination techniques and recommended the ICUMSA cane sugar method (Schneider, 1979), showing that it yields reproducible results. This method has therefore been adopted in this work. Recently, Lionnet and Moodley (1995) have discussed the effects of the concentration of the impurities, the type of impurities and the crystal size on impurity transfer. Finally, Vaccari (1996) reviews the work done to-date and notes that there is a degree of confusion concerning possible mechanisms for impurity transfer. Purely mechanical inclusions of mother-liquor are implied by some of the results available in the literature while other data suggest co-crystallisation/adsorption processes.

Vaccari (1996) is the first worker to suggest an interfacial breakdown mechanism.

The general conclusions from the above are that the more important impurities are colour, potassium, calcium and polysaccharides. The factors that have an effect on the impurity transfer are the rate of sucrose crystallisation, the concentration and type of the impurities, and the crystal size. There is much less information on possible mechanisms for impurity transfer into the sucrose crystal.

The literature was reviewed, in more detail, with respect to the main factors mentioned above.

1.1.1 **Factors that affect impurity transfer**

The main factors reviewed here are the crystallisation rate, the concentration and type of the impurities, the temperature, viscosity and diffusivity, the crystal size and, finally, the agitation.

1.1.2 **Crystallisation rate and shape factors**

Many workers (VanHook, 1981; Mantovani *et al.*, 1985, 1986; Lionnet, 1987, 1988; Donovan and Williams, 1992; Lionnet and Moodley 1995; Vaccari, 1996) confirm that the colour transfer increases as the rate of crystallisation of sucrose increases. Saska (1991) shows that the uptake of dextrans is similarly affected by the rate of crystallisation of sucrose. Guo and White (1984) show that higher growth rates result in higher levels of impurities in the crystals due to more inclusions.

A similar trend has been found with other crystals. Ozum and Kirwan (1976) found a critical growth velocity above which the growth front becomes unstable and breaks down, causing impurity capture. This phenomenon was found with ice and sucrose or sodium chloride as impurities, in metallic melts and in various organic systems.

Mullin (1993) reviews the literature and shows that rapid growth, rapid healing of etch pits, and dissolution followed by re-growth generally increase impurity transfer. These effects were investigated during the crystallisation of sodium chlorate, hexamine and sodium chloride crystals.

In view of the importance of the sucrose crystallisation rate, it is useful to look at how this is measured. Nyvlt *et al.* (1985) show that there are many ways in which the sucrose crystallisation rate can be measured - they define a linear growth rate, a volumetric growth and a mass growth rate.

Mullin (1993) follows a similar approach for the crystallisation rate in general and shows that there is no simple or generally accepted method of expressing the rate of growth of a crystal since this has a complex dependence on temperature, surpersaturation, habit, system turbulence, etc. However, for carefully defined conditions, crystal growth rate may be expressed as a mass dependent rate, G, in kg/s/m^2, and a mean linear velocity, v, in m/s.

These two basic rates are related, require some characteristic crystal dimension for their calculation and depend on volume and shape factors. A precise calculation of the volume or surface area of a solid body of regular geometric shape can only be made when its length, breadth and thickness are known. For particulate matter in general these three dimensions can never be precisely measured. Thus, the need for shape factors, which are based on one or more dimensions of the particle.

Both types of crystal growth rate, G and v, and shape factors are well used in the sugar industry. Vaccari *et al.* (1996), Guimaraes *et al.* (1995), Grimsey and Herrington (1994), Bennett and Fentiman (1969) and Day (1971) have used them for sucrose. Kraus and Nyvlt (1994) have used them for work with glucose. Finally, they have been reviewed in detail by Bubnik and Kadlec in 1992, for sucrose. These authors show that it is possible to calculate G and v using the measurement of one or two of the crystal dimensions. This and the use of well defined shape factors for the sucrose crystal, yield the crystal surface area, characteristic dimensions and the number of crystals per unit mass. This approach has been applied to sucrose and other crystallisation work.

1.1.3 **The concentration of the impurity**

Again the effect of the concentration of the impurity is well documented in the literature, both for sucrose and for other crystals. Donovan and Williams (1992) and Lionnet and Moodley (1995) show that the colour in the sucrose crystal is a function of the level of colour in the feed liquor.

Saska (1991) shows similar trends with dextrans.

Boistelle (1975) shows that the concentration of the impurity affects the existence of an adsorption layer. Sodium chloride with lead as impurity, was the type of system investigated. Mullin (1976) shows that even traces of an impurity, at levels as low as a few parts per million, can profoundly affect the crystal. Finally, a concentration effect is implied in Ozum and Kirwan's (1976) work involving aluminium/copper melts, organic systems, sodium chloride/water and sucrose/water solutions.

1.1.4 **Effect of the type of impurity**

As far as sugar is concerned, Honig in 1953 had already noticed that starch was highly incorporated into the sucrose crystal. Mantovani *et al.* studied colour inclusions in 1985. Vaccari *et al.* (1991) give clear evidence that cane and beet liquors behave differently with respect to colour transfer. This immediately implies species effects since the colour bodies in beet and cane are known to be very different. Generally, transfer in cane is higher (Lionnet and Moodley, 1995) and it is known that cane contains more phenolics and monosaccharides than beet. Donovan and Williams (1992) show experimental evidence that molecular mass affects the transfer rate; the higher the molecular mass the higher the transfer of the colour body.

Saska (1991) shows a similar molecular mass effect for the incorporation of dextrans into the sucrose crystal. The same author shows that the ratio of dextran in the crystal to dextran in the liquor was about 0,3 while for potassium or sodium the same ratio was only 0,003. Similar trends are mentioned by Vaccari (1996). Pautrat *et al.* (1995) mention the transfer of polysaccharides and their effect on the keeping quality of the sugar.

Guo and White (1984) used potassium and calcium as inorganic species, glucose as an organic impurity and molasses to provide colour as the impurity. Lithium was also selected by these workers, as a species not normally present in cane.

One impurity well investigated in the beet industry is the trisaccharide, raffinose, which is however not found in cane. Aquilano *et al.* in "Crystallisation as a Separation Process" (Myerson and Toyokura, 1990) show that raffinose consists of the sequence fructose-glucose-galactose and is

able to enter the kinks on the sucrose crystal. The galactose portion then hinders the entrance of other sucrose molecules. Glucose and fructose do enter the sucrose crystal, but there is no hindering effect. Mantovani (1997) confirms the impact of raffinose and investigates effects due to its concentration. He also works with glucose and fructose, highlighting the differences between these three sugars. VanHook (1997a) reports on glucose, fructose and raffinose. He points out that fructose, glucose and raffinose are found at different locations in the sucrose crystal. He then comments on the chemical and crystallographic properties of the impurity and of the crystal. If both these aspects are similar, the impurity is highly incorporated in the crystal, as is the case for raffinose. Glucose does not fit in sucrose and is therefore weakly adsorbed. Later work by VanHook (1997b) involves X-ray diffraction analyses to show that the raffinose molecules are accommodated within the growing sucrose crystal in such a way as not to change the normal spatial dimensions between the sucrose molecules. Thus the raffinose is chemisorbed on the surface of the growing sucrose crystal and not built into the normal sucrose lattice. VanHook (1997c) notes that a similar conclusion has been made for the presence of dextran in the sucrose crystal.

Species effects are available in the literature for many other crystals. Boistelle (1975) discusses the behaviour of nickel, copper and iron with various organic crystals. Zumstein *et al.* (1990) show different behaviours for the crystallisation of L-isoleucine with L-leucine, L-valine and L-alpha-amino butyric acid as impurities. Similarly Witcamp and Rosmalen (1990) show that cadmium and phosphate impurities behave differently during the crystallisation of calcium sulphate.

Finally Nyvlt (1976) states that the parameters which influence the occurrence of adsorption include the steric arrangement of molecules, their charge and dipole moment, as well as the electric field at the crystal surface.

1.1.5 **Effect of temperature**

The effect of temperature on the crystallisation rate of sucrose is well documented in the literature. It is expected that temperature will also have an effect on the rate at which impurities are transferred but this is much less documented. It is instructive to look at the activation energy concept, for the crystallisation of sucrose, as a guide to the investigation of temperature effects on impurity transfer.

Mullin (1993) reviews the effect of temperature on crystallisation in general. If crystallisation is assumed to consist of a two-step process, namely a transport mechanism by which the molecules approach the crystal, followed by their incorporation into the crystal, Mullin states that the activation energy of the transport process is generally in the range 10 to 20 kJ/mol, while that of the incorporation step is about 40 to 60 kJ/mol. The rate of incorporation therefore increases more rapidly with temperature than does the transport rate. Thus, at high temperatures, similar to those found in the crystallisation of sucrose, growth rate could be limited by the transport process. Experimental work quoted by Mullin (1993) confirms this, showing that the rate of crystallisation of sucrose is diffusion controlled at temperatures above 40°C. For sodium chloride the process is transport limited above 50°C.

The relationship between a reaction rate constant and temperature is given by the Arrhenius equation

$$k = A_{pf}\, e^{-Ea/RT}$$

where k is the reaction rate constant, A_{pf} the pre-exponential factor, E_a the energy of activation, R the gas constant and T the absolute temperature. Activation energies for the crystallisation of sucrose are well documented in the literature, and some typical results are shown in Table 1.1.

Table 1.1

Activation energies in kJ/mol for the crystallisation of sucrose

Transport	Incorporation	Whole process	Temperature/°C	Reference
12-17	60-69	-	40-60	Maurandi and Mantovani (1982)
21-38	-	-	45-55	as above
15-24	60-70	-	-	Maurandi *et al.* (1984)
-	-	19-29	60-80	Honig (1959)
-	-	30	60-80	VanHook (1944, 1945)
-	-	31-42	60-80	VanHook (1997d)

1.1.6 **Viscosity and diffusivity**

The two-step mechanism (Mullin, 1993) for the crystallisation process has already been mentioned. In that mechanism viscosity and diffusivity could play an important role in crystallisation and impurity transfer.

Honig (1959) shows that viscosity is important in the crystallisation of sucrose, a point which is clearly evident industrially when sucrose is crystallised from progressively more and more viscous and impure liquors. Two points are raised by Honig. Firstly, the region of importance is the boundary layer between the crystal and the bulk of the solution; secondly, sucrose concentrations are high and so are the temperatures. This impacts on viscosity since the viscosity of sucrose solutions is dependent on concentration and temperature. Chen and Chou (1993) give the viscosity of sucrose solutions at various temperatures and concentrations. Peacock (1995) gives an empirical formula to calculate the viscosity of sucrose solutions if the temperature and concentration are known.

The presence of impurities in sucrose solutions generally increases the viscosity (Chen and Chou, 1993). In the present work the sucrose solutions do contain impurities but these are at relatively low concentrations. Thus data for pure sucrose solutions should yield good approximations.

Particles in solution have to jostle their way through the solvent to meet and then react. As mentioned in Section 1.1.2.4 this diffusional mechanism is important for the crystallisation of sucrose and it is logical to assume that it could impact on impurity transfer. Again the diffusivities of the various non-sucrose species have to be considered in a boundary layer and with sucrose concentrations at saturation and higher.

Theoretical approaches yield relationships between the diffusion coefficient (D) and viscosity (η) indicating that D can be estimated if η is known. VanHook (1945) and Gladden and Dole (1953) show, however, that these relationships do not hold in highly concentrated sucrose solutions, a result which has been confirmed experimentally by Saska and Oubrahim (1989).

Although in the present work it is the diffusivities of the non-sucrose species which are of interest, it is still useful to look at some results pertaining to sucrose itself. The diffusivity of sucrose has

been investigated by many workers (VanHook and Russel, 1945; Gladden and Dole, 1953; Honig, 1959). Some results for sucrose in aqueous solutions can be summarised as follows:

- VanHook (1945) shows that the diffusion coefficient of sucrose increases with temperature and decreases with concentration. The activation energy for diffusion, E_d (equation 2.25) was about 19 kJ/mol, from 10 to 90°C.

- Gladden and Dole (1953) show a linear decrease in the diffusion coefficient as the concentration of sucrose increases, at 25°C, varying from about 2 x 10^{-7} cm^2/s at 40% sucrose by mass to 0,2 x 10^{-7} cm^2/s at 70%. The value of E_d increased linearly with the concentration of sucrose over the range 25-35°C; E_d was about 30 kJ/mol at a sucrose concentration of 62% but rose to 40 kJ/mol at 74%.

- Maurandi (1981) shows that the diffusion coefficient of sucrose decreases as supersaturation increases.

- Heffels (1986) and Heffels *et al.* (1987) have also studied the diffusivity of sucrose. The results which apply best to the present work are those of Heffels who measured the diffusion coefficient of sucrose in concentrated aqueous solutions and concluded that his results were correct, for high concentrations, particularly if extrapolations from values measured at low concentrations had been used. Heffels *et al.* give the results shown in Table 1.2.

Table 1.2

The diffusion coefficient of sucrose at 70°C as a function of concentration (% mass/mass) from Heffels (1986)

Sucrose concentration %	$D/10^{-9}$ m^2/s
50	7,4
60	5,5
70	4,2
75	3,8
80	2,8

Heffels *et al.* also provide data which allow the calculation of the activation energy for the diffusion coefficient of sucrose in water (D_{suc}). The data include D_{suc} for concentrations from 50 to 80% (mass/mass) and temperatures of 50 to 80°C. The values of D_{suc}, the concentrations of sucrose (50 - 80% mass/mass) and the temperatures (50 - 80°C) have been used in a multiple linear regression to yield equation 1.1

$$\ln D_{suc} = -3289 \frac{1}{T} - 0{,}0386\ C \qquad \text{.....1.1}$$

where D_{suc} is the diffusion coefficient of sucrose, T the temperature in K and C the concentration in grams of sucrose in one hundred grams of solution. The saturation concentration of sucrose for various temperatures is given by Chen and Chou (1995) and equation 1.1 can then be used to calculate the diffusion coefficients of sucrose at saturation. This has been done in Table 1.3.

Table 1.3

Values of D_{suc} at saturation calculated after Heffels (1986) and from the data of Chen and Chou (1995)

Temperature/°C	Conc at saturation/% (kg/100 kg)	$D_{suc}/10^{-6}$ cm²/s
50	72,04	2,35
60	74,02	2,94
70	76,45	3,59
80	78,74	4,31

It is now possible to relate the logarithm of the diffusion coefficient, at saturation, to the reciprocal of the absolute temperature, to obtain the energy of activation of diffusivity, at saturation, E_{DSat}. Then, E_{DSat} is equal to 19 kJ/mol. This calculation has been repeated for a supersaturation of 1,3 a value chosen to represent an upper practical limit for the supersaturation range found in the present work, and the activation energy is now 20 kJ/mol, a value very similar to that at saturation. Activation energies for viscosity were calculated as described in Section 2.5, for similar sucrose concentrations and temperatures, and values of 1 - 11 kJ/mol were obtained.

For the investigation of impurity transfer it is the diffusivities of the selected impurities which are relevant. Again, these diffusivities should be in concentrated sucrose solutions, near to or above saturation, and at the relevant temperatures. It should be noted that the concentration of the impurities is low in the present work and thus conditions are not too dissimilar to those for pure sucrose solutions.

The diffusion coefficients of some non-sucrose species of interest here, have been investigated by Chang and Myerson (1985, 1986). These workers studied the diffusivity of KCl, NaCl, urea, and glycine in aqueous solutions and show that the coefficients decrease with increasing concentration in the supersaturated range. They postulated that this is due to the formation of molecular clusters.

Shoemaker *et al.* (1974) give an experimental method to measure diffusivities in the type of solutions applicable to this work, namely with relatively low concentrations of impurities, high sucrose level and high temperatures. The method cannot, however, be used for sucrose concentrations at saturation and above because of experimental difficulties, particularly the occurrence of crystallisation in the equipment. Some extrapolation will therefore be necessary. It is expected from the work of VanHook (1945) and Gladden and Dole (1953) that the diffusion coefficients will decrease as the sucrose concentration increases.

The experimental method (Shoemaker *et al.*, 1974) used to measure the diffusivity of some of the non-sucrose species used here is described in Section 3.6.6. It involves the use of a porous frit, containing the diffusing species, placed in a bath consisting of an aqueous sucrose solution of high concentration.

Taylor and Wall (1954) used this method and mixtures of sugars and KCl to show that each substance diffuses independently. This is relevant here since K^+, Ca^{2+}, Li^+ and Ni^{2+} are used together. Wall and Wendt (1958) show that the frit method gives a good approximation for the differential diffusion coefficient. The coefficient applies to a concentration which is somewhere in between the initial frit concentration and the final bath one. Work with KCl and $ZnSO_4$ showed that the initial frit concentration makes little difference to the measured value of D. The outside bath has the most influence and since this consists of a concentrated sucrose solution here, the conditions are as close as practically possible to the sucrose crystallisation process. Finally, Wall

et al. (1952) show that there is no bulk flow of solution through the porous frit; that mechanical circulation in the bath, to ensure uniform concentration, does not disturb the solution in the frit, and that a sharp initial concentration boundary is formed.

The frit method was calibrated by using potassium chloride solution, at 25°C. The diffusion coefficient for K^+ at 25°C is 1,96 x 10^{-9} m^2/s (Atkins, 1994). The method was then used to measure the diffusion coefficients of K^+, Li^+, Ca^{2+} and Ni^{2+} at 70°C in concentrated sucrose solutions.

1.1.7 The effect of crystal size

Mantovani *et al.* (1986), Mann (1987), Lionnet (1988; 1995), and Vaccari *et al.* (1991) show that the size of the sucrose crystal influences the crystallisation rate and the colour transfer. Mullin (1993) generally shows that large crystals, and/or fast growth, increase the likelihood of inclusions with experimental evidence from work with hexamine, ammonium perchlorate and terephthalic acid. There is also similar evidence from work with sodium chloride. Generally the larger the crystal the higher the transfer.

Guo and White (1984) show that larger crystals contain more inclusions, perhaps because the bigger crystals are faster growing.

1.1.8 The degree of agitation

Mullin (1993) shows that agitation has a marked impact on the crystal growth, but if the agitation is sufficiently high the effect tends to an asymptotic maximum. In the present work agitation is set at a constant level as described in Section 3.1.

1.2 Models of impurity transfer

Although there are many theories for crystal growth (Mullin, 1993; Garside, 1991; Jansic, 1984; Nyvlt *et al.*, 1985) and a number have been applied to the crystallisation of sucrose (Maurandi, 1982; Heffels *et al.* 1987; Heffels and Jong, 1988; VanHook, 1981; 1973, 1945, 1944; Maurandi

et al. 1984; Mantovani, 1997), there is much less in the literature concerning the transfer of impurities into crystals.

As far as the transfer of impurities into the sucrose crystal is concerned, inclusion of mother-liquor has been mentioned by Mantovani *et al.* in 1985. Saska (1991) and Donovan and Williams (1992) mention the possibility of Langmuir type adsorption isotherms for colour and dextran. VanHook (1997b, 1997c), using X-ray crystallography, shows that raffinose and dextran are not built into the sucrose lattice but are chemisorbed on the surface of the growing crystal.

Guo and White (1984) show that the liquor trapped in inclusions in the crystals is an important source of impurities.

The literature contains more information for crystals other than sucrose. The main ideas involved are partition coefficients, adsorption isotherms, a two-step model and an interfacial breakdown mechanism. These are discussed below.

1.2.1 **Partition coefficients**

Nyvlt (1976) notes that, as a unit operation, crystallisation although a powerful purification process, yields crystals which may not be completely pure. Physical adsorption of impurities, for example, can occur on the growing crystal and this leads to partitioning between the solid and the solution. As the crystals grow, exchange reactions occur on the surface of every new layer. He presents various partition functions, for example the logarithmic partition law

$$\ln \frac{X_o}{X_o - X} = C \ln \frac{Y_o}{Y_o - Y}$$

where X_o and Y_o are the initial concentrations of the impurity in the solution and crystalline species respectively, and X_o-X and Y_o-Y are the concentration differences after a given time. C is a constant; if $C > 1$ then the crystal is enriched with the impurity and if $C < 1$ then the crystal is purified.

The degree of adsorption is influenced by the steric arrangement of the molecules in the impurity, the charge and dipole moment of the impurity and by the electric field at the crystal surface.

VanHook (1997b) elaborates on the importance of the steric and chemical similarities between the impurity and the crystal. If the impurity is similar both chemically and crystallographically, it may be incorporated into the lattice structure of the growing crystal. Its distribution will be uniform in the crystal. Raffinose for example has a combination of chemical and crystallographic characteristics similar to those of sucrose and this causes strong adsorption. Glucose on the other hand does not fit the sucrose molecule well and thus is only weakly adsorbed. As mentioned earlier raffinose molecules are accommodated within the growing sucrose crystal in such a way as not to change the normal spatial dimensions between the sucrose molecules. High temperatures and high concentrations of raffinose favour this chemisorption. Essentially the same conclusions apply to the incorporation of dextran in the sucrose crystal. Glucose and dextran are found in cane sugar, but raffinose is present in beet sugar only.

Myerson (1990) shows that impurities adsorb preferentially on specific crystal faces, an observation well documented for the incorporation of colour into the sucrose crystal (Mantovani *et al.* 1985; Vaccari *et al.*, 1991).

Witcamp *et al.* (1990) and Zumstein *et al.* (1990) have proposed a partition coefficient (P_i) defined as follows:

$$P_i = \frac{\text{(conc. impurity/conc. reference) in crystal}}{\text{(conc. impurity/conc. reference) in solution}}$$

.....1.2

Ideal behaviour occurs when P_i is constant over a wide range of concentration of the impurity in the solution. In this case, the impurity will tend to substitute for the crystalline species, a process called isomorphous substitution. P_i will be affected by other factors such as the rate of crystallisation, the temperature and the crystal size. These must therefore be kept constant.

Zumstein *et al.* (1990) give the following results for the crystallisation of L-isoleucine in the

presence of L-leucine, L-valine and L-α-amino butyric acid as impurities. Under acidic crystallisation conditions all three impurities behaved ideally, as far as P_i is concerned. Plots of the ratio of concentrations of the impurity to L-isoleucine in the crystal versus that in the solution were linear and went through the origin. $P_{L\text{-leucine}}$ and $P_{L\text{-valine}}$ were found to be 0,2 and 0,1. When the crystallisation process involves cooling, the results were different. The relationships between the ratio of concentration in the crystal and that in the solution were still linear but the lines did not go through the origin and the behaviour is thus non-ideal in terms of P_i.

Witcamp *et al.* (1990) worked with calcium sulphates, the impurities being phosphate and cadmium ions. The phosphate and cadmium intakes in $CaSO_4.2H_2O$ behaved ideally, with P_{PO4} and P_{Cd} both being equal to 0,002 and the range of concentration in the solution covering a factor of four. The results were similar with $CaSO_4.1/2H_2O$, except that P_{PO4} and P_{Cd} were now about 0,0002, or ten times smaller. Finally, these authors show that the partition coefficient for several metal ions in $CaSO_4$ is a function of the ionic radius of the metal ion. This is shown in Figure 1.1.

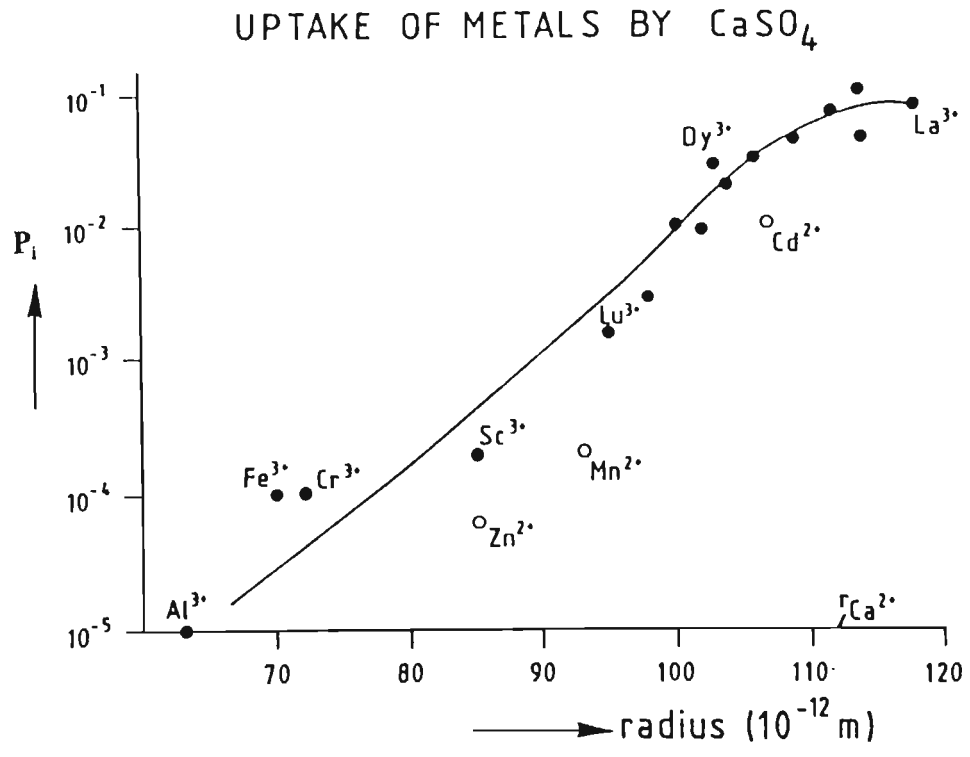

Figure 1.1 **Partition coefficient in $CaSO_4$ as a function of metal ion ionic radius (Witcamp *et al.*, 1990).**

The concept of partition coefficients and the approach presented by Zunstien *et al.* (1990) and by Witcamp *et al.* (1990) have not been applied to the crystallisation of sucrose. If this can be done successfully, the results may help in understanding the mechanisms of impurity transfer in the sucrose crystal.

1.2.2 **Adsorption isotherms**

Adsorption from solution is well described in Adamson (1976) and in Atkins (1994). The simplest or ideal isotherm, the Langmuir isotherm, is based on three assumptions:

- adsorption cannot proceed beyond a monolayer coverage
- all sites are equivalent and the surface is uniform
- the ability of a molecule to adsorb at a given site is independent of the occupation of neighbouring sites.

The independence and equivalence of all adsorption sites is often the one assumption which is violated. The Freundlich isotherm assumes that the adsorption enthalpy changes logarithmically with the concentration. Adamson (1976) states that the Freundlich isotherm suits adsorption from solution. Finally the Brunauer, Emmett and Teller (BET) isotherm deals with multilayer adsorption.

Different isotherms represent experimental behaviour more or less well, often only over restricted ranges of concentrations, and they remain empirical. Nevertheless, if the parameters of a given isotherm fit the data and are known, they can characterise the process. As mentioned previously, some impurities have been shown to adsorb on the sucrose crystal surface; it is thus necessary to investigate this aspect.

1.2.3 **Two-step model for crystallisation**

Mullin (1993), Karpinski (1980), Maurandi (1982) and Smythe (1971) treat crystallisation as a two-step process; the first step involves the transport of the molecule to the crystal surface, while the second step involves its incorporation into the crystal lattice.

Mullin (1993) discusses the process in detail and depicts it diagramatically as shown here in Figure 1.2, where C, C_i and C* are concentrations in the solution, at the crystal/solution interface and at saturation, respectively.

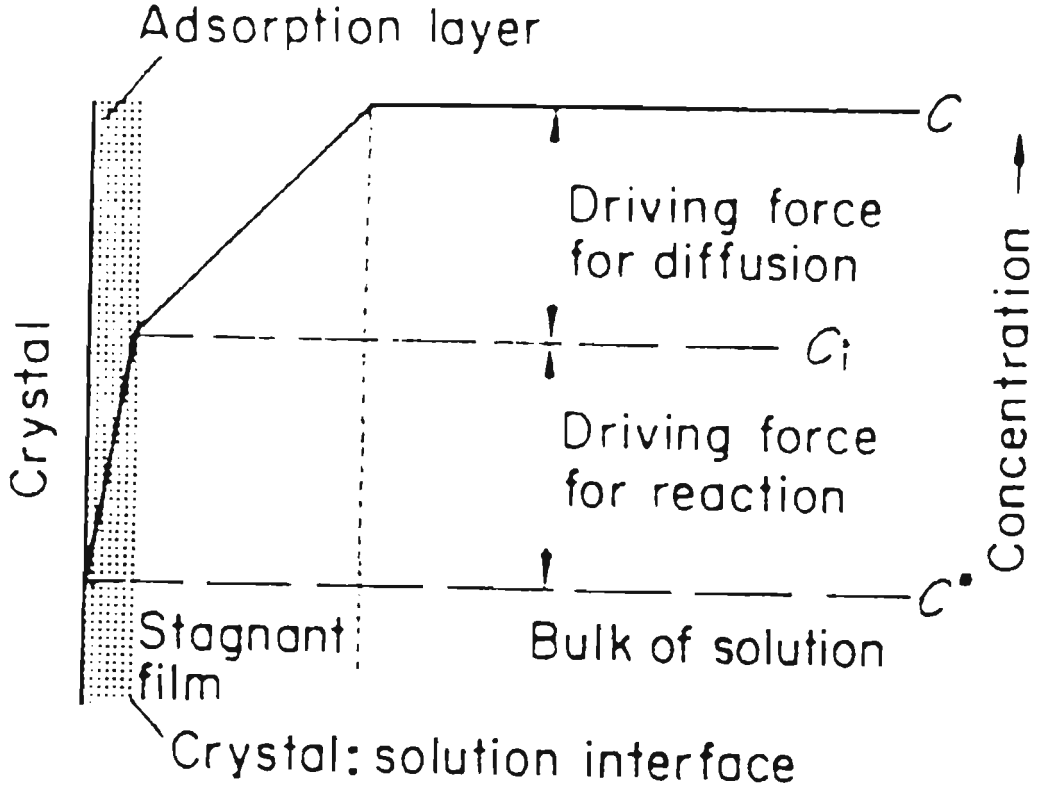

Figure 1.2 Concentration driving forces in crystallisation from solution (Mullin, 1993).

Mullin notes that this is a pictorial representation; in reality the process must be much more complex. He empirically derives equations 1.3, 1.4 and 1.5, for a mass transfer rate, dm/dt, during crystallisation.

$$\frac{dm}{dt} = k_d A(C - C_i) \qquad \text{.....1.3}$$

$$\frac{dm}{dt} = k_r A(C_i - C^*) \qquad \text{.....1.4}$$

$$\frac{dm}{dt} = K_G A(C - C^*)^g \qquad \text{.....1.5}$$

where k_d is a coefficient of mass transfer by diffusion, k_r a rate constant for the integration process, K_G an overall crystal growth coefficient and g an exponent by which the concentration difference (C - C*) must be raised for the data to fit the equation. This exponent has no fundamental significance. A is the surface area of the crystals, while m is their mass.

The situation is however complicated by the fact that the assumption of a first-order surface reaction is highly questionable. Thus Mullin suggests raising (C_i - C*) to a power, r. Solution of the equations now becomes impossible analytically except for simple cases when r = 1 or r = 2, and generally the relationships between the crystallisation rate, K_G, k_d and k_r remain obscure.

Sobczak (1990) has however proposed an integral method which allows reasonable values for k_d and k_r to be estimated.

Smythe (1990) shows that a value of 2 for r results in good fits for the sucrose crystallisation process, with pure sucrose, well stirred conditions and within a temperature range of 20 to 70°C.

Maurandi (1982) shows that both steps are active at intermediate temperatures but that transport is rate limiting at high temperatures. Similar conclusions are reached by Heffels and Jong (1988).

A point made by Garside (1991) needs to be kept in mind. He notes that this model assumes that the process takes place at steady state. Under those conditions there is no accumulation of solute at any point in the concentration field and so the rates of the two steps are always the same. It is incorrect to refer to one as being faster than the other; the concentration at the surface takes up a value so that the rates of the two steps are equal. One of the two steps is rate limiting in that it cannot proceed faster and thus causes the other to slow down so as to preserve the steady state.

1.2.4 **Interfacial breakdown**

Vaccari (1996) points out the confusion which exists with respect to the mechanisms of impurity, in particular colour, transfer. Thus some authors state that it is the physical inclusion of mother-liquor which is important while others mention preferential adsorptions of impurities and accommodation into the crystal lattice. Vaccari (1996) is the first worker to suggest an interfacial breakdown process at the crystal/solution interface for the incorporation of impurities in the sucrose crystal.

Mullin (1976) and Nyvlt (1982) discuss the "constitutional supersaturation" mechanism for impurity capture. When a crystal grows in the presence of impurities, the impurities are rejected at the solid/liquid interface. If the impurities cannot diffuse away from the surface fast enough, the impurity concentrations near the crystal surface will be higher than in the bulk of the solution, somewhat further away. This affects the equilibrium solubility in the boundary layer and just outside it. The supersaturation at or in the layer will be lower than that in the bulk and the driving force for crystallisation is thus higher a short distance from the crystal face, towards the bulk. This results in interfacial instability. Mullin (1976) shows that this process is similar to the "constitutional supercooling" well known by metallurgists. At high constitutional supercooling the interface breaks down and dendritic branching occurs, for example in the casting of metals.

Burton *et al.* (1953), Edie and Kirwan (1973) and Ozum and Kirwan (1976) present mathematical treatments for constitutional supercooling and constitutional supersaturation. Ozum and Kirwan (1976) show that the mechanism applies to aluminium/copper systems in melt crystallisation, to various organic crystallisation systems, and to the freezing of water with sodium chloride or sucrose present as impurities. They show the following main points:

- a critical minimum crystallisation velocity exists above which the interfacial breakdown takes place

- stirring is important - at high levels of agitation the breakdown is reduced; conversely at high growth rates or low agitation levels the level of impurity in the crystal is high.

These authors have developed a mathematical solution for the boundary layer model, for a broken, trapping interface, namely

$$K_e = \frac{K_a}{K_a + (1 - K_a)e^{-\frac{V\delta}{D}}} \qquad \text{.....1.6}$$

where

$$K_e = \frac{\text{conc. of impurity in crystal}}{\text{conc. of impurity in liquid bulk}},$$

$$K_a = \frac{\text{conc. of impurity in crystal}}{\text{conc. of impurity in interface}},$$

V is the linear growth velocity (in m/s), δ is the boundary layer thickness (in m) and D is the diffusion coefficient of the impurity (in m^2/s).

Rearrangement of 1.6 gives

$$\ln\left(\frac{1 - K_e}{K_e}\right) = \ln\left(\frac{1 - K_a}{K_a}\right) - \frac{\delta}{D} V$$

and a plot of V against $\ln\left(\frac{1 - K_e}{K_e}\right)$ should be a straight line with a slope of $-\frac{\delta}{D}$ and an intercept equal to $\ln\left(\frac{1 - K_a}{K_a}\right)$.

Since K_e and V can be measured, K_a and the ratio δ/D can be calculated for transfers fitting this model. The literature provides values for the boundary layer thickness for sucrose. Maurandi and Mantovani (1981) give a range of $1{,}8 \times 10^{-5}$ to $1{,}1 \times 10^{-4}$ m; VanHook (1973) quotes 1×10^{-3} to 1×10^{-4} m and Mullin (1993) gives 1×10^{-5} to 2×10^{-4} m.

1.3 **Aims and limitation of this work**

The literature survey was used as a guide in setting the following three main objectives for this work:

- To propose a parameter to quantify the rate at which selected impurities are incorporated into the sucrose crystal. Establish the validity and usefulness of the parameter and investigate the factors that influence it.

- To investigate mechanisms by which impurity transfer into the sucrose crystal could take place.

- To obtain results which must apply to the crystallisation of sucrose under industrial conditions.

The third objective required that the experimental work be done at the pilot plant rather than the laboratory scale, because of the difficulties in representing industrial conditions, for example the large number of crystals, the crystal size distribution, the degree of agitation, etc., at the laboratory scale.

The selection of the impurities to be studied in the present work needed careful consideration. From a sugar quality point of view colour, starch, potassium and calcium are important since they are present in sugar cane liquors and are found in commercial sugar crystals. These species were also selected by Guo and White (1984). Lithium has been used as a tracer ion in sugar work because it is not present in cane (Morel du Boil, 1980: Guo and White, 1984); it was included as a second monovalent ion. Nickel was included for a similar reason, being divalent like calcium. Finally, dyes have been mentioned (Mantovani *et al.*, 1986) in connection with colour transfer work with sucrose crystals and it was decided to include methylene blue, acid blue 25 and methyl blue. These three particular dyes were chosen because some have been used before (Mantovani *et al.*, 1986) and because they have different molar masses, namely 374, 416 and 800 g/mol, respectively. The selection of these different chemical species also makes the results more general.

There is little to no information in the literature regarding the existence of a parameter describing the rate at which impurities are incorporated into the sucrose crystal. The availability of such a parameter and an investigation of the factors that affect it would help in understanding the incorporation of impurities into the sucrose crystal.

Again, there is little information on mechanisms of impurity transfer during the crystallisation of sucrose. This has caused the approach taken in the present work to be somewhat wider and less fundamental than could be desired. The general procedure has been to investigate many relevant processes, for example adsorption, partition coefficients, transport phenomena such as viscosity and diffusivity, and activation energies, in an attempt to throw light on possible mechanisms of impurity transfer. It is not expected that clear, fundamental results will be produced because of

the complexity of the transfer process and because many basic parameters cannot be changed independently of each other. Thus, changing the temperature changes solubilities, viscosities, diffusion coefficients, equilibrium constants, etc. These difficulties must be responsible for the dearth of information in the literature, particularly for the crystallisation of sucrose under industrial conditions. The work is not made easier by the analytical problems caused by the very low levels of the impurities, in highly concentrated sucrose solutions. The concentrations of sucrose in the liquors used vary from about 65 to 80% (mass/mass); the concentrations of the impurities on the other hand, vary from a few milligrams to a few grams per kg of solution. These however do not necessarily result in analytical difficulties. It is the analysis of the sucrose crystal itself which needs great care. Here the impurities are at concentrations of a few mg/kg, but these low levels have an important impact on the quality of the crystal.

CHAPTER 2

THEORETICAL CONSIDERATIONS

The literature survey in Chapter 1 shows that the main factors affecting the transfer of impurities into the crystal are the sucrose crystallisation rate, the concentration and type of impurity, characteristics of the crystal, and physical factors such as temperature, viscosity, diffusivity, etc. In this chapter, the theory underlying the quantification of the effects of these factors will be developed. The first step in these calculations is to obtain mass balances in and out of the crystalliser.

2.1 Material balances

Material balances in and out of the crystalliser described in Chapter 3 are required to yield the mass of crystals, mother-liquor, massecuite, etc., which cannot be obtained directly. The mass of the crystals is needed in order to calculate a simple mass based crystallisation rate for sucrose, which is subsequently used in the calculation of the rate at which impurities are transferred into the crystal. The system consists of a batch crystalliser with continuous feed and condensate withdrawal. Both are linear, in terms of mass, with time.

2.1.1 Mass balance

The following masses are determined by weighing for each run:

Mass of feed liquor,	M_f
Mass of condensate water,	M_{cw}
Mass of seed,	M_s
Mass of wash liquor,	M_{wl}

At any time the mass of massecuite, M_{mc}, is then given by equation 2.1:

$$M_{mc} = M_f + M_s + M_{wl} - M_{cw}$$

..... 2.1

For most runs, seed slurry (2 cm^3) is used for seeding and M_s can be taken as 0 since the mass of slurry is negligibly small when compared to the mass of massecuite. The wash liquid is the feed itself (as done in industrial crystallisers, to save energy) and M_{wl} is included in M_f. Then

$$M_{mc} = M_f - M_{cw}$$

Massecuite consists of mother-liquor, M_m, and of sucrose crystals, M_c, thus

$$M_{mc} = M_m + M_c$$

..... 2.2

Another equation is still needed to solve for M_m and M_c. This can be obtained through the brix, sucrose or colour balances.

2.1.2 **Brix balance**

Since the sucrose crystal consists of sucrose plus very small amounts of impurities and water it can be assumed that the crystal has a brix of 100%. B_m and B_{mc} are the brix (%) contents of the mother-liquor and of the massecuite, respectively, and are obtained by analysis. Then

$$M_{mc}\, B_{mc} = M_m\, B_m + M_c\, 100$$

..... 2.3

By eliminating the mass of crystal from equations 2.2 and 2.3:

$$M_m \left(\frac{B_m}{100} - 1 \right) = M_{mc} \left(\frac{B_{mc}}{100} - 1 \right)$$

one obtains the mass of mother-liquor:

$$M_m = \frac{M_{mc} \left(\frac{B_{mc}}{100} - 1 \right)}{\left(\frac{B_m}{100} - 1 \right)}$$

.....2.4

This together with the mass of massecuite can then be used to calculate the mass of crystal at any time from equation 2.2.

2.1.3 **Sucrose balance**

A sucrose balance is obtained in the same way as the brix balance, but with P_m and P_{mc} (pol % mother-liquor and pol % massecuite) replacing B_m and B_{mc}. Again the crystal is taken as pure sucrose, namely $P_c = 100\,\%$. Since the pol analysis is independent of the brix analysis, this balance can be used as a check.

2.1.4 **Colour balance**

Colour is expressed on brix in the sugar industry and it is treated as if it was a single substance; in reality it is mixture of many diverse compounds such as caramels, phenolics and pigments. C_{mc}, C_c and C_m are the massecuite, crystal and mother-liquor colours, respectively, which are determined by analysis.

Equation 2.5 represents a colour balance:

$$C_{mc} \frac{B_{mc}}{100} M_{mc} = C_c \frac{B_c}{100} M_c + C_m \frac{B_m}{100} M_m$$

.....2.5

As in Section 2.1.2, $B_c = 100$. Then:

$$C_{mc} \frac{B_{mc}}{100} M_{mc} = C_c M_c + C_m \frac{B_m}{100} M_m$$

.....2.6

But $M_{mc} = M_m + M_c$

and

$$C_{mc} \frac{B_{mc}}{100} M_{mc} = C_c (M_{mc} - M_m) + C_m \frac{B_m}{100} M_m$$

$$M_m \left(C_m \frac{B_m}{100} - C_c \right) = C_{mc} \frac{B_{mc}}{100} M_{mc} - C_c M_{mc}$$

Thus

$$M_m = \frac{M_{mc}\left(\frac{C_{mc}\,B_{mc}}{100} - C_c\right)}{\left(\frac{C_m\,B_m}{100} - C_c\right)}$$

$$M_m = \frac{M_{mc}\left(\frac{C_{mc}\,B_{mc} - 100\,C_c}{100}\right)}{\left(\frac{C_m\,B_m - 100\,C_c}{100}\right)}$$

and

$$M_m = \frac{M_{mc}\left(1 - \frac{C_{mc}B_{mc}}{C_c 100}\right)}{1 - \frac{C_m B_m}{C_c 100}}$$

.....2.7

Again, M_c can be obtained from equation 2.2. Colour is not a conserved quantity, but the change has been measured to be less than 5% on mass. Thus the colour balance will only be used as a check for very large errors.

2.2 Crystallisation rate of sucrose

The sucrose crystallisation rate is known to have an effect on the transfer of impurities into the crystal (Donovan and Williams, 1992; Lionnet, 1988; Vaccari, 1996). A number of definitions

of crystallisation rates have been proposed in the literature, the one generally considered the most useful (Bennett and Fentiman, 1969; Bubnik and Kadlec, 1992; Day, 1971; Kraus and Nyvlt, 1994.) being a mass growth rate, G, involving the mass of crystal produced per unit time and per unit crystal surface area. In order to determine G, in kg/s/m^2, a knowledge of the crystal length and width, the crystal mass, and crystal shape factors, as discussed below, is required.

2.2.1 **Sucrose crystal shape factors**

Crystal dimensions have usually been obtained by sieving the sample of crystals into various size fractions (Bubnik and Kadlec, 1992; Bennett and Fentiman, 1969; Broadfoot and Bartholomew, 1995; Guimaraes *et al.*, 1995). It will be shown in Section 3.4.2, that the image analysis system used in this work to obtain crystal dimensions has many advantages over sieving. The approach taken here is based on that of many workers (Bubnik and Kadlec, 1992; Kraus and Nyvlt, 1994) but uses crystal dimensions obtained from the image analysis procedure. This approach assumes that all the crystals are of the same size. This is a simplification which has been used by many workers (Bubnik and Kadlec, 1992; Grimsey and Herrington, 1994; Guimaraes *et al.*, 1995; Mullin, 1993; Van Hook, 1973; etc.) and found to be adequate and to yield useful results.

For one crystal, the image analysis yields two linear dimensions, the crystal length, L, along the b-axis and the width, W, along the c-axis as shown in Figure 2.1. A characteristic crystal linear dimension (Bubnik and Kadlec, 1992,), L_c, as defined by equation 2.8 is needed to calculate a linear crystal growth rate and to calculate a crystal mass growth rate (see Section 2.2.2).

$$L_c = (L^2 W)^{1/3} \qquad \text{.....2.8}$$

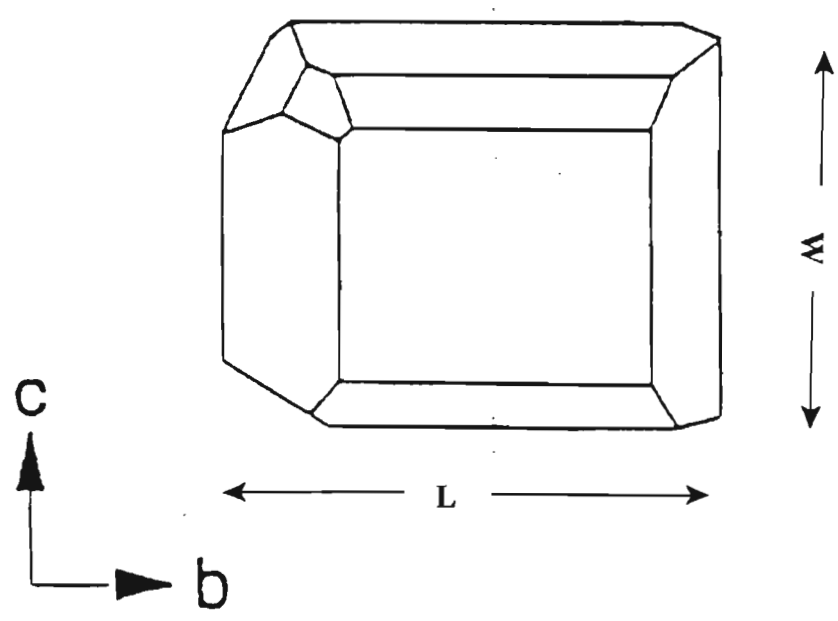

Figure 2.1:The b and c axes of the sucrose crystal.

A volume shape factor, α, defined by equation 2.9 is needed to calculate both the sucrose mass growth rate and a rate of impurity transfer (see Section 2.3).

$$\alpha = \frac{m}{\rho L^2 W} \qquad \text{.....2.9}$$

where m is the mass of one crystal and ρ the density of sucrose.

A surface area shape factor, β, defined by equation 2.10, is needed for the mass growth rate and the rate of impurity transfer

$$a = ß\ L_c^2$$

.....2.10

where a is the surface area of one crystal.

From equations 2.8 and 2.10:

$$a = ß\ (L^2\ W)^{2/3}$$

.....2.11

From equations 2.9 and 2.11:

$$a = ß\ (\frac{m}{\alpha\rho})^{2/3}$$

.....2.12

A crystal shape factor, F, is defined by equation 2.13:

$$a = Fm^{2/3}$$

.....2.13

From equations 2.12 and 2.13:

$$ß\ (\frac{m}{\alpha\rho})^{2/3} = Fm^{2/3}$$

and

$$F = \frac{ß}{(\alpha\rho)^{2/3}}$$

.....2.14

Equations 2.8 to 2.14 apply to one crystal. For a mass M_c of N crystals of average size L and W, needed for the derivation of the rate of impurity transfer,

$$N = \frac{M_c}{m} = \frac{M_c}{\alpha\rho L^2 W}$$

.....2.15

The surface area, A_c, of the N crystals is now

$$A_c = Na = \frac{M_c}{\alpha\rho L^2 W} \times ß\ (L^2 W)^{2/3}$$

and

$$A_c = \frac{M_c \beta}{\alpha\rho\ (L^2 W)^{1/3}}$$

.....2.16

The actual values of α, F and ß, to be used in this work were determined as follows.
The shape factor, α, is defined by equation 2.9

$$\alpha = \frac{m}{\rho L^2 W}$$

Eighty to 100 crystals, produced from different runs in the pilot crystalliser, were divided into eight groups, based on size. The average length (L) and width (W) of each group was determined as will be described in Section 3.4.2. The average mass was then obtained by weighing each group consisting of a number of crystals and dividing the total mass by the number of crystals in the group. The results obtained are shown in Table 2.1.

Table 2.1

Data for the calculation of the volume shape factor, α

Number of crystals	Average for one crystal		
	Mass/kg	L/μm	W/μm
10	$7{,}0 \times 10^{-9}$	212	144
10	$8{,}0 \times 10^{-9}$	231	157
10	$5{,}9 \times 10^{-8}$	554	340
10	$7{,}0 \times 10^{-8}$	566	371
10	$1{,}50 \times 10^{-7}$	705	450
10	$1{,}63 \times 10^{-7}$	801	486
10	$2{,}30 \times 10^{-7}$	836	550
10	$2{,}72 \times 10^{-7}$	960	601

A straight line was fitted by least squares linear regression to obtain

$$m = 539{,}2\ L^2\ W$$

for eight sets of observations with an r^2 value of 0,969, as shown in Figure 2.2. Then,

$$\alpha = 539{,}2/\rho$$

which gives a value of $0{,}34 \pm 0{,}03$ ($t_{0{,}025;6} = 2{,}45$. Standard error of coefficient = 22,3) for α since $\rho = 1587$ kg/m^3 for sucrose (Bubnik and Kadlec, 1992). These authors have reviewed the work on the sucrose crystal shape factors and quote a value of 0,31 for crystals from beet sugar and a sizing technique similar to that used here. This compares well to the value obtained in the present work, but with sizing by sieving Bubnik and Kadlec obtained a value of 0,75 for α. The different

value obtained with sieving is probably due to the fact that the sucrose crystal is not square (see Figure 2.1). Sieving thus yields a characteristic dimension which is different to L_c.

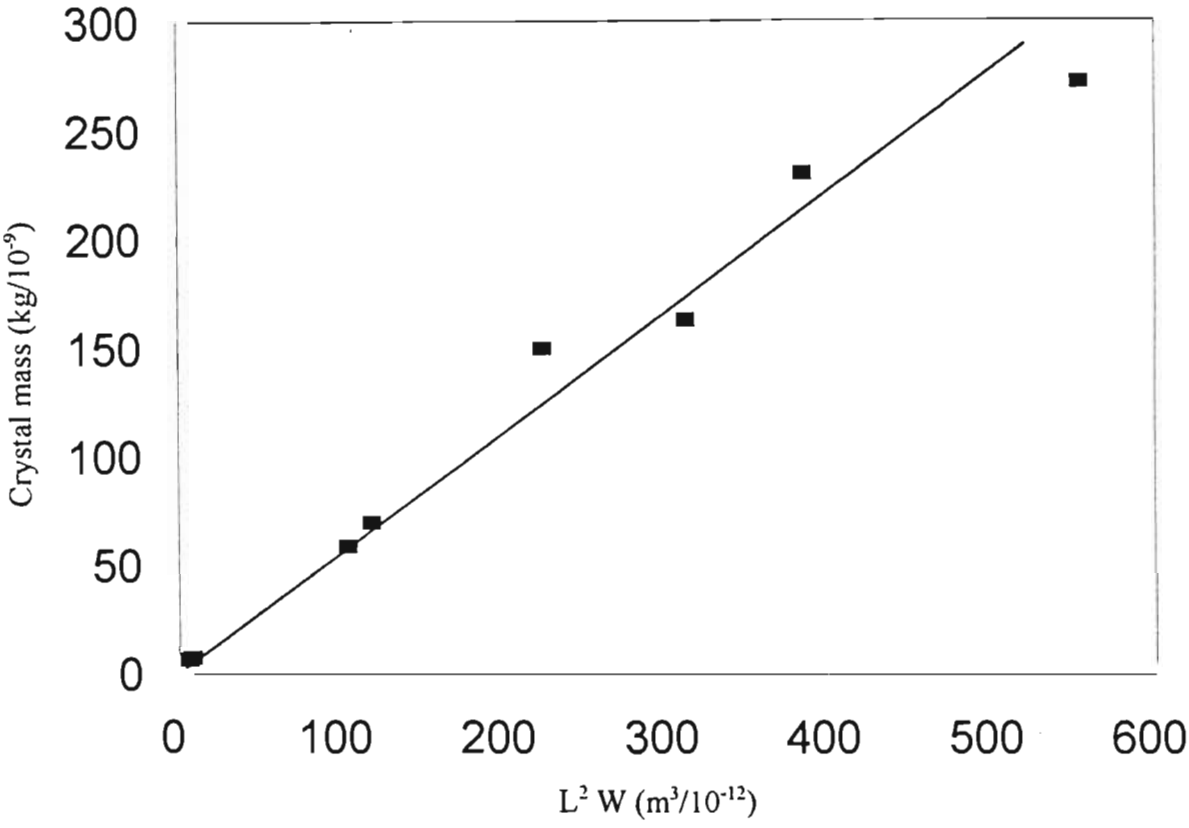

Figure 2.2:The relation between crystal mass and L^2W.

The values of the two other interrelated shape factors, F and ß, are necessary for the calculation of the sucrose growth rate and the impurity transfer rate. The crystal shape factor F, is a function of the shape of crystal. Bubnik and Kadlec (1992) report that F varies between 3,92 and 4,90 $mm^2/mg^{-2/3}$, averaging 4,47, for sucrose crystals. Bennett and Fentiman (1967) give values of 4,12 ± 0,05 and 4,55 ± 0,12 $mm^2/mg^{-2/3}$ and state that F is 4,41 for a cubic shape, 7,19 for a tetrahedron and 3,49 for a sphere. In this work the average value of 4,47 $mm^2/mg^{-2/3}$ will be used as recommended by Bubnik and Kadlec.

Finally, ß, the surface area shape factor, given by equation 2.10, can now be obtained from

equation 2.14

$$ß = F(\alpha\rho)^{2/3}$$

and with F = 0,0447 $m^2/kg^{-2/3}$, α = 0,34 and ρ = 1587 $kg/m^{-2/3}$, ß is equal to 2,96.

2.2.2 **Sucrose mass growth rate**

The sucrose mass growth rate, G, will now be derived following an approach proposed by Bennett and Fentiman (1969) and Bubnik and Kadlec (1992).

A linear crystal growth rate, l_g, is defined by equation 2.17:

$$l_g = \frac{dL_c}{dt}$$

.....2.17

From equation 2.9

$$m = \alpha\rho L_c^3$$

and thus

$$\frac{dm}{dt} = 3\alpha\rho L_c^2 \, dL_c/dt$$

.....2.18

A mass growth rate, G, is now defined by equation 2.19:

$$G = \frac{dm}{dt}\frac{1}{a}$$

.....2.19

From equation 2.10

$$a = \beta L_c^2$$

From equations 2.10, 2.17 and 2.19:

$$G = 3\alpha\rho L_c^2 \frac{dL_c}{dt} \frac{1}{\beta L_c^2}$$

which simplifies to

$$G = \frac{3\alpha\rho}{\beta} l_g$$

.....2.20

Equation 2.20 will be used throughout this work to quantify the rate at which sucrose is being crystallised. G will therefore be calculated using the following quantities:

α, the volume shape factor, which has been found to be equal to 0,34 (see Section 2.2.1);

ρ, the density of sucrose which is equal to 1587 kg/m^3 (Bubnik and Kadlec, 1992);

β, the surface area shape factor, which is equal to 2,96 (see Section 2.2.1);

l_g, the linear crystal growth rate, which is calculated by dividing the crystal characteristic linear dimension, L_c (in m), by the crystallisation time, t (in s). The value of L_c for the seed (<5 μm, see Section 3.3) is assumed to be negligibly small in comparison to that of the final crystal.

2.3 Rate of impurity transfer

There is no clear information in the literature about the definition of the rate at which impurities are incorporated into the sucrose crystal. A simple rate of impurity transfer, based on the mass of impurities incorporated into the sucrose crystal, per unit time and per unit crystal surface area, is proposed.

This impurity transfer rate, R_i, is defined by equation 2.21

$$R_i = \frac{\text{Mass of impurity in crystals}}{\text{Crystallisation time x Total surface area of crystals}}$$

.....2.21

The mass of the impurity in the crystals is the product of the mass of crystals (M_c, kg) and the concentration of the impurity in the crystal (X_i, kg/kg crystal), and the time is again the crystallisation time in seconds. Equation 2.21 deals with the total number of crystals and the surface area is therefore that of the N crystals, given by equation 2.16. Then

$$R_i = \frac{M_c X_i}{t\frac{M_c \beta}{\alpha \rho L_c}} = \frac{\alpha \rho L_c X_i}{t \beta}$$

.....2.21

The sucrose mass growth rate, G, is an instantaneous rate whereas R_i is an average between time 0 and t.

The rate R_i, (kg/s/m^2) given by equation 2.21 and which applies to each impurity, will be used throughout this work to quantify the rate at which the selected non-sucrose species are incorporated into the sucrose crystal. R_i will be calculated by using equation 2.21. The quantities

α, ρ, L_c, β and t are all available (see Section 2.2.2) while X_i is obtained by chemical analysis. The effect of temperature on both G and R_i will now be discussed.

2.4 The Arrhenius model for the effect of temperature

An empirical observation is that many processes have rate constants that follow the Arrhenius equation:

$$k = A_{pf}\, e^{-Ea/RT}$$

.....2.22

where k is the rate constant, E_a the activation energy, R the gas constant, T the temperature and A_{Pf} the pre-exponential or frequency factor. Equation 2.22 can also be expressed in the form:

$$\ln k = \ln A_{pf} - \frac{E_a}{RT}$$

The Arrhenius parameters, A_{pf} and E_a, can be regarded as empirical quantities that allow the investigation of the variations of rate constants with temperature. E_a is the minimum energy that reactants must have to form products and A_{pf} is a measure of the rate at which collisions or encounters occur, irrespective of their energies.

A plot of ln k versus 1/T, for processes following the Arrhenius equation, gives a straight line of intercept ln A_{pf} and slope $-E_a/R$.

If only two sets of measurements are available, it can easily be shown that

$$E_a = R \left(\ln \frac{k_2}{k_1} \right) \frac{T_1 T_2}{T_2 - T_1}$$

.....2.23

In this case it is assumed that E_a is constant over the temperature range T_1 to T_2.

If the activation energy E_a is not constant with temperature, then a plot of ln k versus 1/T shows curvature. The slope at any point of the curve represents an activation energy at that temperature.

Activation energies can also be defined for processes such as viscosity and diffusivity through an approach similar to that for equation 2.22. This yields equations 2.24 and 2.25:

$$\eta = A_{fv}\, e^{Ev/RT} \qquad \text{.....2.24}$$

$$D = A_{fd}\, e^{-Ed/RT} \qquad \text{.....2.25}$$

and plots of ln η or ln D versus 1/T should allow E_v and E_d to be estimated.

Mullin (1993) notes that typical diffusion controlled processes give activation energies of 10-20 kJ/mol, while processes where the limiting step is a surface integration one show values of 40-60 kJ/mol. Since the rate of integration increases faster with temperature than diffusion does, the rate of crystal growth could be limited by diffusion at high temperatures but by integration at low temperatures. At intermediate temperatures both processes are involved and the Arrhenius plot should show curvature.

This approach will be used to investigate the effect of temperature on G and, more interestingly, on the R_i values for the various non-sucrose species, for which there is no documentation in the literature.

2.5 Viscosity of the mother-liquor

Honig (1959) shows that viscosity plays an important role in the crystallisation of sucrose, which implies that some diffusional mechanism is involved. Two points are relevant with respect to the effect of viscosity on impurity transfer during the crystallisation of sucrose:

- The region of interest is the boundary layer, between the bulk of the solution and the crystal itself.

- Sucrose concentrations are in the supersaturated range, at the various temperatures, during crystallisation.

The investigation of the effects of temperature on viscosity must therefore deal with sucrose solutions at saturation and above.

The solubility of sucrose in water, and the viscosity of sucrose solutions at various temperatures and sucrose concentrations, are available in Chen and Chou (1993). These viscosities can also be calculated from a formula given by Peacock (1995), namely:

$$\log_{10} \eta = 22{,}46\ Z - 0{,}114 + \frac{(30 - T)}{(91 + T)} (1{,}1 + 43{,}1\ Z^{1{,}25}) \qquad \text{.....2.26}$$

where $Z = \dfrac{\text{sucrose conc. in \% by mass}}{1900 - 18 \times \text{sucrose conc. in \% by mass}}$, T is the temperature in °C

and Z, 1900, 18 are empirical quantities yielding the best fit.

The data required to obtain the viscosity of sucrose saturated solutions over a range of temperatures are shown in Table 2.2.

Table 2.2

Viscosities of saturated sucrose solutions over a range of temperature

Temperature /°C	Solubility /% by mass	Viscosity /Pa s	
		Chen and Chou (1993)	Calculated (Peacock, 1995)
40	70,01	1,14	1,13
45	71,00	1,05	1,03
50	72,04	0,96	0,96
55	73,10	0,92	0,91
60	74,20	0,88	0,88
65	75,32	0,85	0,85
70	76,45	Not available	0,84
75	77,59	Not available	0,83

It can be seen that the viscosities obtained from Chen and Chou (1993) and those calculated by the formula agree well. Equation 2.24 can now be used to obtain E_v for sucrose saturated solutions at the selected temperatures. A plot of ln η versus 1/T is shown in Figure 2.3.

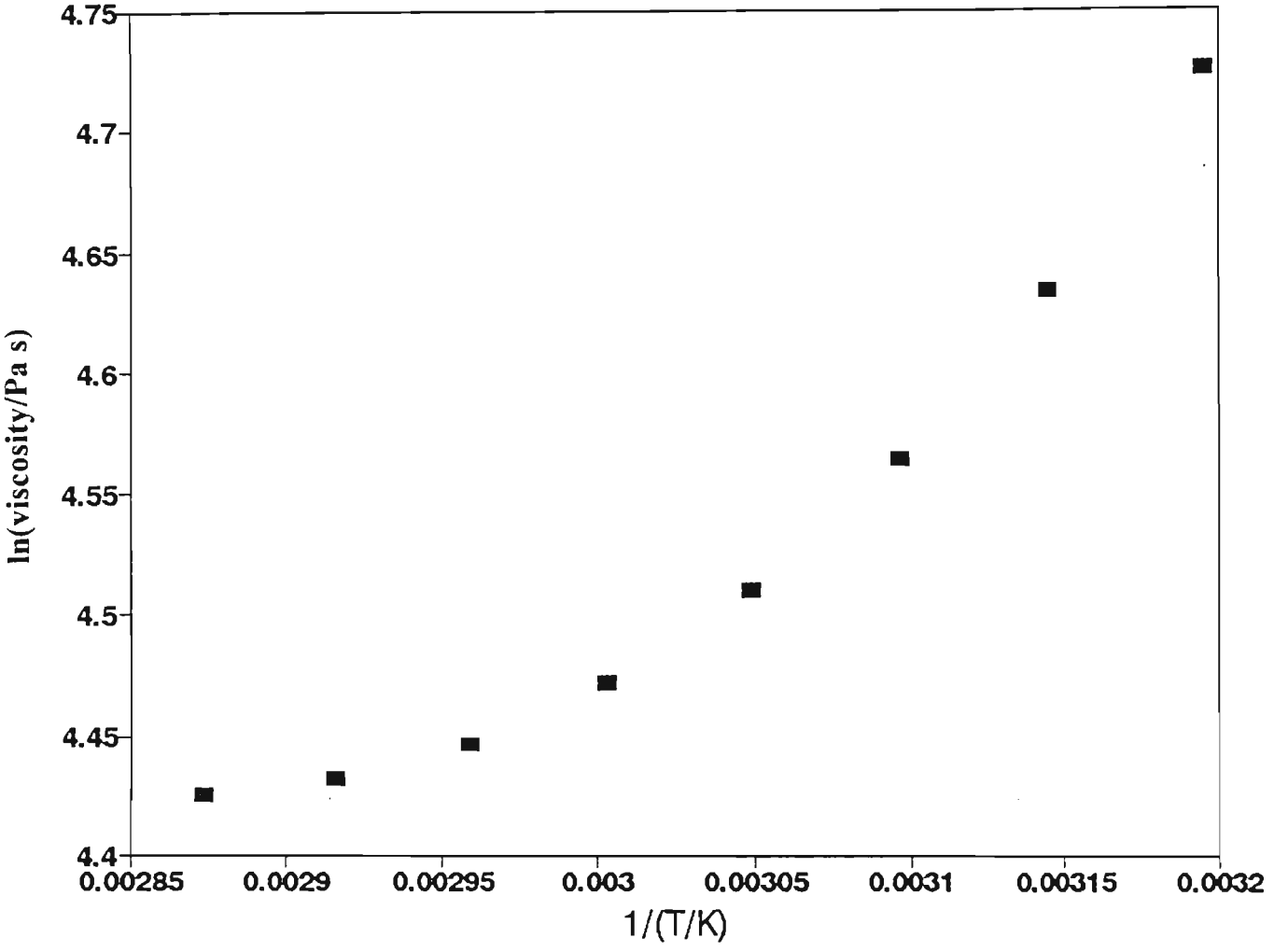

Figure 2.3: **A plot for the determination of the activation energy of viscosity for saturated sucrose solutions.**

If it is assumed that the plot is linear over several 5°C ranges equation 2.23 can be used to calculate E_v at set temperatures. The results are shown in Table 2.3.

Table 2.3

Values of E_v at selected temperatures, for saturated sucrose solutions

Temperature /°C	E_v /kJ/mol
45 - 50	12
50 - 55	9,8
55 - 60	6,7
60 - 65	4,8
65 - 70	2,7
70 - 75	1,9

The procedure has been repeated for a supersaturation of 1,3, where the supersaturation is defined by the formula

$$\left(\frac{\text{actual sucrose concentration in grams/100 g water}}{\text{saturation sucrose concentration in grams/100 g water}} \right).$$

The value of 1,3 has been chosen to represent an upper practical limit for the supersaturations found in this work. The activation energies at saturation and at a supersaturation of 1,3 are plotted against temperature in Figure 2.4. Since the range of temperatures involved in this project will be 60-80°C, this corresponds to E_v values between 11 and 1 kJ/mol.

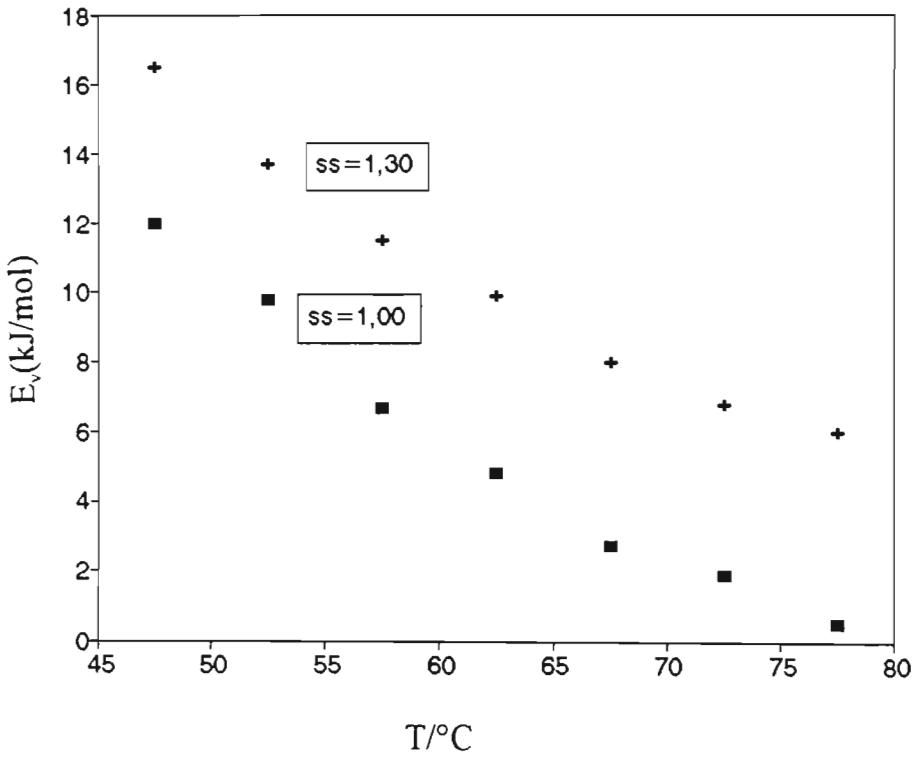

Figure 2.4: **The variation of E_v with temperature for pure sucrose solutions at a constant saturation of 1,00 and a constant supersaturation of 1,30.**

2.6 Diffusivity of sucrose and of the contaminants

Diffusivity has been discussed in Section 1.1.2.5 and for the investigation of impurity transfer it is the diffusivities of the selected impurities which are relevant. Again, these diffusivities should be in concentrated sucrose solutions, near to or above saturation, and at the relevant temperatures. It should be noted that the concentrations of the non-sucrose species (for example colour, K^+, Li^+, etc.) should be low because of the relatively high purities of the liquors used here.

The theory behind a method for the determination of these diffusivities follows an approach suggested by Shoemaker *et al.* (1974).

A component present in a non-uniform concentration, at constant pressure and temperature and without external fields, will diffuse in such a way as to render its concentration uniform. Fick's first and second laws relate the flux (amount per unit cross-sectional area per unit time) to functions of concentration gradients. Shoemaker *et al.* (1974) show that for a solution contained in a porous frit suspended in a bath, the mass of solute Q(t), with diffusion coefficient D, in the frit at time t is related to D through a fairly complicated expression involving concentrations and the physical dimensions of the frit. Simplifying assumptions can however be made to yield an equation of the form

$$Q(t) = a\, e^{-bDt}$$

where a and b are constants for a given frit.

If there are no large volume or density changes in the bath then the loss of mass of the species in the frit will be proportional to the increase in concentration of the diffusing solute, in the bath. If W_t and W_∞ are these concentrations at time t and after equilibrium has been reached, respectively, and W is given by $(W_\infty - W_t)$ then

$$W = a'.e^{-b'Dt} \qquad \text{.....2.27}$$

or $$\ln W = \ln a' - b'Dt$$

and a plot of ln W versus t should give a straight line with a slope equal to - b'D. The quantity b' is the "frit constant" and can be obtained by using a solution of known diffusion coefficient. In this work a potassium chloride solution has been used. Hence values of D for each impurity can be calculated.

2.7 **Adsorption isotherms**

Adsorption processes have been mentioned in the literature in connection with the presence of impurities in the sucrose crystal (Donovan and Williams, 1992; Grimsey and Herrrington, 1994). Adsorptions at solid surfaces can lead to physisorption in which interactions between the adsorbate and the adsorbent are weak and chemisorption which involves stronger interactions with energies similar to those of chemical bonds. Both are well documented in the literature, particularly with respect to gas adsorption on metal surfaces and to catalysis.

The Langmuir adsorption isotherm is well known and its use requires that there be no interaction between adjacent molecules on the solid surface, that the energy of adsorption be the same for all the adsorption sites on the surface, and that the adsorbed molecules form a monolayer only.

The Langmuir adsorption isotherm is:

$$\theta = \frac{KP}{KP + 1} \qquad \text{.....2.28}$$

where θ is the fraction of the surface covered by the adsorbate; K is the equilibrium constant for adsorption, defined by the ratio k_a/k_b; k_a is the rate constant for adsorption, and k_b the rate constant for desorption; P is the equilibrium partial pressure or concentration of the species being adsorbed. It will be shown later that the Langmuir model does not fit the results obtained here.

Freundlich has proposed an isotherm for cases when the heat of adsorption varies logarithmically over the surface. This equation is:

$$\theta = C_1 P^{1/C_2}$$

.....2.29

where θ is the fraction of the surface covered, C_1 is a constant, P is the equilibrium partial pressure or concentration, and C_2 is another constant.

This model has been shown to apply to adsorption in solutions and fits the data from this work.

Finally, the BET isotherm (Atkins, 1994) was also tested in this work. This isotherm deals with multilayer adsorption and its derivation yields the following equation:

$$V/V_{mon} = c\,(p/p^*)/\{(1 - p/p^*)[1 - (1 - c)\,(p/p^*)]\}$$

.....2.30

where V is the volume of adsorbate, $V_{mon.}$ is the volume of adsorbate if there were complete monolayer coverage only, c is a constant for a particular system, p is the equilibrium pressure, and p^* is the vapour pressure of the bulk liquid adsorbate. The isotherm requires the heat of adsorption for the first layer to be higher than that of the second and higher layers. This expression can be reorganised into a form which lends itself to a linear plot with the intercept giving $c\,V_{mon}$ and the slope yielding $(c - 1)/c\,V_{mon}$. These results may be solved for c and V_{mon}. In all cases fits were poor and it was concluded that this model does not apply for this work.

2.8 Conclusions

The theoretical aspects of a relatively wide range of topics have been covered in this Chapter, as could be expected from the comments made in Section 1.3. The two main points of the Chapter, however, are the selection of G, the sucrose crystallisation rate, and the derivation of an impurity transfer rate, R_i. Both quantities will be utilised extensively in this work.

CHAPTER 3

EXPERIMENTAL

The information contained in Chapters 1 and 2 has been used to formulate an experimental plan. The rate at which impurities are transferred into the sucrose crystal, and the effect of a number of factors on this rate must be investigated. The experimental plan devised to achieve this is described in this Chapter. The materials, equipment and analytical techniques used and the experiments performed will also be described.

3.1 Crystallisation equipment

In order to perform the experimental work, sucrose has to be crystallised. The central feature of the crystallisation equipment is thus a pilot plant scale evaporative crystalliser. This crystalliser and its ancillary equipment, which were designed and built at the Sugar Milling Research Institute (Bruijn, 1964), are described below.

3.1.1 Evaporative crystalliser

The crystalliser and its ancillary equipment are shown in Figure 3.1. Some of the important features of the crystalliser are as follows:

- The working volume of the crystalliser is 20 litres and the nucleating volume is 7 litres.
- The heat input is through a 220 V, 2,2 kW circular heating mantle specially manufactured to fit outside the bottom part of the vessel. The mantle is a "wrap-around" type and can be tightened to fit securely. The energy input can be changed through a voltage controller and this controls the evaporation rate which is a linear function of the voltage and increases by about 0,06 g of condensate per second for every ten volts increase. Changing the voltage from 180 to 220 V increases the evaporation rate by about 50%. Increasing the concentration of sucrose in the feed liquor from 65 to 73% reduces the amount of water to be evaporated by about 35%. Both factors were used to obtain large changes in the crystallisation rate.

- Stirring speed is adjustable from 0 to 175 rpm.
- Sampling during the crystallisation process is possible through a sampling port and vacuum system.
- Nucleation is instigated by injecting 2 cm^3 of a suspension of ball milled sucrose crystals (2 to 10 μm) in alcohol, through the seed port. This port contains a septum which is removable.
- Vacuum is provided by a dedicated vacuum pump.
- Feed of liquor to the crystalliser is through a speed controlled peristaltic pump and dripper for visual check. This system allows precise feed control. The feed is kept at 60°C and enters the crystalliser, at the bottom, through a perforated feed ring. The feed mass is recorded continuously.
- The baffle tube enhances circulation vertically, from the outer to the inner regions, as is the case in industrial vessels.

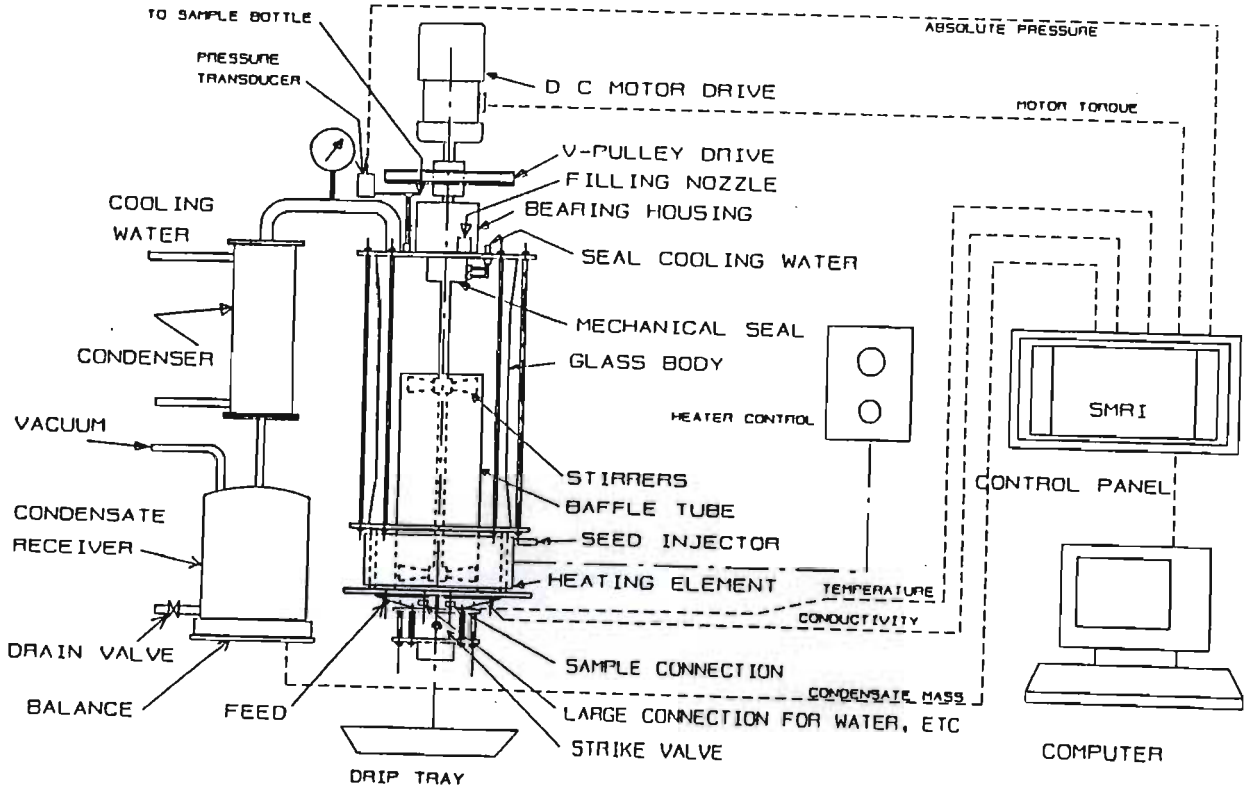

Figure 3.1 Pilot evaporative crystalliser and ancillary equipment.

3.1.2 **Ancillary equipment**

The ancillary equipment consists of various devices, most of which are commercially available, to measure and display the following parameters:

- Stirrer torque in arbitrary units.
- Absolute pressure in kPa.
- Conductivity in arbitrary units.
- Massecuite temperature in °C.
- Boiling point elevation in °C. This is given by the difference between the massecuite temperature and the boiling point of water at the same pressure. The latter is calculated by the computer using the following formula (Keenan *et al.*, 1969) where P is the pressure measured in bars:

  $Temp/°C = 23,782 + 280,43P - 667,32P^2 + 1002,9P^3 - 781,38P^4 + 241,28P^5$
- Masses of condensate and of feed in kg.

3.1.3 **Data logging**

All the signals are routed into a personal computer (PC) through relevant interfaces. The PC uses a data logging program to plot the data on the screen against real time, to display instantaneous values and to store the data on disc for future retrieval by commercial spreadsheet programs. A typical screen display is shown in Figure 3.2.

Figure 3.3 shows the data logged from a typical crystallisation and the various stages have been marked.

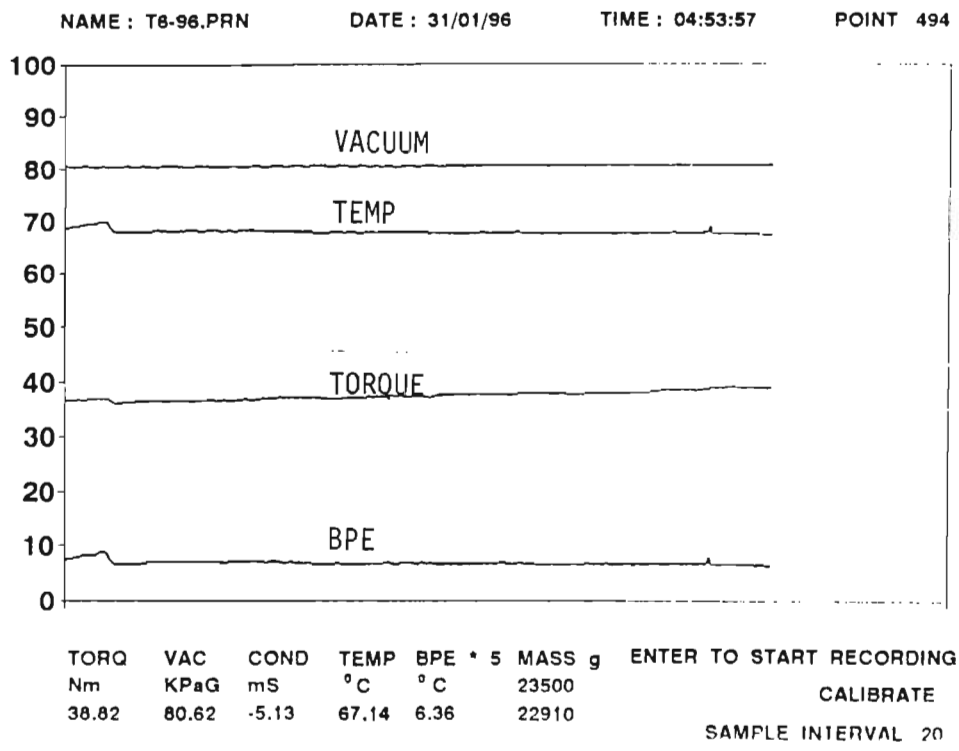

Figure 3.2 **Typical screen display from the crystalliser data logging system.**

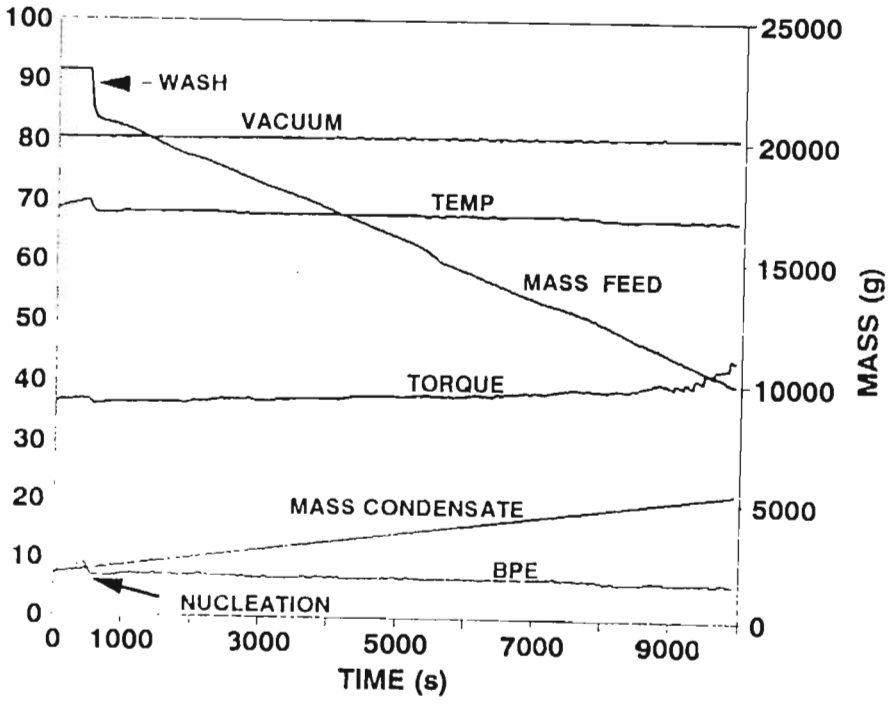

Figure 3.3 **Data logged from a typical crystallisation run.**

3.1.4 **Operation**

A typical run consists of the following steps:

(i) Starting the vacuum pump and drawing about 10 litres of feed into the vessel.

(ii) Switching the heat on and evaporating the liquor to the required concentration for nucleation, as determined by the boiling point elevation (BPE). Spencer and Meade (1948) show that BPE is directly proportional to the concentration of sucrose in solution and that the BPE value for nucleation depends on the purity and temperature of the sucrose solution. In this work, trial and error was used to establish that a BPE of about 8°C resulted in good nucleation. The stirrer is on, at maximum speed setting, throughout the run.

(iii) Introducing the seed material as described in Section 3.1.1, on page 50.

(iv) Introducing the feed itself (1 kg) as a wash material, about 5 minutes after nucleation, to reduce the number of nuclei and thereby improve the crystal size distribution by dissolving the smaller crystals. This process is used industrially, where a narrow crystal size distribution is required in terms of sugar quality.

(v) The crystalliser is then controlled according to the program for that run. BPE, torque, mass of water evaporated and of feed, and/or conductivity may be used for control.

(vi) At the end of the crystallisation a "tightening" period may or may not be used. This involves the evaporation of water without the addition of feed. Again this is common in industry.

Conditions in the crystalliser can be controlled and kept at the selected levels. The absolute pressure in the vessel affects many other parameters (temperature, viscosity, etc.) and thus needs to be kept as constant as possible. This is achieved by using a dedicated vacuum pump (Sihi, liquid ring), a bleed to atmosphere through a needle valve and a pressure gauge. As mentioned

earlier, the absolute pressure in the crystalliser is displayed on the computer screen. The evaporation rate is controlled by selecting the required voltage. Condensate flow is then monitored, together with the feed rate. Again these parameters are displayed.

Absolute pressure, feed rate, condensate production and temperature in a typical run are shown in Figure 3.4.

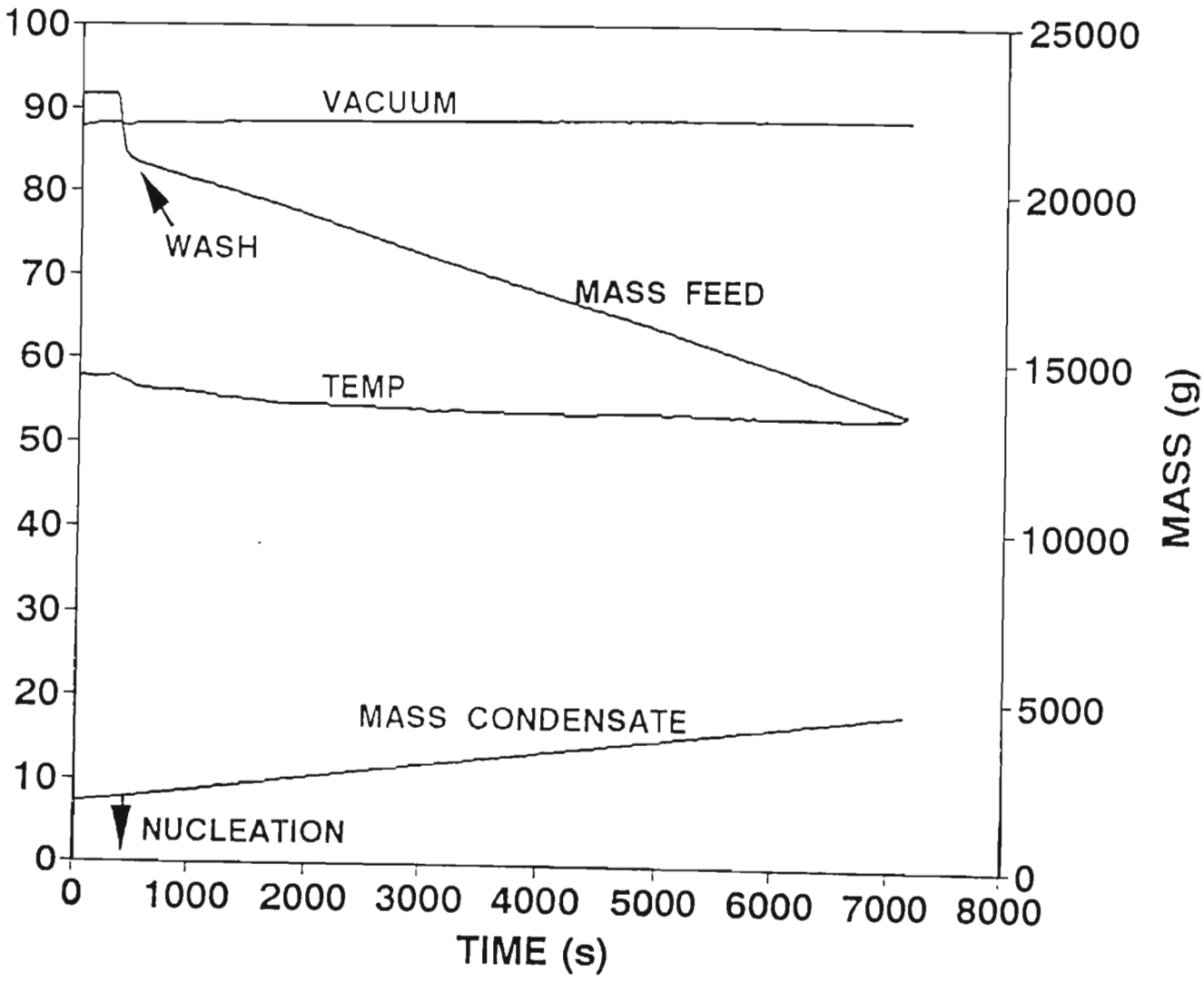

Figure 3.4 **Pressure, feed rate, condensate production and massecuite temperature during a typical crystallisation run.**

At the end of the run the vacuum is broken and the crystallised mass, called a massecuite in the sugar industry, is discharged and immediately centrifuged in a laboratory centrifuge. The run off (called molasses or jet) is sampled. The wet sugar is added to an equal mass of saturated refined sugar solution, mixed well manually and centrifuged again. This sugar is allowed to air dry and is referred to as "unaffinated" sugar.

The following materials are sampled:

- Feed liquor (about 500 g).
- Massecuite (about 500 g).
- A small sample (about 10 g) of massecuite in glycerol saturated with sucrose, for crystal size measurements.
- Run-off (about 500 g).
- Sugar (about 1 kg).

Liquors, massecuite and run-off samples are kept in a freezer (-10°C) prior to analysis. Samples for crystal size measurements and sugars are kept at room temperature in sealed labelled containers.

3.1.5 **Comparison with industrial crystallisers**

It is important to ensure that the pilot crystalliser yields results which can be transferred to industry. Two approaches were used to compare the pilot crystalliser to industrial crystallisers:

- General approach - Liquors from industrial crystallisers were sampled and crystallised in the pilot crystalliser. The colour of the sugar crystals produced and colour transfers (crystal colour/feed liquor colour) were then compared to those published by those refineries, for the time period during which the samples were taken. Colour was measured as described in Section 3.4.4.3 and the comparison is given in Table 3.1. It is evident that the agreement is acceptable.

Table 3.1

General comparison between the pilot crystalliser (P) and industrial crystallisers (I)

Refinery	Feed Colour		Sugar Colour		Colour Transfer	
	I	P	I	P	I	P
A	268	240	24	20	0,090	0,085
B	290	367	22	26	0,076	0,071
C	709	856	25	24	0,035	0,028

- Direct comparison - Samples of feed liquors, massecuites and sugar were taken during industrial crystallisation, at a large central refinery. The sampled feed liquors were then crystallised in the pilot crystalliser, under conditions as close as possible to those used in the industrial vessels. Feed liquors, sugars produced, etc. were analysed. The results obtained from the industrial vessels and from the pilot crystalliser are compared in Table 3.2, and the agreement is good.

Table 3.2

Direct comparison of the pilot crystalliser (P) with industrial units (I)

	Feed 1		Feed 2		Feed 3		Feed 4	
	I	P	I	P	I	P	I	P
Feed: Colour	248		594		1090		2516	
Massecuite:								
Temp /°C	78,5	79,3	82,4	80,4	84,5	80,6	82,0	81,2
Brix /%	90,2	92,2	91,0	91,6	90,0	89,2	92,2	92,3
Colour	261	273	734	645	1229	1200	2513	2505
Sugar Colour	12	12	26	22	38	36	54	52
Colour transfer:								
on feed	0,048	0,048	0,044	0,037	0,035	0,033	0,021	0,021
on massecuite	0,046	0,044	0,035	0,034	0,031	0,030	0,021	0,021
Crystal: width /μm	399	394	392	341	405	354	323	306

3.2 Centrifugation

After removal from the evaporative crystalliser, sugar crystals are separated from the massecuite in a Martin Christ laboratory centrifuge without wash addition. Some operational details are:

- Speed of rotation - 3000 rpm.
- Charge mass - 2 kg.
- Basket diameter - 200 mm.

3.3 Materials used

The sugar liquors used as feed to the crystalliser were obtained as required from a local refinery and thus represent actual industrial streams. Sucrose solutions were prepared by dissolving refined sugar in water. The non-sucrose species investigated are as follows:

- Colour

  Colour in the sugar industry cannot be defined. To increase colour levels, aliquots of highly coloured refinery streams were added to the feeds. This again represents actual industrial conditions.
- Potassium

  Potassium chloride, AR, from Associated Chemical Enterprises (ACE).
- Calcium

  Calcium chloride dihydrate, CP, from ACE.
- Lithium

  Lithium hydroxide monohydrate, commercial grade, was neutralised with commercial grade hydrochloric acid.
- Nickel

  Nickel chloride, hexahydrate, AR, from ACE.
- Starch

  Soluble starch, AR, from Hopkins and Williams Ltd.

- Dyes

  Methylene blue, $C_{16}H_{18}ClN_3S.3H_2O$, from Merck, molecular mass 373,9. This is soluble in water and was used as a 1% (m/v) solution in water.

  Methyl blue, $C_{37}H_{27}N_3Na_2O_9S_3$, from Riedel-de Haën, molecular mass 799,8. Soluble in water and a 1% (m/v) solution was used.

  Acid blue 25, $C_{20}H_{13}N_2O_5SNa$, from Sigma, molecular mass 416,4. Soluble in water and used as a 1% (m/v) solution.

- Polysaccharides

  Carboxymethyl cellulose, sodium form, food grade from Chemimpo. This was dissolved as required, in the sugar liquors, with heat and stirring.

  Carrageenan, food grade, from Chemimpo. This was dissolved in the sugar liquors, as required, using heat and stirring.

- Slurry for nucleation

  Nucleation is instigated by the introduction of 2 cm^3 of a standard sucrose slurry. This slurry is prepared by ball milling 800 g of refined sugar and 2 litres of methylated spirits in a slurry ball mill. This mill is 600 mm in diameter by 200 mm long and is fitted with a leak-proof, full diameter cover. It uses 2 500 steel balls of 10 mm diameter and turns at about 75 rpm. Milling takes 12 hours and the product is then diluted to 6 litres with methylated spirits. The slurry is kept in well sealed containers. The required amount is introduced into the crystalliser with a syringe. The slurry consists of small, irregular pieces broken off the sucrose crystals. It is difficult to determine an average size for the pieces because many are too small to be measured by the image analysis system. Those pieces that can be measured are about 5 μm in length.

3.4 **Analytical techniques**

The analytical work consists of four main sections. The first deals with two aspects which are of primary importance in this investigation, namely the laboratory affination of the sucrose crystals and the use of an image analysis system to measure the length and width of the crystals. The second section deals with the analysis of potassium, calcium, lithium and nickel ions in the sugar liquors and crystals. The third section covers a number of analyses such as colour, total dissolved solids (or brix), sucrose content (or pol), starch, etc., in the sugar materials, which are particular

to the sugar industry. Finally, miscellaneous analyses are described in the fourth section.

3.4.1 **Affination of sugar**

The "affination" of sugar crystals is a critical part of the study of impurity transfer. It has received attention from many workers (Mackintosh and White, 1969; Guo and White, 1984; Michael and Thelemaque, 1984; Lionnet and Moodley, 1995).

Crystalline sugar as produced by the usual crystallisation process is considered to consist of two components: a thin film of mother-liquor on the surface and a crystal, a concept that has been confirmed experimentally (Michael and Thelemaque, 1984). When crystalline sugar is separated from massecuites by centrifuging, the amount of mother-liquor film left on the crystal depends on the conditions (speed of rotation, amount of wash liquid, etc.) during centrifuging. These conditions cannot be controlled with the precision required to always leave the same amount of mother-liquor on the crystal. Since the concentration of impurities in the film can be 100 times greater than that in the crystal itself, it is essential to develop a technique which results in reproducible film removal. Michael and Thelemaque (1984) investigated various laboratory affinations and developed a procedure which met the reproducibility criterion. These authors show that, when samples of raw sugar were affinated three times, the affinated crystal colour was within the analytical error for raw sugar colour (± 40 colour units) after the first affination, as shown in Table 3.3.

Table 3.3

Affinated sugar colours after repeated affinations of the same sugar

Number of affinations	Sample			
	1	2	3	4
1	822	824	830	791
2	825	763	845	818
3	820	814	824	781

As a check a few sugar samples were affinated twice during the present work; in all cases the

colours were within analytical error.

The method developed by Michael and Thelemaque (1984) is described below.

Three hundred grams of the air dried unaffinated sugar (Section 3.1.4) is stirred mechanically with 600 g of a saturated refined sugar solution for 15 minutes. This process softens the mother-liquor film and predisposes it for easy removal. The mixture is filtered, under vacuum, using a sintered glass funnel. The process is repeated on the filtered crystals but with manual stirring using a glass rod. Then 600 g of a saturated sucrose solution made up with 95% methanol solution is added to the second crop of filtered crystals and the sugar stirred with a glass rod, then filtered as before. A final stirring followed by filtration is done but in this case only 300 g of 100% methanol saturated with sucrose is used. The now affinated sugar is spread on clean paper and allowed to air dry.

The sugar crystals thus produced are free of the mother-liquor film and are called "affinated crystals". All the analyses quoted in this work, except for the determination of crystal length and width, were performed on this affinated crystal.

3.4.2 **Measurement of crystal length and width**

This involves the use of a commercially available image-analysis system, called Kontron Videoplan. This system consists of the following equipment:

A 286-10 computer with math co-processor and 1,2 MB floppy disk and 41 MB hard disk
Digitizing tablet
Charge coupled device video camera
Video graphic printer
Colour monitor
Olympus microscope.

The system is first calibrated with a 1 mm objective micrometer.

Massecuite (Section 3.1.4) is mixed with sucrose saturated glycerol on a 1:1 mass basis. The mixture is allowed to stand at room temperature to eliminate air bubbles and is then lightly spread on a microscope slide. The lengths of the long (L) and short (W) axes of 200 crystals are measured. This is done by positioning the cursor at one end of the crystal being measured, anchoring it there and then moving it to the other end. The system can read that distance and using the calibration, converts it to micrometers. All the lengths and widths are stored in the PC, in separate fields for future processing.

Figure 3.5 shows that the standard deviations of the length and of the width tend to constant values after about 140 crystals have been measured. This indicates that 200 crystals is a suitable sample size.

Figure 3.6 shows a view of sugar crystals, as seen on the monitor screen, for size measurement. The image analysis package produces a number of statistical results for the lengths and widths measured. Figure 3.7 is an example of these results, concerning the crystal length (shown as DMAX on the print-out) for a specific sample (UK 290795). A histogram is produced and various statistics, including the mean (206,78) and standard deviation (52,09), are calculated and printed. The standard deviation in this case is smaller than that shown in Figure 3.5; this is because of the differences between the various experiments.

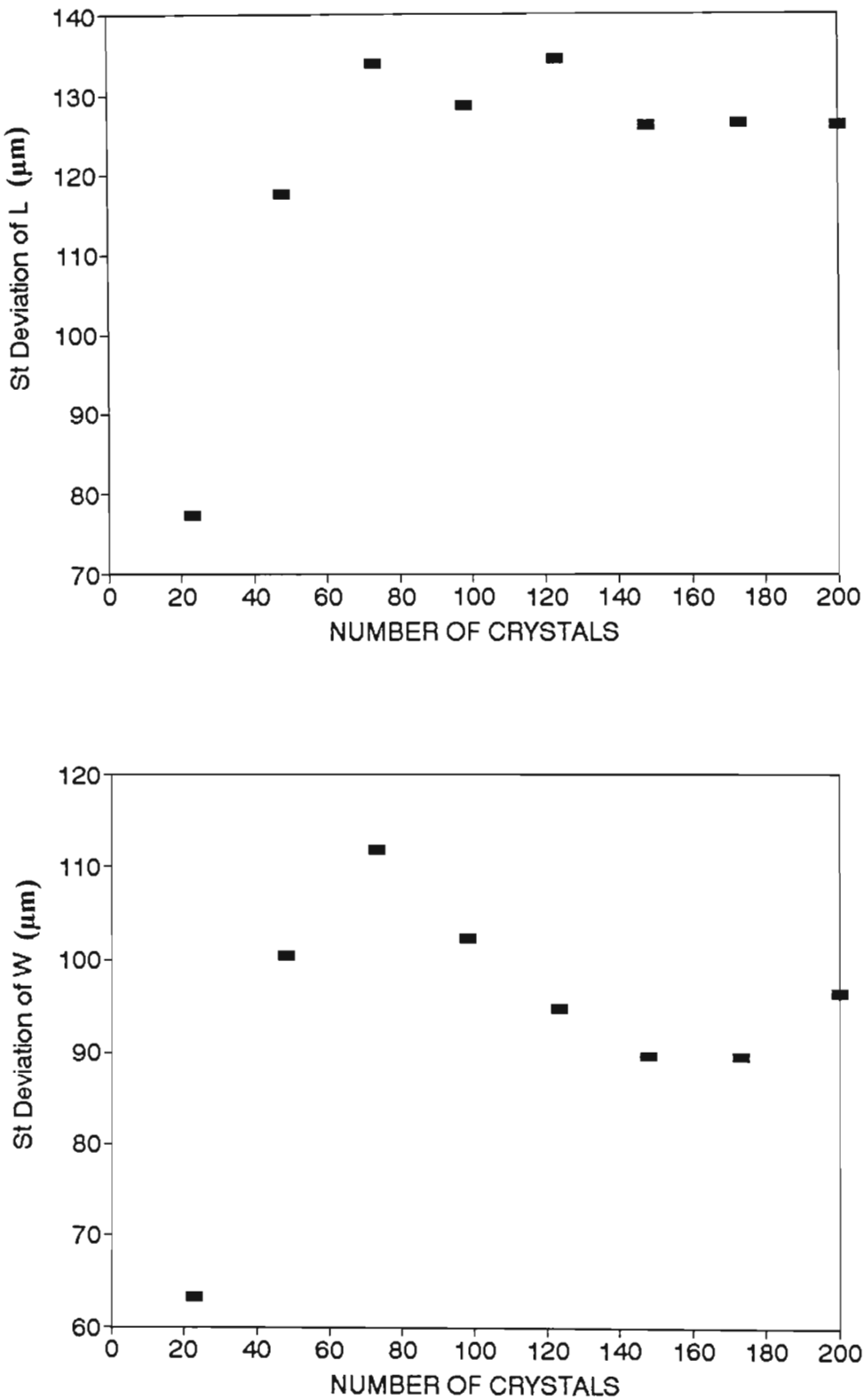

Figure 3.5 **Standard deviation of crystal (a) length and (b) width with number of crystals measured.**

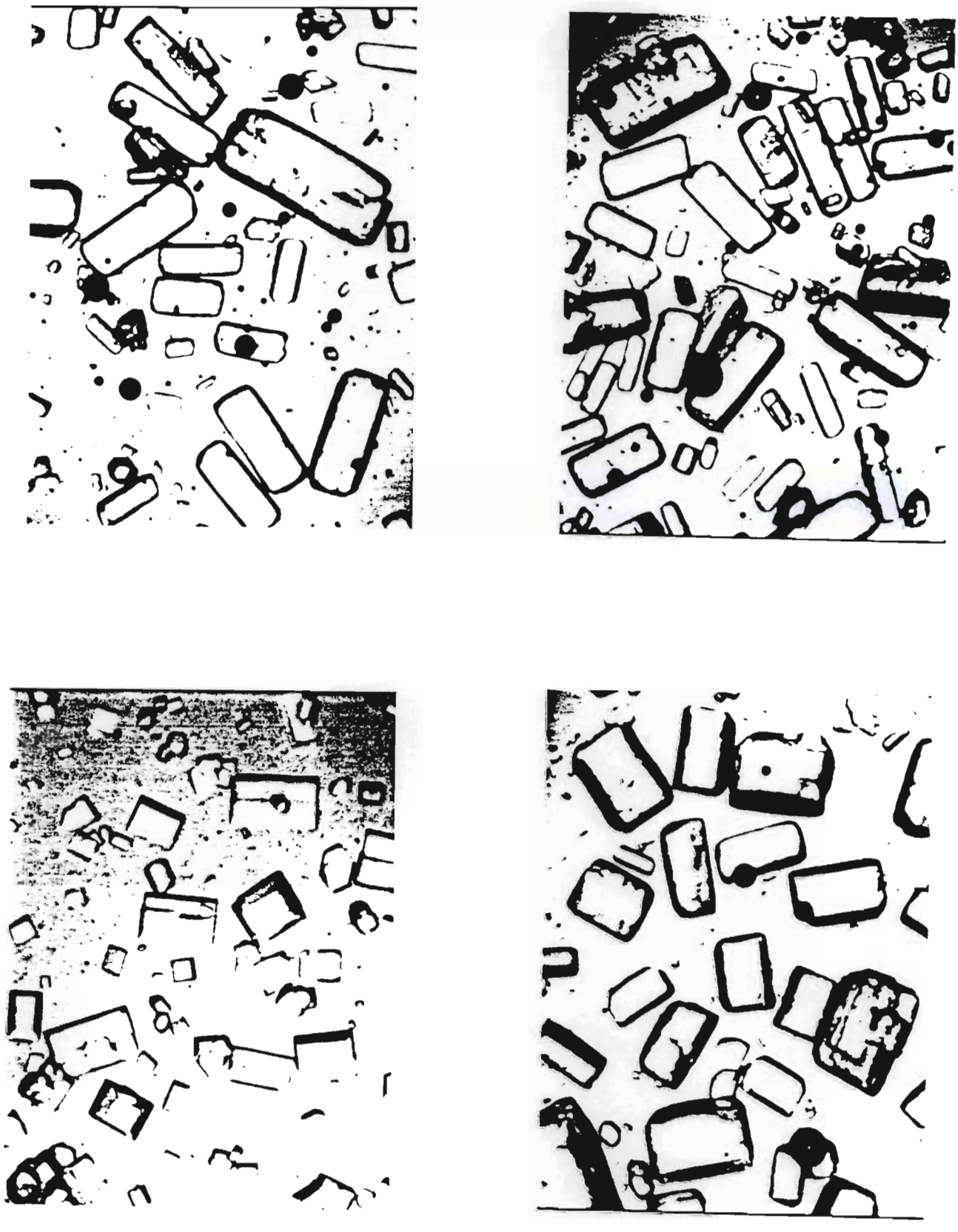

Figure 3.6 **Sugar crystals as seen on the monitor screen for size measurement.**

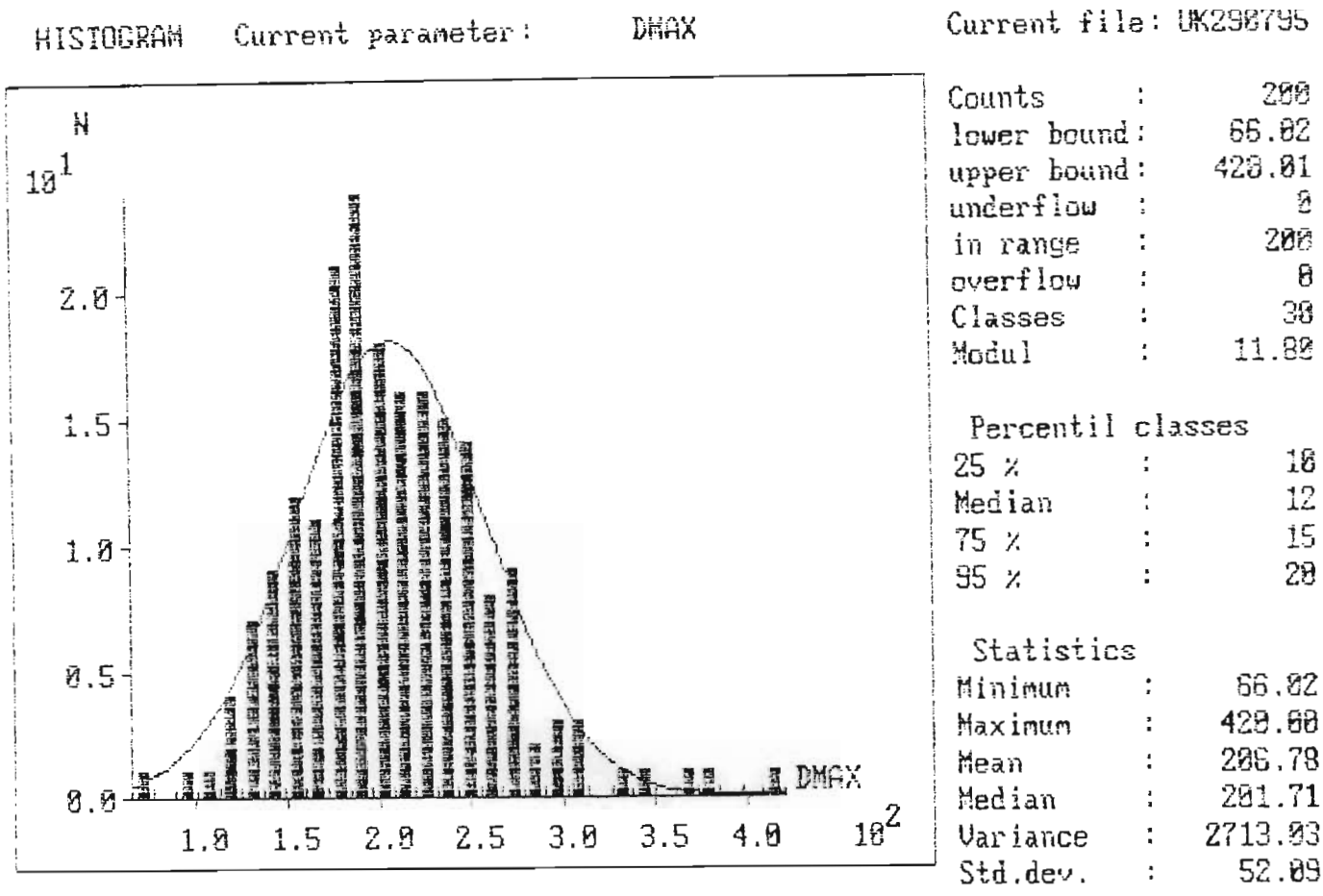

Figure 3.7 Data obtained from the image analysis system for the crystal length measurements.

As mentioned in Section 2.2, crystal size analyses in the sugar industry have usually been done by sieving. The image analysis system used here has many advantages when compared to sieving:

- The image analysis technique, contrary to sieving, does not require the separation of the crystals from the mother-liquor. This separation can result in the formation of conglomerates, particularly with high purity massecuites. The dispersion of a small quantity (10-20 g) of massecuite in sucrose saturated glycerol (about 100 cm^3) stops the crystallisation process.

- Some types of sugar crystals need further treatment to prevent caking and/or conglomeration before sieving. With high purity materials it is often impossible to completely prevent conglomeration.

- Sieving does not distinguish between crystal length and width.

- Actual measurements in the image analysis can be automated. Even the present, non-automated, system is faster than sieving.

3.4.3 **Analysis of metal ions**

Calcium, potassium, lithium and nickel ions were analysed by atomic absorption (Guo and White, 1984) using a Varian Spectra AA 20. The standard solutions were made by diluting commercially available stock solutions (UnivAR, from Saarchem Pty Ltd.) with distilled and deionised water. The sugar materials were diluted as required, to the maximum of 5% (m/v) sucrose in water, again using distilled and deionised water.

Some key details are given in Table 3.4.

Table 3.4

Details for the atomic absorption analyses

Species Analysed	Concentration of Standard/ mg/l	Suppressant	Lamp Current/ mA	Fuel	Oxidant	Wavelength Monitored/ nm
Ca^{2+}	1 to 4	Potassium chloride	3,5	Acetylene	Nitrous oxide	422,7
K^{+}	0,5 to 2	Cesium chloride	5	Acetylene	Air	766,5
Li^{+}	1 to 4	Potassium chloride	5	Acetylene	Air	670,8
Ni^{2+}	15 to 60	None	3,5	Acetylene	Air	352,4

The ionisation suppressants are AR grade chemicals, dissolved in distilled deionised water, added to give a final concentration of cesium or potassium of 1000 µg/l in all solutions, including the blank.

3.4.4. **Analyses particular to sugar**

Most of these analyses are described in detail in the Laboratory Manual for the South African Sugar Factories, 3rd Edition, 1985. Some of the key details are given here.

3.4.4.1 **Total dissolved solids**

This is called "brix" in the sugar industry and is determined by refractometry. The angle of refraction of a beam of light through an aqueous solution of sucrose is dependent on the concentration and temperature of the solution. Refractive indices of sucrose solutions and brix at 20°C, at a wavelength of 589 nm are given in Table 1 on page 377, of the above mentioned reference. The table was constructed (Bates, 1942) by reading the refractive indices of aqueous sucrose solutions of accurately known concentrations. In the sugar industry brix is considered equal to the total dissolved solids. This is based on the assumption (Spencer and Meade, 1948) that most sugars in solutions of equal concentrations have the same refractive indices. Any deviation from this assumption has little impact in this work because the refinery liquors used for crystallisation contain sucrose at concentrations which are very high relative to the concentrations of the impurities.

All brix values given here were measured on dilute, filtered solutions read at 20,0°C in a RFM 500 Bellingham and Stanley refractometer . The brix value corresponds to the mass of dissolved solids in 100 mass units of solution.

3.4.4.2 **Sucrose content**

The apparent sucrose content of a material, or "pol", is expressed as a percentage by mass. It is determined by the direct polarisation method and for most of the materials found during refining, pol can be considered as being equal to true sucrose because of the high concentration of sucrose

present, as mentioned in Section 3.4.4.1.

The saccharimeter is used to measure the pol content of the materials. The operation of this instrument is based on the measurement of the optical rotation of the plane of polarised light by the sucrose solution and this is proportional to the concentration under specified conditions. Readings are taken at 20°C on filtered solutions, with light at 589 nm on a Polartronic Universal saccharimeter from Schmidt and Haensch.

Modern saccharimeters are fitted with the International Sugar Scale and will give a reading of 100 when 26,000 g of pure sucrose are present in 100 cm^3 of an aqueous solution, read in a 200 mm cell at 20°C. The pol content (g/100 g solution) is then calculated from

$$\text{Pol \%} = \frac{\text{Saccharimeter reading x 26,00}}{\text{mass (g) of 100 cm}^3 \text{ of solution}}$$

The mass in grams of 100 cm^3 of the solution is the apparent density at 20°C. This is a function of the brix of the solution and is available in Table 8 on page 391 of the Laboratory Manual for the South African Factories. The table was constructed (Bates, 1942) by actual measurements on sucrose solutions.

3.4.4.3 **Determination of colour**

All colour values quoted here were measured on diluted solutions, after filtration through a membrane filter (Millipore) with a pore size of 0,45 μm. Unless stated otherwise the measurement was performed on solutions at pH 7,0 ± 0,2, the pH being adjusted with sodium hydroxide or hydrochloric acid. The absorbance was read in an LKB Biochrom spectrophotometer at 420 nm (the standard wavelength, in the Sugar Industry, for the measurement of colour), against distilled water, in a cell of known path length. The concentration of dissolved solids in the solution, in g/cm^3, is obtained from the brix (Table 8, page 391, Laboratory Manual for South African Factories). Then

$$\text{Colour} = A_s \times 10\,000/(b \times c)$$

where A_s is the absorbance, b the cell length in mm and c the concentration of total solids in g/cm^3. Colour is in "colour units", expressed on brix.

3.4.4.4 Determination of starch

Starch in sugar products is measured by colorimetry, using the starch/iodine colour complex. A known mass of sample (10 ± 0,01 g for liquors; 25 ± 0,1 g for sugar) is added to 30 cm^3 of distilled water. The starch is precipitated by the addition of absolute alcohol. It is filtered off, dissolved by heating and reacted with a mixture of acidified potassium iodide and potassium iodate. The absorbance of the resulting starch/iodine complex is read against a blank of distilled water, at 600 nm. A reagent blank, using distilled water in the place of the sugar aliquots, is also read and its absorbance is subtracted from that of the sample. The resulting absorbance value is used in conjunction with a calibration curve based on potato starch (found in Section 6.3.5.2 of the Laboratory Manual for South African Factories) to yield the starch content of the sample in mg/kg. The detailed methods are found in the above-mentioned publication on pages 194, 284 and 325.

3.4.4.5 Determination of total polysaccharides

Total polysaccharides in sugar products are measured by alcohol precipitation followed by filtration, drying and weighing.

The sugar product is diluted to 30 brix using distilled water and centrifuged for 5 minutes in a Martin Christ III Universal Junior Centrifuge, with head 5010, at a speed of 3500 rpm. A known mass (30 ± 0,1 g) of the supernatant is taken and acidified absolute ethanol (200 cm^3 of 1:1 HCl added to 1 ℓ of absolute ethanol) added (150 cm^3). The mixture is allowed to stand for 16 hours and then filtered through a Gooch crucible containing asbestos. The precipitate is washed with ethanol and the crucible and contents dried (105°C) for 3 hours. The crucible is cooled in a desiccator, weighed and then ignited in a muffle furnace (650°C) to burn all the polysaccharides. It is then cooled and weighed again. The mass loss yields the polysaccharide content which is expressed as mg per kg of sample.

The detailed method is given in the Laboratory Manual for South African Factories on page 329.

3.4.4.6 The measurement of viscosity

Traditionally in the sugar industry, viscosity has been measured by the rotating cylinder method. Commercially available viscometers, such as the Brookfield, provide pre-calibrated equipment which are adequate for measuring the viscosity of Newtonian fluids such as sucrose solutions. A specific calculation converts the scale reading to the viscosity.

In this work a Brookfield HBT viscometer was used. This instrument was checked against two standard fluids (Brookfield viscosity standards: fluids 6 000 and 100 000) with viscosities of 97,2 and 59,2 Pa s at 25°C. The measured viscosities were 95 and 57 Pa s respectively. These are within 5% of the standard values which is considered adequate.

The material to be analysed is held in a large diameter container placed in a water bath. The viscosity is measured when the temperature of the material has reached the set temperature.

3.4.5 Determination of dye content

The wavelength of maximum absorption for each dye in a sucrose solution, was determined. Dye solutions of 25 mg/l in 30% (m/m) sucrose solutions were scanned over a wavelength range of 350 to 750 nm, against a 30% (m/m) sucrose solution in a LKB Ultrospec II spectrophotometer. As an example, the absorption spectrum recorded for acid blue 25 is shown in Figure 3.8.

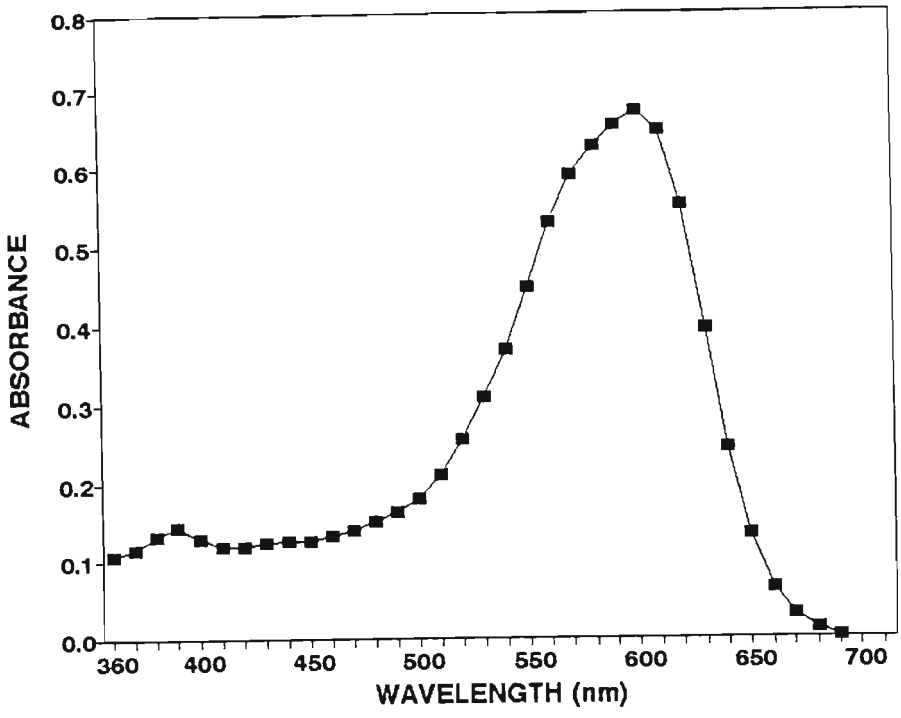

Figure 3.8 **The absorption spectrum of a 25 mg/l solution of acid blue 25 in 30% (m/m) sucrose solution, recorded against a blank of 30% (m/m) sucrose solution.**

The absorption maxima for all the dyes used in this work are shown in Table 3.5.

Table 3.5

Wavelength of maximum absorption for dyes dissolved in 30% (m/m) sucrose solution

Dye	Wavelength/nm
Methylene blue	665
Methyl blue	607
Acid blue 25	602

Calibration curves were then prepared for each dye. Aliquots of aqueous dye stock solutions were added to 30% (m/m) sucrose solutions and the optical absorbance (A) read against a 30% (m/m) sucrose solution in the LKB spectrophotometer. The calibrations were linear over the

range 0,25 to 2,50 mg dye/l. As an example the calibration for acid blue 25 is shown in Figure 3.9.

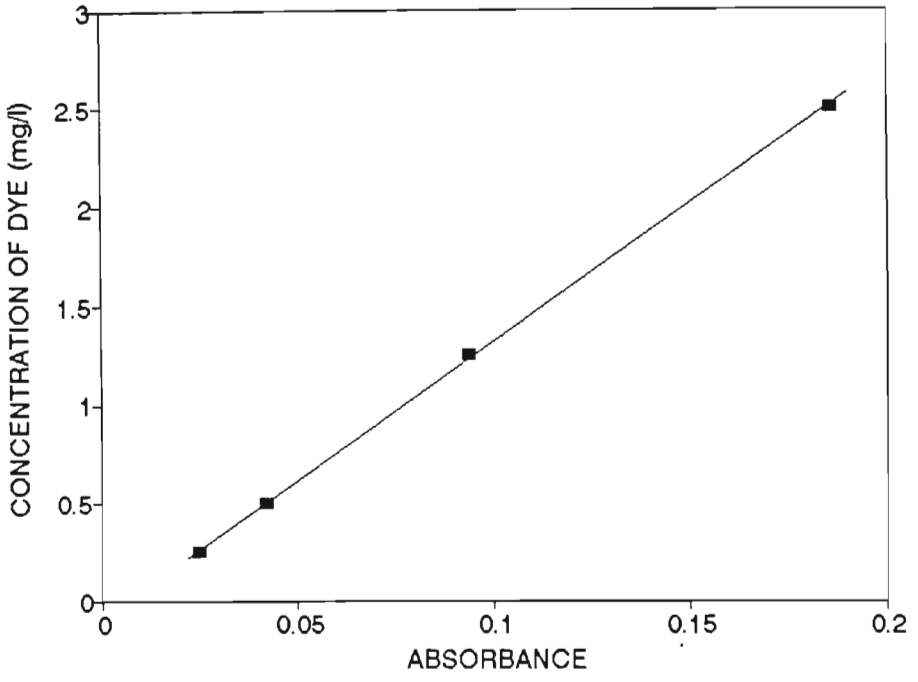

Figure 3.9 The calibration curve for acid blue 25 in 30% (m/m) sucrose solution, recorded against a blank of 30% (m/m) sucrose solution, at a wavelength of 602 nm.

The following calibration equations were obtained:

mg methylene blue/l	=	-0,0720 + 0,966A
mg methyl blue /l	=	-0,107 + 19,1A
mg acid blue 25/l	=	-0,0857 + 13,9A

In all cases four concentrations of dye were used to generate the calibration curve and the regression r^2 values were all greater than 0,9997. The intercepts are not equal to zero, but the differences are small. Sugar liquors and crystals could then be analysed for dye concentrations, by dilution to 30% (m/m) sucrose, reading in the spectrophotometer at the appropriate wavelength, in 1 cm glass cuvettes, and then using the above calibration equations.

3.4.6 **X-ray powder diffraction**

X-ray powder diffraction techniques were used to test whether the incorporation of impurities changes the sucrose crystal lattice.

The analyses were done by Mrs L Turner of Minemet Technologies (Pty) Ltd, on their own equipment. This consisted of a Phillips X-ray diffractometer, using a cobalt target tube and a wavelength (λ) of cobalt radiation of 1,790197 Å. The goniometer is fitted with a graphite monochromator.

The sucrose crystals were ground in a pestle and mortar, sieved through a 38 μm screen and the sieved fraction used for the analysis.

Scans were run from $2\theta = 6°$ to 60° at a scanning speed of 1° per minute, chart speed of 10 mm per minute, full scale deflection of 2×10^4 and 4×10^4 counts per second, time constant = 1, gain = 16 and generator setting at 50 kilovolts and 24 milli-amperes. D-spacings were read off tables calculated using the Bragg equation

$$\lambda = 2d \sin \theta$$

The purpose of this analysis was to compare the results obtained from sucrose crystals containing very low concentrations of impurities with those from crystals with very high levels of impurities. The latter were selected from crystallisation runs yielding crystals with higher levels of starch, calcium, colour and potassium.

The crystals with very low levels of impurities were prepared specially for this experiment by purifying a sucrose liquor, with activated carbon. The pure crystals had very low colours (less than 10 units), very low starch, about 5 mg/kg of calcium and 2 mg/kg of potassium. The concentrations of impurities in the impure crystals were 2000-5000 mg/kg for starch, 300-420 colour, 18-20 mg/kg of potassium and 30-70 mg/kg of calcium.

It is stressed that the purpose of this analysis was to obtain qualitative information on the lattices of the pure and impure crystals.

3.5 Expression of the concentration of impurities

The concentration of impurities in sugar liquors is usually expressed either on sample or on total dissolved solids, using a mass on mass basis. In the present work it was considered that neither of these approaches would fully reflect the concentration driving force behind the incorporation of the impurity into the sucrose crystal. Since crystallisation is driven by evaporating water, it was felt that the concentration of the impurity expressed on the water present in the liquor would be more meaningful. Therefore the concentrations of all the impurities, except colour, have been expressed as mg impurity per kg water in the liquor. The concentrations of the impurities in the sugar crystals must obviously be expressed on the crystal itself, that is, mg impurity per kg crystal.

Colour in the sugar industry has a specific meaning, as shown in Section 3.4.4.3, and this was not altered.

3.6 Experiments performed

The objective of this work is to study the transfer of selected impurities into the sucrose crystal by investigating the main factors which affect this transfer. The experimental approach involved performing sets of experiments. Within each set a number of runs were performed in which one main factor was changed, while all the others were kept as constant as possible. A total of 39 such sets of experiments were performed and each set was identified by a name, such as AB25, CS15, W136, etc. These codes will be found throughout this work, as set identifiers. A list of all the codes is given in Appendix 1.

The following basic quantities were always measured for each run within the sets:

the sucrose crystallisation rate, G ($kg/m^2/s$)

the mass of sucrose (kg) crystallised per second

the rate of impurity transfer, R_i ($kg/m^2/s$), for each relevant impurity

the concentration of each relevant impurity in the feed liquor, F_i, expressed as mg impurity per kg of water in the liquor

the concentration of each relevant impurity in the crystal, X_i, expressed as mg impurity per kg of crystal

the temperature, T, at which the crystallisation run was performed

and the characteristic dimension, L_c (m) of the crystals.

In addition, a certain number of sets required the following quantities:

the viscosity (Pa s) of the mother-liquor

the concentration of sucrose in the feed liquor, expressed as kg per kg liquor.

The possibility that the presence of impurities in the sucrose crystal is due to the simple inclusion of mother-liquor in the crystal was investigated experimentally in sets KL15 and R15. The other main factors investigated were the rate at which sucrose crystallises, the temperature at which the crystallisation takes place, the type and concentration of the impurity, the viscosity, and, finally, the diffusivity of the various species.

3.6.1 **Testing for mother-liquor inclusion in the sucrose crystal**

Impurities can find their way into the sucrose crystal basically by two different mechanisms.

Mother-liquor can be trapped into microscopic crevasses in the growing crystal or impurities can enter the crystal surface by other mechanisms, such as adsorption and co-crystallisation, without the mother-liquor, as such, being involved. The first mechanism would be species independent but this would not be the case for the second. The ratios of the concentrations of the impurities in the mother-liquor and in the crystal would be similar if the first mechanism predominates.

Sets of experiments involving three or four different impurities, at different concentrations in the feed liquors, were performed under the same crystallisation conditions. Feed liquors and crystals were analysed for the various impurities. Some basic experimental conditions are given in Table 3.6.

Table 3.6

Experimental conditions to test for mother-liquor inclusion

Set	Species	Average concentration in feed/mg/kg water	Temp/ °C	G/ kg/m²/s	Crystallisation time/s	L_c/m
KL 15	Lithium Potassium Starch	1120 4495 16570	70	$1,8 \times 10^{-5}$	7800	0,000262
R 15	Colour Calcium Potassium Starch	8810 3730 4630 2165	63	$1,3 \times 10^{-5}$	9600	0,000229

3.6.2 The effect of the sucrose crystallisation rate on impurity transfer

The rate at which sucrose is crystallised (G, kg/m²/s) has an effect on the rate at which non-sucrose species are transferred (R_i, kg/m²/s) into the crystal. The aim of this set of experiments was to measure this effect.

G was varied by changing the energy input (see Section 3.1.1) into the crystalliser, which changes the time needed for the crystallisation of the same masses of feed liquor. The temperature of the

crystallisation and final crystal size were not allowed to change (by keeping the feed mass, volume of slurry and condensate mass the same) and the concentrations of non-sucrose species in the feeds were kept constant within each set. Typical data for some of the sets are given in Table 3.7.

Table 3.7

Typical data to determine the effect of G on impurity transfer rates

Set	Temp/ °C	Concentration in Feed			Crystal		Crystallisation time/s	G
		Colour/ colour units	Potassium	Lithium	L	W		
			/mg/kg water		/µm			/10^{-5} kg/m²/s
COND 16	62,8	-	-	1772	264	192	7200-15900	0,9-1,7
HRM 16	62,8	2856	-	1692	302	140	7810-12900	1,0-1,6
X 19 FL	65,5	413	3240	-	317	236	2480-19200	0,9-4,6
X 19 J2	65,0	1341	5116	-	313	193	4000-16810	0,9-5,0
X 19 J4	67,5	6978	6109	-	436	175	4390-20590	1,1-3,2
GHR	67,3	965	-	-	250	180	7810-17700	0,8-1,5
GHR	67,6	-	6389	-	288	151	9430-15700	0,7-1,4

3.6.3 Effects of temperature

The objective of this set of experiments was to measure the effect of temperature on the rate of crystallisation of sucrose and on the rate of impurity transfer.

In the present work, the temperature range that could be used was limited. Below 55°C, the massecuite in the crystalliser was too viscous. This caused a reduction in circulation resulting in secondary nucleation and charring. Above about 85°C, thermal decomposition started to take place and colour, for example, increased. All the tests were therefore performed between 60 and 80°C. Feed liquor quality needed to be constant for each run in a given set. Normally a set would consist of three runs, one each at 60, 70 and 80°C. The temperature was obtained by setting the absolute pressure in the crystalliser to the required level. The crystallisation runs were

then performed using the same feed mass and quality for all the runs in a set. There were no duplicates within any one set, but 14 sets were performed thus providing replication.

The temperature sensor in the crystalliser was calibrated against a certified thermometer.

Initial data on the feed liquors used in these investigations are given in Table 3.8.

Table 3.8

Details on the sets of experiments performed to investigate the effect of temperature

Set	Feed Liquor Quality				
	F_c/ Colour units	F_K	F_{Li}	F_{Ca}	F_{st}
		/mg/kg water			
AP 13	13830	17370	2160	4765	-
HT 14	930	5480	-	-	3575
MT 13	-	2800	860	2525	-
HRB 15	1040	2910	-	100	-
HTA 13	865	9900	-	-	-
NB 16	1480	2660	-	-	-
HTD 13	630	12765	-	-	2260
ST 13	2050	-	-	5320	900
SCA 13	195	-	-	4115	1800
F 13	-	3090	-	-	-
F 46	-	3680	-	-	-
W 135	785	7145	-	1225	-
W 246	745	7750	-	1400	-
CMC 13	210	3680	-	-	-

3.6.4 The effects of type and concentration of non-sucrose species

The type and concentration of non-sucrose species present in the feed liquor are expected to have an effect on the transfer of these species into the sucrose crystal. The objective here was to

measure the rate of impurity transfer and the effect of concentration on it, for each of the selected non-sucrose species.

A set of crystallisation runs, normally consisting of five runs, involved preparing five sub-samples of the same feed liquor spiked with differing amounts of the impurities selected for this set. Other factors such as temperature, sucrose crystallisation rate, crystal size, etc., were kept constant for all the runs. Typical details concerning 11 of the sets are given in Table 3.9.

Table 3.9

Typical conditions for the measurement of the rates of impurity transfer for various impurities

Sets	Temp/° C	G/ 10^{-5} kg/m^2/s	Crystal		Number of runs	Species monitored
			Length/ µm	Width/ µm		
TR 18	69,7	1,8	224	184	8	Colour,K^+,Ca^{2+}
S 16	62,8	1,4	262	187	6	Colour,K^+,Ca^{2+}
KL 15	69,8	1,8	281	228	5	K^+,Li^+,Starch
CS 15	69,4	1,6	237	196	5	Ca^{2+},Starch
LN 15	69,6	1,6	251	200	5	Li^+,Ni^{2+}
CN 15	70,1	1,6	297	213	5	Ca^{2+},Ni^{2+}
R 15	62,9	1,3	246	199	5	Colour,K^+,Ca^{2+},Starch
ML 15	69,4	1,8	285	225	5	Methylene blue
MYB 14	69,5	1,7	280	208	4	Methyl blue
AB 25	69,3	2,0	322	240	4	Acid blue 25
C 16	69,4	1,9	330	250	6	Methylene blue

3.6.5 **Effects of viscosity**

If a transport mechanism is involved during the incorporation of impurities into the crystal, then viscosity would have an effect. The aim of this series of experiments was to investigate this

hypothesis.

A set of crystallisation runs would now involve a number of sub-samples of the same feed liquor, each having a different viscosity but being otherwise similar, which is difficult if not impossible to achieve. Commercially available polysaccharides, namely carboxymethyl cellulose (CMC) or carrageenan, were used to increase the viscosity of the sub-samples. The polysaccharides were dissolved directly into the feed liquors, with heat (60°C) and stirring, at concentrations ranging from 0,2 to 0,5% (m/m). The sub-samples of feed liquor, for a given set, were crystallised, at a given temperature and fixed energy input. The feed rate was then adjusted as required, to maintain a steady concentration, based on boiling point elevation and/or torque, in the crystalliser.

Mother-liquor viscosity was measured, at the temperature of the crystallisation run. The total polysaccharide contents in the feed liquors and resulting affinated crystals were determined.

The use of CMC is known to make solutions non-Newtonian, which could complicate the results.

3.6.6 **Measurement of diffusion coefficients**

The possible model of a transport mechanism for colour transfer has been mentioned in Section 1.1.2.5. Diffusivities of the non-sucrose species could then be relevant and an experimental procedure was developed to measure these quantities. Since the various non-sucrose species diffuse through a layer of highly concentrated sucrose solution at high temperatures, these are the conditions under which diffusivities must be measured.

The experimental approach used here is based on a method suggested by Shoemaker *et al.* (1974). When a porous unglazed porcelain disk (or frit) is filled with a liquid or solution and is then placed in a large bath of another liquid (pure solvent) or a solution of different concentration, the frit loses mass. A plot of the logarithm of the mass lost at time t versus t gives a straight line of slope $-\alpha D$, where α is an "apparatus constant", characteristic of the frit used. The diffusion coefficient, D, can then be calculated.

Here, it is further assumed that the mass loss mentioned above is directly proportional to the

increase in the concentration of a diffusing species in the bath. If W_t and W_∞ are the concentrations at time t and at equilibrium, respectively, and $W = (W_\infty - W_t)$ then the logarithm of W plotted versus time gives a straight line of slope $-\alpha D$.

The apparatus used for measuring the diffusion coefficients consisted of a lagged plastic container capable of holding about eight litres of bath solution. A circulator was located in the container to stir the contents gently and to maintain the set temperature. The frit (porosity 3, diameter 80 mm) was devised from a Buchner funnel, with the stem and rim shortened. The frit was fitted with two stainless steel legs and could stand with its base off the bottom of the container, to allow circulation. The apparatus is shown schematically in Figure 3.10.

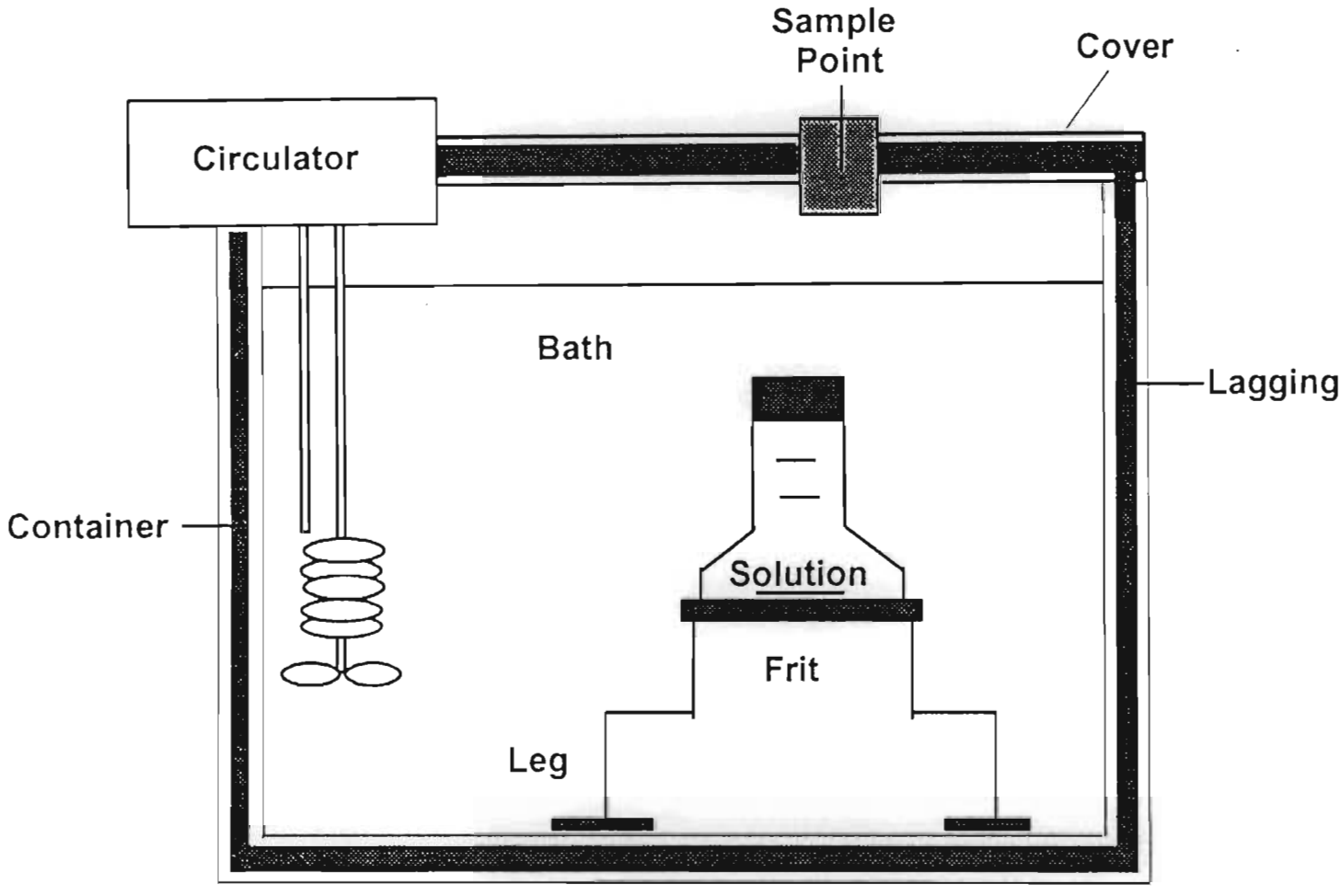

Figure 3.10 Diagram of the diffusivity apparatus.

It was necessary to calibrate this apparatus in order to obtain α. This was done by allowing potassium chloride to diffuse in water at 25°C. The frit was filled with a solution of potassium chloride (1 molar) and placed in the bath, containing 5800 cm^3 of water. Samples (10 cm^3) of the bath solution were removed every 15 minutes for 6 hours. When a sample was taken, 10 cm^3 of water were added to keep the volume constant in the container. The samples were analysed for potassium and the results corrected for the addition of water. The frit constant could then be calculated by making use of the value of D for the potassium ion (1,96 x 10^{-9} m^2/s) available in the literature (Atkins, 1994, page C28).

A similar procedure was used to measure the diffusion coefficients of the non-sucrose species in sucrose solutions:

- The bath solution consisted of a refined sugar solution of the set concentration, usually between 65 and 75% (m/m) sucrose.
- The frit solution consisted of KCl (20 g), $CaCl_2.2H_2O$ (30 g), $NiCl_2.6H_2$ (40 g) and LiCl (15 g) tested in turn and dissolved in a refined sugar solution of concentration equal to that of the bath for that run.
- The temperature was set at 70°C.
- Samples were taken every 4 hours, from about 8 am to about 5 pm, over a period of just over 100 hours, but no sampling was done between 6 pm and 6 am.
- Each sample taken was replaced by the same volume (10 cm^3) of the bath solution.
- Samples were analysed for K^+, Ca^{2+}, Ni^{2+} and Li^+ by atomic absorption. The results were corrected for the addition of bath solution.

The value of the frit constant as obtained in the calibration was then used to calculate the diffusion coefficients, for each species tested at 70°C in concentrated sucrose solutions.

CHAPTER 4

RESULTS

The experimental programme of this work consisted of six main series of experiments, as described in Section 3.6. The results obtained from each of these sets are presented in this Chapter. It is also possible to use the results obtained from the six main series of experiments to calculate partition coefficients and adsorption isotherms (see Section 1.2.1 and 1.2.2 respectively). Since these concepts can throw light on mechanisms of impurity transfer, they are evaluated in this Chapter.

Finally, the relevance of the two-step model and of an interfacial breakdown model (see Section 1.2.3 and 1.2.4, respectively) are discussed.

4.1 Testing for mother-liquor inclusion in the sucrose crystal

Two sets of experiments, identified as KL15 and R15, as described in Section 3.6.1, were performed to investigate whether a mother-liquor inclusion process can account for the presence of impurities in the sucrose crystal.

The concentrations of impurities in the feed liquors, F_i, in mg per kg water in the feed liquor (see Section 3.5), and in the crystals, X_i, in mg per kg crystal, for each run within the two sets of experiments are given in Table 4.1. The averaged ratios of the concentrations of selected pairs of impurities, in the feed and in the crystal, can now be calculated and are shown in Table 4.2. The concentrations of impurities in the crystal have been related to those in the feed liquors by linear regressions, using the method of least squares, and these results are given in Table 4.3. Finally, the results for the R15 set, shown in Table 4.3, have been used to generate Figure 4.1. It is stressed that Figure 4.1 has been prepared only to illustrate the differences between the transfers of the impurities, particularly starch, for equal but arbitrary concentrations of the impurities in the feed liquor. This is why the actual points have not been included.

Table 4.1

Concentrations of the impurities in the feed liquors and in the crystals used to test for mother-liquor inclusion in the sucrose crystal

Set	In feed/mg/kg water				In crystal/mg/kg			
	Lithium		Potassium	Starch	Lithium		Potassium	Starch
KL 15	673		3143	10950	1,0		6,5	2065
	2861		1320	2340	1,5		3,0	360
	103		10741	19940	0,1		13,0	3710
	1576		2026	5820	1,0		4,5	575
	376		5244	43800	0,5		8,5	4770
	Colour	Calcium	Potassium	Starch	Colour	Calcium	Potassium	Starch
R 15	11070	4974	5587	2980	168	30,9	8,8	400
	20950	8813	11440	5080	334	76,5	21,0	870
	2400	1068	1226	370	51	4,9	2,1	10
	3600	1355	1848	900	77	13,7	4,6	85
	6030	2453	3943	1490	100	15,8	5,0	165

Table 4.2

Ratios of concentrations of impurities in the feed liquor and in the crystal, expressed as the averages of five runs

Set	Concentration ratios
KL 15	$\frac{K^+/Li^+ \text{ conc. in crystal}}{K^+/Li^+ \text{ conc. in feed}} = 2$
	$\frac{\text{Starch } /K^+ \text{ conc. in crystal}}{\text{Starch } /K^+ \text{ conc. in feed}} = 85$
R 15	$\frac{\text{Colour}/K^+ \text{ conc. in crystal}}{\text{Colour}/K^+ \text{ conc. in feed}} = 10$
	$\frac{\text{Starch}/K^+ \text{ conc. in crystal}}{\text{Starch}/K^+ \text{ conc. in feed}} = 64$
	$\frac{Ca^{2+}/K^+ \text{ conc. in crystal}}{Ca^{2+}/K^+ \text{ conc. in feed}} = 4$

The results in Table 4.2 are seen only as indicating large differences between the pairs of impurities. There is scatter, but ratios varying from 2 (K^+/Li^+) to 85 (starch/K^+) are seen as reasonable indications of large differences in behaviour among the species.

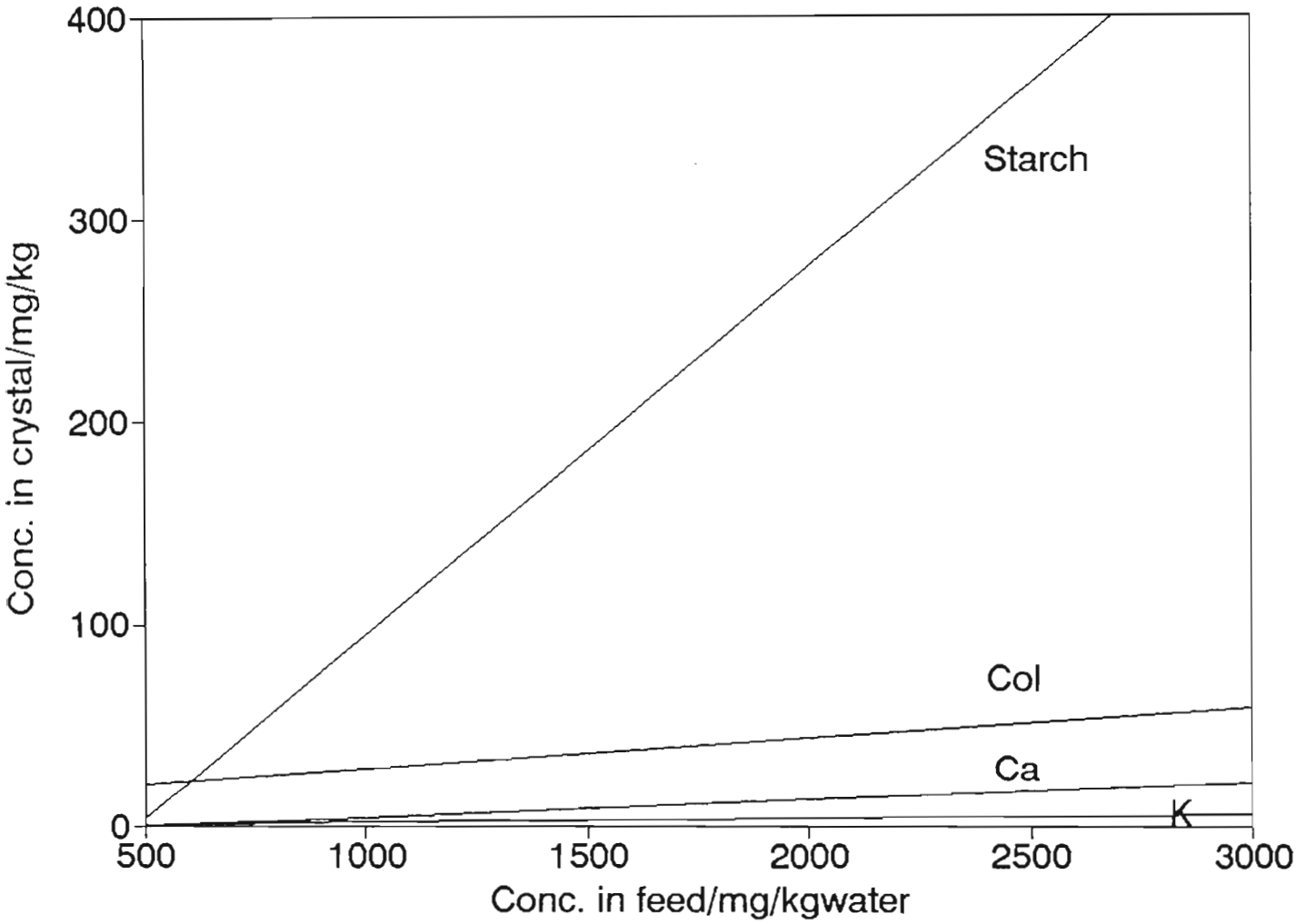

Figure 4.1 **The linear relationships (Table 4.3) used to illustrate the differences between the transfers of colour, calcium, potassium and starch. The data used for these plots are from the R15 set of experiments.**

Table 4.3

Relationships between the concentrations of impurities in the crystal and those in the feed liquors

Set	$X_i = a + bF_i$	n	r^2	95% Confidence interval for b
KL 15	$X_{Li} = 0,34 + 0,00043\ F_{Li}$	5	0,805	0,0003
	$X_K = 2,56 + 0,0010\ F_K$	5	0,967	0,0003
	$X_{st} = 500 + 0,11\ F_{st}$	5	0,870	0,08
R 15	$X_c = 13,8 + 0,015\ F_c$	5	0,994	0,002
	$X_{Ca} = -3,3 + 0,0087\ F_{Ca}$	5	0,962	0,006
	$X_K = -0,37 + 0,0018\ F_K$	5	0,968	0,0006
	$X_{st} = -87,6 + 0,18\ F_{st}$	5	0,989	0,04

The values of the intercepts (a) in Table 4.3 were investigated statistically to test whether they are different from zero. The test statistic $T_{o;o}$ was calculated:

$$T_{o;o} = \frac{(\text{Intercept} - 0)}{s\sqrt{\frac{1}{n} + \frac{\bar{x}^2}{d^2}}}$$

where s is given by $\sqrt{\frac{1}{n-2}\sum (Y_{iobs} - Y_{icalc})^2}$

$\bar{x}$ is the mean of the x_i values

and $d = \sum \sqrt{(x_i - \bar{x})^2}$

$T_{o;o}$ was then compared to the critical value $t_{0,025;\ n-2}$, using the conventional hypothesis testing procedures.

With five observations in each regression and a probability level of 95%, the value of $t_{0,025;\ n-2}$ is 3,18. Only one value of $T_{o;o}$ (4,30) was above the critical value, and this was for the potassium

regression, in set KL15. All the other values of $T_{o;o}$ were much smaller than the critical value, indicating that these intercepts are not statistically different from zero.

The results shown in Tables 4.2 and 4.3 and in Figure 4.1 indicate that both the absolute values and the rates of change are different for the various species. Starch and colour show high transfer values and there are differences among the ionic species. Generally, transfer rates and concentrations in the crystal follow the trend

Starch > Colour > Calcium > Potassium> Lithium.

Since inclusions of the different species are not equally favoured, it can be concluded that a simple physical inclusion of mother-liquor in the crystal is not the only mechanism. This conclusion is strengthened by the following result, based on an observation made by Murray (1972). He noticed that the calcium carbonate precipitate produced during the processing of sugar liquors of high starch content, contained a higher ratio of amylopectin:amylose inside the calcium carbonate crystal while the reverse was found at the surface of the calcium carbonate crystal. This splitting up of the starch molecule was investigated with respect to the sucrose crystal in the present work by performing a crystallisation run using a feed liquor of high starch content. The sucrose crystals were washed with water during the centrifuging step to produce a wash-liquor and washed crystals, in addition to the normal affinated crystal. The feed and wash liquors, and the washed and affinated crystals, were then analysed for their starch content by the usual starch-iodine coloured complex formation as described in Section 3.4.4.4, but the solutions were scanned over a wavelength range of 450 to 700 nm. The spectra are shown in Figure 4.2 where the absorbance ratio, namely the absorbance at each wavelength divided by the maximum absorbance (A_i/A_{max}), has been plotted versus the wavelength. It is evident that the absorption peak is at 575 nm for the feed and wash liquors but at 600 nm for the affinated and washed sugars. The maximum difference is small but consistent and shows that the amylopectin:amylose ratio inside the sucrose crystal could be different to that in the solution. This conclusion is based on the fact that the wavelength at which absorption is a maximum depends on the ratio of amylopectin to amylose in the starch since the amylopectin:iodine and amylose:iodine complexes show maximum absorptions at different wavelengths, namely 550 and 625 nm respectively.

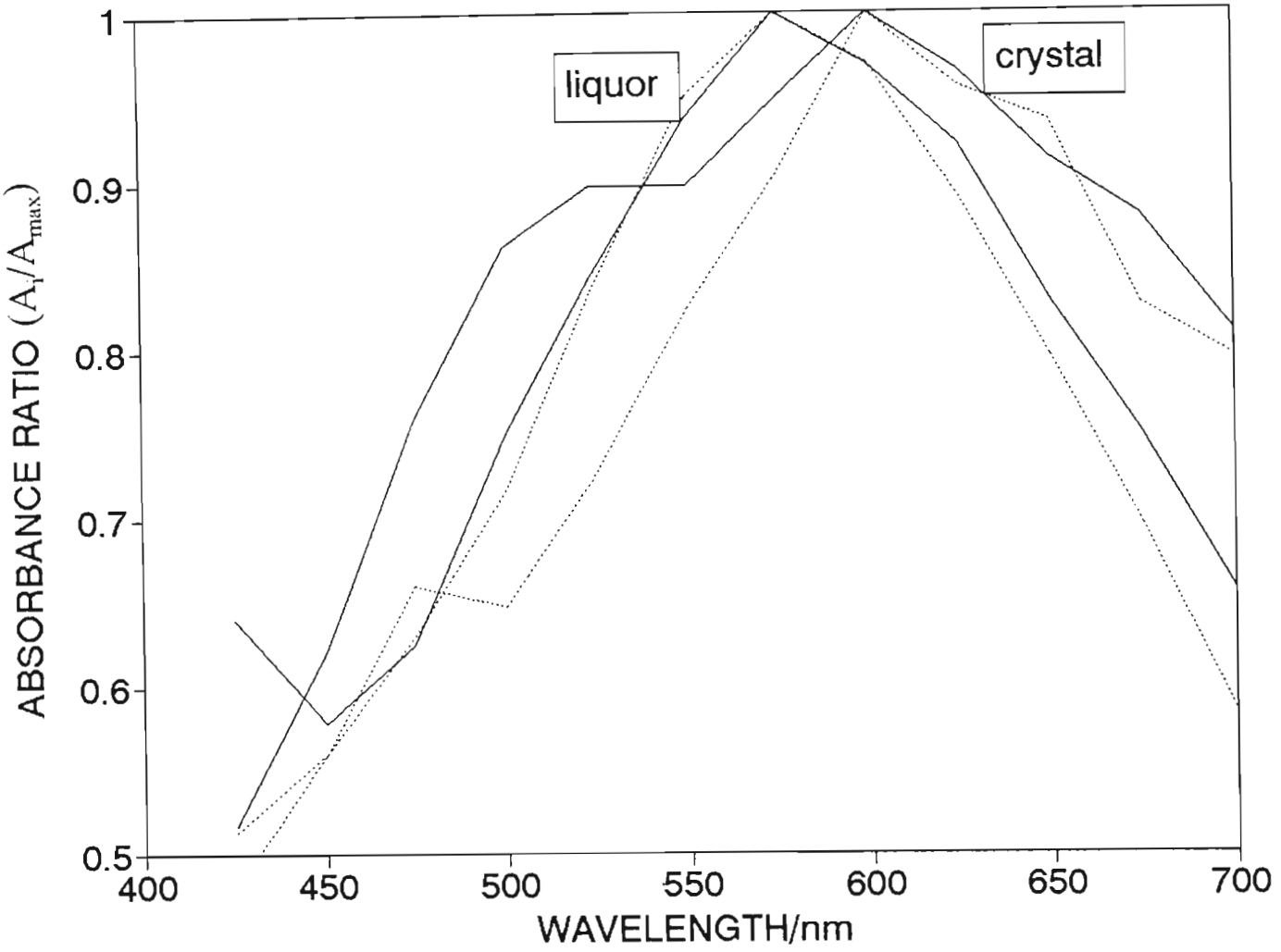

Figure 4.2 **Absorbtion spectra for the starch-iodine complexes formed from the starch present outside and inside the sucrose crystals. The solid lines refer to samples from set R15 while the dotted lines refer to samples from set KL15.**

4.2 The crystallisation rate of sucrose

The rate at which sucrose is crystallised is well documented in the literature. In this work this rate has been quantified through a mass growth rate, G, in $kg/m^2/s$, derived and calculated as shown in Section 2.2.2.

Two aspects will be covered in this section. The first will deal with the numerical values found for G in this work, and these will be compared with values for the crystallisation rate of sucrose published in the literature. Secondly the relationship between G and R_i will be investigated, using results from the series of experiments described in Section 3.6.2.

4.2.1 Values of G obtained in this work

Thirty-nine sets of experiments were performed during this work (see Appendix 1) and, as shown in Section 3.6, G was obtained for each run in the 39 sets of experiments. These values and comparable data from the literature are shown in Table 4.4. In all cases the averages are simple arithmetic averages of all the available values in the sets. The values found in this work compare well with those published, particularly with those from South African refineries.

Table 4.4

The mass growth rate of sucrose crystals, G, obtained in this work and from the literature

	G/kg/m²/s		
	Min.	**Max.**	**Average**
This work	$6,0 \times 10^{-6}$	$2,3 \times 10^{-5}$	$1,5 \times 10^{-5}$
Guimaraes *et al.* (1995)	$0,1 \times 10^{-5}$	2×10^{-5}	-
Grimsey and Herrington (1994)	2×10^{-5}	13×10^{-5}	-
Kraus and Nyvlt (1994)	$0,2 \times 10^{-6}$	4×10^{-6}	-
Lionnet (1989) for South African Refineries	1×10^{-5}	6×10^{-5}	3×10^{-5}
Maurandi *et al.* (1984)	$0,2 \times 10^{-5}$	2×10^{-5}	1×10^{-5}
Bennett and Fentiman (1969)	2×10^{-5}	20×10^{-5}	-

The determination of G does not require that the mass of crystals be known. This is an advantage under industrial conditions where it is usually impossible to obtain this quantity. It has however been shown in Section 2.1 that the mass of crystals can be calculated for the crystallisations performed in the pilot crystalliser and it is thus possible to compare G to a simple mass based crystallisation rate given by the mass of crystals produced per unit time. It is not expected that G and the mass based crystallisation rate will correlate to a high degree (which would imply that G is not much better than the simple mass rate) but some agreement is expected. G and the mass based rate were used in a linear correlation based on the least squares method, to yield equation 4.1:

$$G = -4,0 \times 10^{-6} + 0,013 \times \text{mass of crystal (kg) per second} \qquad \text{.....4.1}$$

with a correlation coefficient of 0,30 (statistically significant at 1%) for 158 pairs of observations. The data has been plotted in Figure 4.3 which shows the expected scatter.

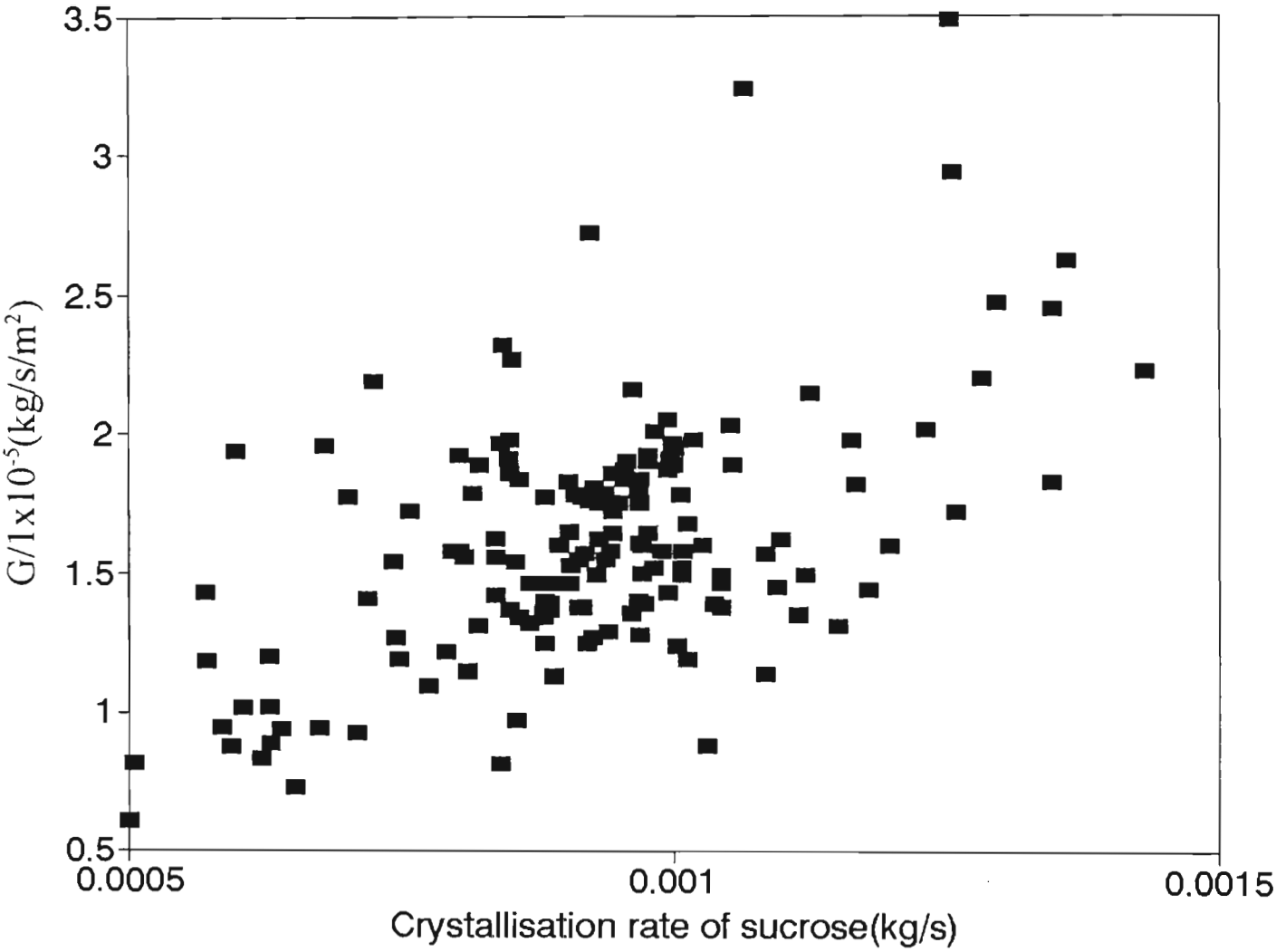

Figure 4.3 **The relationship between G ($kg/m^2/s$) and a simple mass based crystallisation rate (kg/s).**

4.2.2 **The effect of G on the rate of impurity transfer**

The effect of G on impurity transfer rates is now investigated. It was shown in Section 3.6.2 that G was varied by changing the energy input into the evaporative crystalliser while keeping the other factors constant within each set of experiments. Seven sets of experiments were carried out to investigate the effect of G on the transfer rates for colour, potassium and lithium, the details of which were given in Table 3.6, page 75.

The impurity transfer rates, R_i, were then related to G through linear regressions, by the method of least squares, using logarithmic transformations (ln R_i and ln G), to yield equations of the form

$$R_i = a\, G^b \qquad \text{.....4.2}$$

where a and b are regarded as constants.

The results from all the regressions are shown in Table 4.5 while the data from three sets, selected randomly, have been used to produce Figure 4.4. It can be concluded that there is a statistically significant relationship between G and the impurity transfer rates; as G increases, the rates also increase. For colour and for potassium, G is raised to a power close to 1. The higher value for lithium and the decreased reproducibility between the two sets are probably due to low concentrations of lithium in the crystal, and thus lower analytical precision.

Table 4.5

The effect of G on the transfer rate for colour, potassium and lithium

Species	Set	$R_i = a\,G^b$		n	r^2
		a	b		
Colour	HRM 16	3134	1,4	6	0,904
	X19FL	1,6	0,85	9	0,932
	X19J2	15,2	1,0	9	0,988
	X19J4	123	1,1	9	0,914
	GHR	171	1,2	6	0,950
Potassium	X19FL	$1,2 \times 10^{-7}$	0,80	9	0,792
	X19J2	$1,6 \times 10^{-6}$	1,0	9	0,929
	X19J4	$7,5 \times 10^{-6}$	1,1	9	0,964
	GHR	$1,0 \times 10^{-4}$	1,3	6	0,911
Lithium	COND16	$4,4 \times 10^{-6}$	1,2	6	0,916
	HRM16	0,19	2,1	6	0,905

It has been shown in Section 2.3 that R_i is a function of G and of the concentration of impurity in the crystal, X_i. It is established here that R_i does increase with G and that the exponent in the equation $R_i = aG^b$ is generally close to 1 as would be expected. The effect of G on the impurity transfer rates will be investigated in more depth in Section 4.3.5 where data from all the relevant sets of experiments will be used in multiple linear regressions.

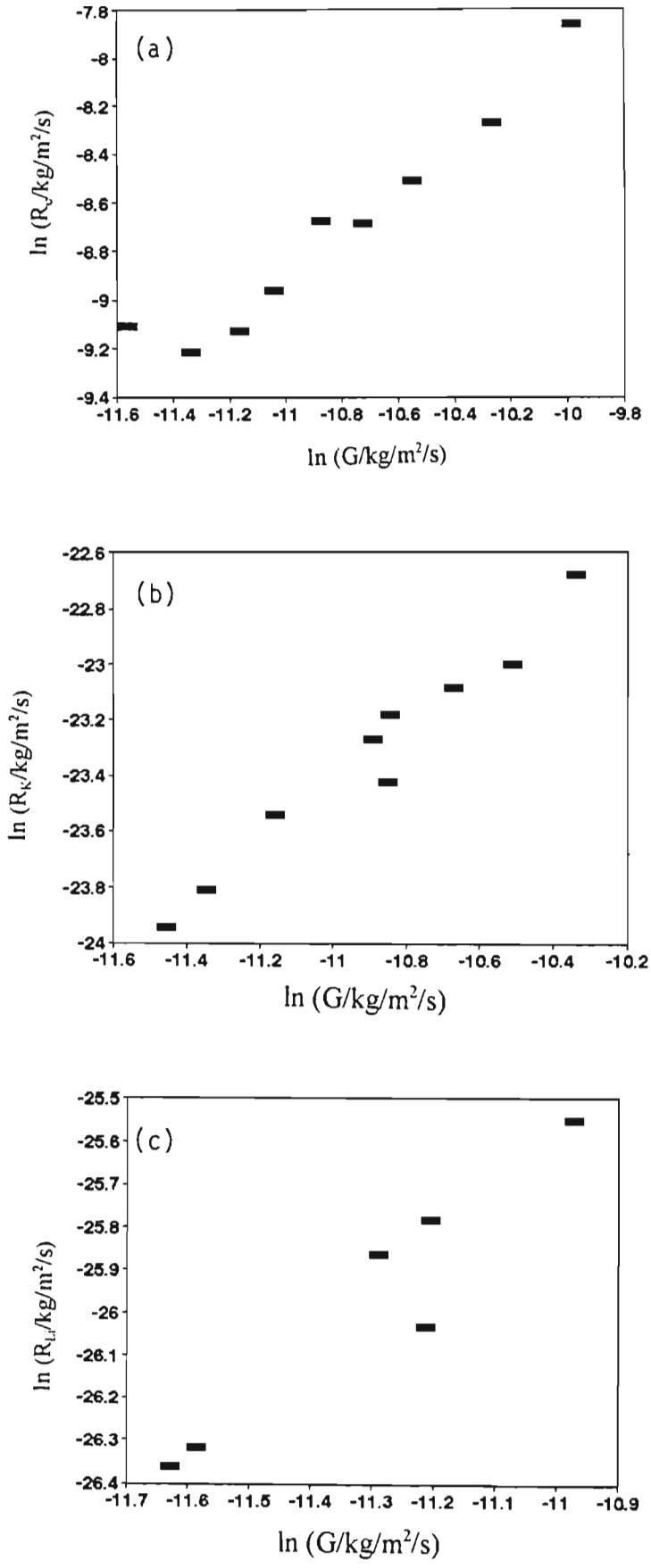

Figure 4.4 **The effect of G on (a) R_c, (b) R_K and (c) R_{Li}.**

4.3 **The effects of temperature**

The effect of temperature was investigated by setting the absolute pressure in the evaporative crystalliser to obtain crystallisation temperatures between 60 and 80°C. The same feed mass and quality were used for all the runs in a set. Table 3.7 in Section 3.6.3 gives the details of 14 sets of experiments involving colour, potassium, lithium, calcium and starch as impurities. The Arrhenius model namely

$$\ln k = \ln A_{pf} - \frac{E_a}{RT}$$

is used to investigate the effect of temperature on G and on the rates of impurity transfer. In each case the logarithm of G or of R_i was related to 1/T through linear regressions using the method of least squares. A linear fit, indicated by a high correlation coefficient and normal residuals shows that the process follows the Arrhenius model. The slope of the line is then equal to $-E_a/R$, where E_a is the activation energy and R the gas constant (8,314 J/K/mol). The results obtained are shown in Tables 4.6 to 4.10. In most cases the confidence intervals are wide, but this could be affected by the small number of observations in each set.

Table 4.6

Results of the Arrhenius plot for G

Set	Number of observations	r^2	E_a/kJ/mol ± 95% confidence interval
AP 13	3	0,991	25,9 ± 30,6
HT 14	4	0,707	9,8 ± 19,3
MT 13	3	0,603	33,6 ± 346
HRB 15	5	0,893	20,8 ± 13,3
HTA 13	3	0,753	8,1 ± 59,1
NB 16	6	0,194	-
HTD 13	3	0,989	14,4 ± 19,1
ST 13	3	0,920	22,4 ± 84,0
F 13	3	0,654	11,7 ± 108
F 46	3	0,086	-
W 135	3	0,900	8,2 ± 34,8
W 246	3	0,112	-
CMC 13	3	0,992	26,8 ± 10,0

Table 4.7

Results of the Arrhenius plot for R_c

Set	Number of observations	r^2	E_A/kJ/mol ± 95% confidence interval
AP 13	3	0,983	35,2 ± 58,3
HT 14	4	0,954	17,0 ± 11,3
HRB 15	5	0,888	34,2 ± 22,4
HTA 13	3	0,878	16,2 ± 77,0
NB 16	6	0,954	17,8 ± 5,4
HTD 13	3	0,960	14,3 ± 52,3
ST 13	3	0,856	29,1 ± 200
SCA 13	3	0,000	-
W 135	3	0,999	12,5 ± 2,5
W 246	3	0,979	11,8 ± 32,5

Table 4.8

Results of the Arrhenius plot for R_K

Set	Number of observations	r^2	E_A/kJ/mol ± 95% confidence interval
AP 13	3	0,979	22,2 ± 40,8
HT 14	4	0,030	-
MT 13	3	0,825	63,6 ± 372
HRB 15	5	0,470	27,3 ± 53,6
HTA 13	3	0,999	13,2 ± 1,0
NB 16	6	0,695	24,2 ± 22,4
HTD 13	3	0,988	27,0 ± 9,7
F 13	3	0,694	23,9 ± 202
W 135	3	0,970	31,3 ± 70,0
CMC 13	3	0,637	15,8 ± 151

Table 4.9

Results of the Arrhenius plot for R_{Ca}

Set	Number of observations	r^2	E_A/kJ/mol ± 95% confidence interval
AP 13	3	0,967	47,7 ± 111
MT 13	3	0,672	73,6 ± 654
ST 13	3	0,760	36,6 ± 84,0
SCA 13	3	0,678	12,8 ± 112
W 135	3	0,938	8,4 ± 27,4
W 246	3	0,579	10,4 ± 113

Table 4.10

Results of the Arrhenius plot for R_{Li}

Set	Number of observations	r^2	E_A/kJ/mol ± 95% confidence interval
AP 13	3	0,999	23,3 ± 4,4
MT 13	3	0,276	28,7 ± 589

The data in Tables 4.6 to 4.10 have been used to produce overall values for the various activation energies, using two different approaches. In the first approach arithmetic averages and 95% confidence intervals for the activation energies for G, R_c, R_K and R_{Ca} were calculated. The formula used for the 95% confidence interval was

$$95\%\ CI = \pm \frac{t_{v;\frac{\alpha}{2}} \times s}{\sqrt{n}}$$

where t_v; $\alpha/2$ is the Student's t value for a degree of freedom equal to v and a probability of $\alpha/2$; s is the standard deviation of the activation energy values and n is the number of observations. For

lithium, the value of n is 2 (see Table 4.10) which was considered too low to yield a meaningful confidence interval.

The second approach involved using all the data for a given impurity (or for G) in one overall regression. For example Table 4.7, for colour, contains information from 10 sets of experiments, or a total of 36 runs; data from all 36 runs were then used in a single regression.

The results obtained by the two approaches are given in Table 4.11. Within experimental error the two approaches yield the same value.

Table 4.11

Activation energies, calculated by two different approaches, for G and for R_i, for a temperature range of 60 to 80°C

	E_a/kJ/mol			
	Aver. ± 95% conf. interval	Single regression approach		
		E_a	n	r^2
G	18 ± 6	14	45	0,44
R_c	21 ± 7	19	36	0,18
R_K	28 ± 11	39	36	0,26
R_{Ca}	32 ± 27	25	15	0,10
R_{Li}	26 ± 34	46	6	0,25
R_{sl}	0	0	13	0,00

The following comments may now be made:

- The single regression approach may not always be successful. This problem is illustrated here with the data from the two series (AP13 and MT13) for lithium, as shown in Figure 4.5. When treated separately, as done in Table 4.10, two reasonably similar values for the activation energy are obtained. The single, overall, regression however yields a relatively large value. As is evident from Figure 4.5 the slopes of the lines from sets AP13 and MT13 are reasonably similar but the intercepts are different, due probably to different crystallisation conditions.

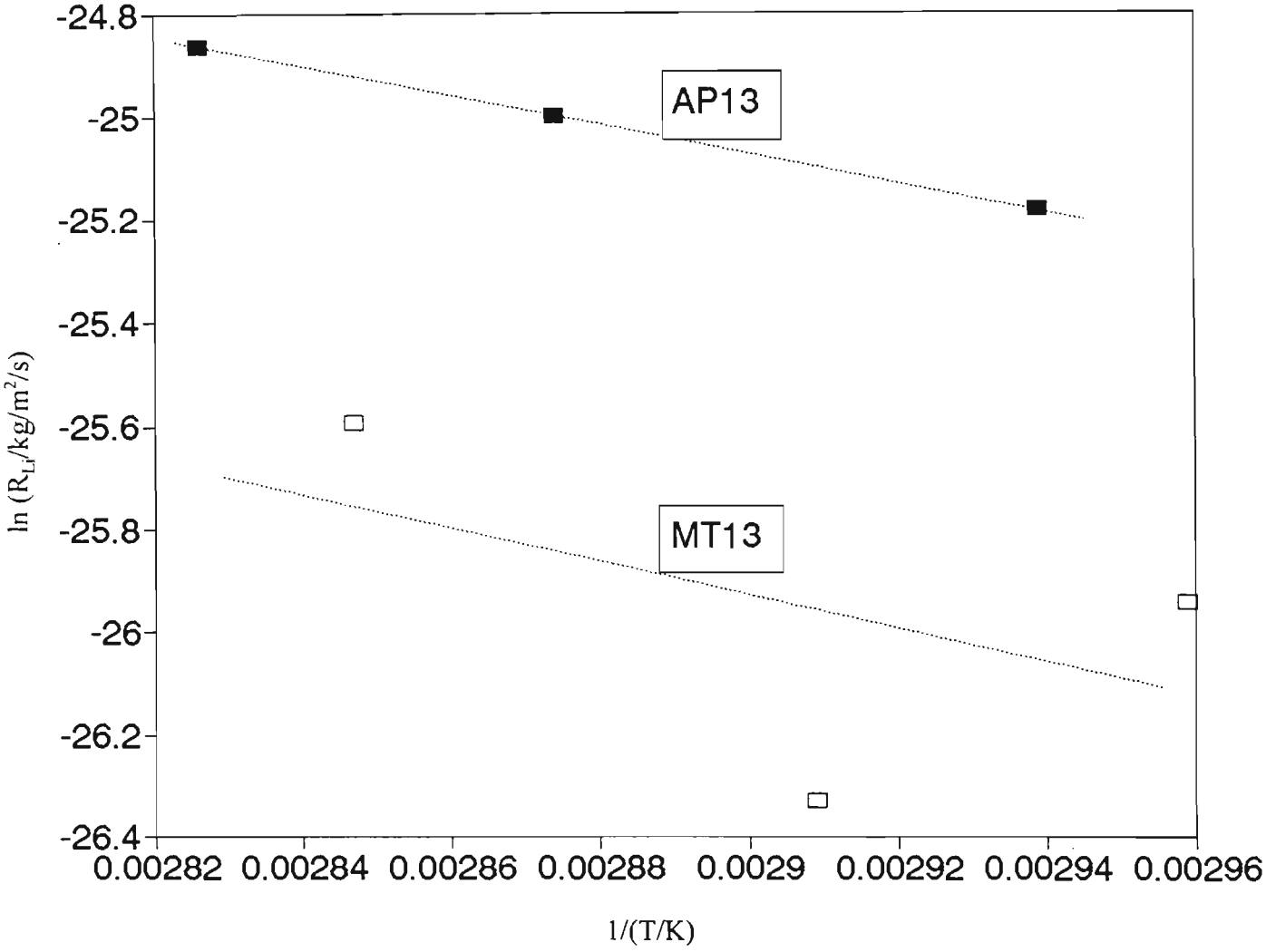

Figure 4.5 The Arrhenius plot for $R_{Li,}$ for sets AP13 and MT13, shown individually.

- The activation energy of the crystallisation rate of sucrose has been well investigated in the literature. Honig (1959) reviews the early work and, at constant supersaturation, gives values of 19-29 kJ/mol over the temperature range 60 to 80°C. VanHook (1945) quotes 30 kJ/mol at 60-80°C. More recently, Maurandi *et al.* (1984) quote values of 21-38 kJ/mol over a temperature range of 40-70°C. The values obtained here are not out of line and compare fairly well with the lower ranges given in the literature.

- There are no values in the literature for the activation energies of rates of impurity transfer and the results given in Table 4.11 can be taken as a first approximation for the activation energies for the transfer of colour, of the ionic species, and of starch in the sucrose crystal. The value for colour is similar to that for G, while the ionic species are somewhat higher but the precision is lower.

- In the case of starch, four sets of experiments were performed. The calculated activation energies varied from + 6 to - 30 kJ/mol, and, statistically, the activation energy for R_{st} was found not to be different from 0, with a calculated value of Student's t equal to 1.3. This result is confirmed by the single regression approach, as shown in Figure 4.6. Except for the two sets, SCA13 and HTD13, the values of the slopes and of the intercepts are different.

- Generally, the precision as measured by the uncertainties, has been low. The activation energies given here must therefore be seen as approximations, to be used to guide future work.

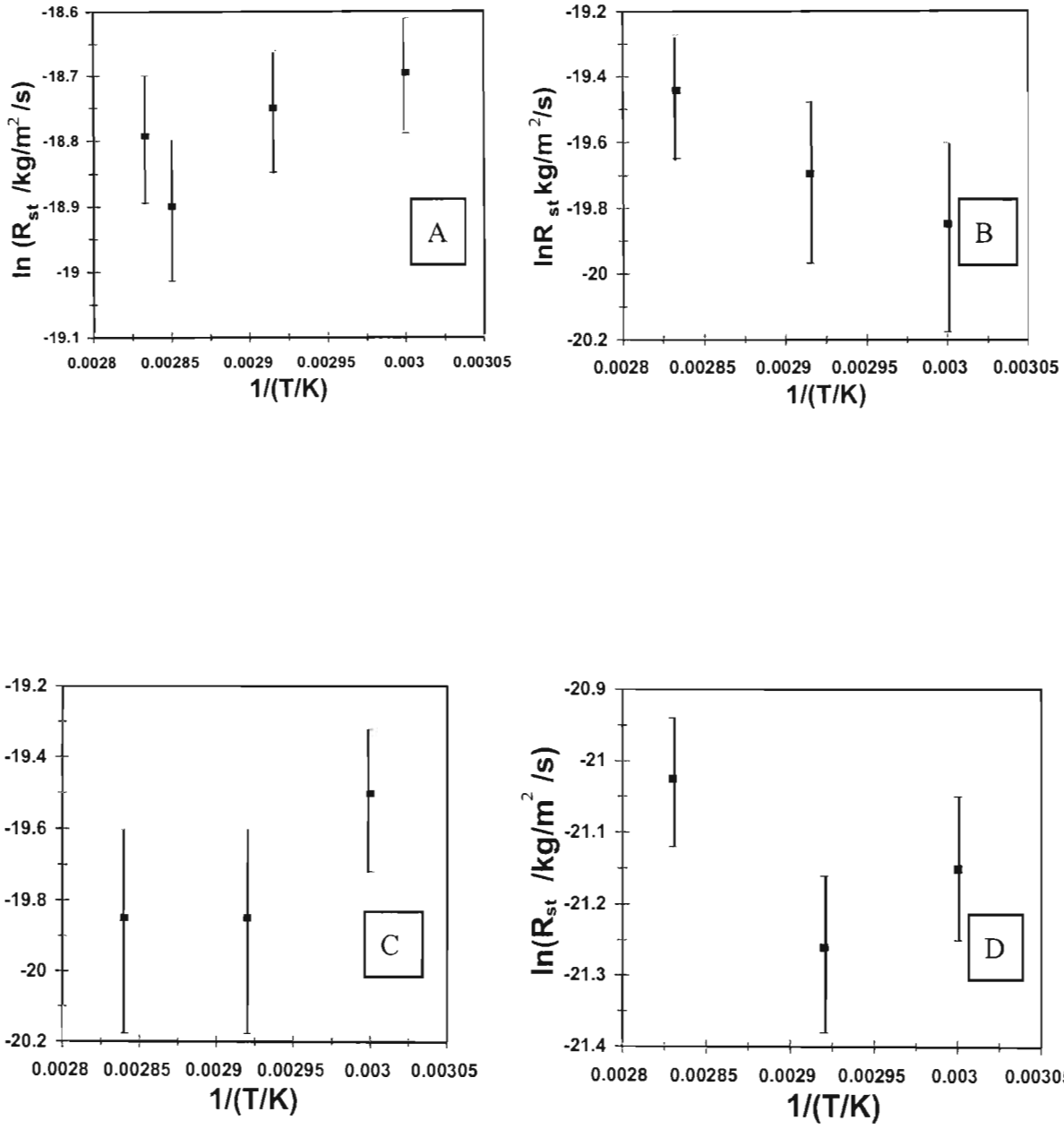

Figure 4.6 **The Arrhenius plot for R_{st}, for sets HT14:(A), SCA13:(B), HTD13:C and ST13:(D), plotted individually.**

Mullin (1993) discusses a two-step model for crystallisation, namely transport followed by surface integration. When the process is controlled by transport (or the diffusion step) the activation energy ranges from 10 - 20 kJ/mol. If it is surface integration controlled, the activation energy ranges from 40 - 60 kJ/mol. The activation energies for G and R_c are similar to those for transport controlled processes but those for the ionic species fall in between the two ranges given above.

Finally, an activation energy around 20 kJ/mol indicates an increase in rate of about 20% for a 10°C rise in temperature. With an E_a value of 30 kJ/mol the increase is now about 40%. Thus, temperature will increase the sucrose crystallisation rate but also the rate at which the selected impurities, except starch, are incorporated in the crystal.

4.4 The effects of type and concentration of non-sucrose species

Both the sucrose crystallisation rate and the temperature influence the rate at which impurities enter the crystal. The control of the rate of impurity transfer through these two factors is however limited since the sucrose crystallisation rate cannot be decreased too far because of throughput and plant utilisation considerations and, as stated in Section 3.6.3, the range of temperatures that is practical is restricted to 60-80°C.

The type and concentration of the non-sucrose species in the feed liquors are expected to have a major effect on the transfer into the crystal. Furthermore both these factors can be controlled by the purification processes used during sugar refining. Thus, the experimental work, as described in Section 3.6.4, was concentrated in that area, using feed liquors spiked with different amounts of the impurities selected for a given set. In total about 20 sets of experiments involving nearly 100 individual crystallisation runs were done. The raw data is in Appendix 2.

The results discussed here are divided into four main sub-sections, based on the experiments carried out in Section 3.6.4:

- Investigating the effect of the type and concentration of the impurity on the rate of

impurity transfer.

- Using multiple linear regression techniques to investigate the effect of type and concentration of the impurity, of the sucrose crystallisation rate, and of the crystal characteristic dimension, on the rate of impurity transfer and on the concentrations of the impurities in the crystal. This approach allows all the relevant runs for a given species to be used in one regression and thus yields overall effects.

- Developing and investigating a partition coefficient for each impurity.

- Investigating adsorption isotherms.

4.4.1 The effects of type and concentration of the non-sucrose species on the impurity transfer rate

It is expected that different impurities will be incorporated into the sucrose crystals at different rates. Sets of experiments (see Section 3.6.4) were performed to investigate the effects of each of the selected impurities. At this stage, however, data for the same impurity but from different sets cannot be grouped together since each set involved different crystallisation conditions, some examples were given in Table 3.8 on page 77.

The effect of the type of impurity and of its concentration in the feed liquor (F_i, mg per kg water in feed) on the impurity transfer rate (R_i, kg/m^2/s) was investigated for each individual set separately by linear regressions, using the method of least squares, to yield equations of the form

$$R_i = aF_i^b$$

where a and b are regarded as constants. The natural logarithm of R_i was regressed against the natural logarithm of F. The results obtained are given in Table 4.12 and allow the following conclusions to be made:

- In most cases high correlation coefficients have been obtained and the fits are normal, indicating a strong relationship between the rate at which an impurity is transferred into the crystal and its concentration in the feed liquor.

- The value of b, the exponent by which F_i is raised, does vary for one given impurity. Nevertheless it is evident that b is less than unity for colour, potassium and acid blue 25; it is close to 1 for calcium, lithium and nickel, and finally, it is higher than 1 for starch and methylene blue.

More general results would be obtained if data for a given impurity from all the sets involving that impurity could be used together. This is investigated in the next Section.

Table 4.12

Investigation of the relationship between the rate of impurity transfer, R_i, ($kg/m^2/s$) and the concentration of the impurity in the feed liquor, F_i, (mg/kg water) for various non-sucrose species

Specie	Set	$R_i = a \times F^b$		n	r^2	95% confidence interval on b
		a	b			
Colour	TR18	$1,9 \times 10^{-6}$	0,68	8	0,970	0,12
	S16	$1,0 \times 10^{-6}$	0,74	6	0,977	0,15
	R15	$0,5 \times 10^{-6}$	0,79	5	0,980	0,21
	T1	$0,8 \times 10^{-6}$	0,66	7	0,910	0,31
Potassium	KL15	$1,8 \times 10^{-13}$	0,66	5	0,995	0,08
	TR18	$1,1 \times 10^{-13}$	0,68	8	0,800	0,34
	S16	$0,6 \times 10^{-13}$	0,74	6	0,823	0,47
	R15	$0,2 \times 10^{-13}$	0,90	5	0,946	0,39
Calcium	S16	$2,7 \times 10^{-13}$	0,57	6	0,934	0,21
	R15	$1,1 \times 10^{-8}$	1,1	5	0,882	0,75
	TR18	$2,2 \times 10^{-14}$	1,2	8	0,720	0,74
	CN15	$3,0 \times 10^{-14}$	0,77	5	0,991	0,13
Lithium	KL15	$2,0 \times 10^{-14}$	0,80	5	0,904	0,48
	LN15	$1,6 \times 10^{-15}$	1,1	5	0,958	0,41
Nickel	CN15	$4,7 \times 10^{-17}$	1,4	4	0,891	0,89
	LN15	$2,8 \times 10^{-12}$	0,23	5	0,975	0,07
Starch	KL15	$1,3 \times 10^{-12}$	0,96	5	0,929	0,48
	CS15	$2,9 \times 10^{-12}$	0,92	5	0,851	0,70
	R15	$6,0 \times 10^{-15}$	1,6	5	0,974	0,47
Methylene blue	C15	$2,4 \times 10^{-13}$	0,89	5	0,679	1,1
	ML15	$2,0 \times 10^{-16}$	2,1	5	0,852	1,6
	MB15	$5,8 \times 10^{-11}$	1,6	5	0,887	1,0
Acid blue 25	AB25	$1,2 \times 10^{-12}$	0,34	4	0,818	0,48

4.4.2 **The use of multiple linear regression**

The results presented in Sections 4.2.2, 4.3 and 4.4.1 show that the rate of impurity transfer depends on the following factors:

- the sucrose crystallisation rate,
- the temperature, and
- the type and concentration of the impurity.

The effects of these factors were measured through individual sets of experiments, each with specific objectives. It is possible to combine all the runs for a given impurity and apply multiple linear regression techniques to the complete data set. This has the following advantages:

- Since all the data are used, the technique yields results which apply to the full range of the factors.

- It may be possible to quantify effects which are too small to be measured through specific experiments. This is so because of the wider range of the factors and the larger number of observations when all the data are combined. In the present work this applies particularly to possible effects of the crystal size, quantified by the characteristic length L_c, on impurity transfer rates.

- There is a wealth of statistical techniques which support multiple linear regressions. This ensures, for example, that only statistically significant independent variables are included in the regression, that correlations between the independent variables can be identified, and that the residuals are well-behaved. It is also possible to transform the independent variables (logarithms, reciprocals, etc.) and to include interactive terms.

The main limitation of the technique is that independent variables which correlate cannot be used together in a regression. The results of Section 4.3 show that G and temperature are related and thus these two factors cannot both be present in any one regression. The approach used here will

be to select all the runs involving a particular impurity to relate R_i to F_i, G and L_c and to relate X_i to F_i, G and L_c. As described in Section 3.6 the experimental part of this work involved 39 sets of experiments, each set involving a number of runs, during which all the above-mentioned quantities were measured.

For the multiple linear regressions the data were sorted out into sets, each relating to one impurity only. Thus, eight new sets of data were obtained, one each for colour, potassium, calcium, lithium, starch, methylene blue, acid blue 25 and methyl blue. Each set contains the following quantities:

R_i (kg/m^2/s), the rate of impurity transfer
X_i (mg/kg), the concentration of the impurity in the sucrose crystal
F_i (mg/kg water in feed), the concentration of the impurity in the feed liquor
G (kg/m^2/s), the crystallisation rate of sucrose
and L_c (m), the characteristic dimension of the sucrose crystal.

The number of observations, the minimum and maximum values and the arithmetic average, for each quantity, in each set, are shown in Table 4.13.

Table 4.13

Number of observations, minimum, maximum and mean values for each variable, in the eight sets of data to be used in multilinear regressions

Species	No. of observations	Variables			
		Names	Min. value	Max. value	Mean value
Colour	82	F_c	100	22430	3510
		X_c	5,2	404	79
		R_c	$2,3 \times 10^{-6}$	$2,0 \times 10^{-3}$	$3,7 \times 10^{-4}$
		G	$6,1 \times 10^{-6}$	$2,2 \times 10^{-5}$	$1,5 \times 10^{-5}$
		L_c	$1,4 \times 10^{-4}$	$3,6 \times 10^{-4}$	$2,4 \times 10^{-4}$
Potassium	59	F_K	330	17671	5205
		X_K	0,8	21	6,4
		R_K	$4,7 \times 10^{-12}$	$9,6 \times 10^{-11}$	$3,1 \times 10^{-11}$
		G	$6,1 \times 10^{-6}$	$2,2 \times 10^{-5}$	$1,5 \times 10^{-5}$
		L_c	$1,4 \times 10^{-4}$	$3,6 \times 10^{-4}$	$2,5 \times 10^{-4}$
Calcium	38	F_{Ca}	217	17531	3763
		X_{Ca}	1	12	4,8
		R_{Ca}	$5,4 \times 10^{-12}$	$7,7 \times 10^{-11}$	$2,5 \times 10^{-11}$
		G	$8,8 \times 10^{-6}$	$2,3 \times 10^{-5}$	$1,6 \times 10^{-5}$
		L_c	$1,4 \times 10^{-4}$	$4,2 \times 10^{-4}$	$2,5 \times 10^{-4}$
Lithium	29	F_{Li}	103	2955	1165
		X_{Li}	0,1	3,4	1,3
		R_{Li}	$5,3 \times 10^{-13}$	$1,7 \times 10^{-11}$	$6,3 \times 10^{-12}$
		G	$1,0 \times 10^{-5}$	$2,3 \times 10^{-5}$	$1,5 \times 10^{-5}$
		L_c	$1,7 \times 10^{-4}$	$4,2 \times 10^{-4}$	$2,5 \times 10^{-4}$

Table 4.13 (Continued)

Species	No. of observations	Variables			
		Names	Min. value	Max. value	Mean value
Starch	31	F_{st}	370	43800	4950
		X_{st}	11	4768	936
		R_{st}	$5,0 \times 10^{-11}$	$2,4 \times 10^{-8}$	$5,2 \times 10^{-9}$
		G	$1,2 \times 10^{-5}$	$2,2 \times 10^{-5}$	$1,6 \times 10^{-5}$
		L_c	$1,9 \times 10^{-4}$	$3,6 \times 10^{-4}$	$2,5 \times 10^{-4}$
Methylene blue	15	F_{myb}	23	31095	4448
		X_{myb}	0,01	81	15,1
		R_{myb}	$5,8 \times 10^{-14}$	$3,6 \times 10^{-4}$	$6,3 \times 10^{-5}$
		G	$1,3 \times 10^{-5}$	$2,2 \times 10^{-5}$	$1,7 \times 10^{-5}$
		L_c	$2,5 \times 10^{-4}$	$3,3 \times 10^{-4}$	$3,0 \times 10^{-4}$
Acid blue 25	4	F_{ab25}	106	435	232
		X_{ab25}	0,9	1,6	1,16
		R_{ab25}	$5,6 \times 10^{-12}$	$9,3 \times 10^{-12}$	$7,7 \times 10^{-12}$
		G	$1,8 \times 10^{-5}$	$2,3 \times 10^{-5}$	$2,0 \times 10^{-5}$
		L_c	$2,5 \times 10^{-4}$	$3,3 \times 10^{-4}$	$2,9 \times 10^{-4}$
Methyl blue	4	F_{mb}	80	230	156
		X_{mb}	2,4	3,0	2,7
		R_{mb}	$1,5 \times 10^{-4}$	$1,7 \times 10^{-11}$	$1,6 \times 10^{-11}$
		G	$1,6 \times 10^{-5}$	$1,9 \times 10^{-5}$	$1,7 \times 10^{-5}$
		L_c	$2,3 \times 10^{-4}$	$2,8 \times 10^{-4}$	$2,5 \times 10^{-4}$

The data in the eight sets described in Table 4.13 were used in multilinear regression routines given in the commercially available package Statgraphics (Statistical Graphics Corporation), version 5.0. The sub-routine "Correlation" was first used with the data for each impurity to test for correlations among the independent variables, since by definition, independent variables must

not be related. An example of the print-out, for the data relevant to colour is shown in Table 4.14, from which it can be seen that there is a weak, negative correlation between G and the reciprocal of the temperature; the correlation between G and the concentration of colour in the feed (F_c) is very weak; finally, there is a positive correlation between G and the characteristic length of the crystal, but L_c is not correlated to F_c. It is thus possible to regress R_c versus F_c and G, and R_c versus F_c and L_c, since the independent variables, F_c and G are not related, and F_c and L_c are also not related.

Table 4.14

Print-out from the Statgraphics package for the "Correlation" sub-routine, to test for intercorrelations between the independent variables in the set of colour data

Mon May 26 1997 08:25:55 AM

Sample Correlations

	Fc	Xc	Ric	G	Lc	recT
Fc	1.0000	.9809	.9423	-.2784	-.2354	.0945
	(82)	(82)	(82)	(82)	(82)	(82)
	.0000	.0000	.0000	.0113	.0332	.3982
Xc	.9809	1.0000	.9673	-.2596	-.2251	.0688
	(82)	(82)	(82)	(82)	(82)	(82)
	.0000	.0000	.0000	.0185	.0420	.5391
Rc	.9423	.9673	1.0000	-.0062	-.1196	-.0238
	(82)	(82)	(82)	(82)	(82)	(82)
	.0000	.0000	.0000	.9562	.2845	.8317
G	-.2784	-.2596	-.0062	1.0000	.4310	-.3620
	(82)	(82)	(82)	(82)	(82)	(82)
	.0113	.0185	.9562	.0000	.0001	.0008
Lc	-.2354	-.2251	-.1196	.4310	1.0000	-.3781
	(82)	(82)	(82)	(82)	(82)	(82)
	.0332	.0420	.2845	.0001	.0000	.0005
recT	.0945	.0688	-.0238	-.3620	-.3781	1.0000
	(82)	(82)	(82)	(82)	(82)	(82)
	.3982	.5391	.8317	.0008	.0005	.0000

Coefficient (sample size) significance level

All the variables were transformed into their natural logarithms, and these values used in the multilinear regressions.

The stepwise, forward multilinear regression sub-routine was then used to relate the rate of impurity transfer to F_i and G in the first case and to F_i and L_c in the second. The routine selects only those independent variables which are statistically significant, at least at 5%. A typical set of results, again applying to colour is shown in Table 4.15. The print-out shows that the two independent variables F_c and G are included in the model, with high statistical significance, as quantified by the F values. L_c, however, is not included (F = 0,0013) at the 5% probability. The coefficients and their standard errors are given. Finally, the correlation coefficient (0,9581) is given.

Table 4.15

Typical print-out from the Statgraphics package for the stepwise multilinear sub-routine for the regression of R_c versus F_c and G, in the set of colour data

Stepwise Selection for COL. Ric

Selection: Forward — Maximum steps: 500 — F-to-enter: 4.00
Control: Automatic — Step: 2 — F-to-remove: 4.00

R-squared: .95909 Adjusted: .95805 MSE: 0.0423091 d.f.: 79

Variables in Model	Coeff.	F-Remove	Variables Not in Model	P.Corr.	F-Enter
1. COL. Fc	0.80701	1852.0207	3. COL. Lc	.0040	.0013
2. COL. G	1.05780	137.4023			

Wed Jun 18 1997 08:51:29 AM Page 1

Further ANOVA for Variables in the Order Fitted

Source	Sum of Squares	DF	Mean Sq.	F-Ratio	P-value
COL. Fc	72.5469748	1	72.546975	1714.69	.000C
COL. G	5.8133596	1	5.813360	137.40	.000C
Model	78.3603343	2			

Wed Jun 18 1997 08:50:31 AM Page 1

Model fitting results for: COL.LRic

Independent variable	coefficient	std. error	t-value	sig.level
CONSTANT	-2.597405	0.976086	-2.6610	0.009
COL. Fc	0.807006	0.018752	43.0351	0.000C
COL. G	1.057804	0.090242	11.7219	0.000C

R-SQ. (ADJ.) = 0.9581 SE= 0.205692 MAE= 0.159445 DurbWat= 1.178
Previously: 0.0000 0.000000 0.000000 0.000
82 observations fitted, forecast(s) computed for 0 missing val. of dep. var.

4.4.2.1 The effects of F_i, G and L_c on the rates of impurity transfer

The procedures described in Section 4.4.2 were used to investigate the effects of F_i, G and L_c on the rate of impurity transfer. The results are given in Tables 4.16 and 4.17.

Table 4.16

The results of the multilinear regressions for the effects of F_i and G on the rate of impurity transfer

Species	Equation	n	r^2
Colour	$R_c = 0{,}074\ F_c^{0,81}\ G^{1,1}$	82	0,958
Potassium	$R_K = 2{,}0 \times 10^{-8} F_K^{0,62}\ G^{1,1}$	59	0,754
Calcium	$R_{Ca} = 1{,}7 \times 10^{-7}\ F_{Ca}^{0,43}\ G^{1,1}$	38	0,645
Lithium	$R_{Li} = 1{,}8 \times 10^{-12}\ F_{Li}^{1,0}\ G^{0,56}$	29	0,820
Starch	$R_{st} = F_{st}^{1,0}\ G^{2,5}$	31	0,999
Methylene blue	$R_{myb} = 1{,}8 \times 10^{-19}\ F_{myb}^{3,6}$	15	0,910
Methyl blue	$R_{mb} = 4{,}4 \times 10^{-7}\ F_{mb}^{0,19}\ G^{1,0}$	4	0,955
Acid blue 25	$R_{ab25} = 4{,}2 \times 10^{-8}\ F_{ab25}^{0,40}\ G^{0,99}$	4	0,993

Table 4.17

The results of the multilinear regressions for the effects of F_i and L_c on the rate of impurity transfer

Species	Equation	n	r^2
Colour	$R_c = 2{,}3 \times 10^{-4}\ F_c^{0,77}\ L_c^{0,69}$	82	0,896
Calcium	$R_{Ca} = 1{,}6 \times 10^{-9}\ F_{Ca}^{0,45}\ L_c^{0,96}$	38	0,557

Correlation coefficient (r^2) values obtained with multilinear regressions involving logarithmic terms can be misleading. It is better to look at the standard errors (see Table 4.18), and to check graphically that the equation obtained does fit the data. The graphical check has been done by using the Equations in Table 4.16, for colour, potassium, starch and calcium to calculate the

values of R_c, R_K, R_{st} and R_{Ca}, respectively, using the relevant values of F_i and G, from the original data sets. Each calculated value of R_i can then be compared to its corresponding one in the original data set. This has been done in Figure 4.7. Detailed statistics, including uncertainties, are in Appendix 3.

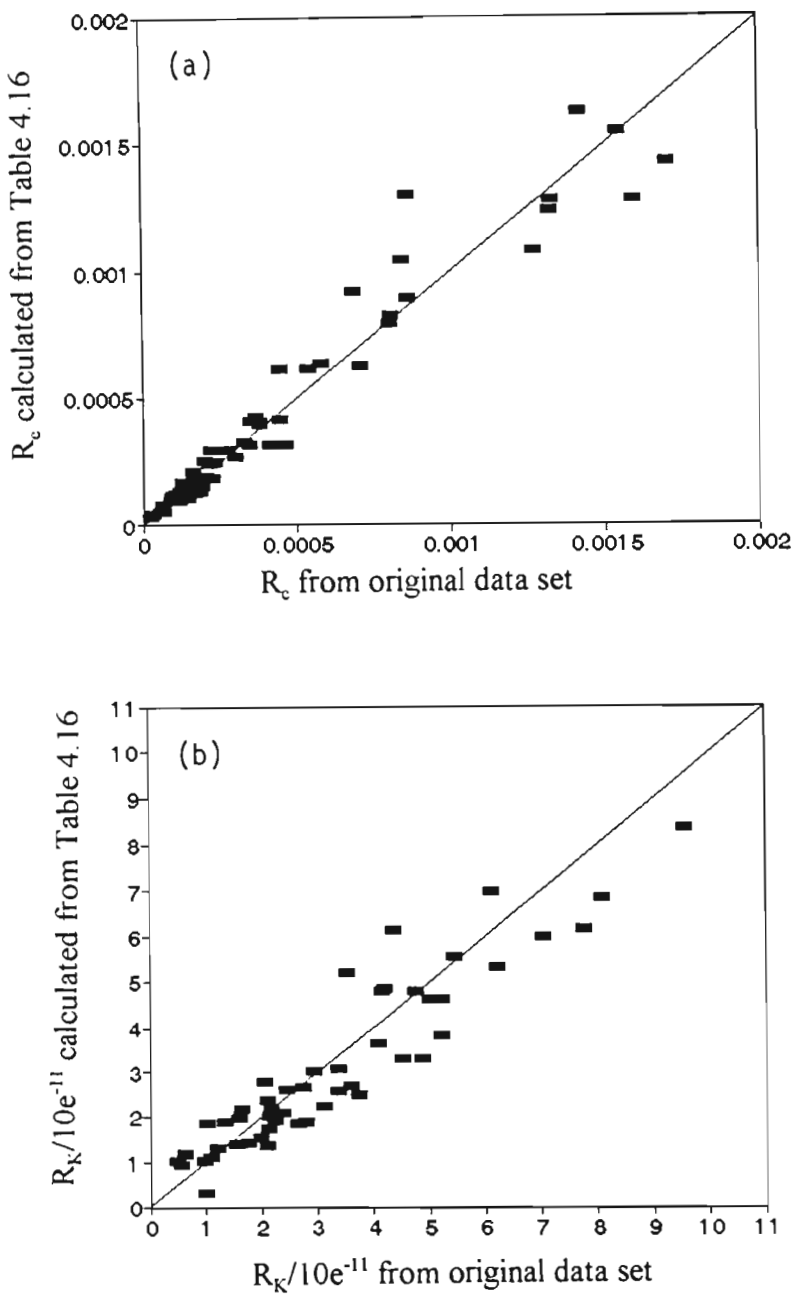

Figure 4.7 **Rates of impurity transfer calculated from the equations in Table 4.16 compared with corresponding values from the original data set. The equivalence line is shown, for (a) colour and (b) potassium.**

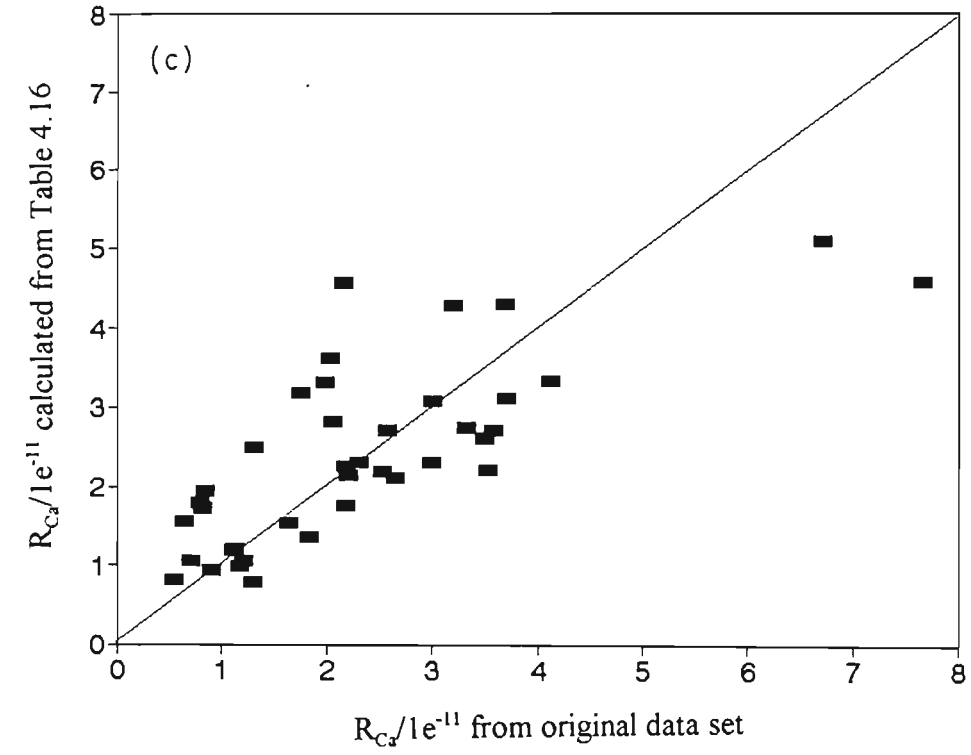

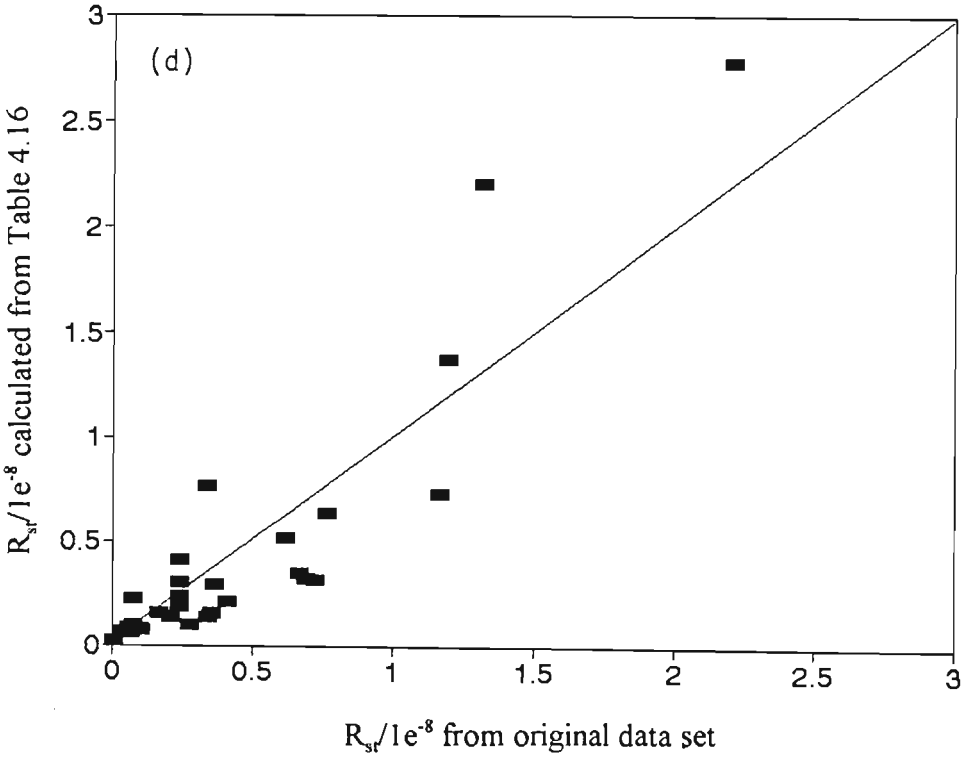

Figure 4.7 (Cont.). Rates of impurity transfer calculated from the equations in Table 4.16 compared with corresponding values from the original data set. The equivalence line is shown, for (c) calcium and (d) starch.

Table 4.18

Coefficients and standard errors for the independent variables in the regression of Tables 4.16 and 4.17

Species	Independent variable	Coefficient	Standard error
Colour	F_c	0,81	0,019
	G	1,1	0,090
Potassium	F_K	0,62	0,047
	G	1,1	0,174
Calcium	F_{Ca}	0,43	0,066
	G	1,1	0,345
Lithium	F_{Li}	1,0	0,092
	G	0,56	0,373
Starch	F_{st}	1,0	0,106
	G	2,5	0,076
Methylene blue	F_{myb}	3,6	0,301
Methyl blue	F_{mb}	0,19	0,079
	G	1,0	0,355
Acid blue 25	F_{ab25}	0,40	0,033
	G	0,99	0,196
Colour	F_c	0,77	0,029
	L_c	0,69	0,233
Calcium	F_{Ca}	0,41	0,080
	L_c	1,2	0,394

The following conclusions can be made on the effect of G, L_c and F_i on the rates of impurity transfer:

- Only nickel yielded data which could not be fitted through the multiple linear regressions. The complete set of results for that impurity showed large scatter and no variable was

statistically significant at the 5% level.

- In the case of methylene blue, G and F_{myb} were unfortunately highly correlated, and G could therefore not be included in the regression. The exponent for F_{myb} (3,6) in Table 4.16, must therefore be viewed with caution.

- In all other cases G was statistically significant at least at 5%.

- G is raised to a power close to 1 for colour, potassium, calcium, lithium (high scatter), methyl blue and acid blue 25. This confirms the results in Section 4.2.2.

- G is raised, to a power higher than 1 for starch only. In this case the increase in the rate of transfer with G is high.

- It is now possible to measure the effect of the crystal characteristic dimension. This factor shows a statistically significant effect on the rate of impurity transfer with colour and calcium. In both cases the rate increases as the crystal becomes larger, a trend which has been found in industry (Mann, 1987; Lionnet, 1987). As a first approximation, the rate of impurity transfer increased by about 65% for a doubling of L_c.

- The effect of the concentration of the impurity in the feed liquors has already been mentioned in Section 4.4.1, where specific sets of experiments were considered. Statistically significant results were obtained in most cases. The results obtained here, as shown in Tables 4.16 and 4.17, confirm the impact of the concentration on the rate of impurity transfer but the agreement between the numerical values from Section 4.4.1 and those from Table 4.16 is not as good as was the case for G. This is shown in Table 4.19.

Table 4.19

Comparison of the exponent b in $R_i = a F_i^b$ from the specific sets and the multilinear regressions

Species	$R_i = a F_i^b$	
	Specific runs	**Multilinear regressions**
Colour	0,7 to 0,8	0,77 to 0,81
Potassium	0,7 to 0,9	0,62
Calcium	0,6 to1,2	0,43 to 0,41
Lithium	0,8 to 1,0	1,0
Nickel	0,9 to 1,0	-
Starch	1,1 to 1,6	1,0
Methylene blue	0,9 to 2,1	(3,6)
Methyl blue	-	0,20
Acid blue 25	0,30	0,40

These results confirm the importance of the concentration of the impurity on its transfer into the sucrose crystal. In the case of colour, the concentration in the feed liquor is raised to an exponent of about 0,8; the metal ions show similar values except for calcium whose exponent could be lower; starch shows a value close to 1. In the case of the dyes the results show low values (0,2-0,4) for methyl blue and acid blue 25 while methylene blue shows high values; the number of observations for these three species is however low.

4.4.2.2 The effect of F_i, G and L_c on the concentration of impurity in the crystal

Most of the results already presented have dealt with the rate at which the impurities are transferred into the sucrose crystal. The experiments described in Section 3.6 have, however, also yielded the concentrations of impurities in the crystal, X_i (mg/kg) and this will now be investigated. Again multiple linear regression techniques will be used to relate X_i to F_i, G and L_c.

The results here were simpler. In all cases (except for calcium which showed large scatter) X_i was statistically significantly related to F_i only, as shown in Table 4.20. This was not the case with R_i, where G, L_c and F_i all showed statistically significant relationships, indicating that R_i is more sensitive, probably because it contains the crystallisation time. Of the three independent variables, F_i is the one which has the widest range; this may contribute to its overriding effect on X_i.

Table 4.20

The results of the multilinear regressions for the effect of F_i on the concentration of impurity in the crystal, X_i (mg/kg)

Species	$X_i = a F_i^b$	n	r^2
Colour	$X_c = 0,12 F_c^{0,80}$	82	0,962
Potassium	$X_K = 0,04 F_K^{0,61}$	59	0,762
Calcium	-	-	-
Lithium	$X_{Li} = 6,5 \times 10^{-4} F_{Li}^{1,1}$	29	0,824
Starch	$X_{st} = 0,08 F_{st}^{1,1}$	31	0,800
Methylene blue	$X_{myb} = 0,01 F_{myb}^{0,89}$	15	0,733
Methyl blue	$X_{mb} = 1,0 F_{mb}^{0,19}$	4	0,955
Acid blue 25	$X_{ab25} = 0,13 F_{ab25}^{0,40}$	4	0,994

The good fits and the fact that no other variable is statistically significant at 5% show that the concentration of the impurity in the crystal is probably completely dependent on the feed quality, over the range of conditions examined in this work.

4.5 Partition coefficients

The experimental data include the concentrations of the impurities in the sucrose crystal (see Section 4.4.2.2). These quantities can be used in partition coefficients.

The concept of partition coefficients has been presented in Section 1.2.1. Witcamp *et al.* (1990) and Zumstein *et al.* (1990) have defined a partition coefficient, P_i, given by

$$P_i = \frac{\text{(conc. impurity/conc. reference) in crystal}}{\text{(conc. impurity/conc. reference) in solution}}$$

.....4.3

P_i will be used in the present work for the impurities selected for investigation and with sucrose as the reference material, while the "solution" will be the feed liquor.

The above-mentioned authors have investigated both organic and inorganic systems and give values of P_i for a number of impurities in those systems. They have also used the concept to investigate possible mechanisms for impurity transfer.

4.5.1 **The calculation of P_i**

The sucrose crystal is considered here (see Section 2.1.3) to consist of pure sucrose. The feed liquors were analysed for sucrose, the results being expressed as % sucrose in feed (gram sucrose/100 gram feed), as described in Section 3.4.4.2. For partition coefficients the concentration of impurity in the feed was not expressed on water in feed but rather on the feed itself, on a m/m basis, but the concentration of colour, however, was on brix (see Section 3.5). An example of the calculation of P_i where i is K^+ follows:

Concentration of sucrose in crystal	100 g/100 g
Concentration of K^+ in crystal	8,8 mg/1000 g
Concentration of sucrose in feed	60,3 g/100 g
Concentration of K^+ in feed	1866 mg/1000 g

$$\text{Then, } P_i = \frac{0{,}88}{100} / \frac{186{,}6}{60{,}3} = 0{,}002844$$

The results obtained from set R15 will now be used to illustrate the application of partition coefficients in the present work. Inspection of equation 4.3 shows that a plot of the ratio (concentration of impurity/concentration of sucrose) in the crystal against the ratio (concentration of impurity/concentration of sucrose) in the feed liquor should be linear with a slope equal to P_i and with the line passing through the origin. These conditions have been used (Witcamp *et al.*, Zumstein *et al.*, 1990) to define an "ideal" behaviour (see equation 1.2, page 14). Set R15 consisted of five runs, each of which had different concentrations of impurities in the feed liquor. The two ratios mentioned above are shown in Table 4.21 for colour, potassium, starch and calcium as impurities. They have been plotted in Figure 4.8.

Table 4.21

Data from set R15 for the calculation of partition coefficients, P_i

Run	Conc. impurity/conc. sucrose in the crystal				Conc. impurity/conc. sucrose in the feed liquor			
	Colour	Potassium	Starch	Calcium	Colour	Potassium	Starch	Calcium
R1	0,000168	$8,8 \times 10^{-6}$	0,000401	$3,1 \times 10^{-5}$	0,0183	0,00309	0,00165	0,00276
R2	0,000334	$2,1 \times 10^{-5}$	0,000867	$7,6 \times 10^{-5}$	0,0364	0,00647	0,00287	0,00470
R3	0,0000510	$2,1 \times 10^{-6}$	0,0000110	$4,0 \times 10^{-6}$	0,0038	0,00066	0,00020	0,00058
R4	0,0000770	$4,6 \times 10^{-6}$	0,0000850	$1,4 \times 10^{-5}$	0,0057	0,00099	0,00049	0,00073
R5	0,000100	$5,0 \times 10^{-6}$	0,000165	$1,6 \times 10^{-5}$	0,0096	0,00164	0,00080	0,00132

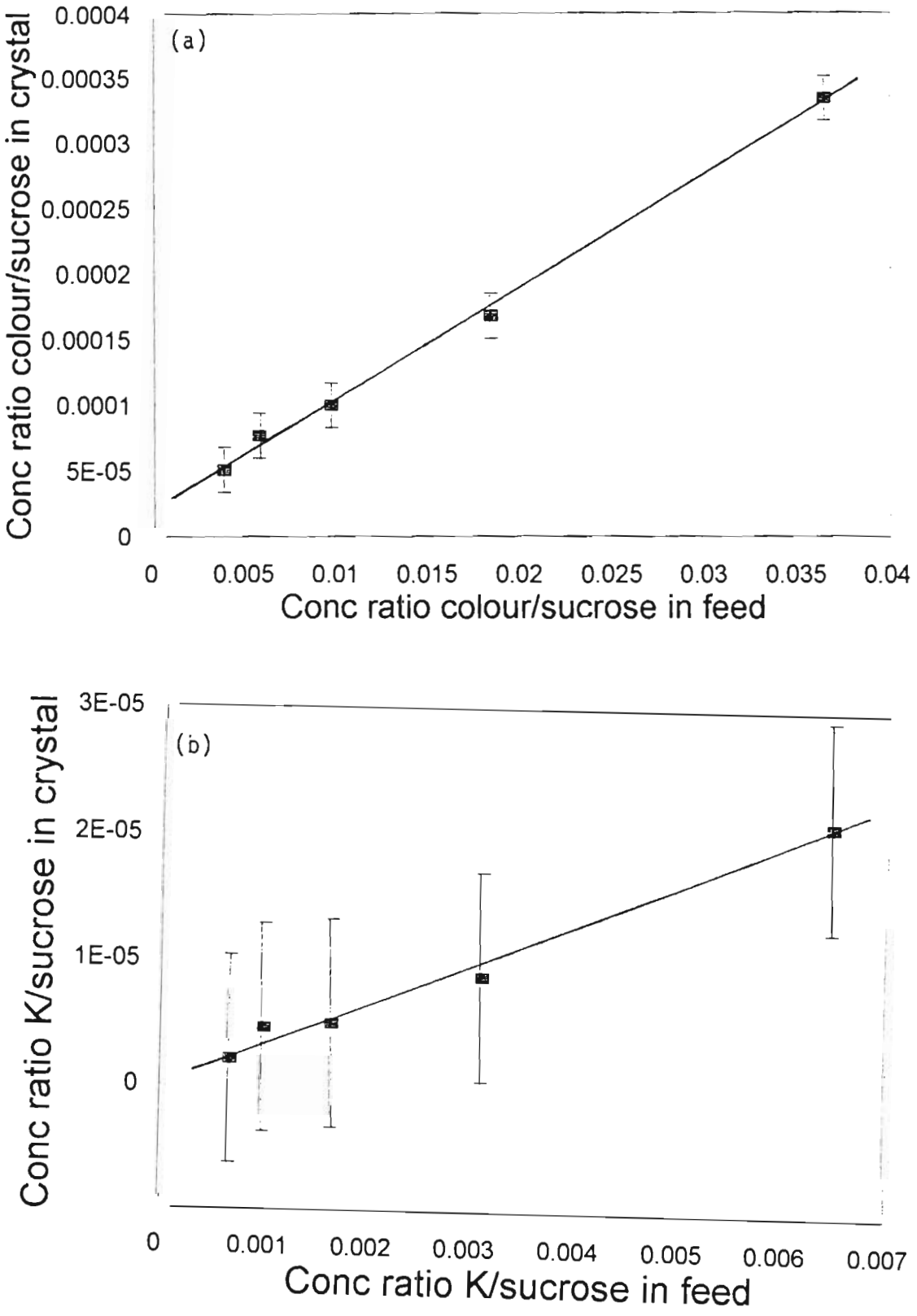

Figure 4.8 **The ratio of the concentrations of the impurity to that of sucrose, in the crystal plotted versus the same ratio but in the feed liquor, for the determination of P_i, for (a) colour and (b) potassium.**

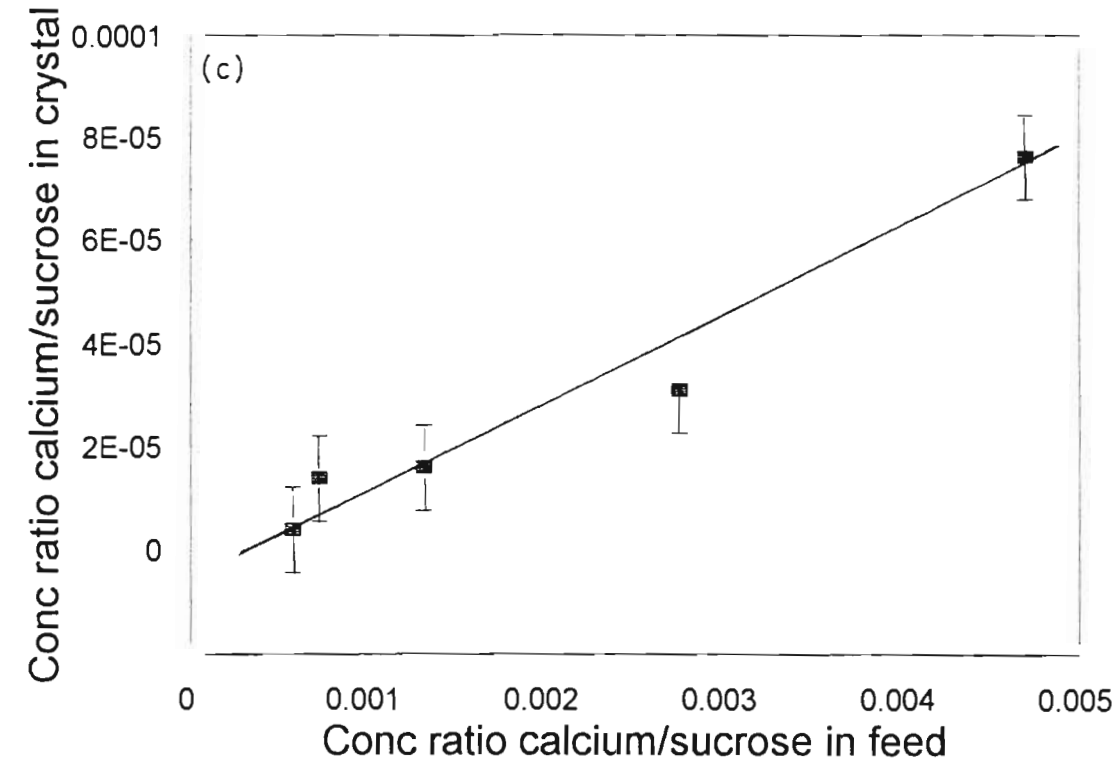

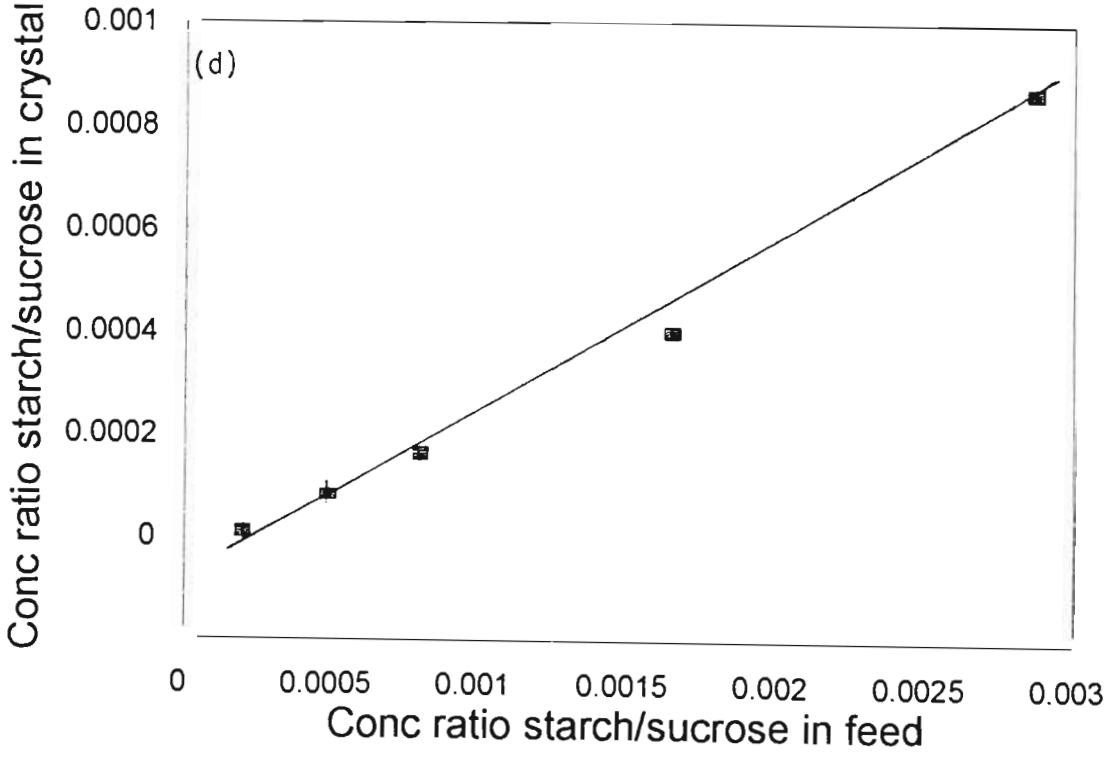

Figure 4.8 (cont.) The ratio of the concentrations of the impurity to that of sucrose, in the crystal plotted versus the same ratio but in the feed liquor, for the determination of P_i, for (c) calcium and (d) starch.

The following comments may be made from the results shown in Figure 4.8:

- There are strong linear relationships between the ratio of the concentration of the impurity to that of sucrose in the crystal and the same ratio but in the feed liquor. This confirms the validity of equation 4.3, if P_i is constant, with the reservation given below.

- With potassium, the straight line passes through the origin for a range of concentrations in the feed covering a factor of seven. According to the definition given by Witcamp *et al.* (1990), this system is "ideal".

- With colour, the straight line does not pass through the origin. The plot of P_{col} versus the ratio of the concentration of colour to that of sucrose in the feed (see Section 1.2.1) is asymptotic and the system is thus not ideal. The conclusion with starch is similar to that for colour, except that the plot of P_{st} versus the ratio of the concentration of starch to that of sucrose in the feed, is asymptotic upwards. Both these results are shown in Figure 4.9.

- The partition coefficient, P_i, can be calculated in two different ways. It can be obtained through a linear regression, as defined by equation 4.3, or its can be calculated for each pair of concentration ratios. If the system is "ideal", the two values will agree. The two approaches are illustrated in Table 4.22 for set R15. Potassium is the only species for which the P_K values obtained by the two methods agree within about 10%.

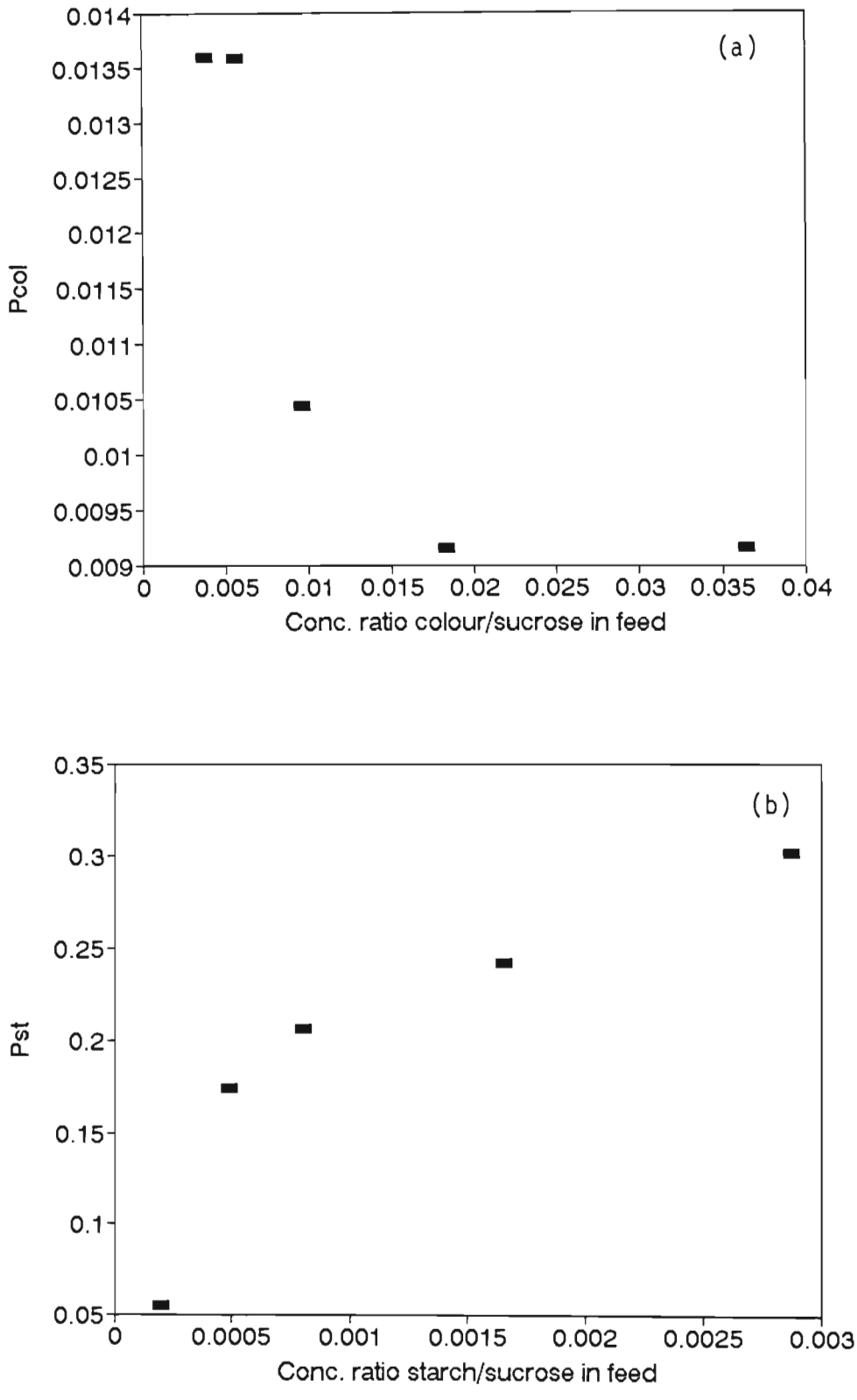

Figure 4.9 **The partition coefficient plotted against the ratio of the concentration of impurity/the concentration of sucrose, in the feed liquor, for (a) colour and (b) starch. These results illustrate non-ideality.**

Table 4.22

The results of the two approaches to calculate partition coefficients (P_i), from the data in Table 4.21

P_i	Regression (Eq. 4.3)	Average from all runs $\left(\frac{X_i/X_{suc}\ \text{crystal}}{F_i/F_{suc}\ \text{feed}}\right)$
P_{col}	0,0085	0,011
P_K	0,0031	0,0034
P_{Ca}	0,016	0,013
P_{st}	0,32	0,20

4.5.2 Values of P_i obtained in this work

The results in Table 4.22 show that all the impurities, except potassium and possibly calcium, behaved in a "non-ideal" way as defined by Witcamp *et al.* (1990). The values of P_i are obtained by calculating the ratio (concentration of impurity/concentration of sucrose, in crystal)/ (concentration of impurity/concentration of sucrose, in feed liquor), for each run in a given set of experiments. This has been done in Table 4.23.

Table 4.23

Partition coefficients for the non-sucrose species

Species	Set	P_i
Colour	R15	0,011
	S16	0,014
	TR18	0,016
	CS15	0,024
	KL15	0,025
	LN15	0,020
Potassium	KL15	0,0036
	R15	0,0034
	S16	0,0042
	TR18	0,0020
Calcium	CS15	0,0013
	R15	0,013
	S16	0,0054
	TR18	0,044
	MX13	0,027
	CN15	0,0018
Starch	KL15	0,29
	CS15	0,49
	R15	0,20
Lithium	KL15	0,0019
	LN15	0,0012
Nickel	LN15	0,0037
	CN15	0,00045
	MX13	0,12
Methylene blue	COND16	0,014
	ML15	0,015
	MB15	0,0018
Methyl blue	MYB14	0,034
Acid blue 25	AB25	0,011

Two main conclusions may be made from the results obtained with the partition coefficients. Firstly, it has been found that the numerical values of P_i obtained in the present work are similar to those reported in the literature, particularly by Witcamp *et al.* (1990) and Zumstein *et al.* (1990). Secondly, the results indicate that exchange reactions/equilibria take place at the surface of the sucrose crystal, which could cause the concentrations of the impurities near the crystal to be different. This confirms that the simple inclusion of mother liquor (see Section 4.1) is not the only important process and suggests that mechanisms based on equilibria could be relevant. This will be investigated in more detail later.

4.6 **Adsorption isotherms**

As was the case in Section 4.5 for partition coefficients, the experimental data can be used to investigate adsorption isotherms. Again these concepts can help in understanding impurity transfer processes.

As discussed in Section 2.7, three isotherms have been considered in this work. The Langmuir isotherm has been give by equation 2.28, which for the present work can be rearranged (Atkins, 1994) to

$$\frac{F_i}{X_i} = \frac{b}{a} F_i + \frac{1}{a}$$

.....4.4

where F_i is the concentration of the impurity expressed as mg per kg water in the feed liquor; X_i is the concentration of the impurity in mg per kg crystal; and a and b are constants. A plot of F_i/X_i versus F_i yields a straight line for adsorptions following the Langmuir model.

The Freundlich isotherm, equation 2.29, can be rearranged for adsorption in solution and, for the present work becomes

$$X_i = C_1 F_i^{1/C_2}$$

.....4.5

where X_i and F_i have been defined in equation 4.4, while C_1 and C_2 are constants. A plot of ln X_i versus ln F_i will yield a straight line if this isotherm is obeyed.

Finally, the BET isotherm, equation 2.30, can be rearranged (Atkins, 1994) for the present work

$$\frac{Z}{(1 - Z)\ V} = \frac{1}{C\ V_{mon}} + \frac{(C - 1)\ Z}{C\ V_{mon}}$$

.....4.6

where Z is the ratio of the concentration of the impurity in the water in the feed to the solubility of the impurity in water; V is the concentration of the impurity in the crystal, expressed as mg/kg crystal; V_{mon} is the quantity of impurity adsorbed to give a monolayer, which, like C, is a constant. A plot of the left hand side versus Z should give a straight line. The following solubilities (Weast, 1986) in g material/100 g water, were used: KCl, 57; $CaCl_2$, 159; starch, 5; LiCl, 130; $NiCl_2.6H_2O$, 599. In the case of colour, a limiting value of 80 000 was used as an approximation for the highest value of colour that could be expected in this work.

4.6.1 **The Langmuir and BET isotherms**

The Langmuir and BET models were tested with the data from the experiments described in Section 3.6.4. Equations 4.4 and 4.6, representing the Langmuir and BET models respectively, were fitted to data from sets R15 and S16.

The results are shown graphically, in Figures 4.10 and 4.11, for the fit of colour and potassium data to the Langmuir and BET isotherms, respectively.

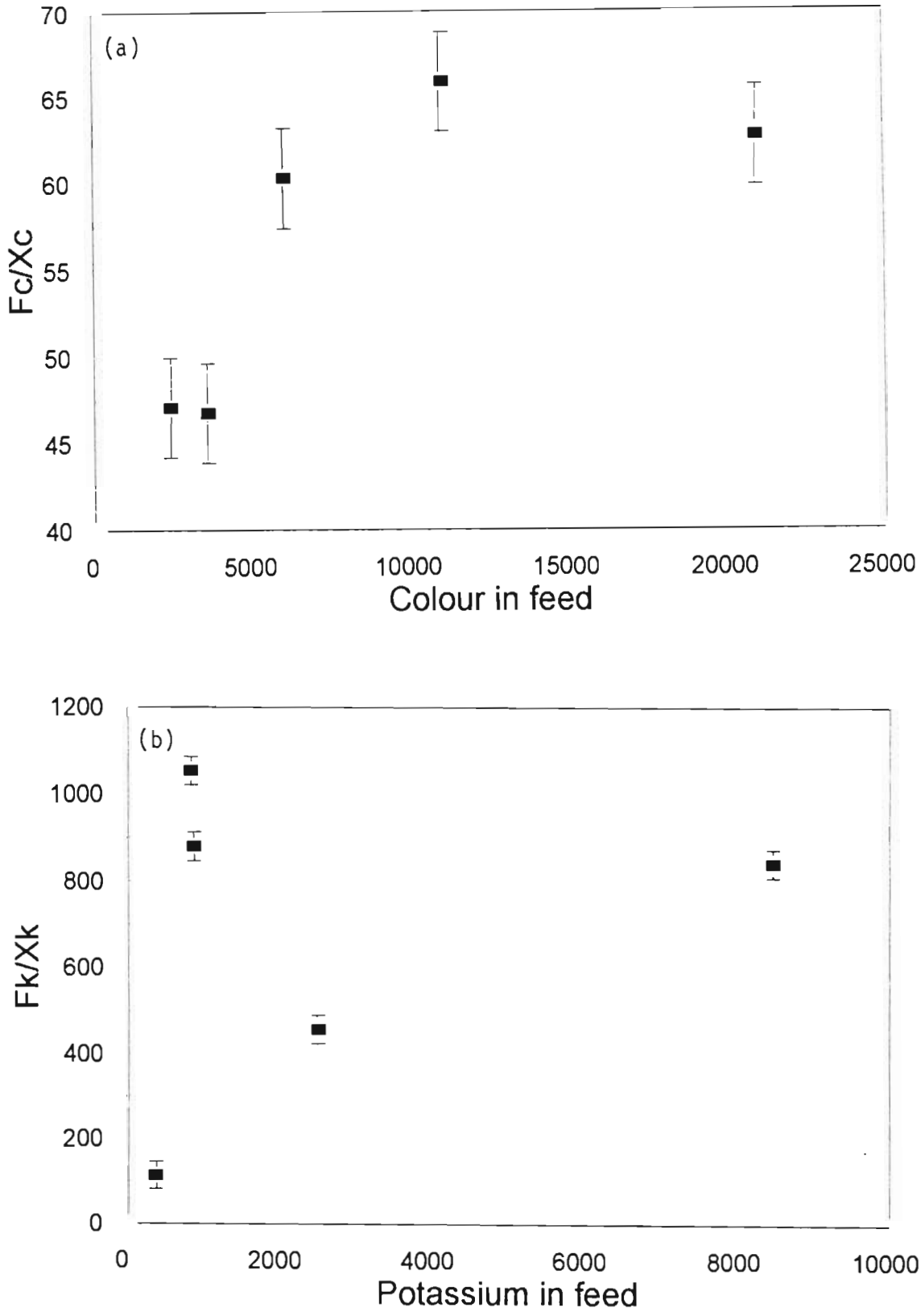

Figure 4.10 **The fit of the Langmuir isotherm to (a) colour data from set R15 and (b) potassium data from set S16.**

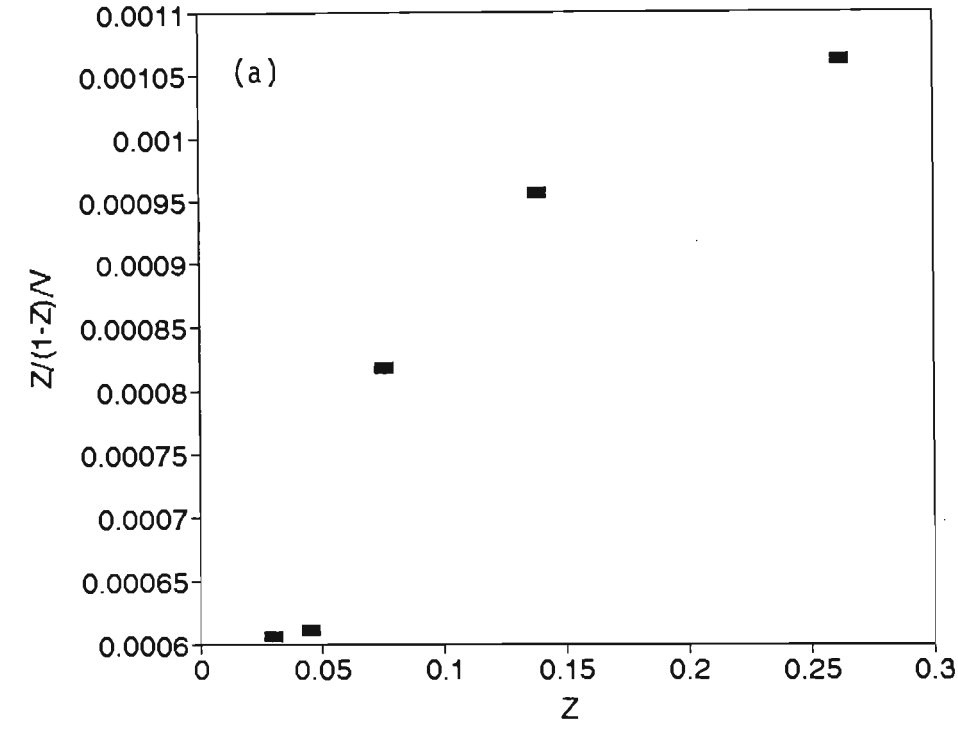

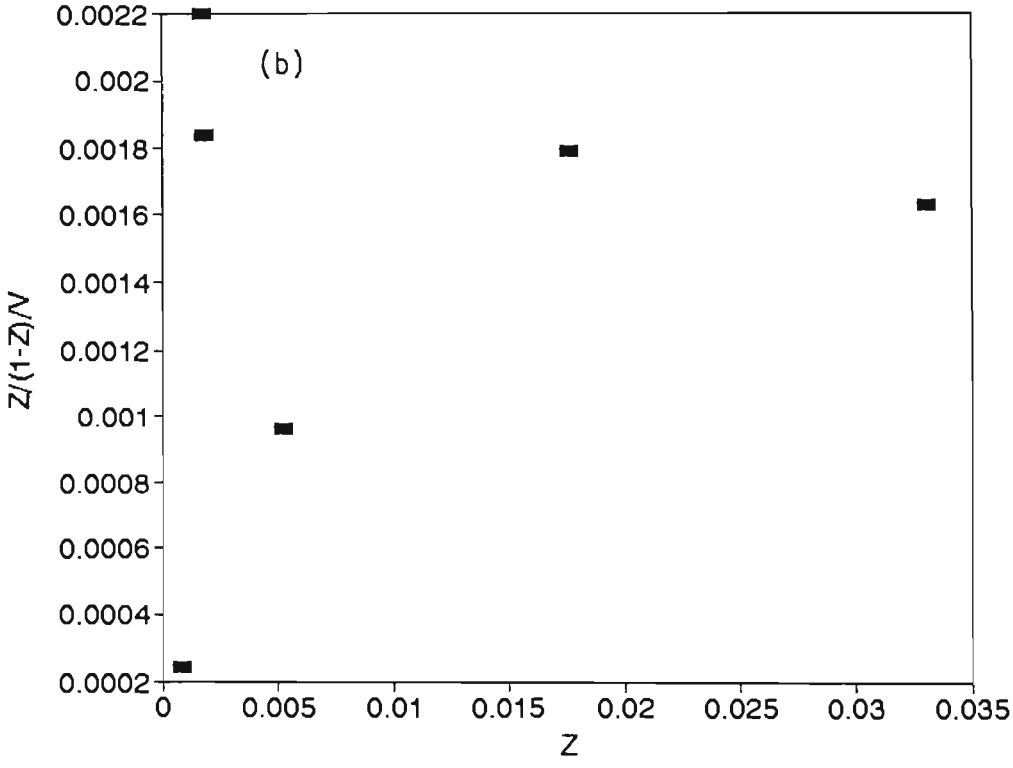

Figure 4.11 **The fit of the BET isotherm to (a) colour data from set R15 and (b) potassium data from set S16.**

As can be seen the Langmuir and BET isotherms do not fit the data from sets R15 and S16. The slopes are not always positive as required by the models, and in most cases, there is scatter and the correlations coefficients are low.

These two isotherms were tested with all the relevant sets of experiments. In all cases the results were similar to those for sets R15 and S16. It can therefore be concluded that the Langmuir and BET isotherms do not describe the data obtained in this work.

4.6.2 **The Freundlich isotherm**

The Freundlich isotherm for adsorption in solution is represented by equation 4.5. This equation is identical to that found in Section 4.4.2.2, when multiple linear regression techniques were used to investigate the effects of G, F_i and L_c on X_i, the concentration of impurity in the crystal. The results given in Table 4.19 show that only F_i was found to affect X_i, for all the impurities, except calcium. It is therefore evident that the Freundlich model will fit the data from this work well. This is illustrated in Table 4.24 and in Figure 4.12, where the data from sets R15 and S16 have again been used as examples.

Table 4.24

Results describing the fit of the Freundlich isotherm to the data from sets R15 and S16

Set	Species	Fit of Equation 4.5			
		Intercept	Slope	No. of observations	r^2
R15	Colour	0,076	0,84	5	0,987
	Potassium	0,0029	0,94	5	0,958
	Starch	0,0010	1,61	5	0,978
	Calcium	0,0015	1,19	5	0,893
S16	Colour	0,120	0,81	6	0,982
	Potassium	0,014	0,73	6	0,679
	Calcium	0,031	0,66	6	0,931

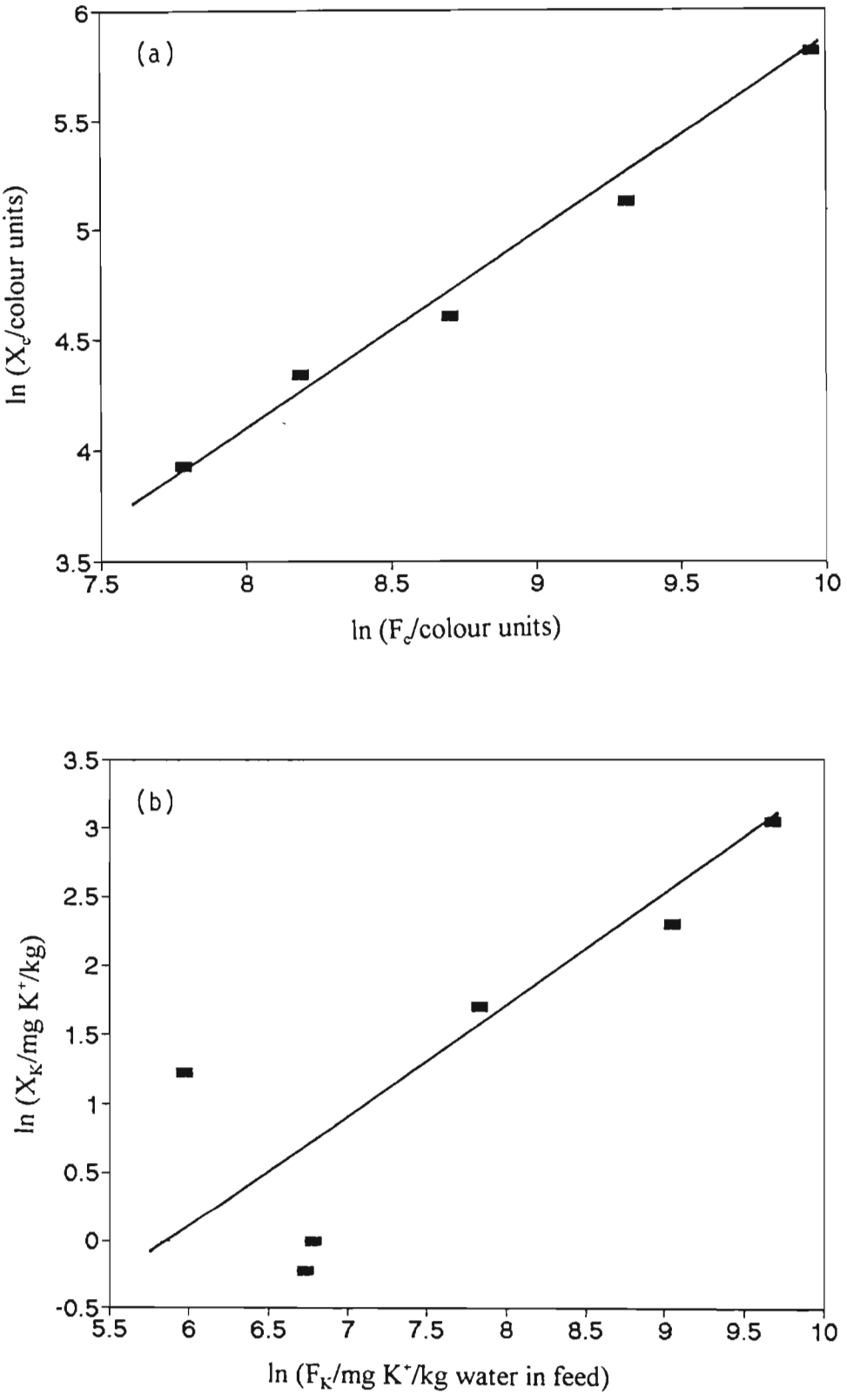

Figure 4.12 The fit of the Freundlich isotherm to (a) colour data from set R15 and (b) potassium data from set S16.

The data from all the sets, for a given impurity, may be used to obtain overall fits for the Freundlich isotherm. As shown earlier this will yield results identical to those obtained in Section 4.4.2.2. These results are reproduced here for the sake of completeness.

Table 4.20

The overall fit of the Freundlich isotherm, namely $X_i = C_1 F_i^{1/C2}$, for the impurities studied in this work

Species	$X_i = C_1 F_i^{1/C2}$	n	r^2
Colour	$X_c = 0,12 F_c^{0,80}$	82	0,962
Potassium	$X_K = 0,04 F_K^{0,61}$	59	0,762
Calcium	-	-	-
Lithium	$X_{Li} = 6,5 \times 104 F_{Li}^{1,1}$	29	0,824
Starch	$X_{st} = 0,08 F_{st}^{1,1}$	31	0,800
Methylene blue	$X_{myb} = 0,01 F_{myb}^{0,89}$	15	0,733
Mehtyl blue	$X_{mb} = 1,0 F_{mb}^{0,19}$	4	0,955
Acid blue 25	$X_{ab25} = 0,13 F_{ab25}^{0,40}$	4	0,994

The overall results with calcium and nickel showed much scatter when the multiple linear regression approach was used. It is possible to use another approach, namely that of averaging the slopes and intercepts of the regressions from each individual set. If this is done, then the Freundlich results for calcium and nickel are

$$X_{Ca} = 0,01 F_{Ca}^{1,0}$$
$$X_{Ni} = 0,06 F_{Ni}^{0,91}$$

for numbers of observations of 38 and 13 respectively. Both these results do not appear out of line when compared to those for potassium and lithium. This problem for obtaining overall results has already been discussed in Section 4.3, in connection with activation energies. Again here, sets with somewhat similar slopes but with intercepts which are very different have been the cause of the poor overall results with the multilinear regressions. This is illustrated in Figure 4.13, using the results for nickel as the impurity under consideration. One difference between these sets was

the value of G, which was between 1,6 and 1,8 x 10^{-5} kg/m^2/s for the run MX13, but between 1,5 and 1,6 kg/m^2/s for LN15 and CN 15.

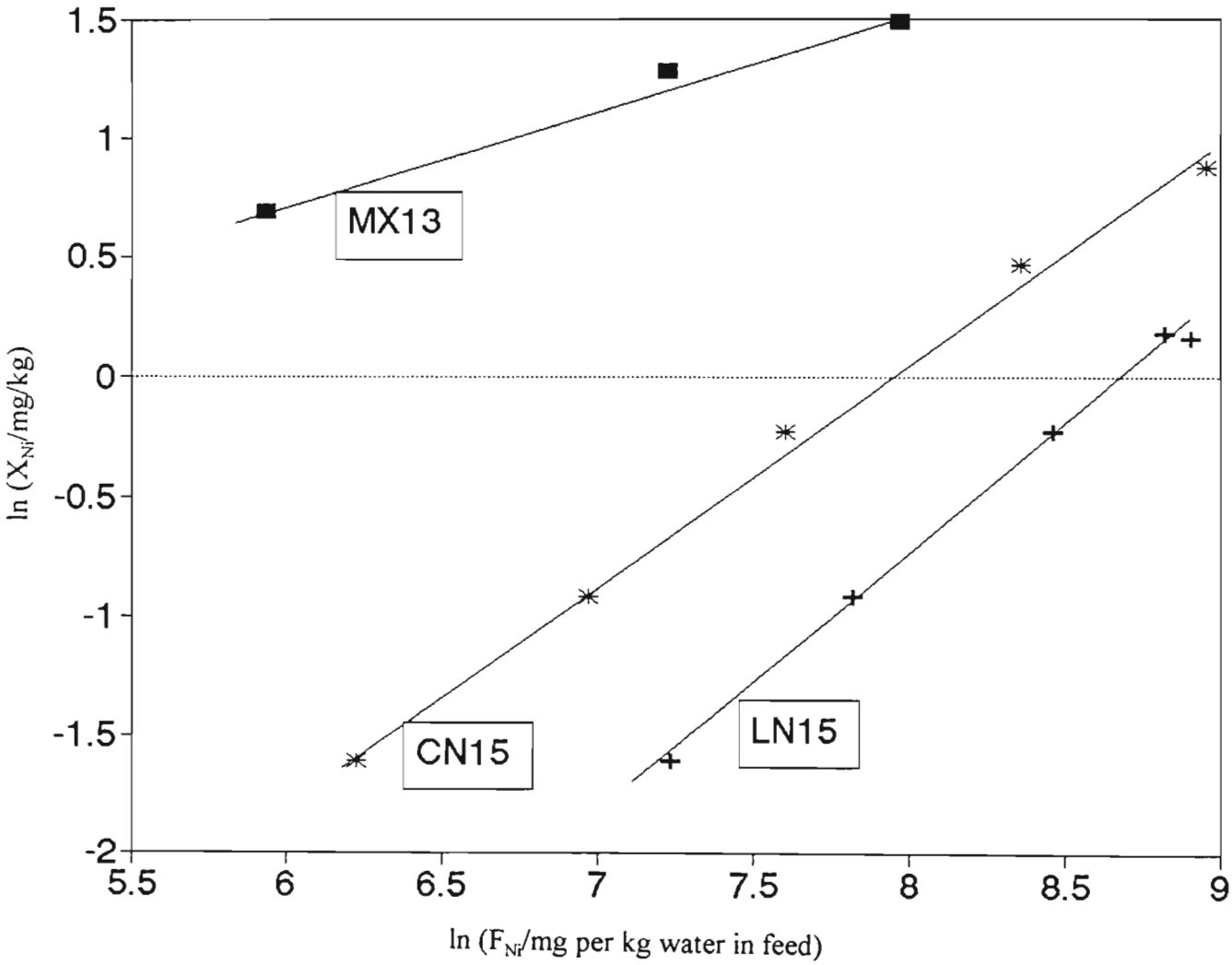

Figure 4.13 The Freundlich plot with nickel as the impurity, for sets MX13, CN15 and LN15, displayed individually.

It can be concluded that the investigation of adsorption isotherms has added little to what had already been found in other sections of the present work, a conclusion which is different to that from partition coefficients. The data fit the Freundlich isotherm, which is the simplest of the three isotherms investigated, a result identical to that obtained with multiple linear regressions.

4.7 The effect of viscosity

The impact of viscosity on the crystallisation of sucrose has been mentioned in Sections 2.5 and 3.6.5. In the present work viscosity has been investigated in two main areas. The first deals with the activation energy aspect of viscosity in highly concentrated sucrose solutions while the second deals with the impact of viscosity on the rate of crystallisation of sucrose and on the rate of impurity transfer. The results are discussed below.

4.7.1 The activation energy of viscosity

The activation energy of viscosity has been studied extensively in connection with the crystallisation of sucrose (Honig, 1959; VanHook, 1944, 1945, 1973; Maurandi, 1982; Maurandi *et al.*, 1984; Heffels *et al.*, 1987, 1988). Using the results of the above workers with solubility and viscosity data for sucrose (Chen and Chou, 1993), it was shown in Section 2.5 that the activation energy of viscosity, at constant supersaturations of 1,0 and 1,3 over a temperature range of 60 to 80°C, ranges from 1 to 10 kJ/mol, which is a small range.

VanHook (1944; 1945) gives a value of 8 kJ/mol, for a temperature of 60-80°C and at constant supersaturation. Under similar conditions, Honig (1959) gives values of 1-5 kJ/mol. Maurandi (1982; 1984), using big, single sucrose crystals in stirred solutions gives E_v values around 14 kJ/mol but does not specify if these are for constant superaturations. The values calculated in Section 2.5 are thus in line with those published in the literature.

4.7.2 **Experimental results**

The experimental work to investigate viscosity has been described in Section 3.6.5. Basically, polysaccharides were added to feed liquors to increase viscosity, and crystallisation was carried out. Two different types of polysaccharides: carboxymethyl cellulose and carrageenan were used. The experimental results obtained are shown in Tables 4.25 and 4.26. These results will be used throughout this Section to investigate the effects of viscosity. The quantity of polysaccharide that could be added to the liquors was limited; amounts around 1% (by mass) caused the feed liquor to loose its fluidity, preventing proper feeding into the crystalliser.

Table 4.25

Mother-liquor viscosities, impurity transfer rates and sucrose crystallisation rates with the addition of carboxymethyl cellulose (CMC)

Set	% CMC in feed (m/m)	Visc./ Pa s	R_i/kg/m^2/s			G/ kg/m^2/s /10^{-5}
			Colour /10^{-4}	Potassium /10^{-11}	Calcium /10^{-11}	
CMC13	0,025	0,090	1,0	7,4	10,4	1,8
	0,05	0,095	1,0	7,6	22,8	1,9
	0,13	0,112	2,1	21,8	20,1	1,6

Table 4.26

Mother-liquor viscosities, impurity transfer rates and sucrose crystallisation rates with the addition of carrageenan

Set	% Carr. in feed (m/m)	Visc./ Pa s	R_i/kg/m^2/s			G/ kg/m^2/s /10^{-5}
			Colour /10^{-4}	Potassium /10^{-11}	Calcium /10^{-11}	
C12	0	0,116	-	1,8	3,9	1,9
	0,40	0,124	-	8,6	9,4	2,0
CM 13	0,03	0,079	2,0	7,7	1,4	2,1
	0,28	0,100	2,4	22,4	4,5	2,2
	0,52	0,131	3,3	15,4	14,7	2,0
CAR13	0	0,100	1,0	2,1	1,6	1,7
	0,25	0,100	1,5	18,3	29,4	1,8
	0,50	0,105	2,3	50,7	61,9	2,1

As expected, the viscosity of the mother-liquor, measured at the crystallisation temperature, increased as more polysaccharide was added. CMC and carrageenan did not however have the same effect per unit amount added, as shown in Table 4.27 using the data from Table 4.26. CMC had a much greater effect.

Table 4.27

The increases in mother-liquor viscosity, based on a value of 100 when no polysaccharide is added

% Polysaccharide in feed (m/m)	Relative increase in viscosity	
	CMC	Carrageenan
0	100	100
0,2	150	109
0,4	200	117

4.7.2.1 **Effects on G**

The addition of carrageenan to the feed liquor did not result in a statistically significant effect on G. CMC, on the other hand, decreased the rate at which sucrose crystallised as shown by equation 4.7

$$G = 1{,}9 \times 10^{-5} - 2{,}4 \times 10^{-5} \ \% \text{ CMC in feed} \qquad \text{.....4.7}$$

with $r^2 = 0{,}715$ for 3 pairs of observations, from the data in Table 4.25. The uncertainty on the slope ($\pm 1{,}9 \times 10^{-4}$) is very large and thus this result must be viewed with caution.

Viscosity, whether caused by carrageenan or by CMC, caused G to decrease, but not at the same rate, as shown in Table 4.28. The eight pairs of data in Table 4.26 have been used for carrageenan, while the three pairs in Table 4.25 have been used for CMC.

Table 4.28

The effect of viscosity and of the type of polysaccharide on G, where G is given a value of 100 when no polysaccharide is added

Viscosity of mother-liquor/Pa s	Relative decrease in G	
	CMC	Carrageenan
0,05	100	100
0,1	76	98
0,2	27	93

The results in Table 4.28 show that the decrease in the crystallisation rate of sucrose was not due entirely to the viscosity. If this was the case the change in G would be similar for both polysaccharides. The type of polysaccharide thus had a pronounced effect, probably through adsorption or other surface effects, which retard the rate at which sucrose can crystallise and which are specific to the particular polysaccharide.

4.7.2.2 Effects on the rates of impurity transfer

Inspection of Tables 4.26 and 4.27 shows that all R_i values tend to increase as the amounts of carboxymethyl cellulose or carrageenan are increased in the feed. This trend is illustrated when the values of the transfer of calcium are plotted against the amounts of carrageenan present in the feed liquors, using the data from Table 4.27. This can be seen in Figure 4.14.

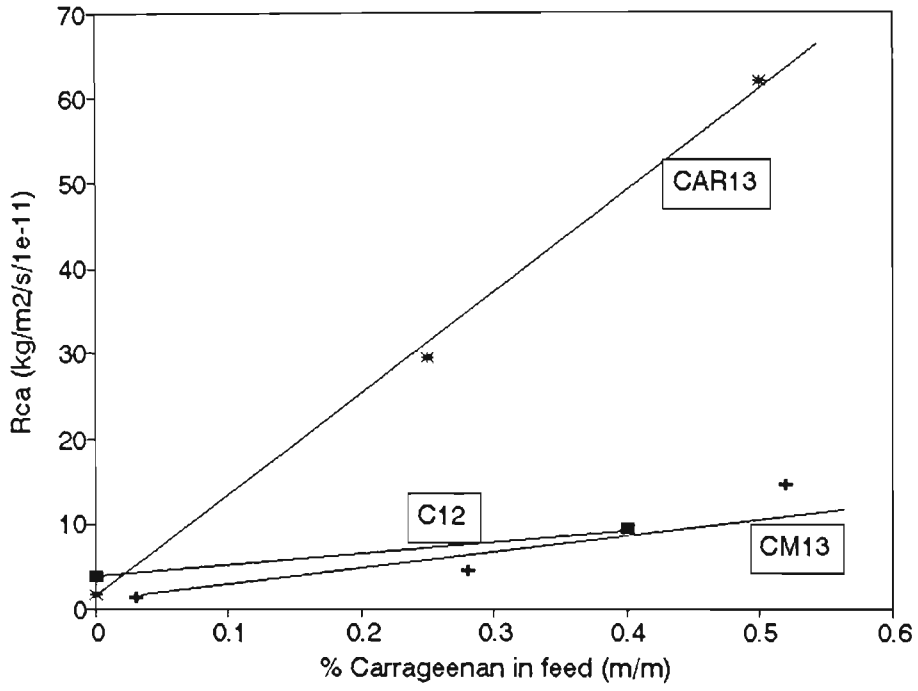

Figure 4.14 The effect of carrageenan on the rate at which calcium is transferred into the sucrose crystal. Data from sets C12, CM13 and CAR13.

The changes in the rates of impurity transfer could be due to the viscosity itself, to the presence of the polysaccharides, through chemical effects, or to a combination of both. There are not enough data to investigate these possibilities.

The following comments may be made:

- In all cases, the presence of the polysaccharides increased the rate at which the impurities

were transferred (see Tables 4.26 and 4.27). This trend is unexpected with CMC since this material decreased G (see Equation 4.7) and as shown in Sections 4.2 and 4.4.2.1, the rates of impurity transfer vary directly with G.

- The magnitude of the increases in the rates of impurity transfer, as the amount of polysaccharide increases, is very large.

- The effect of viscosity itself on the rates of impurity transfer is less consistent. Data from Table 4.26, which relate to the use of CMC, show that viscosity has a large, positive and statistically significant impact on the transfer rates of colour, potassium and calcium. This is not the case when the data from Table 4.27 (carrageenann) are used. Now there is no statistically valid effect of viscosity on the transfer rates of potassium and calcium.

It can be concluded that viscosity had a small but measurable effect on the rate of crystallisation of sucrose. Assuming that carrageenan affected viscosity only (i.e. no surface or adsorption effects) then doubling the viscosity reduced G by about 10%.

The type of the polysaccharide had a marked impact on G. Doubling the quantity of carrageenan had little to no effect, but doubling the quantity of CMC decreased G by 30%.

The impact of the polysaccharides on the impurity transfer rates appear to be independent of any viscosity effect. Both materials tested increased the transfer rates, but with effects of different magnitudes. For example, doubling the quantity of carrageenan increased R_c by 10-15% whereas a similar increase in CMC caused 50-100% increases in R_c. Because of this effect, the impact of viscosity as such on the rates of impurity transfer has not been obtained as was originally planned, since the effects are species specific rather than general.

4.8 **The effect of diffusivity**

As mentioned in Section 1.1.2.5 a transport process has been used to model crystallisation. Viscosity has been involved but it is the diffusivity which is often found in mathematical models

for crystallisation. Diffusivity and viscosity are related by the Einstein-Stokes relationship but this is not the case in highly concentrated sucrose solutions, a result which has been confirmed experimentally by Saska and Oubrahim (1989).

VanHook (1973) also mentions the two-step model for the sucrose crystallisation process and notes that the diffusion coefficient of sucrose decreases as concentration increases. At high temperatures and high supersaturations VanHook used the Nernst theory to consider the effect of an interfacial film. Maurandi (1981) also uses a similar concept and notes, as does Mullin in 1993, that although hypothetical in nature the interfacial film concept is useful in modelling the two-step process.

In the present work it is the diffusivities of the impurities which are of interest. It is however useful to consider results pertaining to sucrose, and it has been shown in Section 1.1.2.5 that the diffusion coefficient of sucrose decreases as supersaturation increases. Furthermore the activation energy of diffusion was found (VanHook, 1945) to be 19-20 kJ/mol. Activation energies for viscosity, for similar sucrose concentrations and temperatures, were calculated in Section 2.5 and values of 1-11 kJ/mol were obtained. Activation energies for G and for the impurity transfer rates are given in Table 4.11, page 99, and the range is from 18 to 32 kJ/mol. It is evident that the activation energies for diffusion are similar to those in Table 4.11, while this is not the case for viscosity.

In the present work diffusivities were measured as described in Section 3.6.6. The frit constant (Schoemaker *et al.*, 1974), was obtained by using a potassium chloride solution, at 25°C. The diffusivity for K^+ at 25°C is 1,96 x 10^{-9} m^2/s (Atkins, 1994). The method was then used to measure the diffusivities of K^+, Li^+, Ca^{2+} and Ni^{2+} at 70°C and in concentrated sucrose solutions. This is discussed below.

4.8.1 **Diffusion coefficients in concentrated sucrose solutions**

As mentioned earlier, the frit must be calibrated by using a substance for which the diffusion coefficient is known. Here, KCl was used. A 1 M KCl solution in water was allowed to diffuse

into pure water, at 25°C. Samples (10 cm^3) were taken and replaced with 10 cm^3 of water, to keep the volume constant. This affects the log law behaviour, but the effect would be small, the volume of water added being less than 2% of that of the bath. The measured concentrations of K^+ were corrected, using a simple material balance, for the removal of samples and addition of water. The results are given in Table 4.29.

Table 4.29

Experimental data for the calibration of the frit with KCl

Sample	Time/s	Concentration of K^+/mg/l	
		Measured	Corrected
Blank	0	8	-
1	660	8	8
2	1560	20	20
3	3360	64	64,1
4	5160	90	90,0
5	6960	108	108,6
6	8760	126	127,0
7	10560	146	147,4
8	12360	154	155,9
9	14160	154	156,4
10	15960	162	164,9
Equilibrium*	-	168	174

*: The equilibrium concentration is obtained by physically mixing the contents of the frit and the bath.

Equation 2.27 in Section 2.6 shows that $\ln (W_\infty - W_t)$ should be linearly related to the time, t. The slope of the line gives $-\alpha D$, where α is the "frit constant". The data in Table 4.29 yield

$$\ln (W_\infty - W_t) = 5{,}35 - 1{,}88 \times 10^{-4} t \qquad \text{.....4.9}$$

with an r^2 value of 0,985 for 10 pairs of observations with a 95% confidence interval on the slope of ± 1,87 x 10^{-5}. This has been plotted in Figure 4.15.

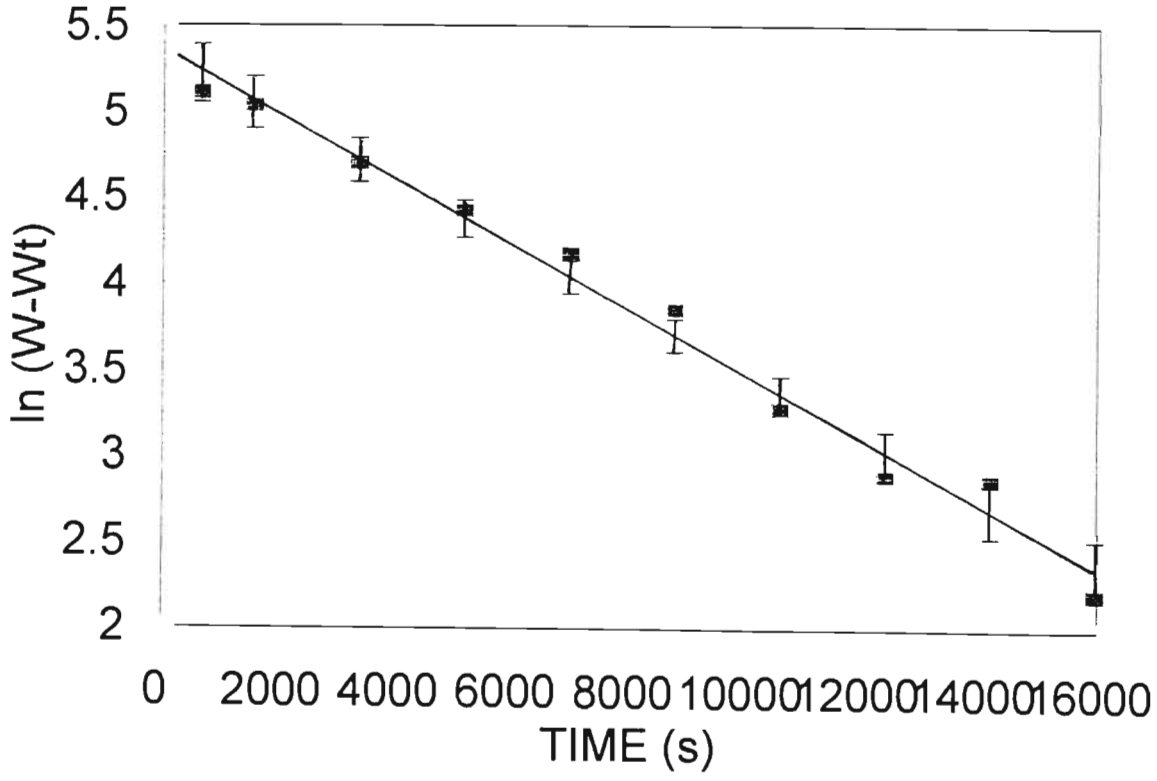

Figure 4.15 The calibration plot to obtain the apparatus constant, α, for the frit used to measure diffusion coefficients. The calibration was performed with a KCl solution.

The linearity obtained confirms that the technique is suitable. The value of α was calculated to be 95 700 m^{-2}.

It is now possible to measure the diffusion coefficients for the selected ions. Sucrose solutions

containing KCl, $CaCl_2$, LiCl and $NiCl_2$, in pairs, were prepared, with sucrose concentrations of 66, 70 and 74% (m/m). These were allowed to diffuse into sucrose solutions of 66, 70 and 74% (m/m) concentration respectively, at 70°C. The diffusion process was found to be very slow and a run required five days, sampling taking place during the period 8 am to 5 pm only. Since it is the results at the highest possible concentration that are most relevant, three runs at 74% (m/m) sucrose were carried out. Typical sets of results are shown in Table 4.30 and in Figure 4.16.

Table 4.30

Experimental data for the diffusivity of Li^+ in a 74% (m/m) sucrose solution, at 70°C

Sample	Time/s	Corrected concentration of Li^+/ mg/kg sucrose
Blank	0	0
1	14 400	0,98
2	79 200	3,05
3	93 600	3,65
4	108 000	4,10
5	165 600	5,77
6	180 000	6,09
7	194 400	6,41
8	252 000	8,20
9	266 400	8,36
10	280 800	8,69
11	338 400	10,14
12	352 800	10,42
13	367 200	10,81
Equilibrium	-	90,0

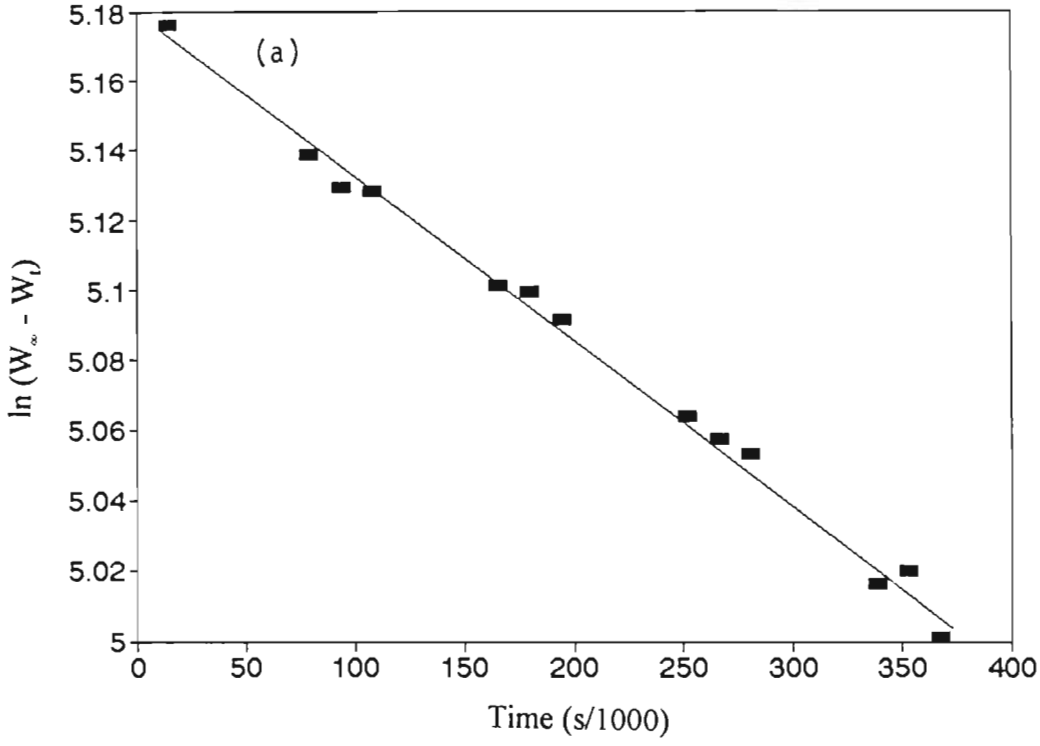

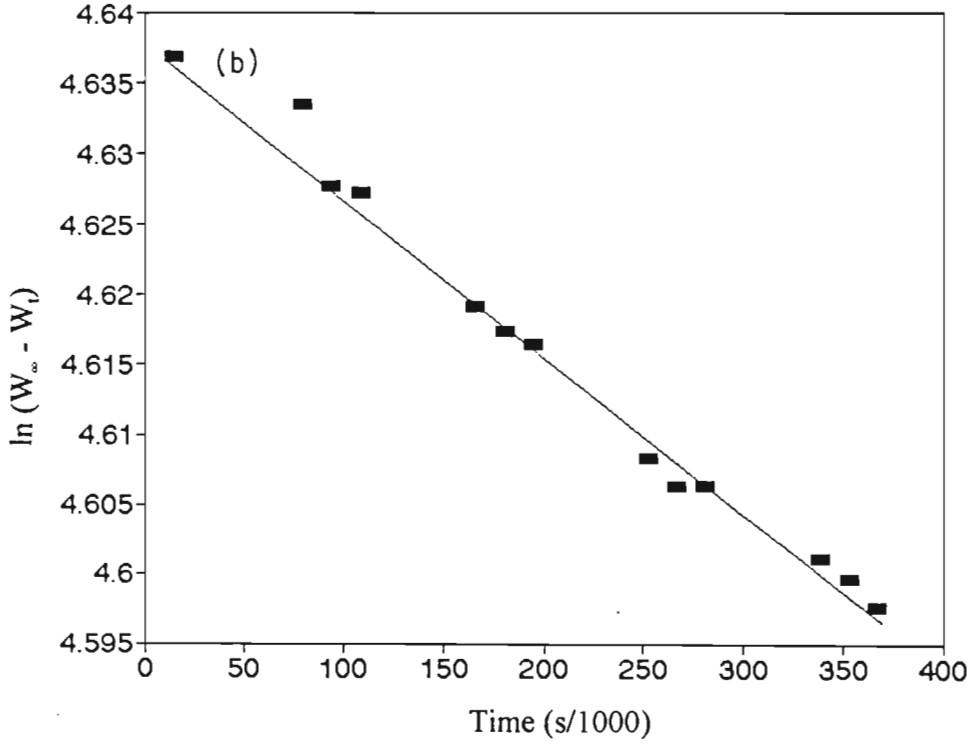

Figure 4.16 **Plots of ln (W_∞ - W_t) versus time, as required by Equation 2.27, for the determination of the diffusion coefficient of (a) K^+ and (b) Ni^{2+}. The slope of the line is equal to $-\alpha D$.**

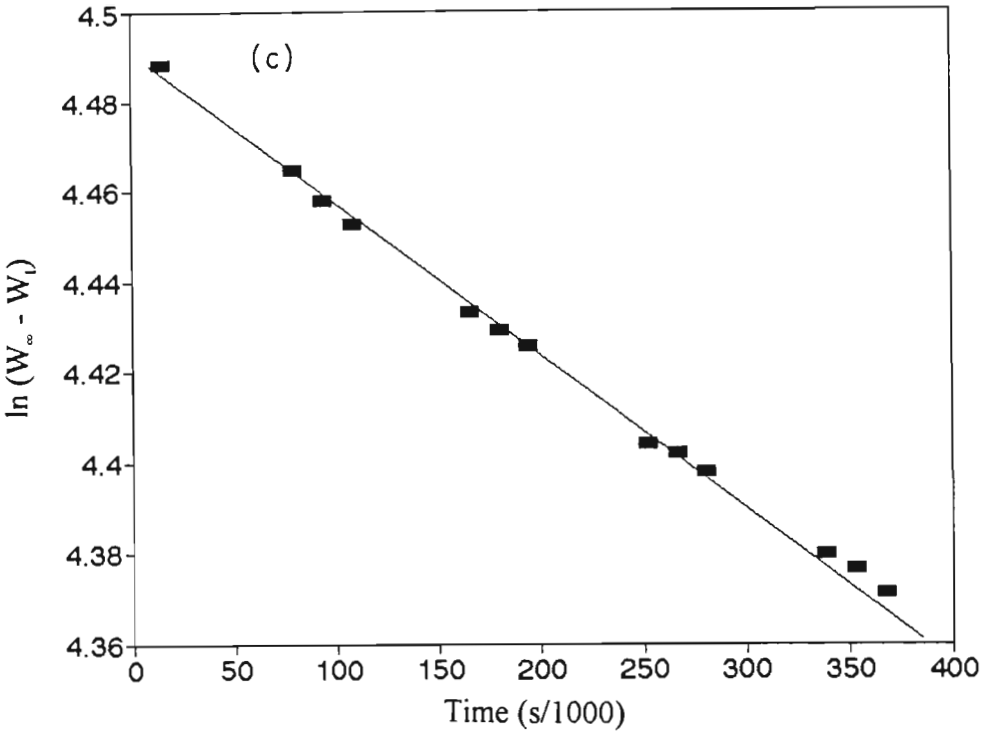

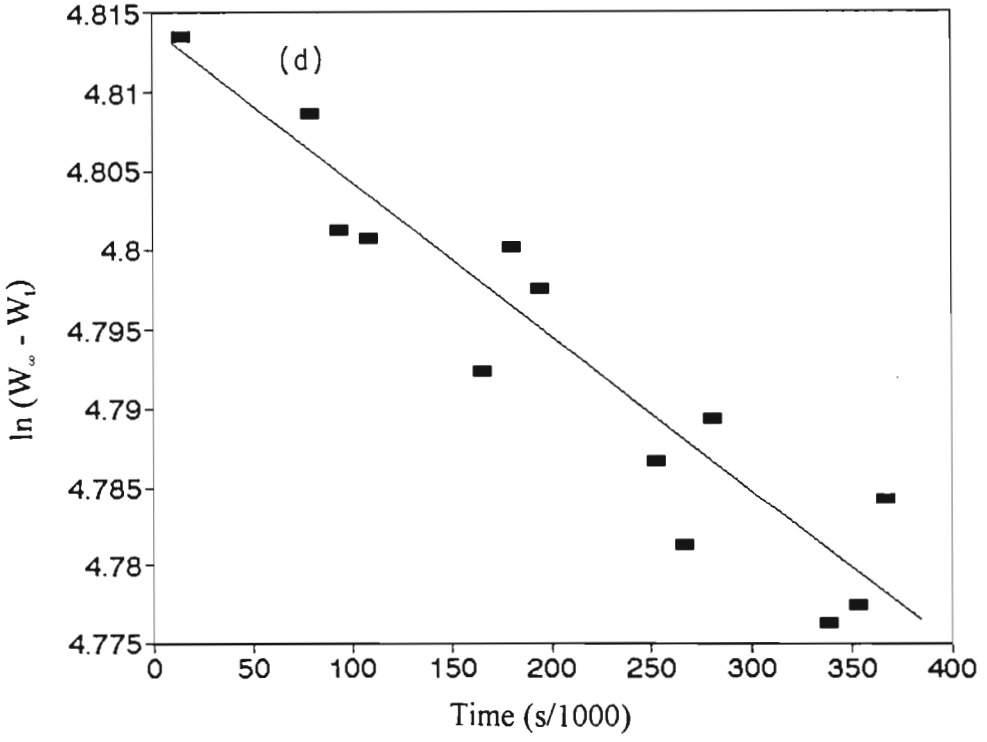

Figure 4.16 (cont.) Plots of ln ($W_\infty - W_t$) versus time, as required by Equation 2.27, for the determination of the diffusion coefficient of (c) Li^+ and (d) Ca^{2+}. The slope of the line is equal to $-\alpha D$.

As shown in Figure 4.16, the linearity for the plots of ln (W_∞ - W_t) versus time was generally good, confirming the validity of the approach. Diffusion coefficients for K^+, Li^+, Ca^{2+} and Ni^{2+} could therefore be calculated, at the different sucrose concentrations and 70°C. This is shown in Table 4.31.

Table 4.31

Diffusion coefficients for the metal ions, at 70°C, with sucrose concentrations of 66, 70 and 74% (m/m)

Set	Sucrose conc./ % (m/m)	$D/10^{-12}$ $m^2/s \pm$ 95% confidence interval			
		K^+	Li^+	Ca^{2+}	Ni^{2+}
1	74	5,8 ± 1	-	-	1,3 ± 0,1
2	74	3,0 ± 0,05	4,5 ± 0,3	2,1 ± 0,3	1,2 ± 0,08
3	74	4,9 ± 0,3	3,4 ± 0,1	1,0 ± 0,2	1,2 ± 0,08
1	70	10,3 ± 0,9	5,6 ± 2,0	4,5 ± 0,7	2,8 ± 0,03
1	66	10,4 ± 0,5	6,3 ± 1,2	3,6 ± 0,9	3,8 ± 0,03

Two effects are evident from the results in Table 4.31. Firstly the diffusion coefficients, D, decrease as the concentration of sucrose increases. The decrease in D, as the sucrose concentration increases, is very similar for lithium, nickel and calcium - in each case D decreases by 3 x 10^{-13} units per unit of increase in sucrose concentration, but potassium shows a larger decrease in its diffusion coefficient, as sucrose concentration rises. Secondly, the absolute values of the diffusion coefficients are low, when compared to diffusion coefficients in water (25°C), for example 1,96 x 10^{-9} m^2/s for K^+, 1,03 x 10^{-9} m^2/s for $Li^+$and 4,59 x 10^{-10} m^2/s for sucrose (Atkins, 1996).

4.9 Models of impurity transfer

One of the main aims of this work is to investigate mechanisms by which impurities could be incorporated into the sucrose crystal. The literature review (Section 1.2) has shown that two main approaches have been linked with crystallisation and impurity transfer, in general. The first treats crystallisation as a two-step process, namely transport to and incorporation into the crystal. The second involves a boundary layer model, for a broken trapping interface.

The possible application of these two models will now be studied.

4.9.1 The two-step model

The two-step model has been described in Section 1.2.3 and it has been pointed out that Smythe (1990) shows that it fits the crystallisation of sucrose.

Equations 1.3, 1.4 and 1.5 (see page 18) can be used to eliminate C_i, the concentration of the impurity in the interface, to yield

$$R_i = K_r \left[(C - C^*) - \frac{R_i}{K_d} \right]^{n'} \qquad \text{.....4.10}$$

where R_i is the observed rate of impurity transfer, K_d a coefficient of mass transfer by diffusion for the impurity, K_r a rate constant for the integration of the impurity into the crystal and (C - C*) is a driving force for the impurity. Here this has been taken as the concentration of the impurity in the feed liquor. This implies that the driving force would be zero if the impurity were absent. Finally, n' is an exponent needed for the equation to fit the data.

The fit of that formula was tested for each impurity, in two ways. Firstly a non-linear regression

routine (Statgraphics, version 5) was used. This involved the known values of R_i and of the concentrations of the impurity in the feed, which the routine then fits into Equation 4.10 by calculating values for K_r, K_d and n'. The routine optimises the fit and yields estimates for K_r, K_d and n'. The following problems were encountered:

- The fitting process was very sensitive to the initial values given for K_d, K_r and n'. The few sets which did not cause the procedure to fail, yielded very different final values for K_d, K_r and n'.

- Response surfaces were very flat and optimisation difficult.

- Values obtained for K_d, K_r and n' gave very poor fits with severe bias in all cases.

It was therefore concluded that, based on the data from the present work, the process of impurity transfer does not fit this two-step model.

This conclusion was confirmed when Sobczak's (1990) integral method was used. This method evaluates K_r, K_d and n' by minimising the sum of squared errors between the observed data and an integral calculated by Sobczak. In all cases the method failed, mostly because the response surface was extremely flat and convergence impossible.

4.9.2 **Interfacial breakdown**

The use of an interfacial film in modelling diffusion effects during crystallisation has been mentioned. Ozum and Kirwan (1976) have investigated a mechanism by which significant quantities of impurities are incorporated into crystals. The mechanism is based on the crystal-solution interface becoming unstable and trapping liquid among the crystalline projections. There is a critical growth velocity above which the growth front is unstable, when the interface breaks down. The mechanism was developed for the incorporation of sucrose and KCl into ice under forced cooling crystallisation and was found to apply to crystallisation from melts and from solutions.

An effective distribution coefficient, K_e, is defined as

$$K_e = \frac{\text{Conc. of impurity in crystal}}{\text{Conc. of impurity in bulk solution}}$$

and the solution (Ozum and Kirman, 1976) of the boundary layer model for a broken, trapping interface, described b an apparent interfacial distribution coefficient, K_a, yields

$$K_e = \frac{X_i}{F_i} = \frac{K_a}{K_a + (1 - K_a)\, e^{-\frac{V\delta}{D}}}$$

where V is a growth velocity (m/s), δ a boundary layer thickness (m) and D the diffusion coefficient (m^2/s) for the impurity under study. The distribution coefficient K_a is given by the ratio of the concentrations of the impurity in the crystal to that in the boundary layer, which is unknown.

A rearrangement of the above equation yields

$$\ln\left(\frac{1 - K_e}{K_e}\right) = \ln\left(\frac{1 - K_a}{K_a}\right) - \frac{\delta}{D}V$$

.....4.11

V in equation 4.11 is equivalent to the growth rate l_g, defined by equation 2.17 in Section 2.2.2. Thus for a process following the interfacial breakdown model of Ozum and Kirwan, a plot of $\ln[(1 - K_e)/K_e]$ versus l_g should be linear. The intercept is equal to $\ln[(1 - K_a)/K_a]$ while the slope is $-\delta/D$.

Data are available from the experiments described in Section 3.6 to test the fit of equation 4.11, using the method of least squares. It should be noted however that these experiments were not designed specifically to test this model. The results will therefore at best yield preliminary conclusions. Detailed results for colour, the impurity for which the largest number of observations is available, are given in Table 4.32.

Table 4.32

The fit of equation 4.11 for colour

Set	$\ln\left(\frac{1 - K_e}{K_e}\right) = a - bl_g$		n	r^2
	a	b		
TR18	4,10	$-1,21 \times 10^7$	8	0,03*
S16	3,79	$-6,28 \times 10^6$	6	0,01*
R15	6,89	$-1,20 \times 10^8$	5	0,76
GHR	3,91	$-1,60 \times 10^7$	18	0,24
MT13	4,22	$-1,60 \times 10^7$	3	0,92
AP13	3,99	$-1,14 \times 10^7$	3	0,92
HT14	3,55	$-6,38 \times 10^6$	4	0,09*
HTAC	3,68	$-1,60 \times 10^7$	3	0,09*
HTDF	3,48	$-4,36 \times 10^6$	3	0,54*
ST13	4,10	$-9,99 \times 10^6$	3	0,78
SCA13	3,29	$-6,89 \times 10^6$	3	0,02*
CS15	3,39	$-9,75 \times 10^6$	3	0,11*
LN15	3,52	$-1,47 \times 10^6$	5	0,02*
KL15	4,04	$-1,60 \times 10^6$	5	0,08*

Generally, the values of r^2 are very low, the regression is not statistically significant in many cases (marked *), and the plots show high random scatter, but no bias. This is not unexpected, as highlighted above. Two observations may however be made:

- in all cases the value of a is positive and the range for a is not wide, (mean = 4,0; Std. error = 0,2),
- the slopes are always negative as required by equation 4.11, but the variation is wide (mean = $1,7 \times 10^{7}$; Std. error = 8×10^{6}).

The results obtained for all the other impurities, except starch, were similar. Data from eight sets of experiments involving starch were used but, in all cases, they did not fit equation 4.11.

These findings were considered sufficiently interesting to warrant a specific set of experiments to investigate the fit of equation 4.11. A large sample of liquor was spiked with the selected impurity and five sub-samples were then crystallised using different energy inputs (see Section 3.1.1) in order to change l_g. As far as possible all the other factors, such as masses of feed and of condensate, temperature, agitation, final crystal size, etc., were kept the same for the five runs. A typical set of experimental data, which in this case represents the experiments with colour as the impurity, is shown in Table 4.33.

Table 4.33

Typical set of experimental data to test the fit of equation 4.11 for colour.

The feed colour was 564 units.

Run	Temp /°C	L /μm	W /μm	Voltage /volts	l_g /m/s	X_c /colour units
1	70,4	253	194	220	$4,1 \times 10^{-8}$	17
2	70,4	258	183	140	$1,4 \times 10^{-8}$	13
3	70,2	260	197	160	$1,9 \times 10^{-8}$	14
4	70,3	253	196	180	$2,8 \times 10^{-8}$	15
5	70,2	254	203	200	$3,5 \times 10^{-8}$	15

The results in Table 4.33 show that the factors not investigated have been kept reasonably constant. The range over which l_g can be changed is limited. The maximum energy input corresponds to 220 volts and this is the upper limit. Below 140 volts circulation in the crystalliser

becomes very slow and this was considered the lowest practical limit. As a result, l_g ranges from about 1,4 to 4,1 x 10^{-8} m/s and this causes a relatively small change in the crystal colour (13-17 units). The difficulty in obtaining wide ranges for the independent variables has been encountered often in this work. This tends to increase the experimental error on the effect of the change of conditions. Equation 4.12 is obtained when the data are used in a linear regression for colour

$$\ln\left(\frac{1 - K_e}{K_e}\right) = 3{,}86 - 8{,}7 \times 10^6 \, l_g \qquad \text{.....4.12}$$

with an r^2 value of 0,91, for five pairs of observations. These results are plotted in Figure 4.17

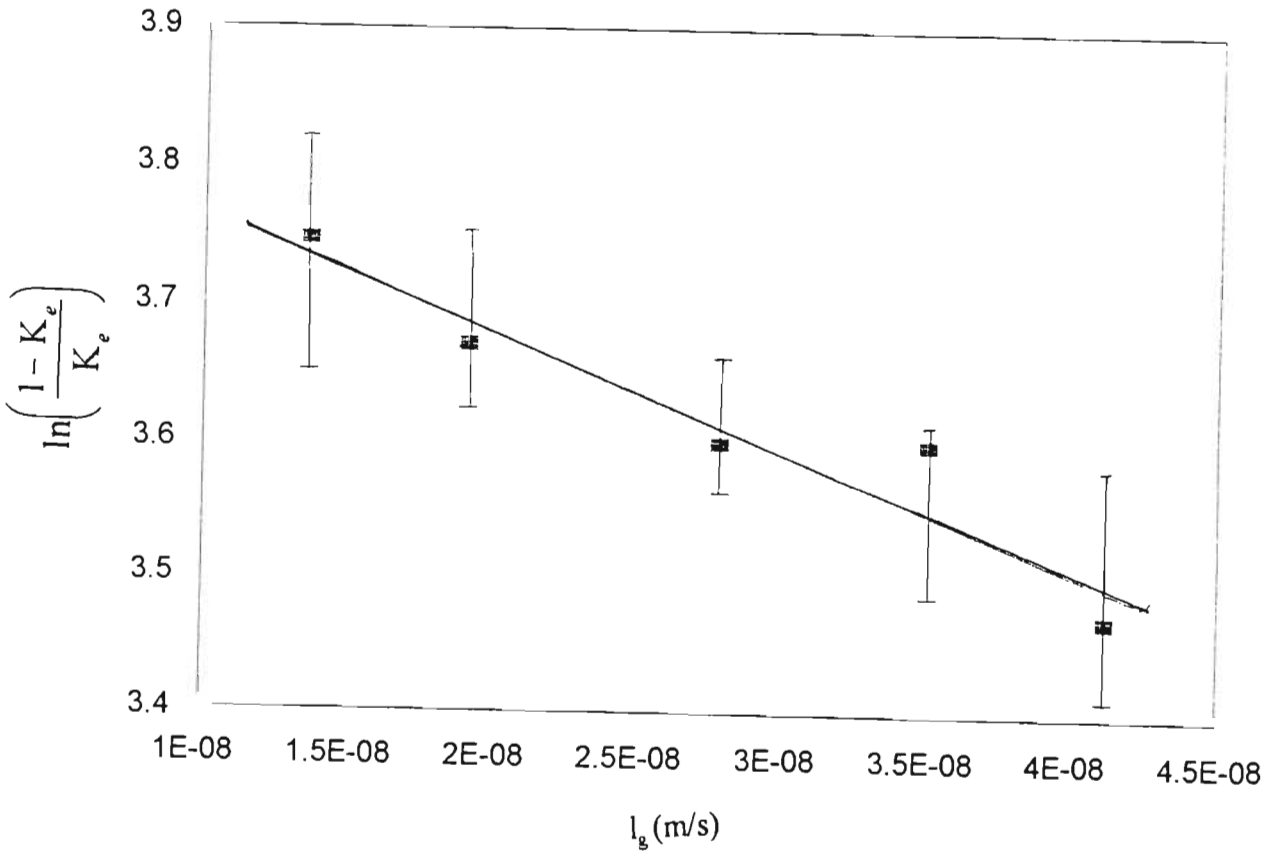

Figure 4.17: The plot to illustrate the fit of data for colour to Equation 4.11.

Equation 4.12 and Figure 4.17 show that the results for colour fit the interfacial breakdown model well.

Similar experiments were done to investigate the other main impurities, namely potassium, calcium, nickel and lithium. The linear regressions yielded equation 4.13 to 4.16, for five pairs of observations, in each case:

Potassium:

$$\ln\left(\frac{1 - K_e}{K_e}\right) = 7{,}79 - 1{,}9 \times 10^7 \, l_g \qquad r^2 = 0{,}94$$

.....4.13

Calcium:

$$\ln\left(\frac{1 - K_e}{K_e}\right) = 6{,}29 - 1{,}4 \times 10^7 \, l_g \qquad r^2 = 0{,}85$$

.....4.14

Nickel:

$$\ln\left(\frac{1 - K_e}{K_e}\right) = 7{,}33 - 2{,}2 \times 10^7 \, l_g \qquad r^2 = 0{,}75$$

.....4.15

Lithium:

$$\ln\left(\frac{1 - K_e}{K_e}\right) = 6{,}66 - 5{,}8 \times 10^6 \, l_g \qquad r^2 = 0{,}90$$

.....4.16

These results have also been plotted in Figure 4.18.

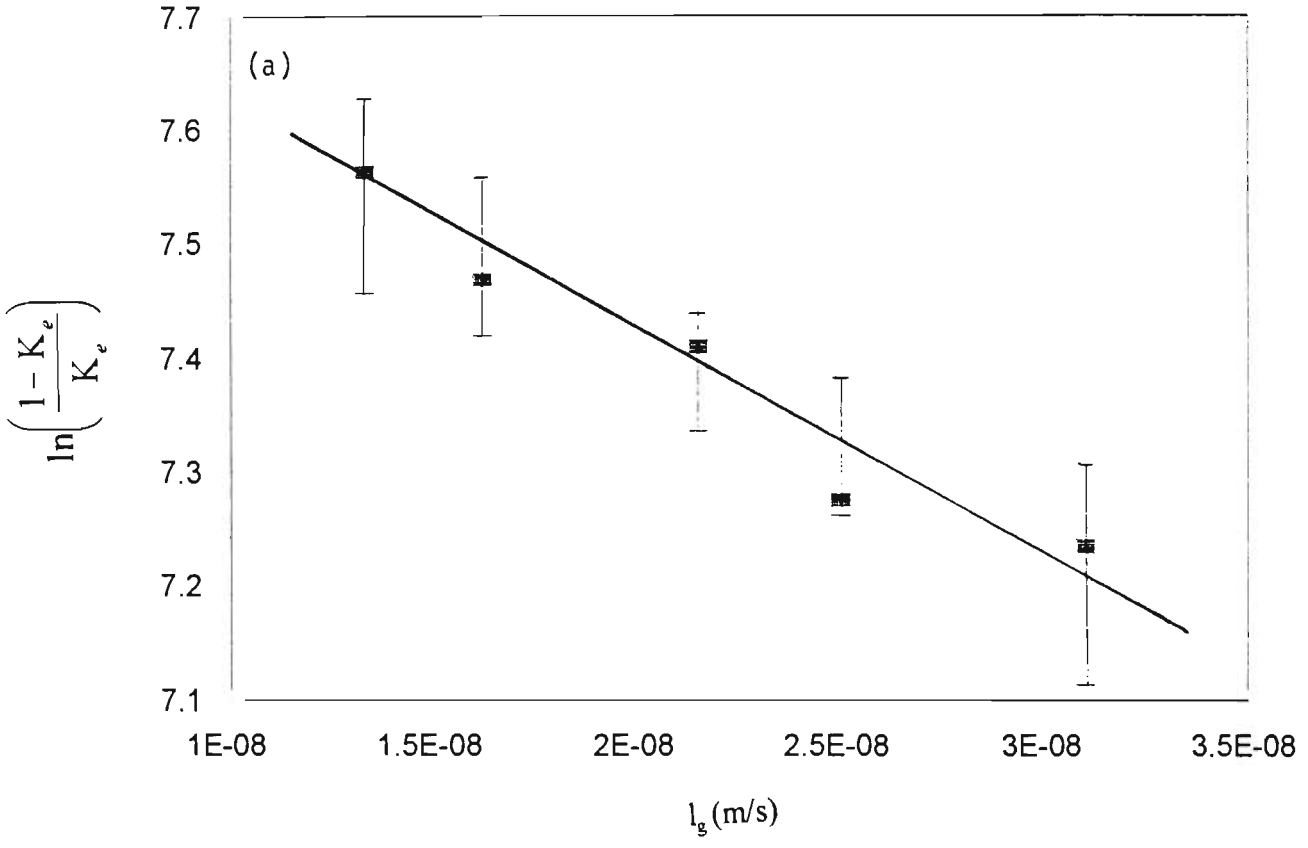

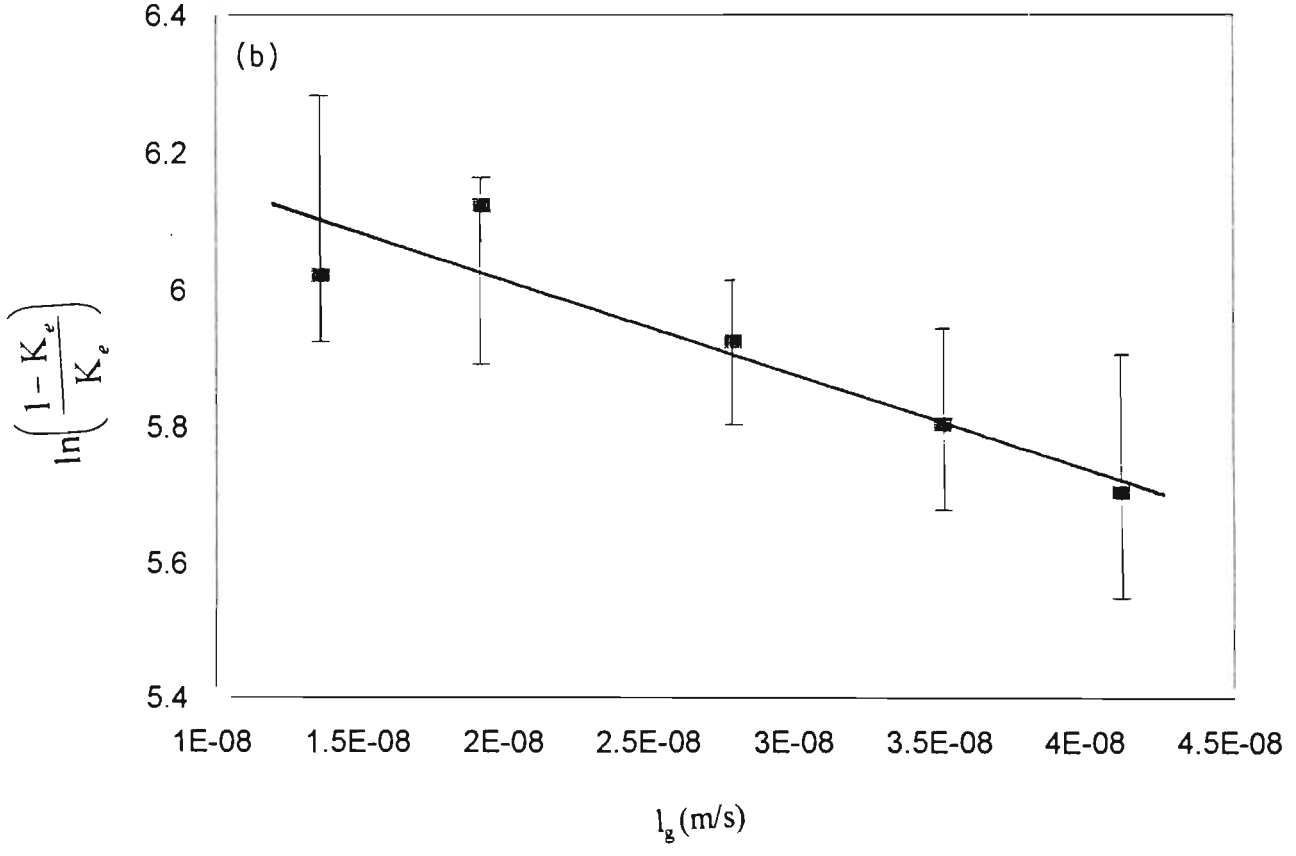

Figure 4.18: The plots to illustrate the fit of Equation 4.11 to data from (a) potassium and (b) calcium as impurities.

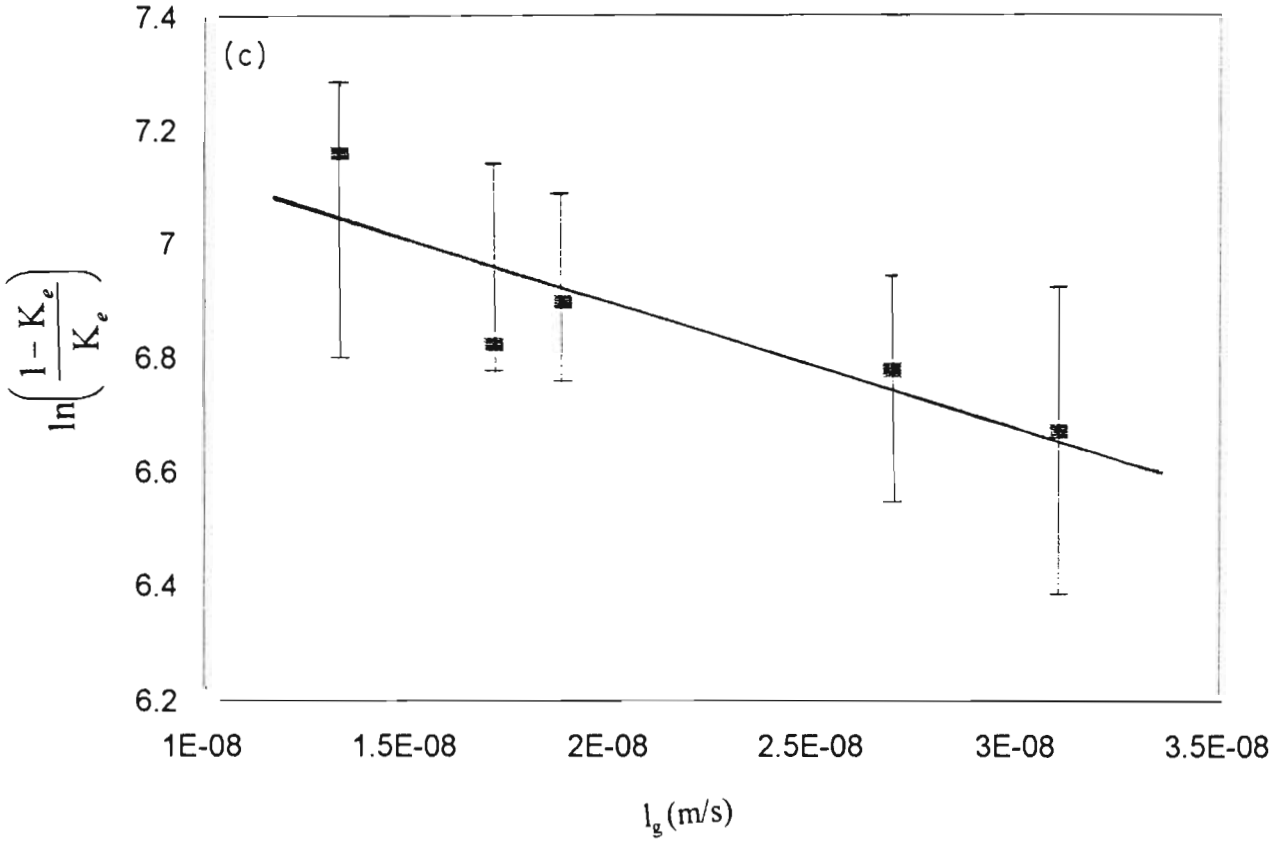

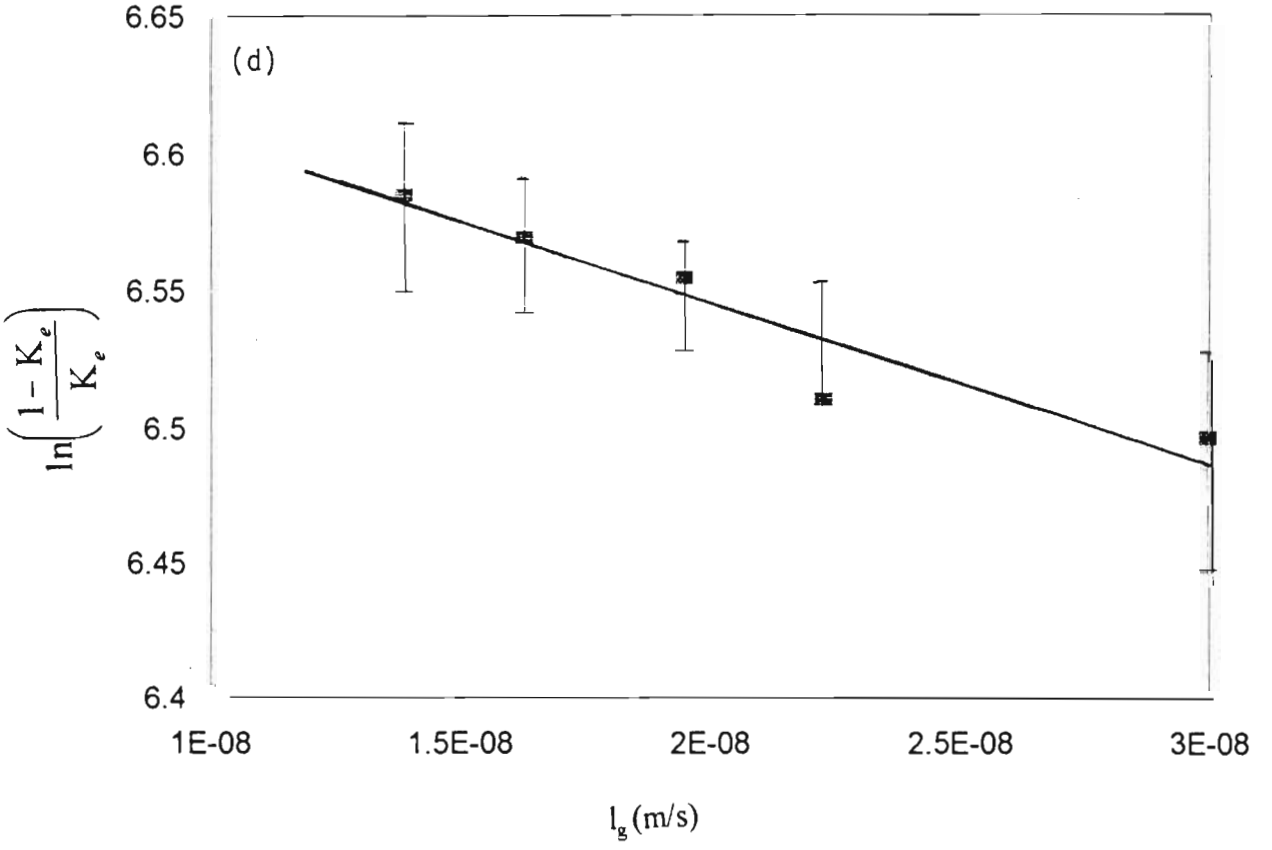

Figure 4.18 (cont.): The plots to illustrate the fit of Equation 4.11 to data from (c) nickel and (d) lithium as impurities.

These results show that, when the experimental conditions are set to investigate only the interfacial breakdown model, that is when extraneous effects are eliminated, good fits are obtained with data from colour, potassium, calcium, nickel and lithium. Starch has generally behaved differently from the above mentioned impurities and this is again the case with the interfacial breakdown model. The fit of the model with data from the experiments involving starch was very poor, with a correlation coefficient of 0,04. The data have been plotted in Figure 4.19 which shows much scatter. These results confirm the lack of fit obtained with the rest of the data, for starch.

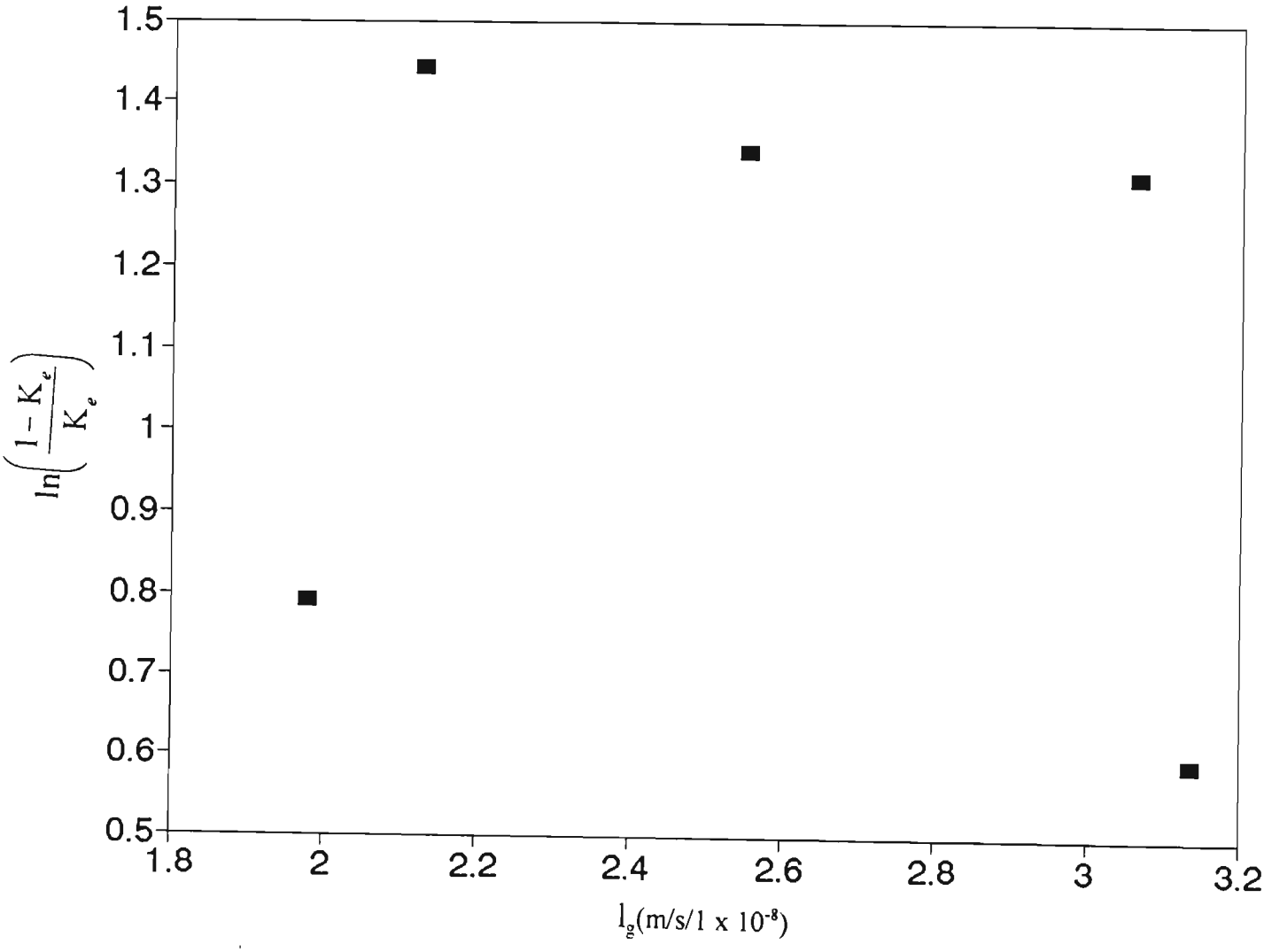

Figure 4.19: Plot to illustrate the lack of fit of the starch data to Equation 4.11.

Equation 4.11 shows that the slope of the line is equal to $-\delta/D$, where δ is the film thickness and D the diffusion coefficient. The diffusion coefficients (D, m/s^2) for potassium, calcium, nickel and lithium (as chlorides) in solutions containing 66,70 and 74% sucrose (m/m), at 70°C, were measured as described in Section 3.6.6. The results are given in Table 4.31 and are shown again here, in Table 4.34.

Table 4.34

Diffusivity coefficients for the metal ions, at 70°C, with sucrose concentrations (m/m) of 66, 70 and 74%

Set	Sucrose conc./ % m/m	$D/10^{-12}m^2/s$			
		K^+	Li^+	Ca^{2+}	Ni^{2+}
1	74	5,8	-	-	1,3
2	74	3,0	4,5	2,1	1,2
3	74	4,9	3,4	1,0	1,2
1	70	10,3	5,6	4,5	2,8
1	66	10,4	6,3	3,6	3,8

D decreases with increasing sucrose concentration. The crystallisation process took place at a sucrose concentration of about 78% (m/m), but diffusion coefficients could not be measured at this high concentration of sucrose because of experimental problems, mostly due to sucrose crystallising in the equipment. The results in Table 4.34 have therefore been used to estimate D at 70°C but for a sucrose concentration (m/m) of 78%. This was done by extrapolating the values of D against the corresponding sucrose concentrations, each impurity being treated separately. The linear regression technique yielded four equations relating D to the sucrose concentration, a typical example (for potassium) being

$$D = 6,9 \times 10^{-11} - 8,8 \times 10^{-13} \times \text{Conc. of sucrose}$$

with an r^2 value of 0,76. The equations were then used to calculate D for each impurity, but at

a sucrose concentration of 78% (m/m). The following values for D were obtained: $6{,}6 \times 10^{-13}$, $2{,}8 \times 10^{-12}$, $1{,}2 \times 10^{-12}$ and $4{,}4 \times 10^{-13}$ m^2/s, for potassium, lithium, calcium and nickel, respectively. This also allows the calculations of δ, the film thickness.

Geankoplis (1993) shows that it is possible to estimate D/δ, the reciprocal of the slope in equation 4.11, independently, using the correlation

$$K_L = 0{,}13\left(\frac{(P/V)\mu}{\rho^2}\right)^{1/4} / N_{sc}^{2/3}$$

where K_L is a mass transfer coefficient equal to D/δ, P is the power input into the crystalliser, V is its working volume, μ is the viscosity of the solution, ρ its density and N_{sc} the Schmidt number given by $\mu/\rho D$. This correlation was chosen because it applies to a range of particle size similar to that found with the sucrose crystals in the crystalliser (particles less than 600 μm), in a slurry stirred mechanically.

The right hand side of Geankoplis' correlation can be calculated. The following data were used:

P, the power was taken at 70% of that of the stirrer motor; P is then equal to 175 W.

V, the working volume, was taken as the average value between the volume at the nucleation point (6×10^{-3} m^3) and that at the end of the run (13×10^{-3} m^3). V is thus 9×10^{-3} m^3.

The temperature in the crystalliser is 70°C; the mother-liquor was analysed and showed a concentration of sucrose (m/m) of 78%. Under those conditions, the correlations of Peacock (1995) show that the viscosity of the solution is 12×10^{-3} Pa s while its density is 1368 kg/m^3.

Finally, the diffusion coefficients taken are those at 78% (m/m) sucrose and 70°C, given earlier.

It is now possible to calculate the values of K_L for potassium, calcium, nickel and lithium. The ratio δ/D, given by the reciprocal of K_L, is also the slope of equation 4.11. The two values may therefore be compared, as done in Table 4.35.

Table 4.35

Comparison of the value δ/D obtained from the slope of Equation 4.11 and that calculated independently from Geankoplis' correlation

Impurity	Slope (δ/D)		Difference % $\left\{\frac{(a)-(b)}{(a)}\right\} \times 100$
	(a) Equation 4.11 (Interfacial model)	(b) According to Geankoplis	
Potassium	$1,9 \times 10^7$	$1,1 \times 10^7$	42
Calcium	$1,4 \times 10^7$	$7,2 \times 10^6$	49
Nickel	$2,2 \times 10^7$	$1,4 \times 10^7$	36
Lithium	$5,8 \times 10^6$	$4,1 \times 10^6$	29

Geankoplis states that the correlation can deviate by up to 60%. The results obtained in Table 4.35 show relatively large deviations but these are below 60% and the agreement is considered acceptable. The film thickness can now be estimated and is found to be between 7×10^{-6} and 13×10^{-6} m.

It can be concluded that experimental evidence has been obtained to show that the transfer of selected impurities, but not starch, involves an interfacial breakdown process.

4.10 X-ray powder diffraction of sucrose crystals

Work done by VanHook (1997a; 1997b) has shown that fructose, glucose and raffinose, when incorporated into the sucrose crystal, do not change the normal spatial dimensions between the molecules in the crystal.

The experimental technique described in Section 3.4.6 was used to test this observation but now

with starch, colour, potassium and calcium as impurities. Two types of crystals were used. The first involved a sugar liquor specially purified by using activated carbon and containing levels of the abovementioned impurities as low as possible. This liquor was then crystallised in the crystalliser. Sub-samples of the same liquor were then spiked with high levels of the selected impurities and crystallised. These runs yielded affinated crystals with low and high impurity contents which were submitted for x-ray diffraction analyses. Typical XRD results are shown in Figures 4.20 (a) to 4.20 (d). Visual inspection of the spectra shows very little evidence of any shift in the angular position of the sucrose peaks between the purer crystals (Figure 4.20 (a)) and those with high concentrations of impurities. This suggests that little lattice displacement has occurred when higher concentrations of impurities are present; in all cases the lattice spacing parameters show no evidence of change and have remained true to the sucrose standard. It is stressed that the approach used here is qualitative. It has only been shown that there are no large differences in the lattice structures of the pure and impure crystals.

4.11 **Conclusions**

This has been a fairly long chapter, covering results from ten main sections. It has been shown that a simple inclusion of mother-liquor cannot account for the presence of impurities in the sucrose crystal. The rate at which sucrose is crystallised, the temperature, the type and concentration of the impurity all impact on the rate of impurity transfer. Partition and diffusion coefficients have been investigated. Experimental evidence has been obtained to show that the transfer of all the impurities selected, except starch, is by an interfacial breakdown process. This involves a film thickness which has been estimated.

These main findings will be discussed in detail in Chapter 5.

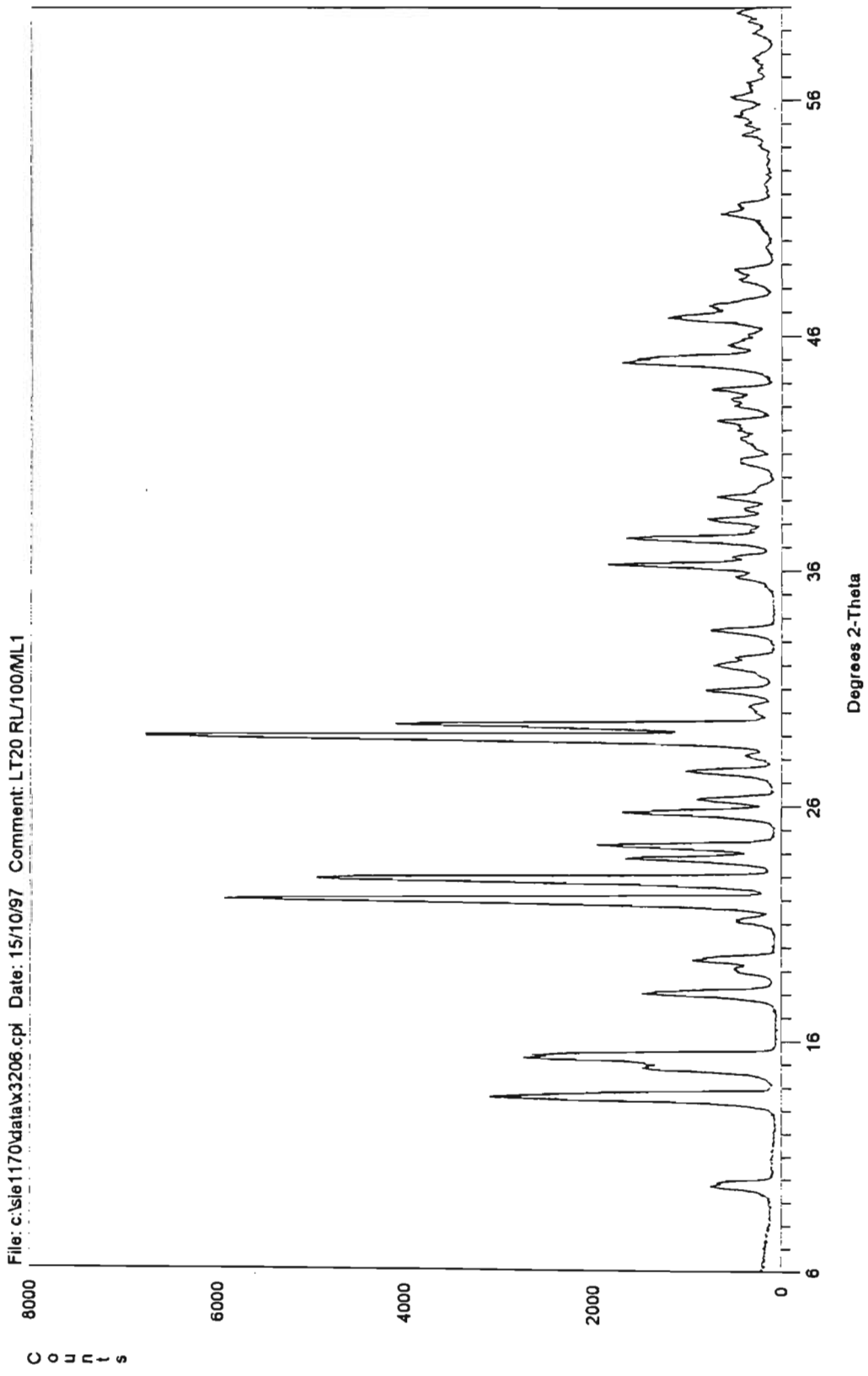

Figure 4.20 (a) **Run ML1. Purer crystal: starch 80 mg/kg, colour 10, K^+ 2 mg/kg, Ca^{2+} 5 mg/kg.**

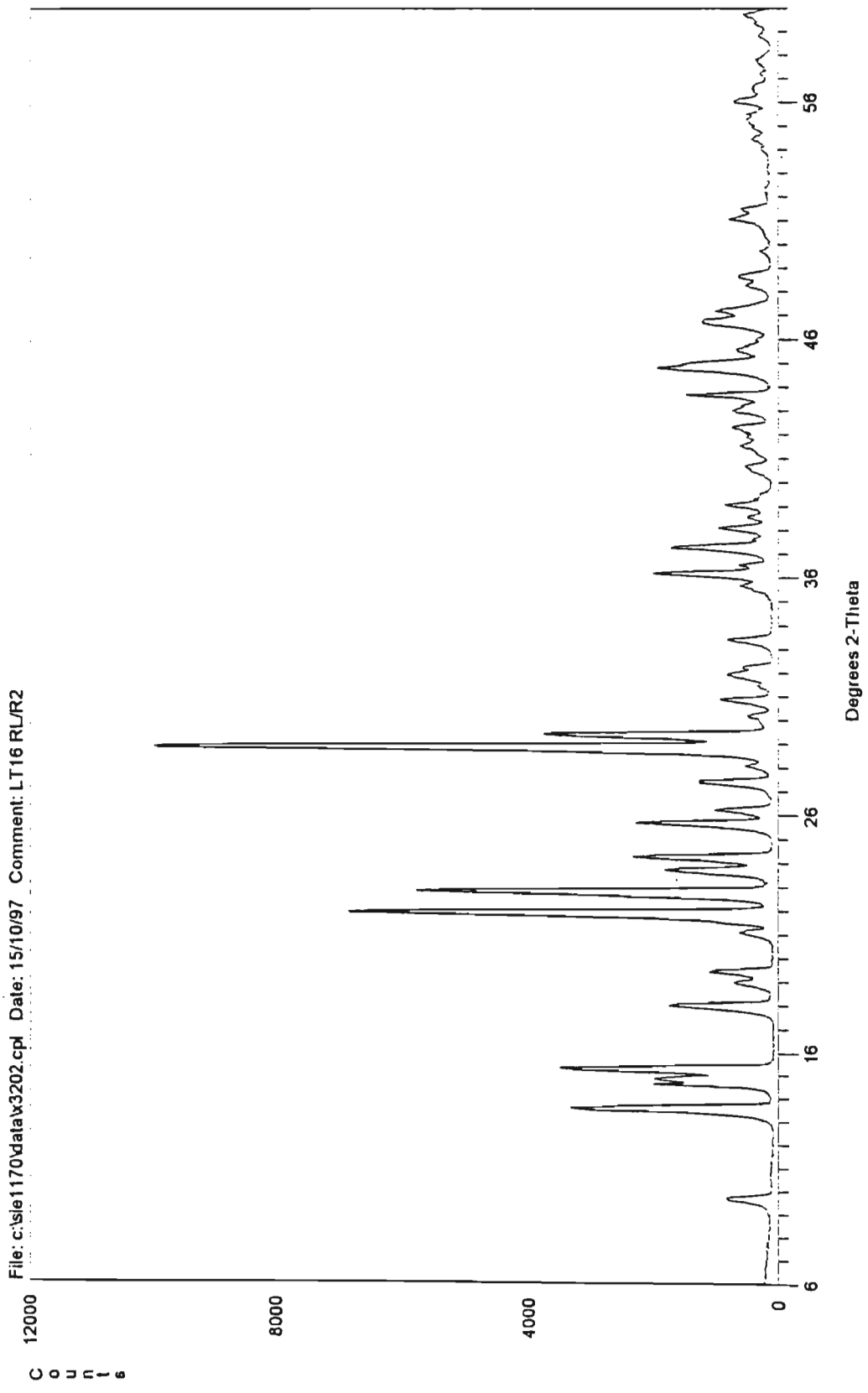

Figure 4.20 (b) **Run R2. Impure crystals: colour 335, K^+ 21 mg/kg, Ca^{2+} 80 mg/kg.**

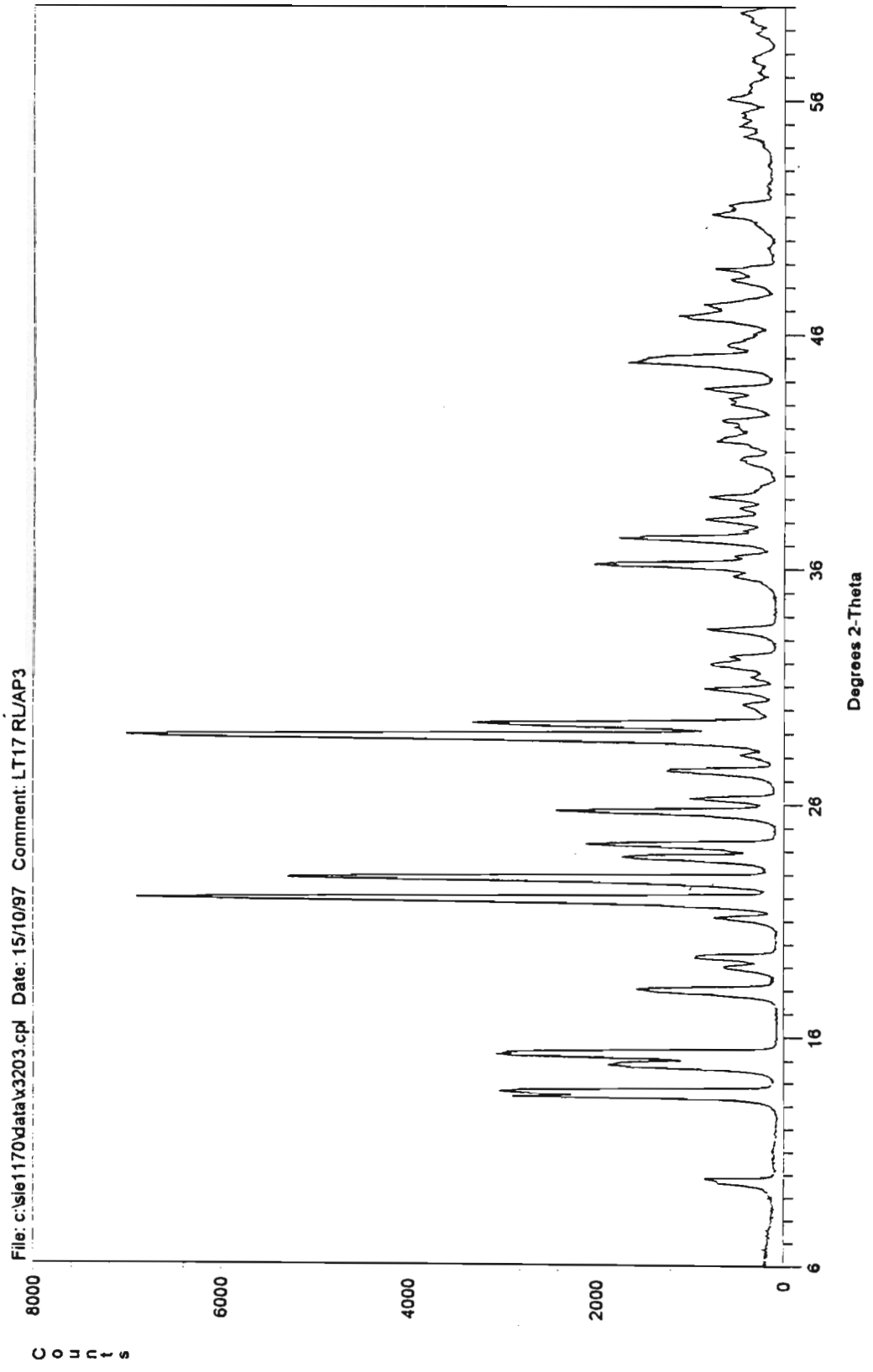

Figure 4.20 (c) **Run AP3. Impure crystals: colour 340, K^+ 18 mg/kg.**

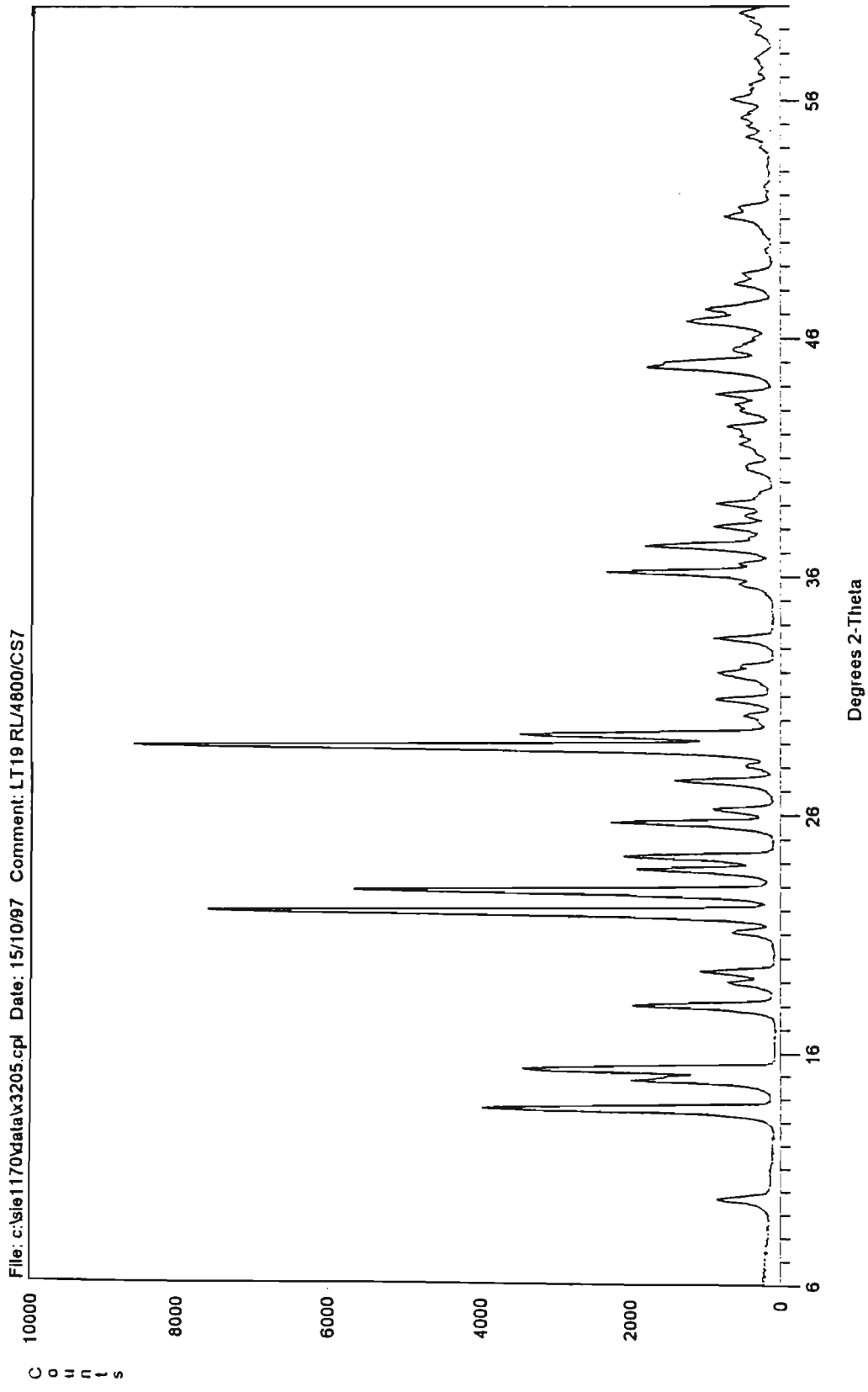

Figure 4.20 (d) **Run CS7. Impure crystals: starch 5000 mg/kg, colour 30.**

CHAPTER 5

DISCUSSION

The results obtained from the present work have been presented individually in Chapter 4. In this Chapter the results will be discussed as a whole and the accent will be on what has been found through the present study. This will be done bearing in mind the three main objectives and the limitations of this work, as set out in Section 1.3, on page 21.

5.1 Basic causes for impurity transfer

It could be suggested that the presence of impurities in the sucrose crystal results from a simple, mechanical inclusion of droplets of mother-liquor. The study of the transfer of colour, potassium, lithium, calcium and starch, under identical crystallisation conditions (Section 4.1) shows that this is not the case. This conclusion is based on three main results:

- The ratio of the concentrations of selected pairs for impurities in the feed and in the crystal are very different, as shown in Table 5.1. If straightforward mechanical inclusion had occurred, then these ratios would be equal to 1.

Table 5.1

Ratios of concentration of pairs of impurities in the feed and in the crystal

Pair of impurities	Ratio of concentration in crystal/in feed
K^+/Li^+	2
Ca^{2+}/K^+	4
Colour/K^+	10
Starch/K^+	64-85

- The concentrations of impurities in the crystal have been found to be linear functions of the concentration in the feed liquor, as shown by Table 4.3 and these data have been used to generate Table 5.2. Although the concentration in the feed is the same for each species, there are large differences for the concentrations in the crystal.

Table 5.2

Concentrations of various impurities in the crystal, for the same concentration in the feed, calculated from the linear functions in Table 4.3, page 83

Concentration in feed /mg/kg water	Concentration in crystal /mg/kg			
	Li^+	K^+	Ca^{2+}	Starch
500	0,6	0,7	0,0	176
1000	0,8	1,3	4,4	266
2000	1,2	2,6	13,1	466

The results indicate that the trend in the transfer is

$$\text{starch} >> \text{colour} > Ca^{2+} > K^+ > Li^+.$$

- Evidence of a change in the wavelength of maximum adsorption for starch present inside the crystal as compared with that for starch in the feed liquor (see Section 4.1 and Figure 4.2) has been found. This indicates the possibility of some molecular rearrangement as the starch is transferred into the sucrose crystal.

It is therefore possible to conclude that a simple, mechanical inclusion of impurities is highly unlikely. This therefore justifies continuing the investigation.

5.2. The rate of impurity transfer, R_i

One of the main objectives of this work has been to propose and investigate a parameter to quantify the rate at which the selected impurities are incorporated into the sucrose crystal. A new concept, namely R_i representing the mass of impurity transferred into the crystal, per unit crystal surface area and per unit crystallisation time, has been derived and investigated.

As discussed in Section 3.6, this work involved 39 sets of experiments and, in each case, R_i ($kg/m^2/s$) was measured for each impurity. These measured R_i values have been used to obtain the information shown in Table 5.3; the minimum and maximum are the single lowest and highest values, respectively, while the average is an arithmetic average of all the measured values. The individual ranges are wide and there are large differences between the various species. This indicates that this parameter is sensitive to crystallisation conditions and to the type of impurity.

Table 5.3

Ranges and averages for R_i, using all the values measured in the 39 sets of experiments

Species	$R_i/kg/m^2/s$		
	Minimum	**Maximum**	**Average**
Colour	$1,3 \times 10^{-5}$	$2,0 \times 10^{-3}$	4×10^{-4}
Potassium	$4,7 \times 10^{-12}$	$9,6 \times 10^{-11}$	3×10^{-11}
Calcium	$5,4 \times 10^{-12}$	$7,7 \times 10^{-11}$	4×10^{-11}
Lithium	$5,3 \times 10^{-13}$	$1,7 \times 10^{-11}$	6×10^{-12}
Starch	$5,0 \times 10^{-11}$	$2,9 \times 10^{-8}$	5×10^{-9}
Methylene blue	$5,8 \times 10^{-14}$	$3,6 \times 10^{-4}$	6×10^{-5}

The factors that affect R_i were then considered. The effect of the rate of crystallisation of sucrose, G, on the impurity transfer rates was investigated through two main series of tests. The first

involved the effect of G only on R_i (Section 4.2.2), while the second used the relevant data from all 39 sets of experiments (Section 4.4.2.1). Two clear results emerge:

- There is a strong relationship between R_i and G; as G increases so does R_i
- the effect of G can be quantified by a relation of the form

$$R_i = a\ G^b$$

and, except for starch, b varies from 1,0 to 1,1. For starch b is equal to 2,5, which indicates a much more pronounced effect.

Industrially, G cannot be reduced much because of throughput and plant utilisation considerations and, thus, the rate of impurity transfer cannot be controlled through G.

The effect of temperature on reaction rates is usually investigated through the Arrhenius model. This has been done in the literature and in the present work for the rate of crystallisation of sucrose. The value of the activation energy for G measured in the present work, namely 18 kJ/mol, is not out of line and compares well with the lower range given in the literature. More interestingly, this is probably the first time that activation energies for the transfer of impurities in the sucrose crystal have been measured. For colour the value is about 19 kJ/mol, or similar to that of G. Activation energies for the inorganic species are higher, namely 25 to 30 kJ/mol but the precision is lower. Starch again behaves differently in that the activation energy for its transfer was not statistically different from 0. This implies that temperature has no effect on the transfer of starch into the sucrose crystal.

Again, two main series of tests (Sections 4.4.1 and 4.4.2.1) have been used to investigate the effect of the type and concentration of the impurity on the rate of impurity transfer. In both cases the concentrations of the impurities in the feed liquors have a marked effect on the rate of transfer into the sucrose crystal and there are differences among the species. The results have been expressed through relations of the form

$$R_i = \propto G^a F_i^b \text{ or } R_i = \propto F_i^c L_c^d$$

for each species, as shown in detail in Section 4.4.2.1. The values of c are summarised in Table 5.4.

Table 5.4

Values of c in $R_i = \propto(G^a, F_i^c, L_c^b)$, from the results in Table 4.18

Species	Range for c
Colour	0,7 to 0,8
Potassium	0,6 to 0,9
Calcium	0,4 to 1,2
Starch	1,0 to 1,6
Dyes	0,2 to 2,1

The effect of concentration for colour and potassium are similar. The range for c with calcium is wide but inspection of Table 4.18 shows more consistent results from the multiple linear regression technique and a value of 0,4 for c would appear more correct. The effect of concentration for starch is high, and there are large differences among the dyes. Possible reasons for these were not investigated here.

Finally an interesting observation that can be made from the results in this section concerns the activation energy. Mullin (1993) discusses the process of crystallisation in general and notes that it can consist of a transport step, followed by a surface integration one. The activation energies of these two steps are different; the transport step shows E_a values of 10-20 kJ/mol while the incorporation one shows values of 40-60 kJ/mol. The activation energies measured in this work are closer to those for the transport process. This indicates that transport phenomena may be involved in mechanisms for impurity transfer.

5.3 Impurities in the crystal

As discussed in Section 3.6, the concentrations of impurities in the sucrose crystal, X_i (mg/kg), are available. This parameter has been used to investigate the second main objective of this work, namely the mechanisms of impurity transfer.

Two processes namely adsorption isotherms (Section 4.6) and partition coefficients (Section 4.5) were considered. The first process confirmed the overriding influence of the concentration of the impurity in the feed liquor (see Section 4.6.2), an observation which had already been made through regression analyses (see Section 4.4.2.2). This is summarised in Table 5.5.

Table 5.5

Values of b in the relationship $X_i = a\ F_i^b$

based on data from Table 4.19

Species	Value of b
Colour	0,8
Potassium	0,6
Calcium	1,0
Lithium	1,1
Starch	1,1
Dyes	0,2 - 0,9

More interestingly, the data from the present work was shown (see Section 4.5.1) to fit the definition of the partition coefficient, P_i, given by equation 4.3, on page 121. P_i values for the selected impurities were calculated and are compared with published values in Table 5.6.

Table 5.6

Partition coefficients from the present work and values from the literature

Impurities	P_i	Remarks
Colour	0,02	
Calcium	0,02	The present work; in sucrose
Other inorganics	0,003	crystals.
Starch	0,3	
Dyes	0,01-0,03	
L-leucine	0,2	Zumstein *et al.*, (1990); in L-
L-valine	0,1	isoleucine
Cadmium	0,002	Witcamp *et al.*, (1990); in
Lead	0,002	$CaSO_4.\ 2H_2O$
Cadmium	0,0002	Witcamp *et al.*, (1990); in
Lead	0,0002	$CaSO_4.\ ½H_2O$

Two main points may be made. Firstly the concept of a partition coefficient applies well to the crystallisation of sucrose in the presence of the selected impurities. Secondly, the results show that exchange reactions/equilibria must take place at the surface of the growing sucrose crystal. These suggest that a mechanism of impurity transfer involving equilibria could be relevant.

5.4 Viscosity and diffusivity

Physical aspects such as viscosity and diffusivity have been shown to impact on the crystallisation of sucrose (Sections 1.1.2.5; 2.5; 3.6.5). It is expected that these parameters will also affect the transfer of impurities, and they have therefore been investigated.

The results obtained when viscosity was investigated have been somewhat disappointing in that it was not possible to change viscosity in isolation. The type of polysaccharide used to modify

the viscosity of the liquors had more impact than the viscosity itself, as shown in Section 4.7.2.2. The activation energy of viscosity in sucrose solutions was found to vary between 1 to 10 kJ/mol, at constant supersaturations of 1,0 and 1,3 (Section 4.7.1).

The activation energy of diffusion, for sucrose solutions at saturation and at a supersaturation of 1,3 was found to be 19-20 kJ/mol (Section 4.8), which is much closer to the values for G and for the impurity transfers (18-30 kJ/mol), and agrees with Mullin's (1993) value for transport - limited processes.

The diffusion coefficients of the impurities, in highly concentrated sucrose solutions and at high temperature, are the values of interest here. A simple method has been developed to measure the diffusion coefficients of selected impurities under those conditions. The method is somewhat tedious, needs sampling over very long times and is dependent on the precision of the analytical techniques to measure the very small concentrations of the impurities. It has, however, been useful for the determinations of the diffusion coefficients of some of the impurities. It has not been used for starch and colour, however, due to the effects of the long times and high temperatures, which cause degradation of those two species.

In solutions containing 74% by mass of sucrose, at 70°C, the diffusion coefficients shown in Table 5.7 have been measured.

Table 5.7

Values of the diffusion coefficients in 74% (m/m) sucrose solutions and at 70°C

Species	Diffusion coefficient/m^2/s
Potassium	$4,6 \times 10^{-12}$
Lithium	$4,0 \times 10^{-12}$
Calcium	$1,6 \times 10^{-12}$
Nickel	$1,2 \times 10^{-12}$

These coefficients are much lower than those in water at 25°C, namely, about 1 to 2 x 10^{-9} m^2/s. A restricted number of determinations indicate that the coefficients decrease as the sucrose concentration increases, roughly by 3 x 10^{-13} units per unit increase in sucrose concentration (m/m).

5.5 **Models of impurity transfer**

One of the main objectives of the present work is to propose a model for impurity transfer during the crystallisation of sucrose. Two possibilities were considered. The two-step model (Section 4.9.1), although successful for the crystallisation of sucrose (Smythe, 1990) could not fit the data obtained here for the transfer of impurities into the sucrose crystal. All attempts to fit this model to the data from the present work failed completely. Sobczak's method (1990) was tried extensively with data from the runs involving colour and those for potassium, which separately contained 82 and 59 sets of observations. In all cases the fits were extremely poor, and response surfaces were very flat rendering optimisation impossible.

Vaccari (1996), using results from the cooling crystallisation of sucrose, comments that, in principle, an interfacial breakdown model would fit his observations. Mullin (1993) and Nyvlt (1982) give a description of such a process. Burton *et al.* (1953) and Edie and Kirwan (1973) describe the model in more detail and give some applications.

From the theory derived by the above authors this process yields data that fit equation 5.1

$$\ln\left(\frac{1 - K_e}{K_e}\right) = \ln\left(\frac{1 - K_a}{K_a}\right) - \frac{\delta}{D} V \qquad \text{.....5.1}$$

where K_e is the ratio of concentrations of the impurity in the crystal to that in the bulk of the mother liquor, while K_a is the ratio of the concentrations in the crystal to that in the interface, the

latter concentration being unknown. The width of the interface is δ while D is the diffusion coefficient of the impurity. Finally V is a linear growth velocity, denoted by l_g in the present work.

The fit of the model has been tested in Section 4.9.2 with detailed results being given by Equations 4.12 to 4.16, and in Figures 4.17 and 4.18, for colour, potassium, calcium, nickel and lithium as impurities. In all cases the correlation coefficients are high and good fits are evident from the graphical representations of the results.

Equation 4.11 shows that the slope of the line is equal to -δ/D, where δ is the film thickness, and D the diffusion coefficient. It is possible to estimate the reciprocal of this slope, independently, by using a correlation given by Geankoplis. This has been done and the results are shown in Table 4.36. It is evident that the agreement is acceptable. This gives an independent confirmation for the validity of the interfacial breakdown model. Since values of D can be estimated from the experimental work, it has been possible to estimate the film thickness, for the crystallisation conditions used here, which has been found to range from 7×10^{-6} to 13×10^{-6} m.

Finally, the results obtained with starch show that the data for this impurity do not fit the interfacial breakdown model, as shown by Figure 4.19.

The mechanisms for the transfer of impurities in the crystals can be classified as follows:

(i) surface impurities: these would include impurities in or from the adhering film of mother-liquor, or those actually adsorbed onto the surface. The first possibility can be discarded because of the affination technique discussed in Section 3.4.1.

(ii) internal impurities: these could be in discrete inclusions, or distributed throughout the crystal.

The results obtained here suggest that the impurities are distributed throughout the crystal by an interfacial breakdown process involving the inclusion of impure solution. The interfacial breakdown model is thus relevant to the transfer of the impurities, except starch, but it may not be the sole mechanism. There might well be a combination of mechanisms. The following points

support the above conclusions:

- Values of 19-30 kJ/mol for the activation energies of impurity transfer, which are close to the level expected for processes involving transport (Section 5.2).

- A value of 19-20 kJ/mol for the activation energy for diffusion in concentrated sucrose solution. Again this is close to the values measured for the impurity transfer and indicates that diffusion could be an important parameter.

- The relevance of partition coefficients (Section 5.3), which involve distribution coefficients similar to K_e.

- The x-ray diffraction analyses (Section 4.10) show that there is no deformation in the sucrose crystal lattice by the impurities incorporated into the crystal. This indicates that there is no co-crystallisation but rather a chemisorption process on the surface of the growing crystal, and is therefore not contrary to the interfacial breakdown process.

- Mackintosh and White (1969) show that inclusions in sugar crystals can be seen, and photographed, when the crystals are immersed in methyl salicilate, which has the same retractive index as sucrose. Inclusions are clearly visible in the crystals from the above workers. To produce these crystals they used extensive washing (i.e. dissolution) and regrowth during the crystallisation process and very fast (about two orders of magnitude faster than the rates used in the present work) crystallisation rates. When the same authors used slow crystallisation rates, without dissolution and regrowth, the crystals now produced showed no inclusions. Both types of crystals are photographed in these workers' paper.

  A number of crystals from the present work were immersed in methyl salicilate and photographed, as shown in Figure 5.1.

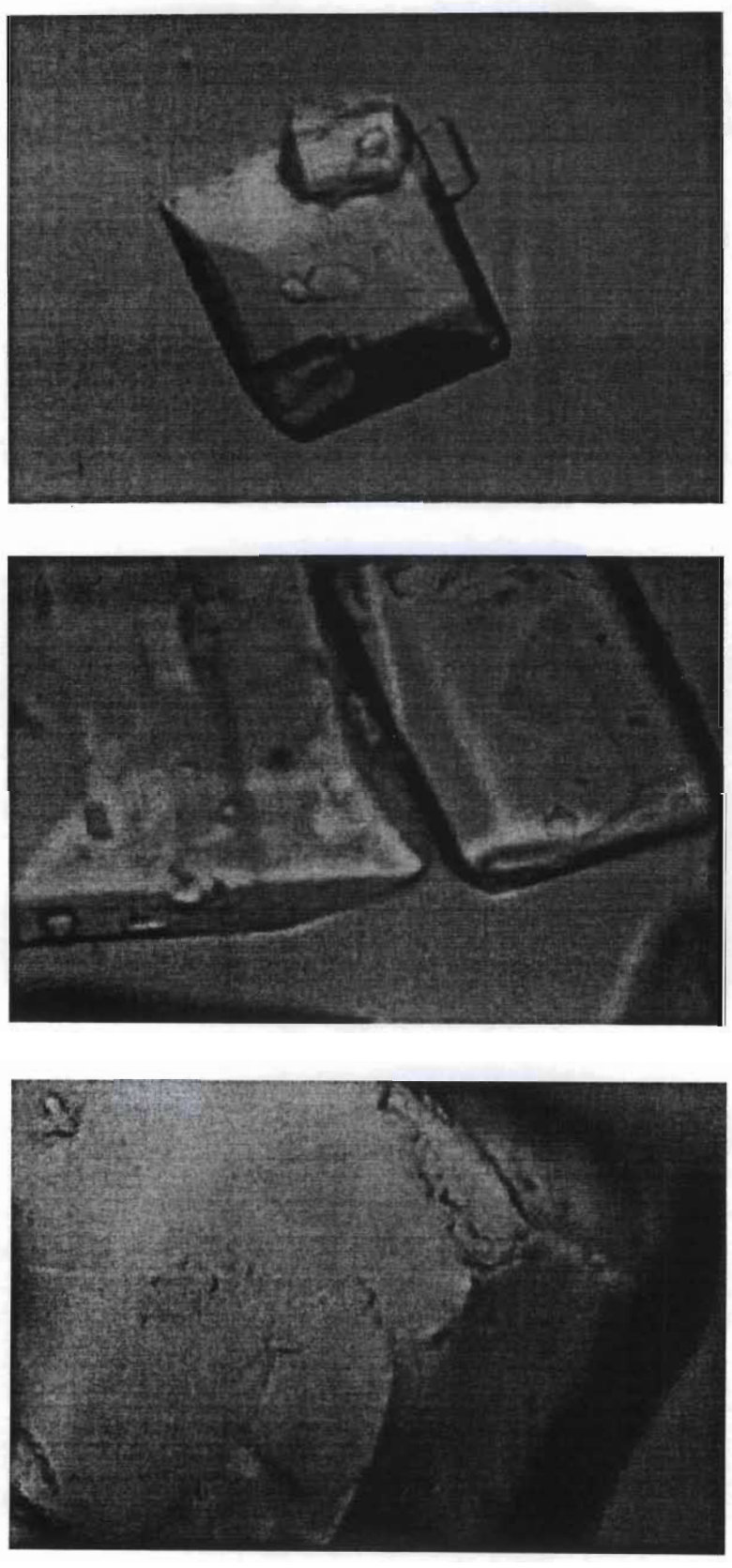

Figure 5.1 **Sucrose crystals from set S16 immersed in methyl salicilate. Magnification 60x and 180x.**

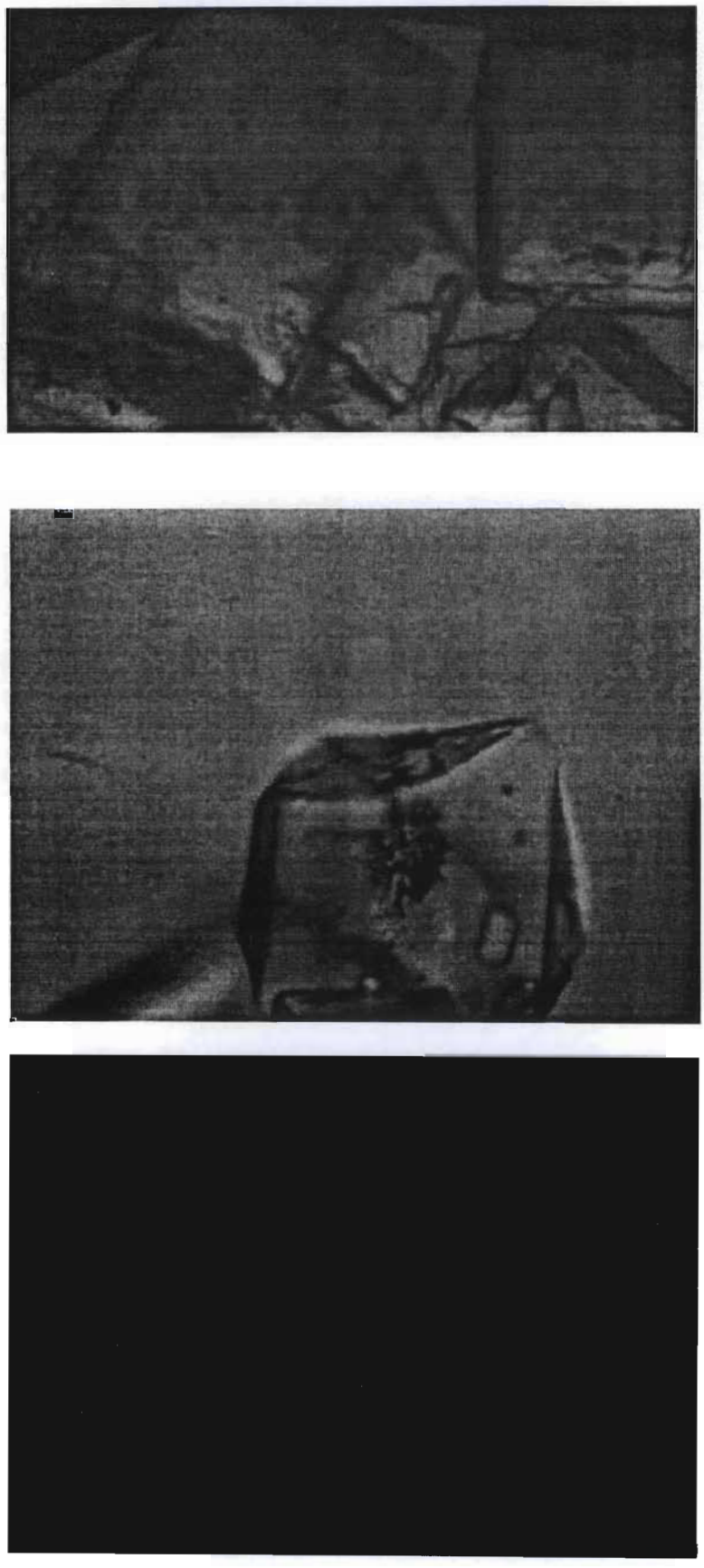

Figure 5.1 (cont.) **Sucrose crystals from set CN15 immersed in methyl salicilate. Magnification 60x and 180x.**

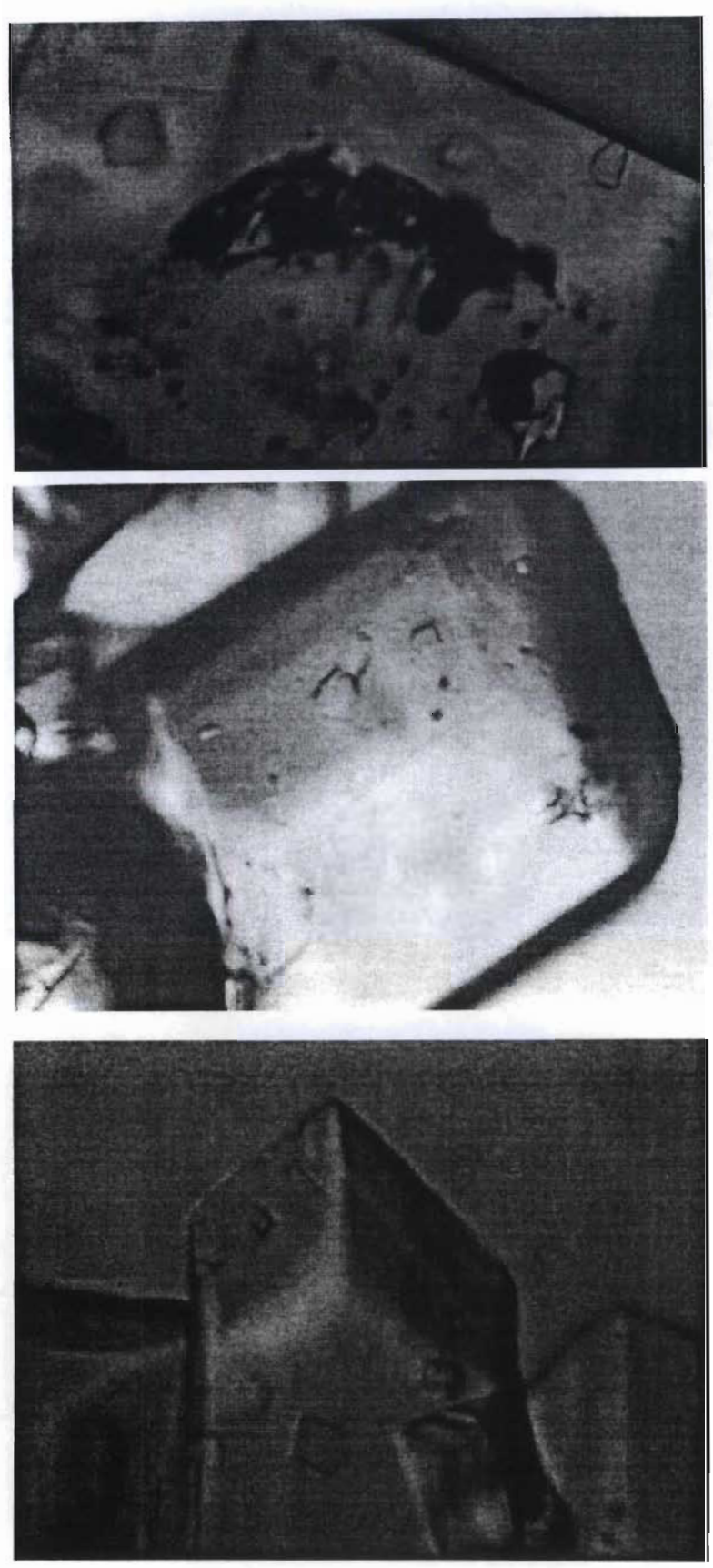

Figure 5.1 (cont.) **Sucrose crystals from set LN15 immersed in methyl salicilate. Magnification 60x.**

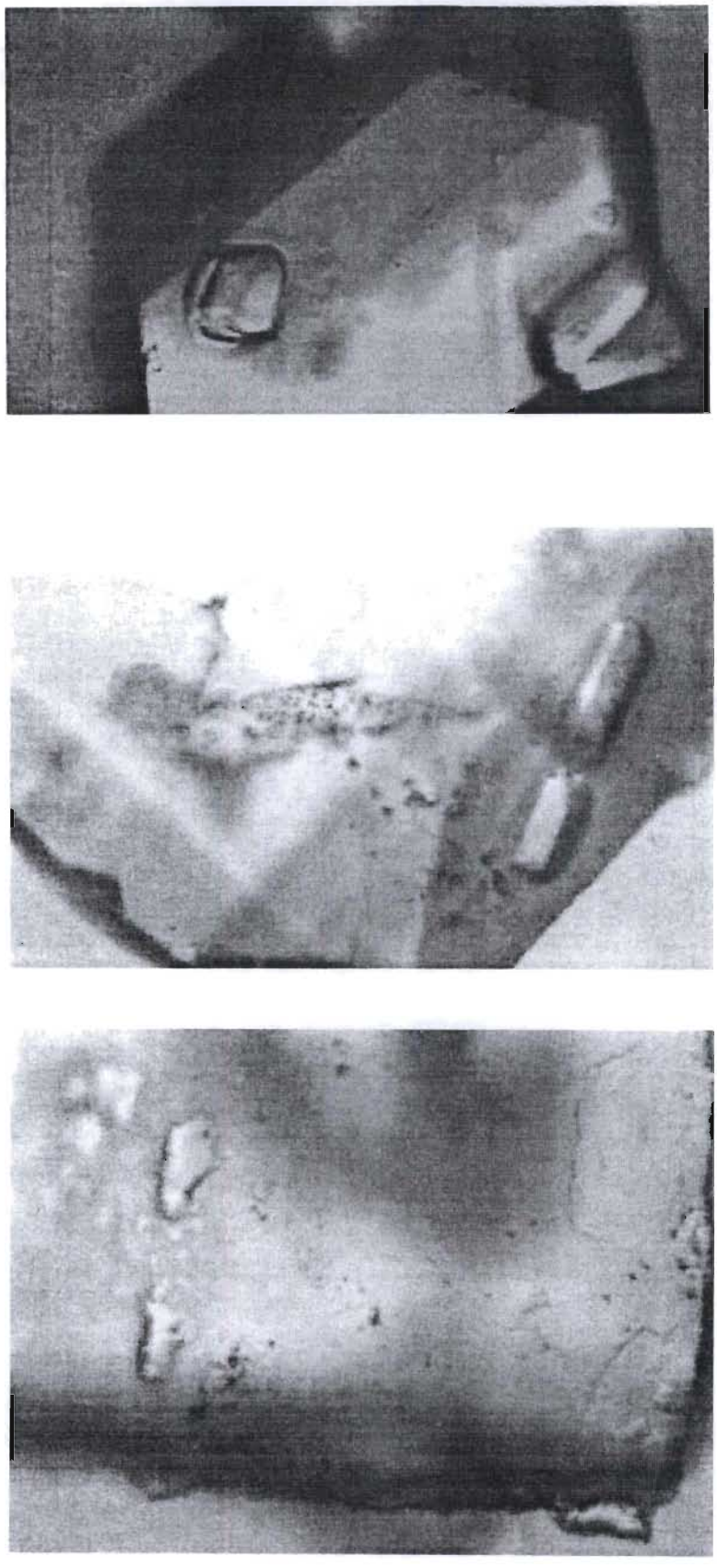

Figure 5.1 (cont.) **Sucrose crystals immersed in methyl salicilate, from set S16. Magnification 180x.**

Apart from the above crystals, many others were examined, by the same technique. In all cases, the conclusions were the same: there is little to no evidence of visible inclusions. The crystals from the present work look similar to those produced by Mackintosh and White (1969) with slow, careful crystallisation.

It can thus be concluded that the type of inclusion discussed by these authors has not been found in the present work.

The interfacial breakdown model has been described in detail by Chalmers (1964) and Burton *et al.* (1953), who both deal with the distribution of solute in crystals grown from melts. Chalmers (1964) shows that the interfacial liquid will in general have a composition that differs from that of the bulk liquid. The liquidus temperature of the interfacial liquid is lower than that of the liquid at a greater distance from the interface. A consequence of this is that the temperature of the interface in an impure liquid is lower than that of the liquidus of the bulk liquid. Supercooling can therefore occur. Actual temperature distributions in the solid and liquid may take the form shown in Figure 5.2. The liquid is supercooled in the sense that it is below its liquidus temperature. This is constitutional supercooling.

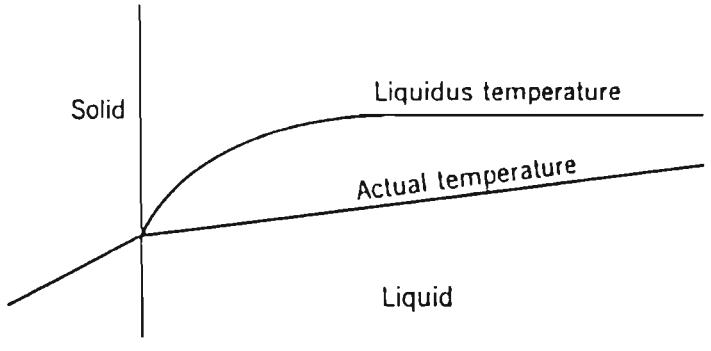

Figure 5.2 Actual temperature of the liquid and its liquidus temperature (Chalmers, 1964).

A small amount of supercooling is sufficient to set up an instability leading to a departure from the conditions of steady-state of the planar interface, which is an assumption implicit in the development of the theory. The instability develops because the growth rate is increased in any localised region that advances ahead of the general interface, in the gradient of supercooling. Such a region would grow as a protuberance until it reaches a region where supercooling and the evolution of latent heat cancel each other. This is shown in Figure 5.2.

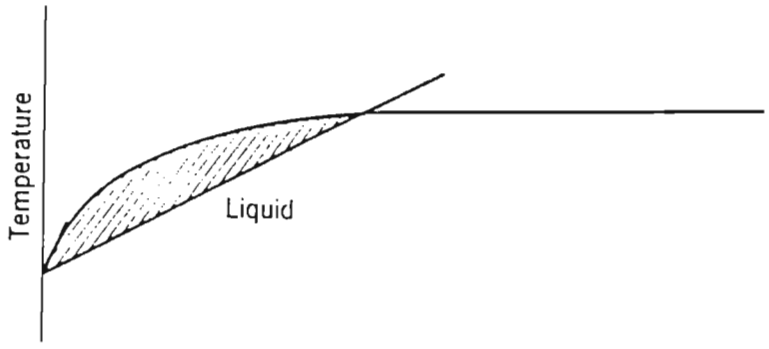

Figure 5.3 Supercooling ahead of planar interface (Chalmers, 1964).

Mullin (1976) compares crystallisation from solutions containing impurities to the model discussed above, for melts. He states that a similar argument may be developed for growth from solution. When a crystal grows in an impure system, impurity is rejected at the solid-liquid interface. If the impurity cannot diffuse away fast enough it will concentrate near the crystal face and affect the equilibrium conditions in the interfacial region. Most of the impurities found in industrial sugar liquors, particularly the inorganic species, increase the solubility of sucrose. Thus, the supersaturation in the bulk somewhat away from the crystal surface, is higher than that at the surface. The driving force, which in this case is the concentration, increases over a short distance from the crystal face towards the bulk solution.

This condition is now called constitutional supersaturation and, as was the case for constitutional supercooling, causes interfacial instability. The growing interface breaks up into finger-like cells in a more or less regular bunched array. In this way the liberated heat of crystallisation is more

easily dissipated and the tips of the protuberances advance clear of the concentrated impurities. The region between the fingers entraps impure solution and a succession of inclusions may be left in the crystal.

Vaccari (1996) appears to be the first to suggest this mechanism for the incorporation of impurities into the sucrose crystal, based on observations comparing evaporative and cooling crystallisation.

The results obtained in this work are believed to provide the first experimental evidence that the constitutional supersaturation model is relevant to the incorporation of colour, potassium and calcium, all important industrial impurities, in the sucrose crystal. The model also fitted the incorporation of exotic species, such as lithium, nickel and a number of dyes, showing that it is fairly general with sucrose.

One noticeable exception however was that of starch, another industrially important impurity. Starch showed a high affinity for the sucrose crystal and it could be possible that chemical or steric effects override the constitutional supersaturation effect. A similar result with raffinose would strengthen this possibility, but this impurity was not studied here, since it is not present in sugar cane.

5.6 Conclusions

The three main objectives of this work are given in Section 1.3 and it is now possible to establish how well they have been met. There is no doubt that the third objective, namely that the results obtained apply to industrial conditions, has been well satisfied. This has been done by using industrial sources for the sugar streams used in the project and by using a pilot scale crystalliser which was shown to operate in a manner similar to that of industrial equipment.

The first objective, that is to propose and investigate a parameter to quantify the rate at which impurities are incorporated into the sucrose crystal, has also been well satisfied. R_i, the rate of impurity transfer, has been derived and shown to be sensitive both to crystallisation conditions and to the type of impurity. The factors that affect it have been identified and their effects quantified.

In industry, refiners are often concerned most with colour. This work shows that they could estimate the rate of transfer of colour using the equation $R_c = 0,07\ F_c^{0,8}\ G^1$. The affinated crystal colour could be estimated using the equation $X_c = 0,12\ F_c^{0,8}$.

The degree of success with the second objective, namely the investigation of mechanisms of impurity transfer, has however been smaller. It is nevertheless felt that valid indications have been obtained as far as the relevance of the interfacial model for all the selected impurities, except starch, is concerned. More work is however required, with the investigation of this model as the main objective. It is also somewhat disappointing that a mechanism for starch, an important industrial impurity, could not be identified. Again this is an area where specific investigations are needed.

Finally, it was noted in the introduction that the knowledge of the mechanism of impurity transfer could help in reducing production costs. The interfacial breakdown model shows that the crystallisation velocity must be slowed down to reduce the impurity transfer rate. This highlights the relevance of cooling, rather than evaporative, crystallisation. This work has also shown the importance of decreasing the concentrations of the impurities in the liquors to be crystallised. This is the approach taken industrially, through a number of purification processes.

REFERENCES

Adamson AW (1976). **Physical chemistry of surfaces**. 3rd ed. John Wiley, New York.

Anon (1994). **International Commission for Uniform Methods of Sugar Analyses**. ICUMSA Publication Department, Colney, Norwich, England.

Atkins PW (1994). **Physical chemistry**. International Student Edition, Oxford University Press, Oxford.

Bates EJ (1942). **Polarimetry, saccharimetry and the sugars**. Circular of the National Bureau of Standards, C440, US Department of Commerce.

Bennett MC and Fentiman YL (1969). **Growth rate of sucrose crystals related to krypton surface area of seeds**. Int. Sug. J. 71:198-202.

Boistelle R (1975). **Survey of crystal habit modification in solution.** In Industrial Crystallisation. Mullin JW (ed.), Plenum Press, New York.

Broadfoot R and Bartholomew HC (1995). **Specific surface area of crystal beds formed from high purity massecuite**. Proc. Aust. Soc. Sugar Cane Technol. 17:222-230.

Bruijn J (1964). **The construction of two laboratory pans**. Proc. S. Afr. Sug. Technol. Ass. 38: 102-105.

Bubnik Z and Kadlec P (1992). **Sucrose crystal shape factors**. Zuckerind. 117, 5: 345-350.

Burton JA, Prim RC and Splichter WP (1953). **The distribution of solute in crystals grown from the melt. Part 1: Theoretical**. Journal of Chem. Phy. 21, 11: 1987-1991.

Burton JA, Kolb ED, Slichter WP and Sturthers JD (1953). **Distribution of solute in crystals grown from melt. Part 2: Experimental**. Journal of Chem. Phy. 21, 11: 1991-1996.

Chalmers B (1964). **Principles of solidification**. John Wiley and Sons, New York.

Chang YC and Myerson AS (1986). **Diffusivity of glycine in concentrated, saturated and supersaturated aqueous solutions**. AIChE J. 32, 9: 1567-1569.

Chang YC and Myerson AS (1985). **The diffusivity of potassium chloride and sodium chloride in concentrated, saturated and supersaturated aqueous solutions**. AIChE J. 31, 6: 890-896.

Chen JCP and Chou CC (1993). **Cane sugar handbook**. John Wiley and Sons, 12th Edition, New York.

Day JC (1971). **The habit modification of sucrose crystals grown in the presence of dextran**. M.Sc. Thesis, University of Queensland, Brisbane.

Donovan M and Williams JC (1992). **The factors influencing the transfer of colour to sugar crystals**. Sug. Proc. Res. Inc., 1992 Conf.: 1-11.

Douwes-Dekker K (1953). **The quality of Natal white sugar ex crop 1953**. SMRI Comm., No. 20A.

Dunsmore A (1997). **The testing of sugars ex the 1996/97 crop**. SMRI Comm., No. 164.

Garside J (1991). **The role of transport processes in crystallisation.** In Advances in industrial crystallisation. J Garside, RJ Darcy and AG Jones (eds.), Butterworth, Oxford: 92-104.

Geankoplis C (1993). **Transport processes and unit operations**. Allyn and Baron Inc., Boston.

Gladden JK and Dole M (1953). **Diffusion in supersaturated solutions. II Glucose solutions**. J. Amer. Chem. Soc. 75: 3900-3904.

Grimsey IM and Herrington, TM (1994). **The formation of inclusions in sucrose crystals**. Int. Sug. J. 96: 504-514.

Guimaraes L, Susana S, Bento LSM and Rocha F (1995). **Investigation of crystal growth in a laboratory fluidized bed**. Int. Sug. J. 97: 199-204.

Guo SY and White ET (1984). **The distribution of impurities in inclusions in sugar crystals**. Proc. Aust. Soc. Sugar Cane Technol.: 333-342.

Heffels SK and de Jong EJ (1988). **Modelling sucrose crystal growth**. Zuckerind. 113, 9: 781-786.

Heffels SK (1986). **Product size distribution in continuous and batch sugar crystallisers**. Ph.D Thesis. Technical University of Delf, Delf.

Heffels SK, de Jong EJ and Sinke DJ (1987). **Growth rate of small sucrose crystals at 70°C**. Zuckerind. 112, 6: 511-517.

Heffels SK, de Jong EJ and Sinke DJ (1988). **Modelling sucrose crystal growth**. Zuckerind. 113, 8: 781-786.

Heffels SK, Weber CHM, de Bruin PR and de Jong EJ (1987). **Mass transfer coefficient of diffusion of sucrose crystals in solution**. Zuckerind. 112, 12: 1075-1081.

Honig P (1953). **Principles of sugar technology**. Vol. 1, Elsevier, Amsterdam.

Honig P (1959). **Principles of sugar technology**. Vol. 2, Elsevier, Amsterdam.

James AM and Pritchard FE (1974). **Practical physical chemistry**. 3rd edition Longman, New York.

Jancic SJ (1984). **Industrial crystallisation**. Delf Univ. Press., D Riedel Publishing Co., Delf

Keenan JH, Keyes FG, Hill PG and Moore JG (1969). **Steam tables**. International Edition. John Wiley & Sons, New York.

Kharpinski DH (1980). **Crystallisation as a mass transfer phenomenon**. Chem. Eng. Sci., 35: 2321-2324.

Kraus J and Nyvlt J (1964). **Crystallisation of anhydrous glucose. III Shape factors and growth rate of crystals**. Zuckerind. 119, 4: 298-303.

Lionnet GRE (1987). **Impurity transfer during A-massecuite boiling**. Proc. S. Afr. Sug. Technol. Ass. 61: 70-75.

Lionnet GRE (1988). **The effect of some operational factors on colour transfer during pan boiling**. Proc. S. Afr. Sug. Technol. Ass. 62: 39-41.

Lionnet GRE (1989). **Some comparisons between refinery pans and the SMRI pilot pan**. SMRI memorandum, 4 pages.

Lionnet GRE and Moodley M (1995). **Colour transfer in the South African cane sugar industry**. Proc. Int. Soc. Sug. Cane Technol. 61: 83-85.

Edie DD and Kirwan DJ (1973). **Impurity trapping during crystallisation from melts**. Ind. Eng. Chem. Fundam. 12, 1: 100-106.

Mackintosh DL and White ET (1969). **Enclave inclusions in sugar crystals**. Proc. Qd. Soc. Sugar Cane Technol. 36: 291.298.

Mann GF (1987). **Modifications to the boiling procedures at Sezela in an attempt to reduce VHP sugar colour**. Proc. S. Afr. Sug. Technol. Ass. 61: 83-85.

Maurandi V (1982). **La reaction de superficie dans le grossissement des cristaux dans les fluides sursatures**. La Sucrerie Belge. 101: 207-221.

Mantovani G (1997). **Morphology of industrial sugar crystals**. In Sucrose crystallisation, Science and Technology. Edited by VanHook AW, Mantovani G and Mathlouthi M. Berlin.

Mantovani G, Vaccari G, Sgualdino G and Rubbo M (1986). **Colouring matter inclusions in sucrose crystals**. Ind. Sac. Italiana. 79: 1-5.

Mantovani G, Vaccari G, Sgualdino G, Aquilano D and Rubbo M (1985). **Sucrose crystal colour as a function of some industrial crystallisation parameters**. Ind. Sac. Italiana. 78: 7-14.

Maurandi V and Mantovani G (1982). **Kinetic and technological aspects of sucrose crystallisation in supersaturated traditional molasses**. La Sucrerie Belge. 101: 85-102.

Maurandi V and Mantovani G (1981). **Kinetic problems in sucrose crystallisation in Quentin syrups of low grade**. La Sucrerie Belge. 100: 143-151.

Maurandi V, Mantovani G and Vaccari G (1984). **Sucrose crystal growth activation energies**. Zuckerind. 109, 8: 734-739.

Mellet P, Lionnet GRE, Kimmerling ZJ and Bennett PJ (1982). **Standards for the analytical precision of sugar and molasses analyses**. Proc. S. Afr. Sug. Technol. Ass. 56: 55-57.

Michael DS and Thelemaque J (1984). **Affination methods for raw sugar**. Sugar Milling Research Institute, Internal Report No. 91/84, 7 pages.

Morel du Boil, PG (1980). **Practical tracers for the sugar industry - the analytical feasibility of using lithium, chloride or potassium**. Proc. S. Afr. Sug. Technol. Ass. 44: 99-104.

Mullin JW (1961). **Crystallisation**. Butterworth, 1st Edition, London.

Mullin JW (1976). **Crystalliser design and operation**. In Industrial Crystallisation. JW Mullin (ed.), Plenum Press, New York.

Mullin JW (1993). **Crystallisation**. Butterworths-Heinemann Ltd., 3rd Edition, London.

Murray JP (1972). **Filtering quality of raw sugars: influence of starch and insoluble suspended matter**. Proc. S. Afr. Sug. Technol. Ass. 46: 116-132.

Myerson AS and Toyokura K (1990). **Crystallisation as a separation process**. ACS Symposium Series 438: 82.

Myerson AS (1990). **Crystallisation research in the 1990's, an overview**. **Crystallisation as a Separation Process**. AS Myerson and K Toyokura (eds.), Amer. Chem. Soc. Symposium Series 438:3-14.

Nyvlt J (1976). **Industrial crystallisation from solution**. Butterworths, London.

Nyvlt J (1982). **Industrial crystallisation - The state of the art**. 2nd Edition, Weinheim.

Nyvlt J, Sohnel O, Matuchova M and Broul M (1985). **The kinetics of industrial crystallisation**. Academia. Prague.

Ozum B and Kirwan DJ (1976). **Impurities in ice crystals grown from stirred solutions**. AIChE Sympsosium Series 153. 52: 1-6.

Pautrat C, Bressan C and Mathlouthi M (1995). **Physico-chemical study of the effect of some polysaccharides on the sucrose crystallisation conditions**. Conf. Int. Tech. Suc. 20th Proc.: 204-215.

Peacock SD (1995). **Selected physical properties of sugar factory process streams**. Sugar Milling Research Institute, Technical Report No. 1714, 46 pages.

Rein PW (1986). **A review of experience with continuous vacuum pans in Tongaat-Hulett Sugar**. Proc. S. Afr. Sug. Technol. Ass. 60: 76-83.

Rein PW, Cox MGS and Love DJ (1985). **Analysis of crystal residence time distribution and size distribution in continuous boiling vacuum pans**. Proc. S. Afr. Sug. Technol. Ass. 59: 58- 67.

Saska M and Oubrahim Y (1989). **Crystallisation rate of sucrose at high impurity concentrations**. Int. Sug. J. 91: 109-115.

Saska M (1991). **Entrainment of dextrans, Na and K in sucrose crystallisation**. Conf. Int. Tech. Suc. 19th Proc.: 133-151.

Shoemaker DP, Garland CW and Steinfeld JI (1974). **Experiments in physical chemistry**. McGraw-Hill. New-York.

Sobczak E (1990). **A simple method of determination of mass transfer coefficients and surface reaction constants for crystal growth**. Chem Eng. Sc. 45, 2: 561-564.

Spencer GL and Meade GP (1948). **Cane sugar handbook**. John Wiley & Sons Inc. New-York.

Taylor GB and Wall FT (1953). **Diffusion of polymer mixtures**. J. Amer. Chem. Soc. 75: 6340-6343.

Vaccari G (1996). **Continuous crystallisation versus boiling crystallisation**. Proc. Sug. Proc. Res. Inst. Workshop on separation processes. MA Clarke, New Orleans.

Vaccari G, Mantovani G, Morel du Boil PG and Lionnet GRE (1991). **Colour inclusions and habit modifications in cane sugar crystals**. Zuckerind. 116. 12: 1040-1044.

Vaccari G, Mantovani G, Sgnaldino G and Dosi E (1996). **Cooling crystallisation of raw juice: Laboratory investigations of sucrose crystal growth kinetics**. Zuckerind. 121. 2: 111-117.

VanHook A (1944). **Kinetics of sucrose crystallisation. Pure sucrose solutions**. Ind. Eng. Chem. 36: 1042-1047.

VanHook A (1945). **Kinetics of sucrose crystallisation. Mechanism of reaction**. Ind. Eng. Chem. 37: 782-785.

VanHook A (1973). **Sucrose crystallisation. Mechanism of growth**. Zuckerind. 23. 9: 499-502.

VanHook A (1981). **Growth of sucrose crystal, a review**. Sug Tech. Rev. 8: 41-79.

VanHook A (1997a). **Kinetics of sucrose crystallisation: mechanism of reaction.** In sucrose crystallisation, Science and Technology. Edited by VanHook A, Mantovani G and Manthlouthi M, Berlin.

VanHook A (1997b). **Influence of adsorbed impurities on the growth rate and habit of sucrose crystals.** In sucrose crystallisation, Science and Technology. Edited by VanHook A, Mantovani G and Mathlouthi M. Berlin.

VanHook A (1997c). **Some notes and speculations on sucrose crystallised from syrups containing raffinose.** In sucrose crystallisation, Science and Technology. Edited by VanHook A, Mantovani G and Mathlouthi M. Berlin.

VanHook A (1997d). **Habit modifications of sucrose crystals.** In sucrose crystallisation, Science and Technology. Edited by VanHook A, Mantovani G and Mathlouthi M. Berlin.

VanHook A and Russel HD (1945). **The diffusivities of concentrated sucrose solutions**. J. Amer. Chem. Soc. 67: 370-372.

Wall FT and Wendt RC (1958). **Determination of differential diffusion coefficient**. J. Amer. Chem. Soc. 62: 1581-1586.

Wall FT, Grieger PF and Childers CW (1952). **A rapid method for measuring diffusion coefficients in solutions**. J. Amer. Chem. Soc. 74: 3562-3567.

Weast RC (1986). **Handbook of chemistry and physics**. 67th edition. CRC Press. Florida.

Witkamp GJ and von Rosmalen GM (1990). **Continuous crystallisation of calcium sulphate phases from phosphoric acid solutions. Crystallisation as a Separation Process**. AS Myerson and K Toyokura (eds.). Amer. Chem. Soc. Symposium Series. 438: 381-394.

Zumstein RC, Gambrel T and Rousseau RW (1990). **Factors affecting the purity of L-Isoleucine recovered from batch crystallisation**. **Crystallisation as a Separation Process**. AS Myerson and K Toyokura (eds.). Amer. Chem. Soc. Symposium Series. 438: 85-99.

APPENDIX 1

Explanation of codes for the experimental sets

Codes	Impurities investigated								Number of runs
	Colour	K^+	Ca^{2+}	Ni^{2+}	Li^+	Starch	Dyes	Polysaccharides	
TEMP 15	✓	✓							5
T 17	✓	✓	✓		✓				7
NBT 15	✓	✓							5
SCA 13	✓		✓			✓			3
ST 13	✓		✓			✓			3
HRB 15	✓	✓							5
HT 14	✓	✓							4
AP 13	✓	✓			✓				3
MT 13	✓	✓	✓		✓				3
HTD 13	✓	✓				✓			3
HTA 13	✓	✓				✓			3
W 16	✓	✓	✓					✓	6
NB 16	✓	✓							6
F 16	✓	✓						✓	6
CMC 13	✓	✓						✓	3
GHR	✓								18
R 15	✓	✓	✓			✓			5
S 16	✓	✓	✓						6
LN 15				✓	✓				5
CN 15			✓	✓					5
C 16		✓	✓				✓	✓	6
KL 15		✓			✓	✓			5
CS 15			✓			✓			5
HRM 16	✓				✓				6
X 19	✓	✓							9
A 14							✓		4
MYB 14							✓		4
MX 13		✓	✓	✓	✓				3
TR 18	✓	✓	✓						8
AB 25		✓	✓				✓		3
ML 15							✓		5
MB 15							✓		5
COND 16					✓		✓		6
AB 29							✓		3

APPENDIX 2

RAW DATA

The raw data are contained in a number of Quattro Pro spreadsheet files, each file having a name such as A LL CA.WQ1.

Details of each file are given first. The following information is listed:

i) The DISC number. Two discs are supplied, numbered 1 and 2.

ii) The name of the file e.g. ALLCA.WQ1.

iii) The type of raw data in a given bunch of files. For example ALLCA.WQ1 to ALLST.WQ1 contain raw data for multilinear regressions. The files AP13 CA.WQ1, AP13CK.WQ1, etc., contain the raw data for set AP13, an so on.

A typical example of each main type of raw data (e.g. multilinear regressions; specific sets, data for Arrhenius plots; data for diffusion coefficients; etc.) has been printed in full, in attached sheets. In all cases the header of the column indicates what the data are. For example with the printed sheet for ALLCA.WQ1, the column headed F_{ca} is the calcium in the feed; X_{ca} is the calcium in the crystal, etc.

Listing of contents of data on discs

DISC 1

ALLCA.WQ1	Data for multilinear regressions
ALLCOL	" " " "
ALLLI	" " " "
ALL MB	" " " "
ALL NI	" " " "
ALL POT	" " " "
ALL ST	" " " "
AP13CA. WQ1	Raw data set AP13
AP13 CK	" " "
AP13 LI	" " "
BET LN15. WQ1	Raw data, BET isotherms
BER S16	" " "
BET CS15	" " "
BET KL15	" " "
BET TR18	" " "
BET R15	" " "
CMC 13K. WQ1	Raw data
F13 CK	" "
F46 CK	" "
HRB15 CK	" "
HT14 K	" "
HTA CK	" "
HTD13 CST	" "

KISKE.WQ1	Raw data for interfacial model
LANGMX13. WQ1	Isotherm data
LANG R15	" "
LANG GS 16	" "
LANG MX13 B	" "
LFAB25	" "
LFC16	" "
LFCACN 15	" "
LFCACS15	" "
LFCCS15	" "
LFKKL15	" "
LFKK15	" "
LFLIKL15	" "
LFLKLN15	" "
LFMBML15	" "
LFNICN15	" "
LFNILN15	" "
LFSTCS15	" "
LFSTKL15	" "
LI15KE.WQ1	Raw data, interfacial model
MT13CA.WQ1	Raw data set MT 13
MT13K	" " "
MX13CANI	" " "
N15KE.WQ1	Interfacial breakdown model
NB16 CK.WQ1	Raw data set NB16

PART AB25. WQ1	Partition coefficient
CN15	" " "
CS15	" " "
IR15	" " "
KL15	" " "
LN15	" " "
MB15	" " "
ML15	" " "
MX13	" " "
MYBI	" " "
TR15	" " "
S16	" " "
TR18	" " "
SCA13CCA.WQ1	Raw data set SCA13
SCA13ST	" " "
ST13ST	" " "
ST15KE.WQ1	Interfacial model, starch
T15KE	" " " "
W135CCAK.WQ1	Raw data
W246 CKCA.WQ1	" "

Fca	Xca	Rca	G	Lc	1/T	
939	2.6	1.11E-11	1.28E-05	0.000234	0.002937	T1T7
839	2.5	1.12E-11	1.35E-05	0.000182	0.003082	T1T7
567	2.65	1.17E-11	1.32E-05	0.000174	0.003063	T1T7
718	2.75	1.64E-11	1.79E-05	0.00031	0.002911	T1T7
819	2.95	1.2E-11	1.22E-05	0.000219	0.002972	T1T7
774	2.45	9.09E-12	1.11E-05	0.000201	0.003003	T1T7
799	2.85	2.19E-11	2.31E-05	0.000418	0.00289	T1T7
303	1.2	7.11E-12	1.78E-05	0.000287	0.002995	S1S6
217	1	5.42E-12	1.61E-05	0.000277	0.002976	S1S6
960	4.4	1.29E-11	8.83E-06	0.000142	0.002992	S1S6
1503	4.3	2.18E-11	1.52E-05	0.000249	0.002973	S1S6
2553	5.75	2.98E-11	1.58E-05	0.000251	0.002979	S1S6
4740	6.9	2.64E-11	1.15E-05	0.000201	0.002952	S1S6
2587	1.9	7.92E-12	1.25E-05	0.000213	0.002959	MT13
2568	1.8	6.42E-12	1.1E-05	0.000204	0.002909	MT13
2437	3.2	2.05E-11	1.92E-05	0.00033	0.002847	MT13
4998	5.45	2.18E-11	1.2E-05	0.000215	0.002939	AP13
4417	7.3	3.49E-11	1.43E-05	0.000252	0.002874	AP13
4848	7.25	4.12E-11	1.71E-05	0.0003	0.002826	AP13
5288	7.8	3.58E-11	1.38E-05	0.00023	0.003003	ST13
5271	7.1	3.69E-11	1.56E-05	0.000257	0.002915	ST13
5408	10.5	7.66E-11	2.19E-05	0.00036	0.002833	ST13
4281	5.2	2.57E-11	1.49E-05	0.000228	0.002999	SCA13
4265	6.1	2.52E-11	1.24E-05	0.00019	0.002916	SCA13
3817	6.3	3.31E-11	1.58E-05	0.000242	0.002837	SCA13
13764	12	6.7E-11	1.68E-05	0.00023	0.002921	CS15
10331	6	3.2E-11	1.6E-05	0.000219	0.002921	CS15
6880	3.8	2.03E-11	1.61E-05	0.00022	0.002922	CS15
17531	4.7	2.16E-11	1.38E-05	0.000189	0.002918	CS15
3469	2.8	1.74E-11	1.87E-05	0.000256	0.002921	CS15
1333	6	3.53E-11	1.95E-05	0.000291	0.002917	AB29
5250	3.6	1.98E-11	1.65E-05	0.000284	0.002916	CN15
1385	1.6	8.13E-12	1.53E-05	0.000251	0.002915	CN15
2779	2.4	1.31E-11	1.64E-05	0.000269	0.002915	CN15
1722	1.6	8.44E-12	1.58E-05	0.00026	0.002912	CN15
10207	6.8	3.68E-11	1.62E-05	0.000267	0.002915	CN15

Typical example of an ALL... file, in this case ALLCA.WQ1.

Xm	XCa	Lc	TIME	L	W	TEMP
6.13	5.45	0.000215	9792	258	149	67.3
5.47	7.3	0.000252	9612	300	178	75
4.47	7.25	0.0003	9612	355	214	80.9

Rca	1/T	RUN
2.18E-11	0.002939	AP1
3.49E-11	0.002874	AP2
4.12E-11	0.002826	AP3

Typical example of a 3 run set, in this case AP13CA.WQ1.

Fc	Fca	Fk	Xc	Xca	Xk		
1160	303	843	27	1.2	0.8	S1 to S6	
240	217	880	12	1	1	BET plot	
4650	960	391	140	4.4	3.4	AUG 96	
7340	1503	2520	159	4.3	5.5		Ko
11430	2559	8469	255	5.75	10.05	KCl	480000
22430	4740	15891	404	6.9	21	CACL2	1420000
						COLOUR	80000

	LHS			RHS	
COL	CA	K	COL	CA	K
0.000545	0.000178	0.002199	0.0145	0.000213	0.001756
0.000251	0.000153	0.001837	0.003	0.000153	0.001833
0.000441	0.000154	0.00024	0.058125	0.000676	0.000815
0.000635	0.000246	0.00096	0.09175	0.001058	0.00525
0.000654	0.000314	0.001787	0.142875	0.001802	0.017644
0.000964	0.000485	0.00163	0.280375	0.003338	0.033106

Typical example of data for the BET isotherm. In this case BERS16.WQ1.

K15 APRIL 98

BX	SG	K mg/l	FEED K mg/kg	K mg/kgW
67.8	1.336	7360	5509	17109
67.95	1.337	7520	5625	17549
68.15	1.339	7480	5586	17539
67.95	1.337	7240	5415	16896
68.05	1.337	7520	5625	17604
	AVG =	7424	5551.883	17339.43

AFF SUGAR K	Ke(on W) K
12.5	0.000721
9.9	0.000571
10.5	0.000606
12	0.000692
9	0.000519

L	W	TIME	lg	ln(1-ke/ke) on W K
308	224	8940	3.1E-08	7.234288
419	290	22860	1.62E-08	7.467632
306	232	12960	2.15E-08	7.408757
291	216	10560	2.5E-08	7.275139
299	202	19800	1.33E-08	7.562995

Typical example of data for the interfacial model. In this case K15KE.WQ1.

DISC 2

AB25.WQ1	Raw data set AB25	
C15	"	"
CN15	"	"
COND16A	"	"
CS15	"	"

DIF	CA66.WQ1	Diffusion tests	
	CA70	"	"
	CA74A	"	"
	CA74C	"	"
	CAC	"	"
	K66	"	"
	K70	"	"
	K74A	"	"
	K74B	"	"
	K74C	"	"
	LI66	"	"
	LI70	"	"
	LI74A	"	"
	LI74C	"	"
	NI66	"	"
	NI70	"	"
	NI74A	"	"
	NI74B	"	"
	NI74C	"	"

Fig 4-2.WQ1	Figure 4.2 in text.
Fig 4-3. WQ1	Figure 4.3 in text.

GHR.WQ1	Raw data set GHR
GHRA	" " "
HRM16A	" " "
HT14ST	" " "
HTD13ST	" " "
KL15k	" " "
KL15STLI	" " "
LN15	" " "
MB15	" " "
ML15MB	" " "
MT13	" " "
R15KCAS	" " "
R15RATIOS.WQ1	Data Tables 4.1, 4.2
R15 T4-3.WQ1	Data Table 4.3
S16. WQ1	Raw data set S16
TR18	" " "
X19A	" " "

BRIX	mg/l	SG	mg/kg	mg/kgBX	TIME	mg/kgBX	
25.2	11	1.10656	9.94	39.45	0		21/4/97
25.6	12	1.1084	10.83	42.29	10800	2.84	Cainf =
26.5	13	1.1126	11.68	44.09	68400	4.64	138.6
25.6	13	1.1084	11.73	45.81	82800	6.37	
25.6	13.1	1.1084	11.82	46.17	97200	6.72	
26.5	15.1	1.1126	13.57	51.21	154800	11.77	
25.5	14.1	1.108	12.73	49.90	169200	10.46	
25.6	14.1	1.1084	12.72	49.69	183600	10.24	
26.5	15.2	1.1126	13.66	51.55	241200	12.11	
25.5	15.2	1.108	13.72	53.80	255600	14.35	
25.5	50.3	1.108	45.40	178.03		138.58	

TIME	LNW
10800	4.910864
68400	4.897507
82800	4.884561
97200	4.881892
154800	4.84287
169200	4.853146
183600	4.854806
241200	4.840193
255600	4.822292

Typical example of a diffusion experiment raw data, here for calcium. DIFCA66.WQ1.

COL	CA	POT	ST	Xc	Xca	Xk	Xst
11070	4974	5587	2985	168	30.9	8.8	401
20950	8813	11440	5077	334	76.5	21	867
2400	1068	1226	370	51	4	2.1	11
3600	1355	1848	900	77	13.7	4.6	85
6030	2453	3043	1486	100	15.8	5	165

COL/K F	ST/K F	CA/K F	COL/K X	ST/K X	CA/K X
1.98	0.53	0.89	19.09	45.57	3.51
1.83	0.44	0.77	15.90	41.29	3.64
1.96	0.30	0.87	24.29	5.24	1.90
1.95	0.49	0.73	16.74	18.48	2.98
1.98	0.49	0.81	20.00	33.00	3.16
1.94	0.45	0.81	19.20	28.71	3.04

IN FEED	Xc	Xca	Xk	Xst
500	21.29	0.03	0.92	4.28
1000	28.79	4.38	1.81	94.91
2000	43.80	13.09	3.60	276.16
3000	58.81	21.80	5.39	457.41

Raw data for Table 4.1 - a typical example.

APPENDIX 3

UNCERTAINTIES AND STATISTICAL DATA

Uncertainties

1. Errors in measurements

The approach given by James and Pritchard (1974) is used to calculate uncertainties in a quantity, using the uncertainties known for the measurements.

James and Pritchard give two equations:

$$\text{If} \quad Y = X_1 + X_2 + X_3 + \ldots$$

and the uncertainties in the X_1's are $\pm \Delta X_1$, then

$$\Delta Y = \left(\Delta X_1^2 + \Delta X_2^2 + \Delta X_3^2 + \ldots\right)^{\frac{1}{2}}$$

$$\text{If} \quad Y = \frac{X_1}{X_2} \times X_3 \ldots$$

then

$$\frac{\Delta Y}{Y} = \left\{\left(\frac{\Delta X_1}{X_1}\right)^2 + \left(\frac{\Delta X_2}{X_2}\right)^2 + \left(\frac{\Delta X_3}{X_3}\right)^2 + \ldots\right\}^{\frac{1}{2}}$$

2. Uncertainties on measured quantities

The International Commission for Uniform Methods of Sugar Analyses (ICUMSA) (1994) publication was used to obtain uncertainties on the sugar analyses. The following was obtained:

Colour: ± 4 units in crystal
± 4 units in liquors less than 1000 colour units
± 10 units in liquors more than 1000 colour units (due to dilution).

Starch: ± 5 mg/kg in crystals
± 20 mg/kg in liquors

Pol : ± 0,1
Sucrose: ± 0,1
Brix : ± 0,1

Lithium, calcium, potassium and nickel, by atomic absorption:
± 0,03 mg/l on standard
± 0,3 mg/l on sugar products, because of dilution.

Temperature: ± 0,1°C. All thermometers were calibrated against a certified thermometer.

Time : ± 15 s (estimated)

Mass: Analytical balance: ± 0,001 g
Pilot plant, 35 kg scale: ± 10 g.

L and W: The system is calibrated using a micrometer scale divided in 1 μm divisions, which can be read. Here ± 5 μm has been taken, conservatively.

3. Calculation of uncertainties

3.1 On L_c

$$L_c = \left(L^2\ W\right)^{\frac{1}{3}}$$

Average value of $L_c = 2{,}5 \times 10^{-4}$ m

$L = 275\ \mu m$

$W = 210\ \mu m$

From James and Pritchard (1974):

$$\frac{\Delta L_c}{L_c} = \left\{ \left(\frac{5 \times 10^{-6}}{275 \times 10^{-6}} \right)^2 + \left(\frac{5 \times 10^{-6}}{275 \times 10^{-6}} \right)^2 + \left(\frac{5 \times 10^{-6}}{210 \times 10^{-6}} \right)^2 \right\}^{\frac{1}{2}}$$

and

$$\Delta L_c = 8{,}8 \times 10^{-6}$$

3.2 On G

$$G = \frac{3\,\alpha\,\ell}{\beta} \cdot \frac{L_c}{t}$$

The uncertainty on α is $\pm$ 0,03 (see page 33). The uncertainty in the density of sucrose (1856 kg/m^3) is taken as $\pm$ 1. The uncertainty in β can be calculated and is $\pm$ 0,26.

Then

$$\frac{\Delta G}{G} = \left\{ \left(\frac{0,03}{0,34}\right)^2 + \left(\frac{1}{1586}\right)^2 + \left(\frac{8,8\ x\ 10^{-6}}{2,5\ x\ 10^{-6}}\right)^2 + \left(\frac{2,96}{0,26}\right)^2 + \left(\frac{15}{9000}\right)^2 \right\}^{\frac{1}{2}}$$

and $\Delta G = \pm 2,6 \times 10^{-6}$ kg/m^2/s

3.3 Other uncertainties

Uncertainties were calculated for the impurity transfer rates, following the approach shown above, to yield:

R_c	±	$5,1 \times 10^{-5}$	kg/m^2/s
R_{Li}	±	$1,7 \times 10^{-12}$	
R_{Ca}	±	$3,6 \times 10^{-12}$	
R_k	±	$4,3 \times 10^{-12}$	
R_{st}	±	$6,7 \times 10^{-10}$	

4. Uncertainties in data for partition coefficients

4.1 Colour

Average value for X_c = 79 colour units

F_c = 3510

Sucrose % liquor = 65,0

$$\text{ratio 1: } \frac{X_c}{\text{Suc. in crystal}} = 7,9 \times 10^{-5}$$

$$\text{ratio 2: } \frac{F_c}{\text{Suc. in feed}} = 0,0054$$

Then, Δ ratio 1 = $\pm 4{,}0 \times 10^{-6}$

$$\Delta \text{ ratio 2} = \left\{\left(\frac{10}{3510}\right)^2 + \left(\frac{0{,}1}{65}\right)^2\right\}^{\frac{1}{2}} = \pm 1{,}0 \times 10^{-5}$$

Similarly:

	Δ ratio 1	Δ ratio 2
Potassium	$\pm 0{,}3 \times 10^{-6}$	$\pm 2{,}7 \times 10^{-5}$
Calcium	$\pm 0{,}3 \times 10^{-6}$	$\pm 1{,}9 \times 10^{-5}$
Lithium	$\pm 0{,}3 \times 10^{-6}$	$\pm 1{,}5 \times 10^{-5}$
Starch	$\pm 5 \times 10^{-6}$	$\pm 1{,}5 \times 10^{-5}$

5. Uncertainties in the data for the isotherms

5.1 Colour

$\Delta F_c = \pm 10$ units

$\Delta X_c = \pm 4$ units

Then $$\Delta\left(\frac{F_c}{X_c}\right) = \left\{\left(\frac{10}{3510}\right)^2 + \left(\frac{4}{79}\right)^2\right\}^{\frac{1}{2}} = \pm 0{,}6$$

5.2 **Potassium**

Similarly: $$\Delta\left(\frac{F_k}{F_k}\right) = \pm\ 0{,}05$$

$$\Delta\left(\frac{F_{Ca}}{X_{Ca}}\right) = \pm\ 0{,}06$$

$$\Delta\left(\frac{F_{Li}}{X_{Li}}\right) = \pm\ 0{,}2$$

Multilinear regression

Multilinear regressions have been used in Tables 4.16 and 4.17 (page 112) for the effects of F_i, G, and L_c on the rate of impurity transfers.

Detailed statistics, including standard errors, significance levels and 95% confidence intervals for all the coefficients are given.

Uncertainties on the dependents have also been plotted.

Model fitting results for: LI.LRli

Independent variable	coefficient	std. error	t-value	sig.level
CONSTANT	-27.053293	4.120711	-6.5652	0.0000
LI.LFli	1.050756	0.092325	11.3811	0.0000
LI.LG	0.560074	0.372777	1.5024	0.1450

R-SQ. (ADJ.) = 0.8200	SE=	0.407454	MAE=	0.331039	DurbWat= 1.826
Previously: 0.0000		0.000000		0.000000	0.000

29 observations fitted, forecast(s) computed for 0 missing val. of dep. var.

Wed May 12 1999 07:18:58 AM Page 1

95 percent confidence intervals for coefficient estimates

	Estimate	Standard error	Lower Limit	Upper Limit
CONSTANT	-27.0533	4.12071	-35.5255	-18.5810
LI.LFli	1.05076	0.09232	0.86093	1.24058
LI.LG	0.56007	0.37278	-0.20636	1.32651

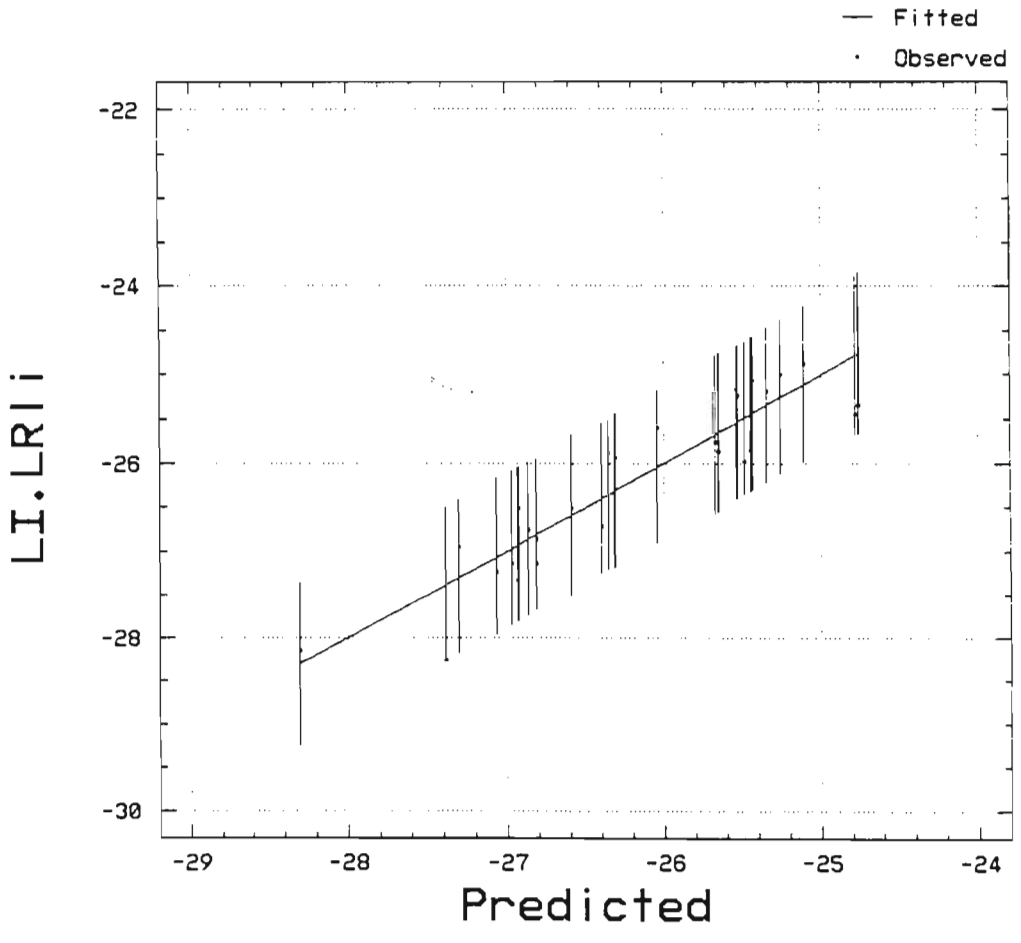

Statistics for the regression with lithium, Table 4.16

Model fitting results for: POT.LRk

Independent variable	coefficient	std. error	t-value	sig.level
CONSTANT	-17.723103	1.862817	-9.5141	0.0000
POT.LFk	0.620736	0.047086	13.1829	0.0000
POT.LG	1.05499	0.173504	6.0805	0.0000

R-SQ. (ADJ.) = 0.7538 SE= 0.385677 MAE= 0.292586 DurbWat= 1.168
Previously: 0.9581 0.205692 0.159445 1.089
59 observations fitted, forecast(s) computed for 0 missing val. of dep. var.

Wed May 12 1999 07:16:40 AM Page 1

95 percent confidence intervals for coefficient estimates

	Estimate	Standard error	Lower Limit	Upper Limit
CONSTANT	-17.7231	1.86282	-21.4556	-13.9906
POT.LFk	0.62074	0.04709	0.52639	0.71508
POT.LG	1.05499	0.17350	0.70734	1.40264

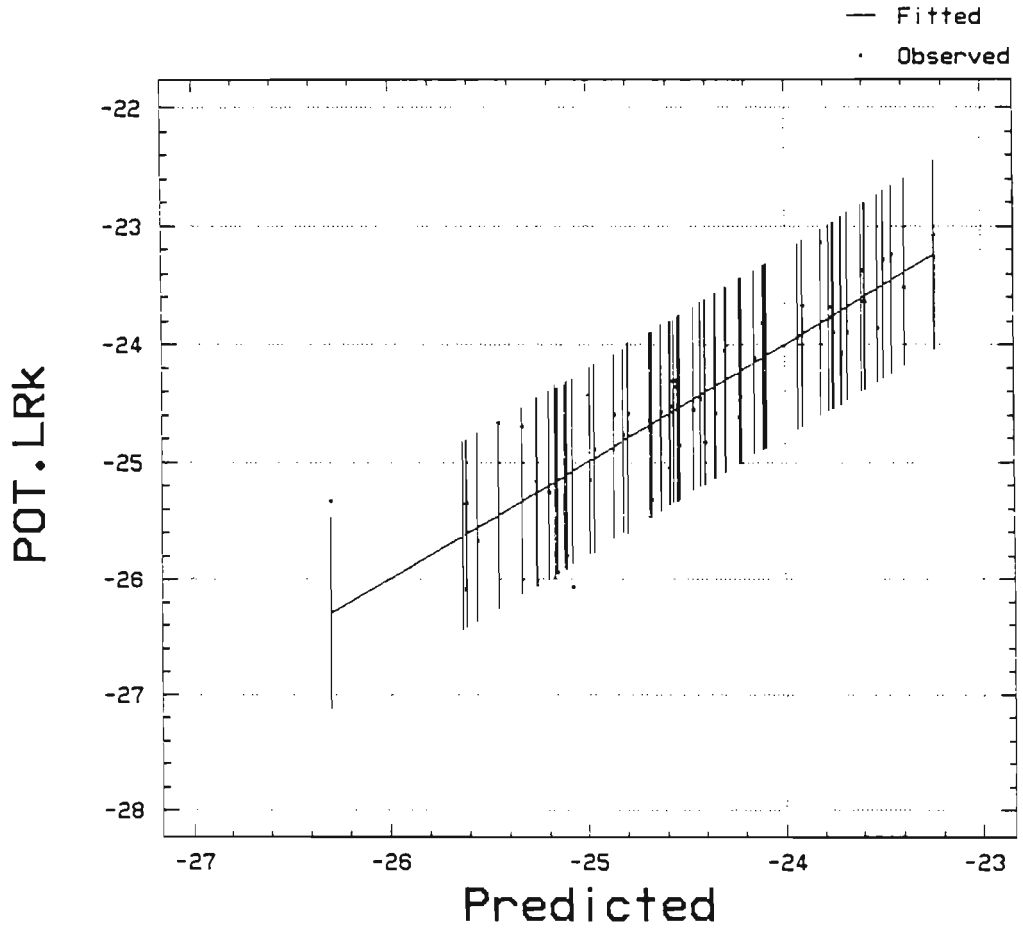

Statistics for the regression with potassium, Table 4.16

ed May 12 1999 07:12:43 AM Page 1

Model fitting results for: COL.LRc

ndependent variable	coefficient	std. error	t-value	sig.level
ONSTANT	-2.597405	0.976086	-2.6610	0.0094
OL.LFC	0.807006	0.018752	43.0351	0.0000
OL.LG	1.057804	0.090242	11.7219	0.0000

t-SQ. (ADJ.) = 0.9581 SE= 0.205692 MAE= 0.159445 DurbWat= 1.089
Previously: 0.0000 0.000000 0.000000 0.000
32 observations fitted, forecast(s) computed for 0 missing val. of dep. var.

Wed May 12 1999 07:13:03 AM Page 1

95 percent confidence intervals for coefficient estimates

	Estimate	Standard error	Lower Limit	Upper Limit
CONSTANT	-2.59740	0.97609	-4.54069	-0.65412
COL.LFC	0.80701	0.01875	0.76967	0.84434
COL.LG	1.05780	0.09024	0.87814	1.23747

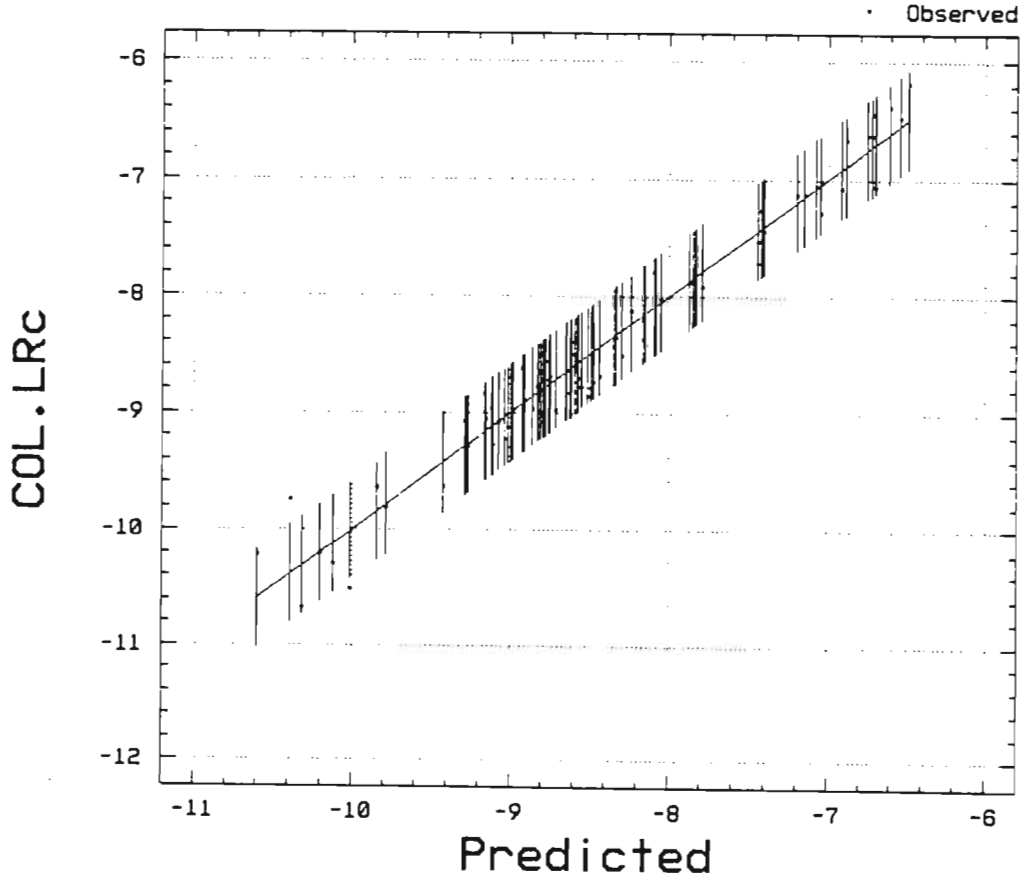

Statistics for the regression for colour, Table 4.16

Model fitting results for: CA.LRca

Independent variable	coefficient	std. error	t-value	sig.level
CONSTANT	-15.749597	4.055454	-3.8836	0.0005
CA.LFca	0.422281	0.068546	6.1605	0.0000
CA.LG	1.100736	0.358982	3.0663	0.0043

R-SQ. (ADJ.) = 0.5774 SE= 0.426242 MAE= 0.350827 DurbWat= 1.066
Previously: 0.0000 0.000000 0.000000 0.000
36 observations fitted, forecast(s) computed for 0 missing val. of dep. var.

Wed May 12 1999 07:42:00 AM Page 1

95 percent confidence intervals for coefficient estimates

	Estimate	Standard error	Lower Limit	Upper Limit
CONSTANT	-15.7496	4.05545	-24.0024	-7.49679
CA.LFca	0.42228	0.06855	0.28279	0.56177
CA.LG	1.10074	0.35898	0.37021	1.83126

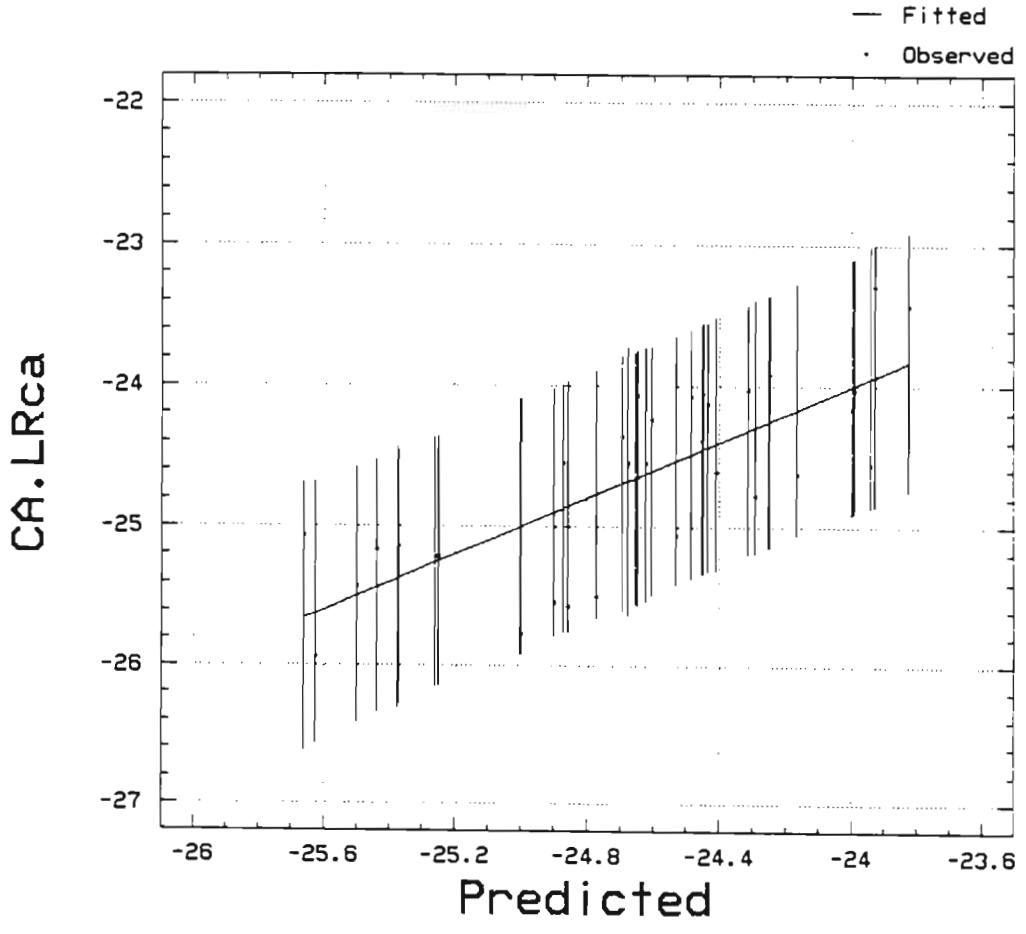

Statistic for the regression with calcium, Table 4.16

Model fitting results for: ST.LRst

Independent variable	coefficient	std. error	t-value	sig.level
ST.LFst	1.010996	0.106592	9.4847	0.0000
ST.LG	2.505086	0.076288	32.8370	0.0000

R-SQ. (ADJ.) =	0.9990	SE=	0.639510	MAE=	0.498916	DurbWat=	1.319
Previously:	0.8104		0.587903		0.448346		0.709

31 observations fitted, forecast(s) computed for 0 missing val. of dep. var.

Wed May 12 1999 07:21:26 AM Page 1

95 percent confidence intervals for coefficient estimates

	Estimate	Standard error	Lower Limit	Upper Limit
ST.LFst	1.01100	0.10659	0.79294	1.22905
ST.LG	2.50509	0.07629	2.34902	2.66115

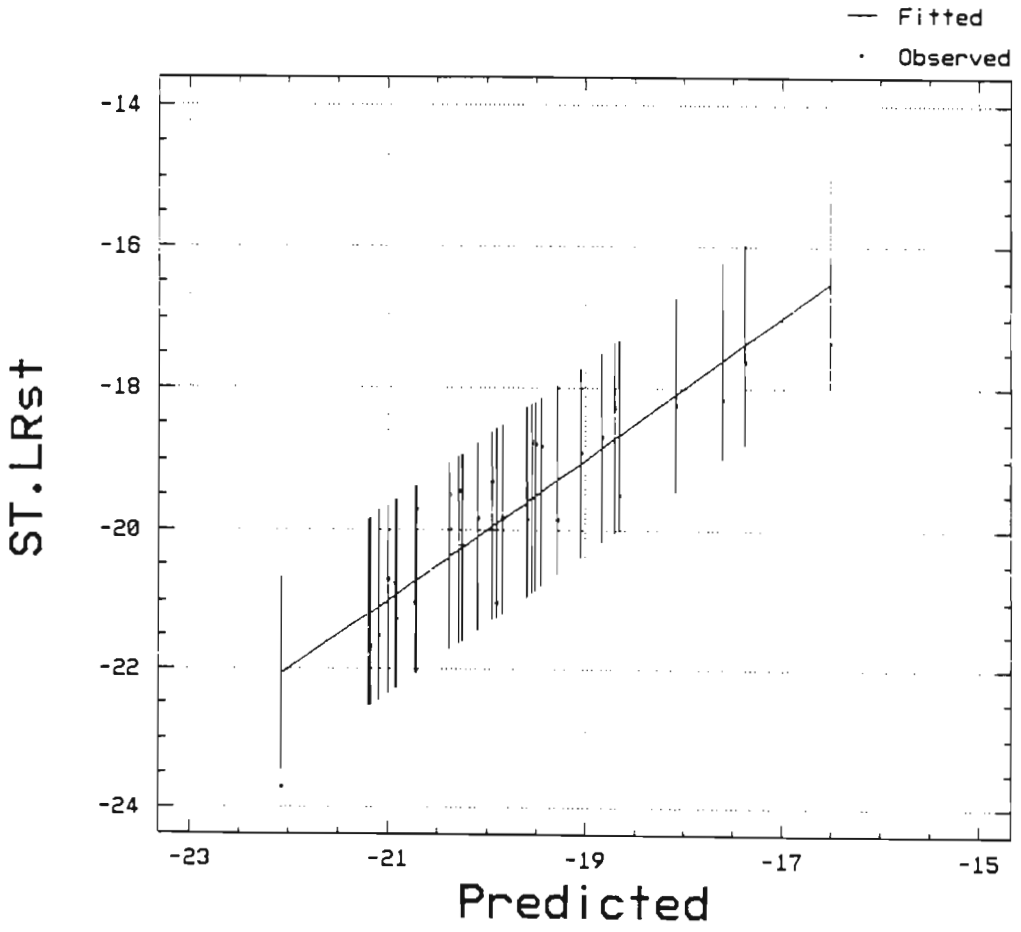

Statistics for the regression for starch, Table 4.16

Model fitting results for: MB.LRmb

Independent variable	coefficient	std. error	t-value	sig.level
CONSTANT	-43.156386	2.028947	-21.2703	0.0000
MB.LFmb	3.583295	0.300919	11.9078	0.0000

R-SQ. (ADJ.) = 0.9096 SE= 2.452873 MAE= 1.995568 DurbWat= 1.113
Previously: 0.9990 0.639510 0.498916 1.319
15 observations fitted, forecast(s) computed for 0 missing val. of dep. var.

Wed May 12 1999 07:23:52 AM Page 1

95 percent confidence intervals for coefficient estimates

	Estimate	Standard error	Lower Limit	Upper Limit
CONSTANT	-43.1564	2.02895	-47.5408	-38.7720
MB.LFmb	3.58330	0.30092	2.93303	4.23356

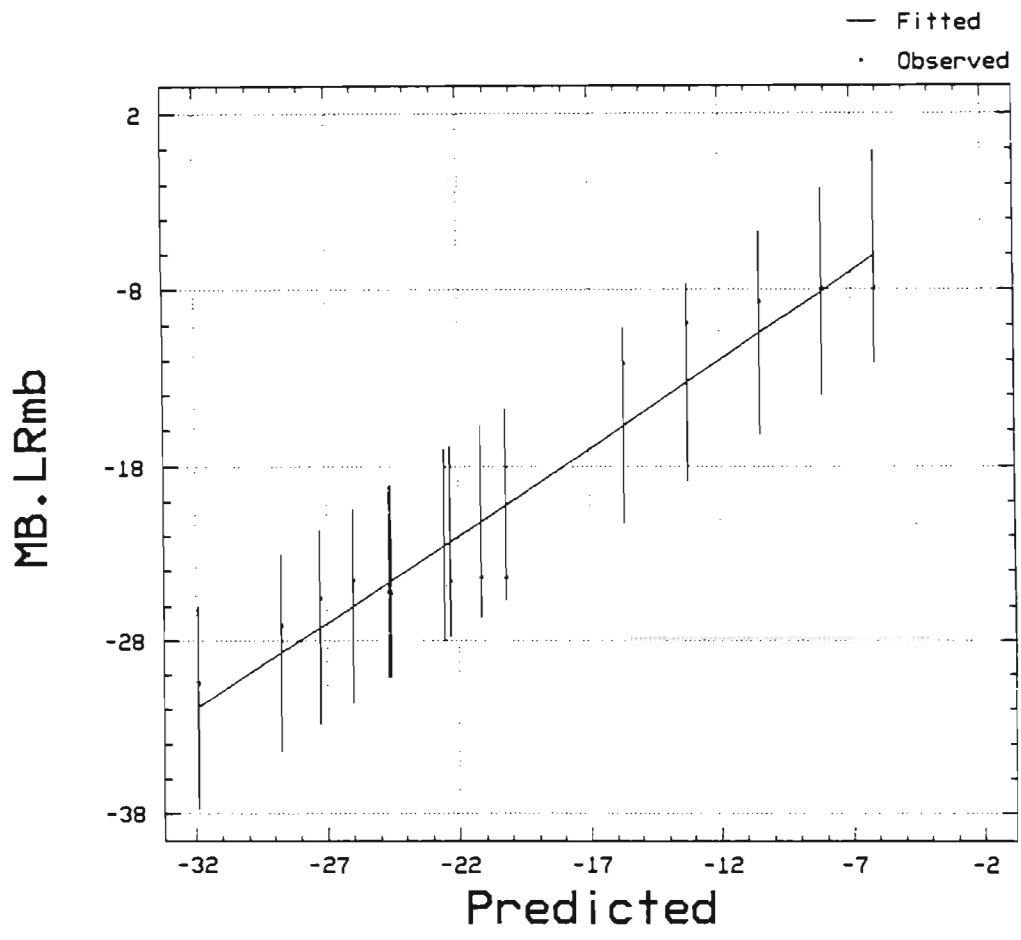

Statistic for the regression with methylene blue, Table 4.16

Model fitting results for: CLC.LRc

Independent variable	coefficient	std. error	t-value	sig.level
CONSTANT	-8.360008	1.90486	-4.3888	0.0000
CLC.LFc	0.765972	0.029118	26.3059	0.0000
CLC.LLc	0.68632	0.233302	2.9418	0.0043

R-SQ. (ADJ.) = 0.8964 SE= 0.323193 MAE= 0.250960 DurbWat= 1.302
Previously: 0.0000 0.000000 0.000000 0.000
82 observations fitted, forecast(s) computed for 0 missing val. of dep. var.

Wed May 12 1999 07:51:44 AM Page 1

95 percent confidence intervals for coefficient estimates

	Estimate	Standard error	Lower Limit	Upper Limit
CONSTANT	-8.36001	1.90486	-12.1524	-4.56763
CLC.LFc	0.76597	0.02912	0.70800	0.82394
CLC.LLc	0.68632	0.23330	0.22184	1.15080

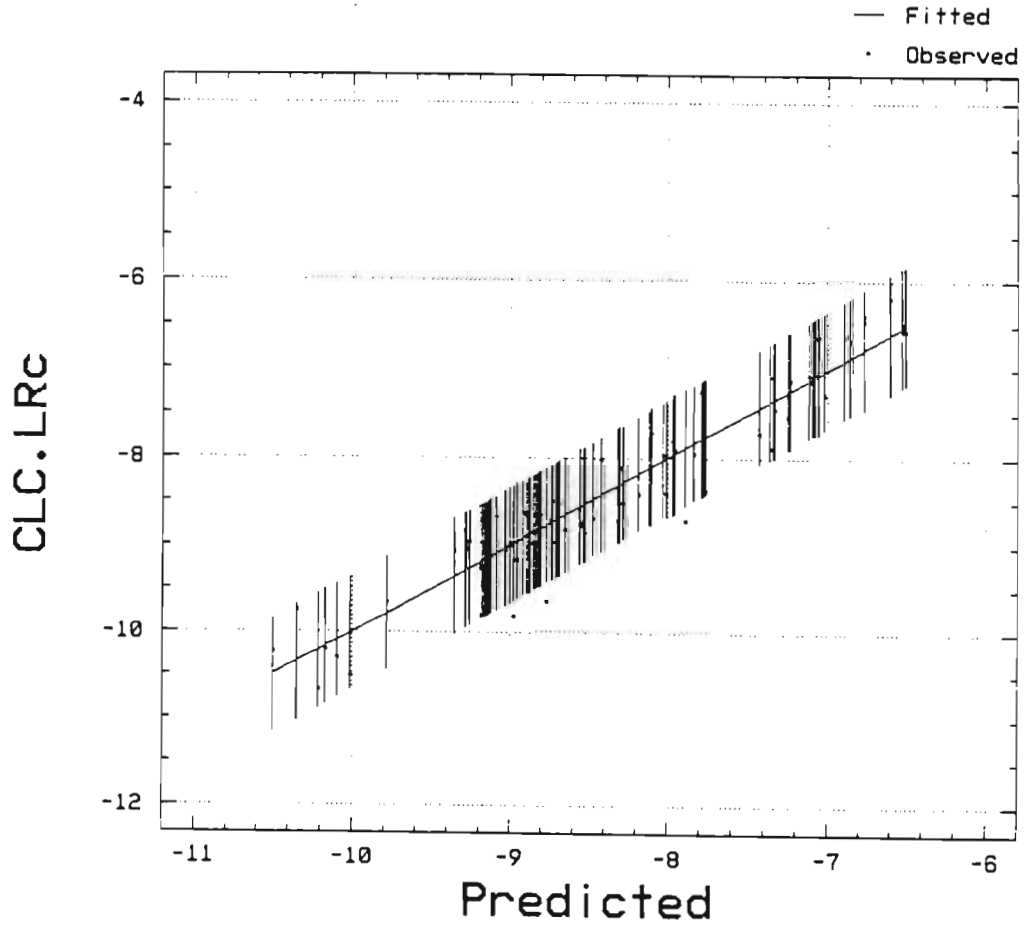

Statistic for the regression with colour, Table 4.17

Model fitting results for: CALC.LRca

Independent variable	coefficient	std. error	t-value	sig.level
CONSTANT	-20.216901	2.930715	-6.8983	0.0000
CALC.LFca	0.448479	0.070226	6.3862	0.0000
CALC.LLc	0.956362	0.350329	2.7299	0.0101

R-SQ. (ADJ.) = 0.5570 SE= 0.436393 MAE= 0.350050 DurbWat= 1.088
Previously: 0.0000 0.000000 0.000000 0.000
36 observations fitted, forecast(s) computed for 0 missing val. of dep. var.

Wed May 12 1999 07:56:09 AM Page 1

95 percent confidence intervals for coefficient estimates

	Estimate	Standard error	Lower Limit	Upper Limit
CONSTANT	-20.2169	2.93071	-26.1809	-14.2529
CALC.LFca	0.44848	0.07023	0.30557	0.59139
CALC.LLc	0.95636	0.35033	0.24345	1.66928

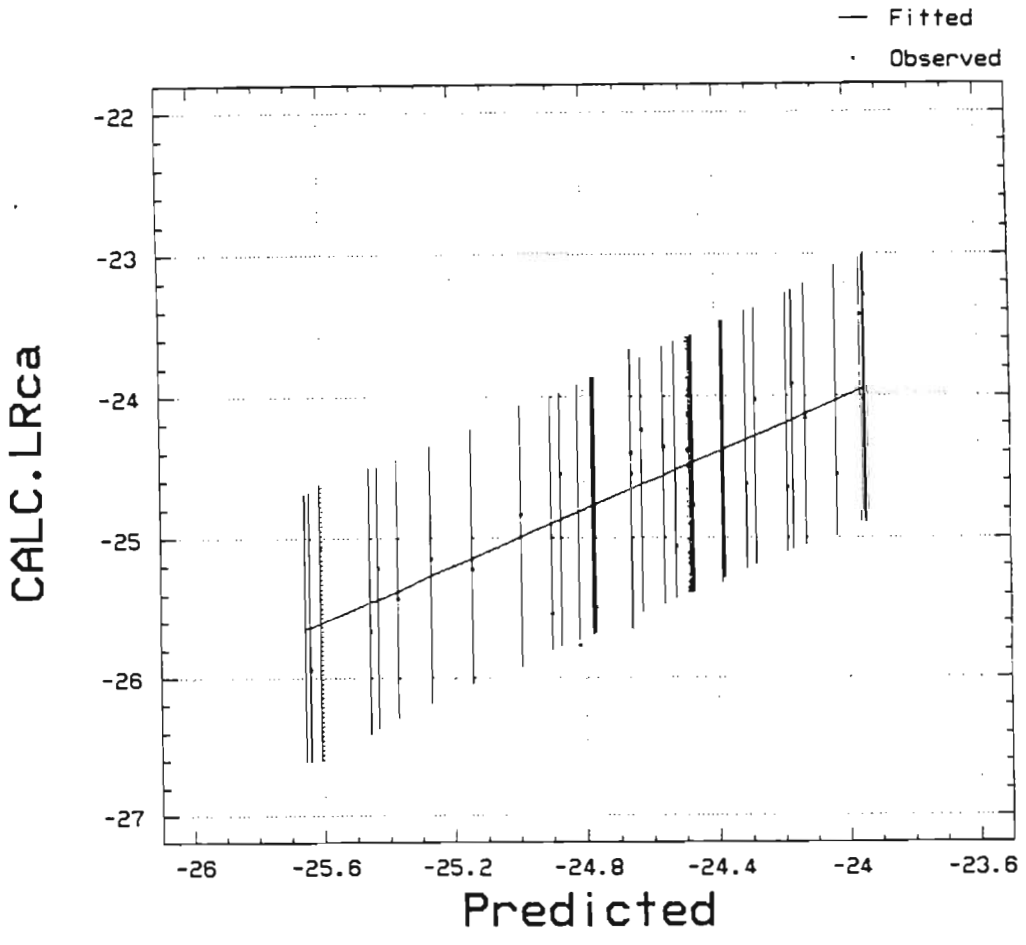

Statistic for the regression with calcium, Table 4.17